

Durham E-Theses

Synthesis and characterisation of potentially electrostrictive polymers

Gimeno, Miquel

How to cite:

Gimeno, Miquel (2002) *Synthesis and characterisation of potentially electrostrictive polymers*, Durham theses, Durham University. Available at Durham E-Theses Online: <http://etheses.dur.ac.uk/3862/>

Use policy

The full-text may be used and/or reproduced, and given to third parties in any format or medium, without prior permission or charge, for personal research or study, educational, or not-for-profit purposes provided that:

- a full bibliographic reference is made to the original source
- a [link](#) is made to the metadata record in Durham E-Theses
- the full-text is not changed in any way

The full-text must not be sold in any format or medium without the formal permission of the copyright holders.

Please consult the [full Durham E-Theses policy](#) for further details.

SYNTHESIS AND CHARACTERISATION OF POTENTIALLY ELECTROSTRICTIVE POLYMERS

The copyright of this thesis rests with the author.
No quotation from it should be published without
his prior written consent and information derived
from it should be acknowledged.

by

Miquel Gimeno

University of Durham



29 JAN 2003

A thesis submitted for the Degree of Doctor of Philosophy at the

University of Durham

October 2002

Acknowledgments

My initial thanks are to Prof. W. James Feast for giving me the opportunity to carry out Ph.D. research work in the IRC in Polymer Science and Technology at the University of Durham, and for his continual help, supervision and support during these three years.

I would like to thank all the people I have met during these three years in the United Kingdom, people who I have been delighted to work or just enjoy my time with, people who have expanded my life experience and knowledge of this country, as well as people from other parts of the world who I have had the fortune to meet and learn from.

From all these past years I have undoubtedly changed and personally enriched myself, but I must not forget to thank the people who initially gave me the opportunity of do that, particularly Prof. F. Albericio for his reference and encouragement and Dr. Neil Cameron for inviting me to come to Durham. I also like to thank my friends at home (Barcelona) for their continual loyalty, and finally my parents to whom I dedicate this work.

ABSTRACT

The work described in this thesis was concerned with the synthesis of electrostrictive polymers. Electrostrictive elastomers, the so-called *artificial muscles*, are a recent area of interest due to their potential for application in robots, smart materials and many high-technology devices. The goal of the project was with the synthesis and characterisation of novel low T_g polymers bearing highly polar groups in order to produce an electrostrictive effect.

The approach to such novel materials was undertaken via two different routes; firstly, the free-radical ring-opening polymerisation of partially fluorinated and alkyl substituted vinylcyclopropane monomers, and secondly, the ring-opening metathesis polymerisation and copolymerisation of partially fluorinated bicyclo[2.2.1]hept-2-ene monomers.

The outcome of the work has been the development of a synthetic route to stable polar polymers with T_g s below room temperature.

Abbreviations

AIBN– 2,2'-azobis(2-methylpropionitrile)

d– Piezoelectric coefficient

DSC– differential scanning calorimeter

EAP– Electroactive polymer

EP– Electrostrictive polymer

EPA– Electrostrictive polymer actuator

T_g– glass transition temperature

GC– Gas chromatography

GPC– gel permeation chromatography

IR– infra-red

nmr– nuclear magnetic resonance

δ– chemical shift

ppm– parts per million

M– Electrostriction coefficient

M_n– number average molecular weight

M_w– weight average molecular weight

PDI– polydispersity index (M_w / M_N)

m– meso

r– racemic

PVDF– poly(vinylidenedifluoride)

TG– thermogravimetry

THF– tetrahydrofuran

VCP– vinylcyclopropane

RROP– Radical ring opening polymerisation

ROMP– Ring opening metathesis polymerisation

Contents

Chapter 1. Introduction and objectives of the work

1.1 Context of the work (1)

1.2 Materials requirements (1)

1.3 Concept of electrostriction (2)

1.4 Existing technologies and applications of polar molecular materials (4)

1.5 The elastomeric state (7)

1.6 The glass transition temperature (8)

1.7 The free-radical polymerization (9)

1.7.1 Initiation (9)

1.7.2 Propagation (11)

1.7.3 Termination (12)

1.7.4 Stereochemistry and tacticity (13)

1.8 Design strategy and free-radical polymerization of
vinylcyclopropanes (14)

1.9 Polar polymers via ring-opening metathesis polymerization (19)

1.9.1 Ring opening metathesis polymerization (21)

1.9.2 ROMP of cycloalkenes (22)

1.9.3 Design strategy and ROMP of partially fluorinated
norbornenes (23)

***Chapter 2. Attempted syntheses of potentially electrostrictive polymers
via radical ring-opening polymerisation of partially
fluorinated vinyl cyclopropane monomers***

2.1 Introduction (25)

2.2 Synthesis and polymerisation of

1,1-difluoro-2-vinylcyclopropane (28)

2.2 a) Introduction (28)

2.2 b) Results and discussions for the ring-opening polymerisation of 1,1-difluoro-2-vinylcyclopropane (31)

2.2 b) (i) Monomer synthesis and characterisation

2.2 b) (ii) Polymerisation of 1,1-difluoro-2-vinylcyclopropane.
Results and discussions (34)

2.2 c) Conclusions (41)

2.3 Approaches to alkyl substituted and partially fluorinated
poly(pentenylenes) (43)

2.3 a) Introduction (43)

2.3 b) Synthesis and characterisation of alkyl substituted dienes (45)

- 2.3 b) (i) Introduction (45)
- 2.3 b) (ii) Synthesis of 4-methyl-1,3-undecadiene (45)
- 2.3 b) (iii) Synthesis of 3,4-dimethyl-1,3-tridecadiene (47)
- 2.3 b) (iv) Synthesis of 1,3-undecadiene (51)
- 2.3 b) (v) Attempted synthesis of 2-alkyl-1,3-butadiene (52)
- 2.3 b) (vi) Synthesis of 1-octen-3-one (53)
- 2.3 b) (vii) Attempted synthesis of
2-pentyl-1,3-butadiene (55)
- 2.3 b) (viii) Synthesis of 2-heptyl-1,3-butadiene (56)

2.4 Conversion of alkyl substituted buta-1,3-dienes to alkyl substituted
vinyl difluorocyclopropane monomers (59)

2.4 a) Introduction (59)

- 2.4 b) Difluorocarbene addition to trans-1,3-undecadiene (59)
- 2.4 c) Difluorocarbene addition to 2-heptyl-1,3-butadiene (63)
- 2.4 d) Analysis of the results and conclusions (69)

- 2.5 Attempted polymerisation of 1,1-difluoro-2-heptyl-2-vinylcyclopropane. Results and discussions (70)

- 2.6 Attempted synthesis of 1,1-difluoro-3-butyl-2-vinylcyclopropane (76)
 - 2.6 a) Introduction (76)
 - 2.6 b) Synthesis of cis-3-octen-1-mesylalcohol (77)

- 2.7 Experimental procedures (79)
 - 2.7 a) General considerations (79)
 - 2.7 b) Synthesis of 1,1-difluoro-2-vinylcyclopropane (80)
 - 2.7 c) Polymerisation of 1,1-difluoro-2-vinylcyclopropane (80)
 - 2.7 d) Synthesis of 4-methyl-undeca-1,3-diene (81)
 - 2.7 e) Synthesis of 3,4-dimethyl-trideca-1,3-diene (82)
 - 2.7 f) Synthesis of 1,3-undecadiene (83)
 - 2.7 g) Synthesis of 1-octen-3-one (84)
 - 2.7 h) First attempted synthesis of 2-pentyl-1,3-butadiene (85)
 - 2.7 i) Second attempted synthesis of 2-pentyl-1,3-butadiene (85)
 - 2.7 j) Synthesis of 2-heptyl-1,3-butadiene (86)
 - 2.7 k) Difluorocarbene addition to undeca-1,3-diene (87)
 - 2.7 m) Synthesis of 1,1-difluoro-2-heptyl-2-vinylcyclopropane (88)
 - 2.7 n) Attempted polymerisation of 1,1-difluoro-2-heptyl-2-vinylcyclopropane
 - 2.7 o) Synthesis of 3-octen-1-mesylalcohol (90)

***Chapter 3 Syntheses and attempted synthesis of potentially
electrostrictive polymers and copolymers via ring-opening
metathesis polymerisation of partially fluorinated
bicyclo[2.2.1]hept-2-ene and cyclopentene monomers***

3.1 Introduction (91)

3.1 a) The Diels-Alder reaction (92)

3.1 b) The ring-opening metathesis polymerization (93)

3.1 c) The hydrogenation of polymers (95)

3.2 Study of the synthesis and hydrogenation of poly(5,5,6-trifluoro-6-trifluoromethylcyclopentylenevinylene)

3.2 a) Synthesis of 5,5,6-trifluoro-6-trifluoromethyl
bicyclo[2.2.1]hept-2-ene (96)

3.2 b) Ring-opening metathesis polymerisation of 5,5,6-trifluoro-6-trifluoromethylbicyclo[2.2.1]hept-2-ene (97)

3.2 c) Hydrogenation of poly(4,4,5-trifluoro-5-trifluoromethyl-1,3-cyclopentylenevinylene) (99)

3.2 d) Structural characterisation of the polymers (100)

- 3.2 d) (i) Nmr spectroscopy (100)
- 3.2 d) (ii) Elemental analysis (116)
- 3.2 d) (iii) IR spectroscopy (116)

3.2 e) Physical characterisation of the polymers (118)

3.2 f) Conclusions (118)

3.3 Study of the synthesis and hydrogenation of poly(5-trifluoromethyl-1,3-cyclopentylenevinylene)

3.3 a) Introduction (119)

3.3 b) Synthesis of 5-trifluoromethylbicyclo[2.2.1]hept-2-ene (119)

3.3 c) Ring-opening metathesis polymerisation of
5-trifluoromethylbicyclo[2.2.1]hept-2-ene (120)

3.3 d) Hydrogenation of poly(5-trifluoromethyl-1,3-cyclopentylenevinylene) (121)

3.3 e) Structural characterisation of the polymers (122)

- 3.3 e) (i) Nmr spectroscopy (122)
- 3.3 e) (ii) Elemental analysis (129)
- 3.3 e) (iii) IR spectroscopy (129)

3.3 f) Physical characterisation of the polymers (131)

3.3 g) Conclusions (131)

3.4 Study of the synthesis and hydrogenation of copoly(5-trifluoromethyl-1,3-cyclopentylenevinylene)-co(pentenylene)s

3.4 a) Introduction (132)

3.4 b) Copolymerisation experiments and results (133)

3.4 c) Structural characterisation of the copolymers (136)

- 3.4 c) (i) Nmr spectroscopy (136)
- 3.4 c) (ii) Elemental analysis of the copolymers (143)

3.4 d) Physical characterisation of the polymers (144)

3.4 e) Conclusions (145)

3.5 Experimental procedures (146)

3.5 a) General considerations (146)

3.5 b) Synthesis of 5,5,6-trifluoro-6-trifluoromethyl
bicyclo[2.2.1]hept-2-ene (146)

3.5 c) Synthesis of 5-trifluoromethylbicyclo[2.2.1]hept-2-ene (147)

3.5 d) General procedure for ring-opening metathesis
polymerisation (148)

3.5 e) General procedure for the hydrogenation of the polymers (149)

4 Future work (150)

References (153)

Appendix chapter 2

Cosy spectrum of 1,1-difluoro-2-vinylcyclopropane AX1

¹⁹F nmr spectrum of 1,1-difluoro-2-vinylcyclopropane AX2
¹³C nmr spectrum of 1,1-difluoro-2-vinylcyclopropane AX3
IR spectrum of poly(1,1-difluoro-2-vinylcyclopropane) AX4
¹H nmr spectrum of 4-methyl-1,3-undecadiene AX5
¹³C nmr spectrum of 4-methyl-1,3-undecadiene AX6
¹H nmr spectrum of 3,4-dimethyl-1,3-tridecadiene AX7
¹³C nmr spectrum of 3,4-dimethyl-1,3-tridecadiene AX8
¹H nmr spectrum of 1,3-undecadiene AX9
¹³C nmr spectrum of 1,3-undecadiene AX10
IR spectrum of 1,3-undecadiene AX11
¹H nmr spectrum of 1-octen-3-one AX12
¹³C nmr spectrum of 1-octen-3-one AX13
IR spectrum of 1-octen-3-one AX14
¹H nmr spectrum of 2-heptyl-1,3-butadiene AX15
¹³C nmr spectrum of 2-heptyl-1,3-butadiene AX16
IR spectrum of 2-heptyl-1,3-butadiene AX17
IR spectrum of 1,1-difluoro-2-heptyl-2-vinylcyclopropane AX18
Expanded ¹⁹F nmr of 1,1-difluoro-2-heptyl-2-vinylcyclopropane AX19
¹H nmr spectrum of 3-octen-1-mesylalcohol AX20
¹³C nmr spectrum of 3-octen-1-mesylalcohol AX21
IR spectrum of 3-octen-1-mesylalcohol AX22

Appendix chapter 3

*IR spectrum of 5,5,6-trifluoro-6-trifluoromethyl
bicyclo[2.2.1]hept-2-ene AX23*
*¹⁹F nmr spectrum of 5,5,6-trifluoro-6-trifluoromethyl
bicyclo[2.2.1]hept-2-ene AX24*
*¹H nmr spectrum of 5,5,6-trifluoro-6-trifluoromethyl
bicyclo[2.2.1]hept-2-ene AX25*
*¹³C nmr spectrum of 5,5,6-trifluoro-6-trifluoromethyl
bicyclo[2.2.1]hept-2-ene AX26*
IR spectrum of 5-trifluoromethylbicyclo[2.2.1]hept-2-ene AX27
¹⁹F nmr spectrum of 5-trifluoromethylbicyclo[2.2.1]hept-2-ene AX28
¹H nmr spectrum of 5-trifluoromethylbicyclo[2.2.1]hept-2-ene AX29

¹³C nmr spectrum of 5-trifluoromethylbicyclo[2.2.1]hept-2-ene AX30
¹⁹F nmr spectrum of copolymer (V) AX31
¹H nmr spectrum of copolymer (V) AX32
¹³C nmr spectrum of copolymer (V) AX33
¹⁹F nmr spectrum of copolymer (VI) AX34
¹H nmr spectrum of copolymer (VI) AX35
¹³C nmr spectrum of copolymer (VI) AX36
¹⁹F nmr spectrum of copolymer (VII) AX37
¹H nmr spectrum of copolymer (VII) AX38
¹³C nmr spectrum of copolymer (VII) AX39
¹⁹F nmr spectrum of copolymer (VIII) AX40
¹H nmr spectrum of copolymer (VIII) AX41
¹³C nmr spectrum of copolymer (VIII) AX42
¹⁹F nmr spectrum of copolymer (IX) AX43
¹H nmr spectrum of copolymer (IX) AX44
¹³C nmr spectrum of copolymer (IX) AX45
¹⁹F nmr spectrum of copolymer (X) AX46
¹H nmr spectrum of copolymer (X) AX47
¹³C nmr spectrum of copolymer (X) AX48
¹H nmr spectrum of copolymer (XII) AX49
¹³C nmr spectrum of copolymer AX50

Chapter 1

Introduction and objectives of the work

1.1 Context of the work

The objective of this project is to produce new polymers with potential for use as electrostrictive materials. The project involves design and synthesis of suitable materials, their characterisation and the investigation of their electrostrictive behaviour. The work of the author in Durham is concerned with the design, synthesis and molecular characterisation of appropriate materials. Their electrostrictive behaviour will be investigated in the group of Professor G.R. Davies in the Leeds IRC Laboratories.

1.2 Materials requirements

The essential requirements for an electrostrictive material, as described at the outset of this work by our colleagues in the physics activity within the IRC, are for a polymer which is an elastomer at room temperature but which has strong electrical dipoles attached at an angle to the polymer backbone. This can be represented as shown in *Figure 1.1*, where the solid line represents the elastomeric polymer backbone and the arrows represent the polar groups.



Figure 1.1 Schematic representation of the requirements for an electrostrictive polymer

There has been previous work in the Durham IRC directed towards the objectives of this project.¹ In that earlier work the polar effect was achieved using nitrile and ester units attached to a poly(1-pentenylene) backbone, *Figure 1.2*. There are two opposing effects on the polymer's properties the first arising from the inherent flexibility of the poly(pentenylene) hydrocarbon backbone, which tends

towards low T_g , and second effect arising from the polar cyano and ester groups which tends to raise the T_g . The alkyl group (R in *Figure 1.2*) was varied to tailor the value of T_g via internal plasticisation. The materials made by Dr. Cochlin were weakly electrostrictive and suffered from the tendency to absorb traces of moisture. Since the electric fields used to obtain the electrostrictive effect are large, the presence of even traces of water (which can migrate in the field) is destructive of the required electrostrictive effect. In this project the author aims to redesign the material to retain the necessary low T_g and to produce a hydrophobic polymer to eliminate the moisture contamination effect.

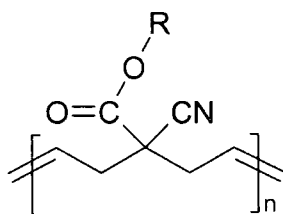


Figure 1.2 The generalised structure of the electrostrictive polymers prepared by R.Cochlin¹

1.3 Concept of electrostriction

Electrostriction has been well known for inorganic crystals and ceramics for many years. Electrostriction was observed as early as 1820 by A.C. Becquerel in inorganic crystals.²

The application of an electric field to any material can displace charge and lead to field-induced elastic strains. The part of the strain proportional to the square of the electric field is called electrostriction.

$$S = dE + ME^2$$

Where S is the strain, E is the electric field applied, d is the piezoelectric coefficient, which is temperature dependent, and M is the electrostrictive coefficient. The electrostriction phenomenon in elastomers is currently an active

field of research in polymer science. There are different explanations of electrostriction at the molecular level for the different materials existing at present; however, a qualitative picture, consistent with the behaviour of the novel material that this project is pursuing, is described below, see *Figure 1.3*.

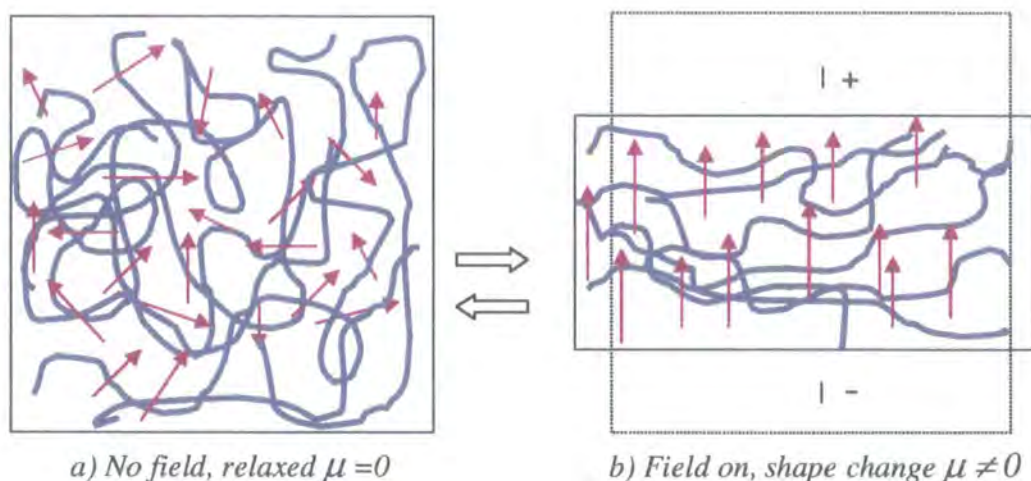


Figure 1.3 Changes produced by the effect of an electric field

In an amorphous rubber, which carries polar groups, the polymer chains are randomly coiled with any associated dipoles randomly directed within the sample, as shown in *Figure 1.3a* in the cartoon on the left; as a result the dipole moment of the bulk material (μ) is zero. On the application of an electric field, a force is exerted on the electric dipoles, which tends to align them with the applied field, this is indicated in the right hand cartoon, *Figure 1.3 b*; the bulk material now has a non-zero value of μ . The movement of the dipoles is, however, restricted by the position of the chains within the sample. In order to maximise the dipole alignment, the polymer chains adopt a different organisation in space, which has the effect of changing the dimensions of the polymer sample while the volume remains constant.

The polymer also changes its properties since the dipole alignment and the chain movement produce more order in the polymer thus reducing elasticity and

giving a more rigid material. On the removal of the electric field, the polymer relaxes and returns to its original, disordered, rubbery state.

1.4 Existing technologies and applications of polar molecular materials

Polar electroactive polymers, mostly PVDF and its copolymers, have found applications which utilise their piezo- and pyroelectric properties. The piezoelectric effect, which can be understood as the generation of electric charge by a crystalline material upon subjection to a stress, exists in natural crystals such as quartz. The piezoelectric effect in polymers was discovered in 1969, and in 1975 the Japanese company, Pioneer Ltd., developed the first commercial products using poled PVDF in piezoelectric loudspeakers and earphones. In the poling process the material is heated above its glass transition temperature and then exposed to a strong electric field, the material is then cooled with the field on and the oriented dipoles become locked in as the material cools below T_g . Films of poled polymers have a permanent electrical dipole across the film. The pyroelectric effect is the property of certain polar crystalline substances to generate an electrical current in an external circuit in response to absorption of heat by the material and poled polymers have found use in pyroelectric detectors. For the purposes of the project we shall describe this class of materials as electroactive polymers, EAPs.

EAPs have been proposed for use in various applications such as sensors, acoustic transducers for underwater navigation and robots. Compared with inorganic crystals, polymers offer the advantages of ease of moulding, flexibility, lightweight, low cost and they do not depolarize while being subjected to very high alternating electric fields. However, the main disadvantages of the common polymers in these applications arise from the relatively high mechanical and electrical losses that occur. For existing technologies EAPs exhibit limitations in one or more of the important performance parameters, such as strain, actuation pressure or speed of response and, in general, their lower efficiency when compared with the commonly used electroactive ceramic materials, like barium titanate (BaTiO_3) or lead-zirconate-titanates (PZTs), inhibits their use. These

limitations are not important for all applications, although for some applications such as mobile microrobots and other high-tech devices a better overall performance or a better performance in one or more specific parameters is required. Hence, one of the challenges in the development and utilisation of EAPs for these specific applications is how to significantly increase and improve these performance parameters. Mechanisms for converting electrical energy into mechanical energy, for instance, are essential for the design of nanoscale transducers, sensors, motors, pumps, artificial muscles or medical microrobots. Electrostrictive polymers (EPs) are quite promising as the active components for a general-purpose actuator technology. As well as the well known piezoelectric materials, electrostrictive materials exhibit shape change in response to electrical stimulation, however, unlike in the piezoelectric phenomenon where such deformation is linear with respect to the applied field (within the elastic limit) and changes sign with the polarity of the field, in electrostriction, the amount of the deformation which occurs with the applied field, is proportional to the square of the field and therefore independent of the polarity of the field. Moreover, since it is an elastomer, it returns to its initial relaxed state when the field is switch off. Some EPAs are commonly described as *artificial muscles* because their performance is potentially comparable to that of natural muscle and, like that of natural muscle is scale invariant; that is to say that the force exerted by an actuator depends on the bulk of active material used.

In recent years, attempts to improve the performance of existing EPs and/or to develop new high performance polymers have had some success. Some electrostrictive materials are already commercially available and relatively cheap and easy to manufacture, they are known as dielectric EAPs and are based on silicone rubbers, thermoplastic polyurethanes or grafted polyglutamates, e.g. Dow Corning Sylgard and Deerfield PT6100S among others. The two main research groups working on these materials appear to be the group of Bar-Cohen *et. al.* in the *Jet Propulsion Laboratory* in the California Institute of Technology, sponsored by NASA, and the group of Pelrine at Stanford Research Institute, (CA).^{3,4,5} The materials studied by these groups do not carry dipoles in the polymer backbone and

their actuation mechanism is different to that outlined in *Figure 1.3*. It is described in terms of the bulk electrical and mechanical properties of the polymer and the actuator effect depends on Coulombic electrostatic forces. A film of the material is constrained within compliant electrodes, when the field is applied the film tends to compress in thickness and expand in length and width due to a combination of the attractive and repulsive electrostatic forces occurring between the charges on the flexible compliant electrodes and the charge distribution in the polymer. The induced actuation strain observed is proportional to the square of the electric field, as in the normal electrostriction (see *Figure 1.3*), these materials require large electric fields for actuation ($\sim 100 \text{ V}/\mu\text{m}$) and can display significant levels of strain (10-200 %).

Other types of EAP actuators are based on solvent swollen polyelectrolyte polymer gels, usually cross-linked polyacrylamides.^{6,7} The use of carbon nanotubes (CNs) in a polyelectrolyte media has been described recently,^{8,9} and is related to the gel systems described above. CNs are fullerene based materials which have an improved response to an electric field, however the relaxation process in these systems is too slow at present to be practically useful when compared to existing technologies and production costs are high.

In the artificial muscles research institute (AMRI) in the University of New Mexico at Albuquerque some prototypes of artificial muscles have been created, using an extension of the polyelectrolyte gel idea, specifically using the perfluorinated ionomer polymer Nafion[™] loaded with metal ions and particles which act as both electrode and active components in these polymer-metal composites (IPMCs).^{10,11} In 1998, a graft elastomer EAP was developed by Su, *et.al.*,¹² this electrostrictive polymer consists of two components, a flexible backbone macromolecule and a grafted polar polymer that can form crystalline domains, the material displays an electric field induced strain of approximately 4 %. In the same year Zhang et al, introduced defects into the crystalline structure of poly(vinylidene fluoride-trifluoroethylene) (P(VDF-TrFE)) copolymer using high energy electron beam irradiation.¹³⁻¹⁵ The resulting material exhibits spontaneous electric polarization at low electric fields giving electrostrictive strains as large as 5

%. The most recent discovery is based on the technology of ferroelectric liquid-crystalline elastomers, which combines polymer backbones with polar liquid crystal structures and is reported to show a further increase in electrostrictive strain at low electric fields.¹⁶

The above examples illustrate the current search for effective electrostrictive materials. There is also a current active area of research concerned with identifying optimal actuator designs that best exploit these electrostrictive polymers' EP capabilities. This engineering design work is outside the scope of this thesis but there are already applications in micro- and minirobots for the dielectric polymers, as well as high-speed devices for sound generation, micropumps or microvalves for inkjet printers, on-chip biological or chemical devices, displays and other optical devices. There are many problems to solve and a major difficulty is in the production of effective compliant electrodes which function in contact with an EP while it undergoes dimensional change without changing their own function.

In this project the author is primarily concerned with the design, synthesis, and characterization of novel potentially electrostrictive materials based on the concept outlined in *Figure 1.3*.

1.5 The elastomeric state

Electrostriction in polymers can only occur in elastomers. Elasticity is the reversible stress-strain behaviour by which a body resists and recovers from deformation produced by a force. Elastomeric materials are able to undergo large deformations without fracture and then return to their original shape.

In order for a polymer to exhibit elasticity, the polymer chains must be highly flexible so that they are able to alter their arrangement and disposition in space when subjected to a force. Also, there must be either cross-links in the form of permanent chemical bonds or physical constraints such as chain entanglements. In the absence of these links, the polymer chains would permanently slip past each other on deformation; that is, they would flow and the deformation would be irreversible.

There must be very low intermolecular forces between the chains, high interchain forces would prevent the chains from moving reversibly past each other. Extensive crystal domains must not be present and the polymer must not be in the glassy state. This means that, at the working temperature of an electrostrictive device, the polymer must be well above its glass transition temperature.

1.6 The glass transition

If the melt of a non-crystallised polymer is cooled it becomes more viscous and flows less readily. If the temperature is reduced low enough the sample becomes rubbery and then as the temperature is reduced further it becomes a relatively hard polymer glass. The temperature at which the polymer undergoes the transformation from a rubber to a glass is known as *the* glass transition temperature, T_g . There are dramatic changes in the properties of the material at the glass transition temperature. Below T_g there is a sharp increase in the stiffness of an amorphous polymer, as well as changes in other physical properties such as heat capacity and thermal expansion coefficient. One of the important aspects of the current project is to maintain the T_g of the polymers produced well below room temperature, this requirement is to insure that they would be elastomers at the intended temperature of use. There are several factors, which affect the glass transition temperature. Main chain flexibility is the most important factor; polymers with flexible backbones have a low T_g . Flexibility is obtained when chains are composed of bond sequences that are able to rotate easily. Large bulky side groups tend to inhibit rotation about the main chain and thus increase the T_g .

For high molecular weight polymers, T_g is essentially independent of molecular weight but as the chain length decreases then T_g will decrease. This is due to the relative increase in the number of the end groups in the polymer sample. Chain ends are able to move more freely than units constrained in the polymer chain and this increase in chain end mobility contributes to a decrease in T_g with decreasing molecular weight.

1.7 Free radical polymerisation

Free radicals are independently existing species which possess an unpaired electron and normally are highly reactive with short life times. Free-radical polymerisations are chain polymerisations in which each polymer molecule grows by addition of monomer to a terminal free-radical reactive site known as an *active centre*. Consequent upon every addition of monomer, the active centre is transferred to the newly-created chain end.

Free-radical polymerisations are a practised method of chain polymerisation. In common with other types of chain polymerisation the reaction can be divided into three distinct steps: *initiation*, *propagation* and *termination*. The general chemistry associated with each step is described in the following three sections by considering for simplicity the polymerisation of a general vinyl monomer, $\text{CH}_2=\text{CHX}$.

1.7.1 Initiation

This stage involves creation of the free-radical active centre and usually takes place in two steps. The first is the formation of free radicals from an *initiator* and the second is the addition of one of these free radicals to a molecule of monomer.

There are two ways in which free radicals can be formed: (i) homolytic scission of a single bond (i.e. homolysis), and (ii) single electron transfer to or from an ion or molecule (redox reactions).

Homolysis can be affected for instance by the application of heat and, for example, the C-N bonds in azo compounds undergo *thermolysis* in the convenient temperature range of 50-100°C. Two examples of free radical initiators are shown in *Figure 1.4*.

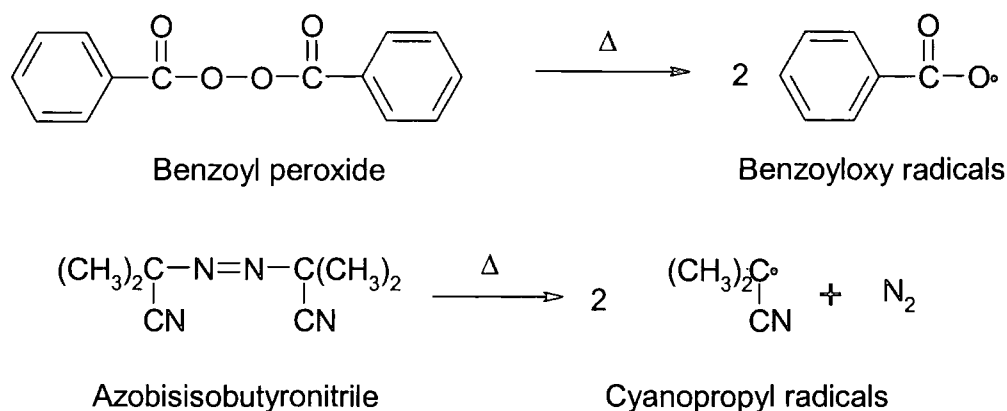


Figure 1.4 Common free radical initiators

Many of the radicals produced undergo further breakdown before reaction with monomer, for example β -scissions of the benzoyloxy radical leading to the phenyl radical and carbon dioxide. Additionally, homolysis can be brought about by photolysis, i.e. the action of radiation, this light energy (usually in the ultraviolet-visible spectral range, generally 250-450 nm) is converted into chemical energy in the form of the reactive intermediates, such as free radicals, which subsequently initiate polymerisation. An advantage of photolysis is that the formation of free radicals begins at the instant of exposure and ceases as soon as the light source is removed. Photoinitiated polymerization and crosslinking of polymers constitute the basis of important commercial processes with broad applicability, including photoimaging and UV curing of coatings and inks. Examples are the dissociation of azobisisobutyronitrile and the formation of free radicals from benzophenone and benzoin.

Redox reactions are another important technique for initiating polymerization. Initiators composed of mixtures of oxidizing and reducing agents, now termed redox initiators, have become very important, particularly in industry where they are used extensively in low-temperature emulsion polymerization, for example in synthetic rubber production. The activation energies for radical generation by redox processes are often low, of the order 40 kJ mol^{-1} (compared to 130 kJ mol^{-1} , approximately, for simple thermal dissociation into initiating radicals) so that they are particularly suitable for low-temperature polymerisations. The

essential feature in redox initiation is a single-electron transfer, generating free radicals, which are sufficiently active to initiate. An active center then is created when a free radical (R^\bullet) generated from the initiator attacks the π -bond of a molecule of monomer. There are two possible modes of addition shown in *Figure 1.5 (a)*, as well as an example of the well-known ferrous ion initiator mixed in this case with cumyl hydroperoxide, although it is also often mixed with hydrogen peroxide or other peroxy compounds, *Figure 1.5 (b)*.

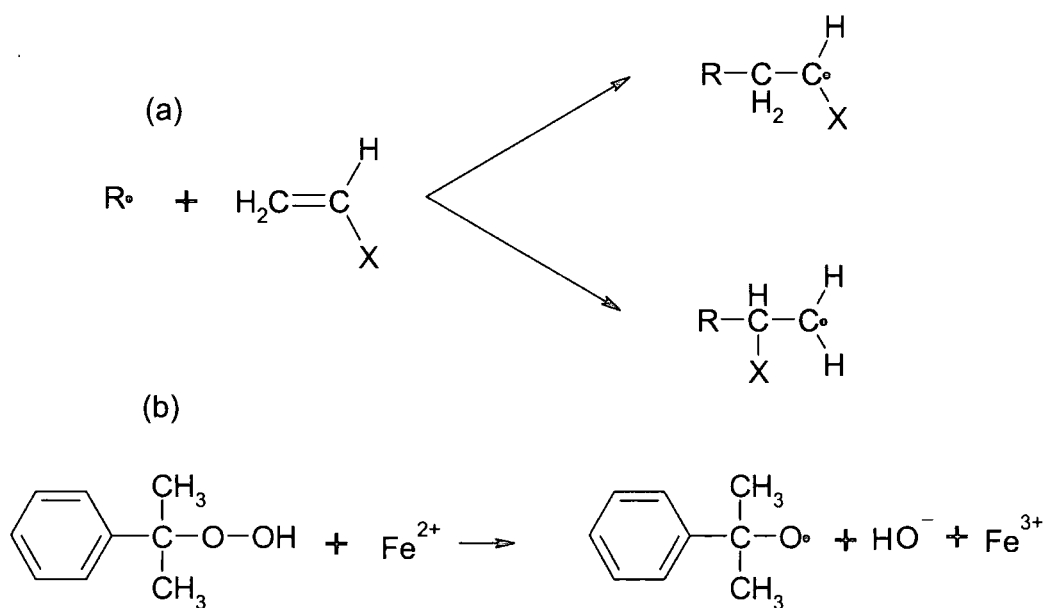


Figure 1.5 Modes of addition (a) and ferrous ion-peroxy mixture redox initiator (b)

The route indicated at the top of *Figure 1.5 (a)* predominates because attack at the methylene carbon is less sterically hindered and yields a product free radical that is more stable because of the effects of the adjacent X group.

1.7.2 Propagation

This involves growth of the polymer chain by rapid sequential addition of monomer to the active centre. As with the second step of initiation, there are two possible modes of propagation as shown in *Figure 1.6*.

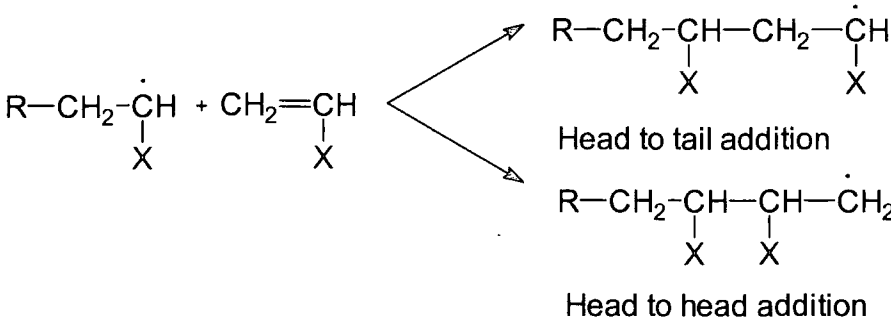


Figure 1.6 Types of addition in free radical polymerisation

The head-to-tail mode of addition predominates for the reasons given in the previous section. Thus, the polymer chains are principally of the structure shown in the *Figure 1.7*. Although, an occasional head to head linkage can be expected.

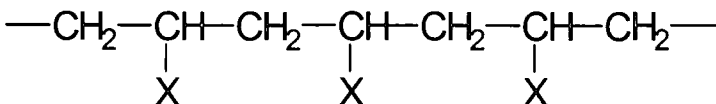


Figure 1.7 Common head-tail structure of the main chain

The time required for each monomer addition is typically of the order of a millisecond, thus several thousand additions can take place within a few seconds.

1.7.3 Termination

In this stage, growth of the polymer chain is terminated. The two most common mechanism of termination involve bimolecular reaction of growing polymer chains. *Combination* involves the coupling together of two growing chains to form a single polymer molecule.

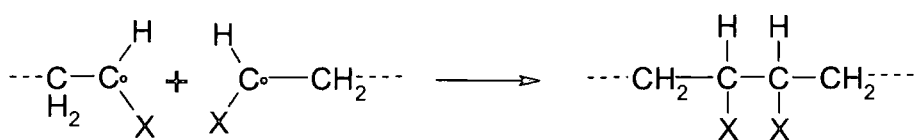


Figure 1.8 Termination by combination

This results in a head-to-head linkage. Alternatively, a hydrogen atom can be abstracted from one growing chain by another in a reaction known as *disproportionation*.

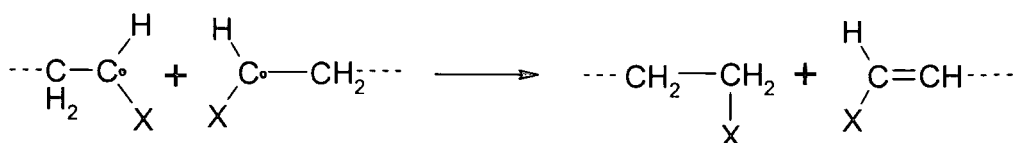


Figure 1.9 Disproportionation termination

Thus two polymer molecules are formed, one with a saturated end-group and the other with an unsaturated end-group. Also the chains have initiator fragments at only one end whereas combination yields polymer molecules with initiator fragments at both ends. In general, both types of termination reaction take place but to different extents depending upon the monomer and the polymerisation conditions.

1.7.4 Stereochemistry and tacticity

The stereochemistry of the polymer can be complicated due to the fact that a substituted carbon atom of a monomer unit in a polymer chain may be chiral and therefore have a *d* or *l* configuration depending on the stereochemistry of addition. Two adjacent chiral centres are known as a diad, and two identical chiral centres give a meso diad and adjacent chiral centres of opposite chirality give a racemic diad.

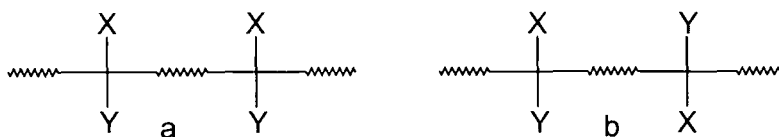


Figure 1.10 Meso diad (a) and racemic diad (b)

Isotactic polymer chains contain diads that are all meso whereas syndiotactic polymer chains contain all racemic diads. Polymers that contain a random (or statistical) sequence of meso and racemic diads are termed atactic.

Nuclear magnetic resonance (NMR) is widely used to study the microstructure of polymers. In sufficiently high resolution NMR, it is possible to detect chiral centre sequences up to heptads.

1.8 Design strategy and free-radical ring-opening polymerisation of vinylcyclopropanes

The polymer synthesis route used by Cochlin was successful.¹ It involved the 1,5-radical addition polymerisation of substituted vinyl cyclopropanes, Figure 1.11.

The main problem was that the polymers were, *vide supra*, moisture sensitive due to the cyano and ester groups and did not have a low enough T_g for practical proposes.

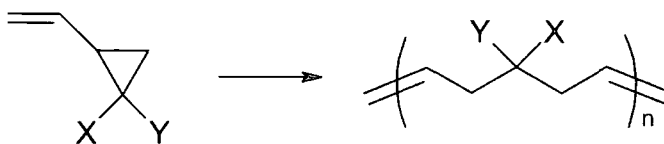


Figure 1.11 Free radical polymerisation of vinyl cyclopropanes

In the current work it was decided, as the first approach, to retain this general method but design X and Y to be highly polar and hydrophobic. It was considered that fluorine atoms and fluoroalkyl groups would be the most suitable for this

propose, and the design of vinyl cyclopropanes (VCPs) with fluorine or fluoroalkyl substitution was selected as the first target for monomer synthesis.

Free radical ring-opening polymerisation was chosen as the way to carry out the polymer synthesis. This type of free radical polymerisation has been widely studied, the first example was published in 1964 by Takahashi.¹⁷ He studied the bulk and solution polymerisation of 1,1-dichloro-2-vinylcyclopropane. Polymerisation failed to occur when ionic initiators were used but when benzoyl peroxide (BPO) or α, α' -azobisisobutyronitrile (AIBN) radical initiators were used a polymeric product was obtained. The purified polymer obtained from the bulk polymerisation of the monomer with BPO was found to be a white solid with a melting point of 70°C and an M_n of 7000. The chlorine content of the polymer was found to be comparable to that of the monomer suggesting that no dechlorination had occurred. Infrared (IR) spectroscopic analysis of the polymer showed that the absorptions due to the cyclopropyl ring (1200 cm^{-1}) had disappeared and absorptions due to a trans double bond (965 cm^{-1}) had appeared. Takahashi proposed the existence of both of the repeat unit structures in the product polymer shown in *Figure 1.12*. There are two kinds of ring opening, the predominant route involves 1,5-addition (*A*) and 1,4-addition is the minor route (*B*).

The following year, Takahashi published a second paper continuing his study of the radical polymerisation of vinylcyclopropanes,¹⁸ in it he described the polymerisation of vinylcyclopropane using AIBN and BPO to give low yields (~15%) of low molecular weight polymer. He studied the IR spectra obtained from the polymers and again he saw the disappearance of the bands corresponding to the cyclopropyl ring and the vinyl group, and the appearance of a band corresponding to the trans double bond.

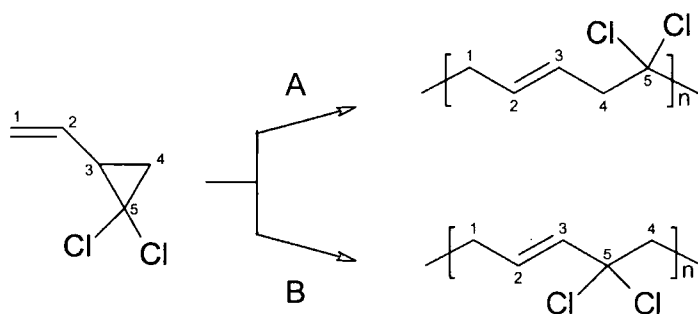


Figure 1.12 The 1,5 (route A) and 1,4(route B) addition types of polymerisation

He compared the spectrum with that obtained from the ring opening polymerisation of cyclopentene using classical ring opening metathesis initiators and saw that the polymers had essentially the same structure. This evidence supported the theory that vinylcyclopropanes underwent radical polymerisation via the mechanism shown in Figure 1.12.

At the same time, similar work was carried out in the USSR by Lishanskii.¹⁹ In 1965, he published his work concerning the polymerisation of VCPs with polar substituents on the ring. His results were only in partial agreement with those obtained by Takahashi. He confirmed the formation of a *trans* double bond as the main pathway, although he also found a small fraction of *cis* double bonds and, from IR spectroscopy, confirmed that the main unit present in this polymer was the 1,5-addition ring opening.

Also he suggested that the chlorine atoms would stabilise the radical formed in 1,5-addition making this more likely than the 1,4-addition. He observed as well that in some samples a unit obtained from 1,2 polymerisation, in which the cyclopropyl ring is retained, was present to an extent of up to 15%, see Figure 1.13.

Polymerisations were carried out in bulk at 80°C using BPO and AIBN. In the case of the isopropenylcyclopropane, he obtained polymers of low molecular weight ($M_n=1800$) in yields of up to 25%. 1-Methyl-1-vinylcyclopropane was not successfully polymerised yielding only a trace of polymer after 2 days reaction time.

From the analysis of the NMR spectra he concluded that the unchlorinated polymer consisted of about 80% 1,5-addition units. The remaining repeat units were thought to be cyclobutane structures, see *Figure 1.14*.

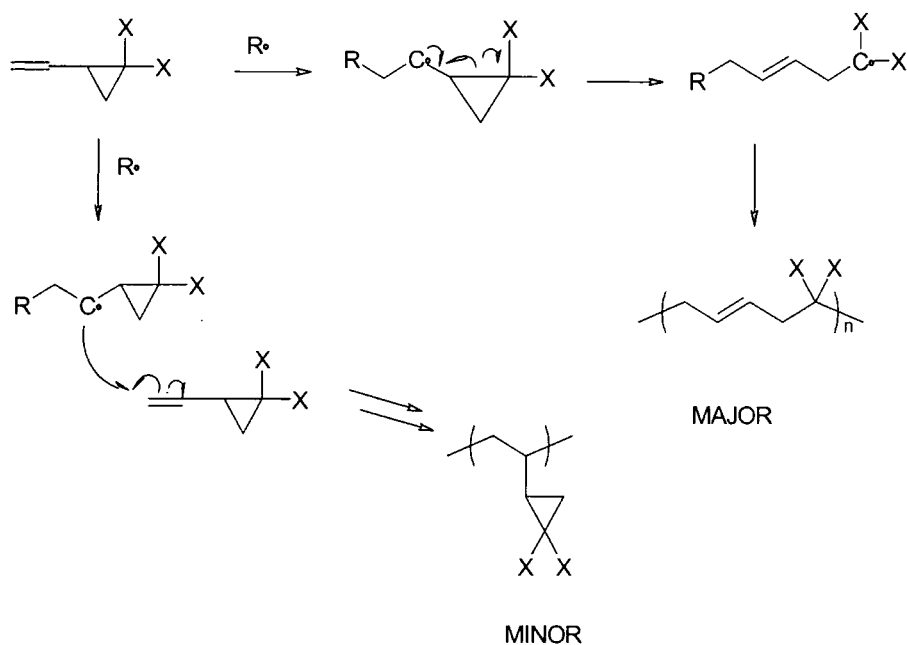


Figure 1.13 The 1,5 and 1,2 competitive polymerisation processes

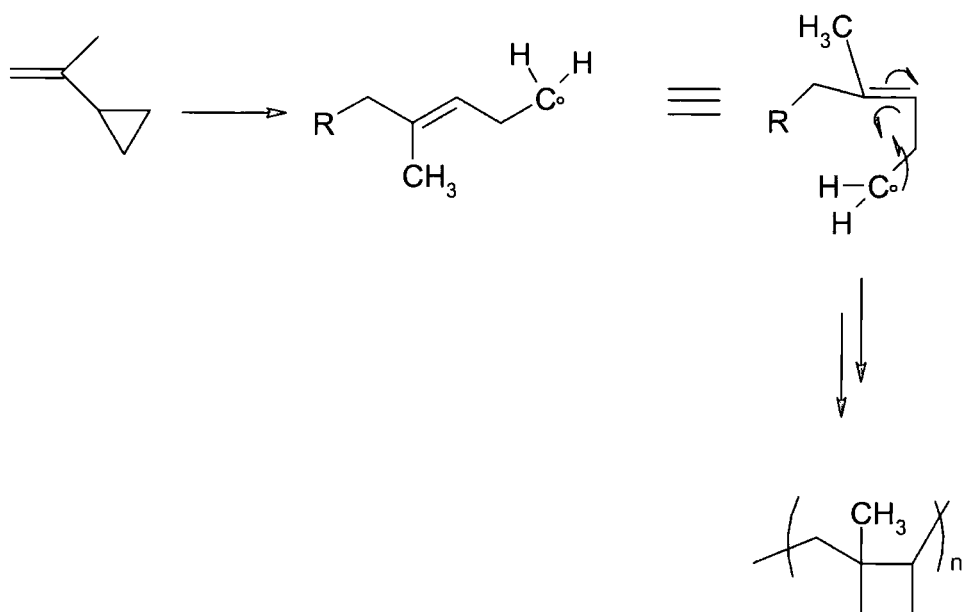


Figure 1.14. Competitive-side reaction in polymerisation of isopropenylcyclopropane

In 1968, Takahashi described the polymerisation of the VCPs shown below,²⁰
Figure 1.15.

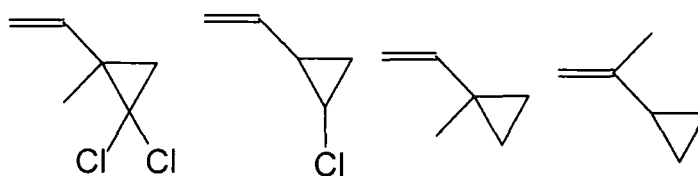


Figure 1.15 Monomers polymerised by Takahashi

Cyclobutane units were not detected in the chlorinated polymers due to the resonance stabilisation of the propagating chain end radical by the chlorine atoms.

Cho and Ahm published a facile polymerisation of ester and cyano substituted vinylcyclopropanes.^{21,22} They polymerised the monomers shown in *Figure 1.16*, at 55°C using AIBN.

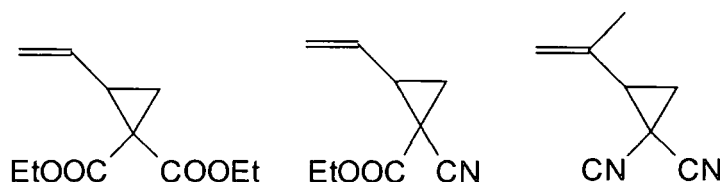


Figure 1.16 Monomers polymerised by Cho

For the first time high yields, up to 60%, of high molecular weight polymers were obtained. The authors studied NMR and IR spectra and concluded that the polymers were exclusively 1,5-addition products and all the double bonds were of *trans* configuration. The polymerisation of VCP derivatives bearing ester groups as well as polymerisation of a series of chlorinated monomers was studied in 1987 by Endo,²³ the yields were fairly low but high molecular weight polymers were obtained.

More recently Sanda²⁴ studied the polymerisation of the monomers shown in *Figure 1.17*. When R was a methyl group only *trans* double bonds were formed, as the steric repulsion of the two-methyl groups would be high in the *cis* isomer.

When R was hydrogen, a *cis: trans* ratio of 33:67 was observed. Sanda was surprised that cyclobutane units were formed when R was methyl as he expected the bulkiness to inhibit the ring formation.

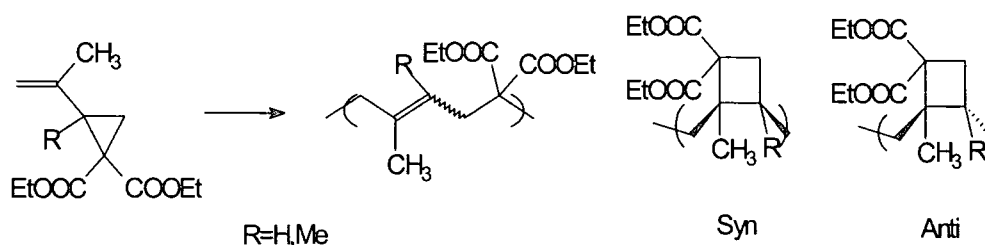


Figure 1.17 Summary of Sanda's work, ref 24

More recently, many studies have been reported concerning the polymerisations of vinylcyclopropanes with ester substituents, including the work done by Dr. Rachel Cochlin.¹

The first experimental part of this thesis is concerned with a description of the synthesis of new substituted vinyl cyclopropanes, their polymerisation and the characterisation of both monomer and polymer.

1.9 Polar polymers via ring-opening metathesis polymerisation

Another known methodology suitable for making the poly(1-pentenylene) backbone is the ring-opening metathesis polymerisation (ROMP) of cyclopentene as shown in Figure 1.18. When this produces a polymer with mainly *trans* configuration of the double bonds in the repeat units, a material with a T_g of -90 °C is obtained.

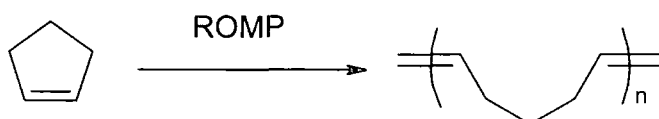


Figure 1.18. ROMP of cyclopentene

The Free-Energy for ring-opening polymerization of cyclopentene is only just negative and the reaction is very sensitive to conditions (e.g. temperature) and to substituents on the ring (i.e. steric effects). Yields are often low, although recently it has been reported that a new catalyst can ROMP cyclopentene monomer with a 60 % yield.²⁵ However, substitution on the cyclopentane ring with polar or other groups was considered, on the basis of earlier work in the Durham group, very unlikely to give successful ring-opening metathesis polymerisation.

By contrast, substituted bicyclo[2.2.1]hept-2-ene systems are very readily polymerised due to the steric strain in the unsaturated five-member ring. The design and synthesis of modified bicyclo[2.2.1]hept-2-ene systems is easy via Diels-Alder chemistry and their ROMP would give the substituted poly(1,3-cyclopentenylvinylidene)s, as shown in *Figure 1.19*. The unsubstituted hydrocarbon polymer, polynorbornene, has a T_g of +37 °C. It is a material which can be heavily plasticised with hydrocarbon oils and has found applications in the automobile industry in the manufacture of vibration damping and sealing components.

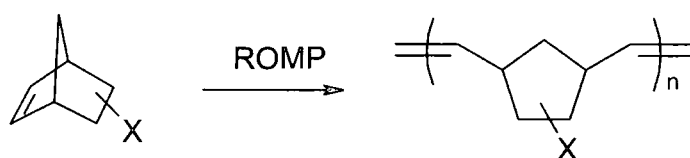


Figure 1.19 ROMP of bicyclo[2.2.1]hepta-2-enes

The inclusion of fluorine substituents on the cyclopentane rings of the general structure shown in *Figure 1.19* tends to raise the T_g to values which vary, depending on the nature and number of fluorine atoms and fluorinated groups attached, from +70 to +180 °C.²⁶ Hydrogenation of the double bonds, which would increase the flexibility in the polymer backbone by replacing the rigid double bonds by freely rotating C-C single bonds, and/or copolymerisation of the monomer with a flexible unit such as cyclopentene, were options considered in order to decrease the T_g . However, the route involving copolymerisation with a nonfluorinated

monomer, would result in a structurally inhomogeneous material and a reduction in the number of polar units which are required for the electrostrictive effect.

1.9.1 Ring-opening metathesis polymerisation

Metathesis in olefin chemistry describes a bond reorganization reaction in which the total number and type of chemical bonds remain unchanged during the transformation of the initial alkenes into equimolar amounts of two new alkenes as shown in *Figure 1.20*. The process requires a catalyst, and the number of catalyst systems that initiate olefin metathesis is very large. Catalysts almost invariably contain a transition metal compound and are sometimes effective by themselves but often require the presence of a second compound (cocatalyst), and sometimes a third (promoter).

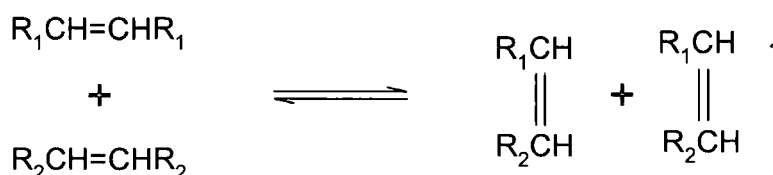


Figure 1.20 Olefin metathesis reorganization scheme

The first examples were reported by Banks and Baily in 1964,²⁷ since then the important field of olefin metathesis in chemistry has developed enormously. Olefin metathesis is valuable in the transformations of substrates such as substituted alkenes, dienes, polyenes and alkynes and has become a general tool in synthetic organic chemistry. Of great importance in respect of the work reported in this Thesis are the metathesis reactions of mono- and polycyclic alkenes, which give polymers, a process recognized initially in 1968.^{28,29}

Among the early applications of the olefin metathesis reaction are the improved utilization of refinery streams, synthesis of high octane fuel components,

production of intermediates for flame retardants, stabilizers, perfumes and novel polymers which may contain functional groups. More recently, with the introduction of the Grubbs' catalyst ($\text{RuCl}_2(\text{PR}_3)_2(=\text{CHR}')$), the ring closing metathesis reaction has become an important tool for natural product and pharmaceutical chemistry.

The 'classical' catalyst systems used in olefin metathesis display different efficiencies, operating conditions, and applicabilities. They may be divided into two categories, heterogeneous and homogeneous. Heterogeneous catalysts systems usually acquire metathesis activity only at high temperatures (100 to 400 °C) and are useful in a continuous flow type of process; they are employed for the metathesis of acyclic alkenes. Homogeneous catalysts, which bring about reactions under mild conditions, are applicable to both the metathesis of acyclic alkenes and cycloalkenes. For both of them the systems most used are derived from molybdenum, tungsten and ruthenium.

1.9.2 ROMP of cycloalkenes

The synthetic potential of the olefin metathesis reaction to polymer chemistry is enormous. The ring-opening polymerisation of cycloalkenes to linear polymers by metathesis provides an interesting class of polymers that differ from conventional polymers in that they maintain the unsaturation of the monomer, as shown for cyclopentene in *Figure 1.18*.

Mono-cyclic alkenes C4 to C12 with the exception of cyclohexene undergo ring-opening polymerisation to produce polyalkenylenes and depending upon the structure of the repeat unit and the double bond configuration these polymers may possess properties ranging from amorphous elastomers to crystalline materials. By careful choice of the catalyst system employed and adjustment of the reaction conditions the double bonds of the poly-alkenylenes can be exclusively or principally of the cis- or trans-geometry. Of particular potential industrial interest is poly(1-pentenylene), because of the availability of the cyclopentene monomer and the useful properties of the polymer. *Trans*-poly(1-pentenylene) is an

elastomeric material, which is competitive in properties with natural rubber (NR); $T_m = 20\text{ }^{\circ}\text{C}$ (NR = $30\text{ }^{\circ}\text{C}$); $T_g = -90\text{ }^{\circ}\text{C}$ ($-70\text{ }^{\circ}\text{C}$) but which has never been successfully commercialised.

Polycyclic alkenes such as bicyclo[2.2.1]hept-2-ene and cyclopentadiene dimer, readily undergo metathesis, although there are exceptions, for example, the fused-ring cyclopentenones shown in *Figure 1.21*.

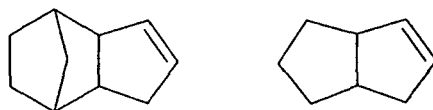


Figure 1.21 Fused rings not suitable for ROMP

Of commercial importance are the specialty polymers produced from bicyclo[2.2.1]hept-2-ene and cyclooctene. The polymer from the bicyclo[2.2.1]hept-2-ene, which gives poly(1,3-cyclopentylenevinylene) (polynorbornene), was the first polyalkylene to be commercially exploited under the trade name Norsorex and poly(1-octenylene) with 80 % *trans* vinylenes is a resilient elastomer marketed under the tradename Vestenamer 80/2.

1.9.3 Design strategy and ring-opening metathesis polymerisation of partially fluorinated norbornenes

Polycyclic monomers are generally more easily polymerised than their monocyclic alkene analogues due to the increased strain,³⁰ bicyclo[2.2.1]heptene (norbornene), was the first monomer shown to undergo metathesis ring-opening polymerisation.^{31,32} the monomer was also relatively cheaply obtained *via* the Diels-Alder reaction of ethylene and cyclopentadiene as it is shown in *Figure 1.22*. Using the same approach, many other bicyclo[2.2.1]heptene derivatives have been synthesized and investigated as monomers for ROMP.

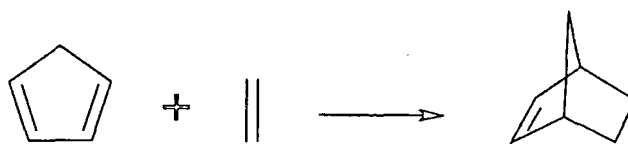


Figure 1.21 The Diels-Alder reaction

An example of a substituent, which is tolerated by the easily prepared conventional metathesis catalysts, is the fluorine group.³³ In this project it was aimed to reproduce the synthesis of partially fluorinated monomers, from the Diels-Alder reaction of fluorinated propenes and cyclopentadiene and carry out their polymerization. Subsequent hydrogenation of the double bonds in the primary product polymers and/or copolymerisation with cyclopentene, again followed by hydrogenation, would give a more flexible material suitable for electrostrictive studies, a generalized target monomer is shown in *Figure 1.23*.

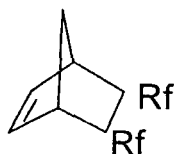


Figure 1.23 Target monomer

The second experimental part of the thesis is concern with the description of the synthesis and characterization of partially fluorinated polymers via ROMP.

Chapter 2

Attempted syntheses of potentially
electrostrictive polymers via radical
ring-opening polymerisation of
partially fluorinated
vinylcyclopropane monomers

2.1 Introduction

Previous work in the IRC at the University of Durham directed towards electrostrictive materials involved the synthesis of substituted vinyl cyclopropane (VCP) monomers incorporating carboxyl and/or cyano groups and their radical ring-opening polymerisation.¹ The synthesis route adopted in that work is summarised in *Figure 2.1*, where X and Y represent ester and/or cyano groups.

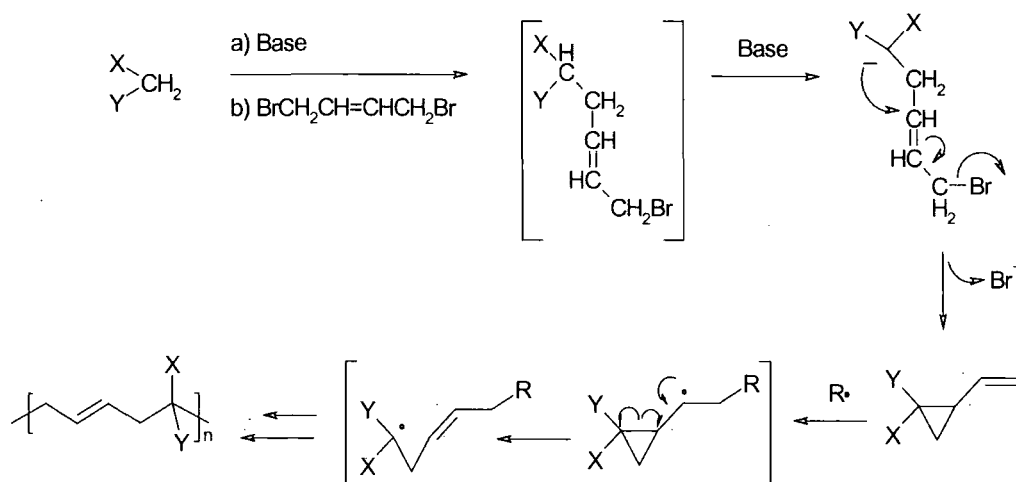


Figure 2.1 Earlier monomer synthesis and polymerisation route

The monomers contained n-alkyl side chains attached at the ester groups, which were able to induce internal plasticisation in the resulting polymers and for such materials T_g s well below room temperature were obtained. The dielectric analysis of the polymers produced by Cochlin displayed some electrostrictive behaviour, however the main disadvantage arose from their capacity to absorb moisture, which inhibited their potential for use.

In the new work reported here fluorine atoms were chosen as the most suitable substituents for our purposes due to the high polarity of C-F bonds and the hydrophobicity of fluoropolymers. The design and synthesis of vinyl cyclopropanes with fluorine substituents was the first target of the work. Radical ring-opening polymerisation (RROP) was selected as the way to carry out the polymer synthesis. The earlier route to the monomer, shown in

Figure 2.1, is not readily adaptable for the present work since difluoromethane is a low boiling point gas and with fluoroalkyl derivatives as starting materials elimination of fluoride ion from the intermediate carbanion is likely to defeat the objective. The first route considered was based on difluorocarbene addition to an alkene in order to give a difluorosubstituted cyclopropane ring. It was thought likely that the monomer should also incorporate an n-alkyl side chain to lower the T_g of the polymer by internal plasticisation. The initial target monomer is shown in generalised form in *Figure 2.2*.

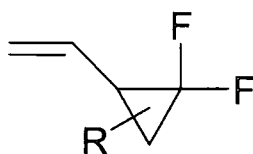


Figure 2.2 Initial target monomer

Two routes to fluorinated vinyl cyclopropanes were considered. The first one was developed by Dolbier et. al. in 1990 and was based on the zinc activated formation of difluorocarbene from dibromodifluoromethane, followed by addition to a double bond.³⁴ This appeared to be a convenient pathway to the desired monomer. The second route was the Buddrus difluorocarbene methodology, initially reported in 1967,³⁵ and referenced several times in the literature;³⁶⁻³⁷ it is based on the formation of the difluorocarbene from chlorodifluoromethane at high temperature (120 °C) in epichlorohydrin in the presence of tetrabutylammonium bromide and hydroquinone, followed by addition to a double bond. Although the Buddrus methodology required fairly drastic reaction conditions, the recovery and purification of the product appeared to be simpler than alternative routes. Seyferth's phenyl(trifluoromethyl)mercury³⁸ and Burton's triphenyl (bromodifluoromethylphosphonium) bromide³⁹ methodologies are effective difluorocarbene sources reported previously, however, they were not considered suitable for this work due to either the hazard of working with volatile mercury compounds, or the requirement for a multistep reagent synthesis. Another more complex difluorocarbene source than the previously reported ones, based on trimethylsilyl-2-fluorosulfonyl-2,2-difluoroacetate ($\text{FSO}_2\text{CF}_2\text{CO}_2\text{SiMe}_3$) as the

carbene source, was described by Dolbier et. al. in January 2000 during the course of this work.⁴⁰ This new reagent appears to give higher conversions for relatively deactivated alkenes; however, the earlier Dolbier Zn-activated debromination of dibromodifluoromethane and the Buddrus methodologies appeared to be more easily accessible and cheaper routes.

The only literature precedent to the present work refers to the ring-opening polymerisation of 1,1-difluoro-2-vinylcyclopropane, which is reported to undergo polymerisation mainly by ring opening via 1,5-addition, giving a symmetrical difluorosubstituted-pentenylene repeat unit in the polymer backbone (See *Figures 1.12, 2.3 and 2.4*). In that study however, no T_g or molecular weight data were reported for the polymer.

The RROP of 1,1-difluoro-2-vinylcyclopropane was repeated in this work. Although it was not expected that a material with a low enough T_g would be obtained, it was felt that the monomer synthesis and polymerisation would provide useful reference points and there were theoretical considerations (see below) which cast doubt on the validity of the structural assignments in the earlier report.

2.2 Synthesis and polymerisation of 1,1-difluoro-2-vinylcyclopropane

2.2 a) Introduction

The general mechanism reported for the RROP of VCP monomers is shown in *Figure 2.3*.^{1,20,37,41-44} Initial radical attack occurs on the least hindered carbon of the vinyl substituent to produce a cyclopropylcarbinyl radical, followed by a rearrangement to an allyl carbinyl radical, which then initiates chain growth. Most of the previously reported RROPs of disubstituted VCPs lead to polymers resulting from breaking of the C₁-C₂ bond in the intermediate cyclopropylcarbinyl radical, this is described as 1,5-addition polymerisation. This is the major pathway established for a large varieties of 1,1-disubstituted-2-vinylcyclopropanes, it is represented by the left-hand side of *Figure 2.3* and leads to polymers of structure A. This is attributed to the radical stabilising effect of the substituents and/or the electron-withdrawing groups' effect in increasing the radical polymerisability and the ring opening ability. The highest conversions and molecular weights are reported for monomers containing cyano or carboxyl substituents on the cyclopropane ring due to their capacity to stabilise the propagating radical.

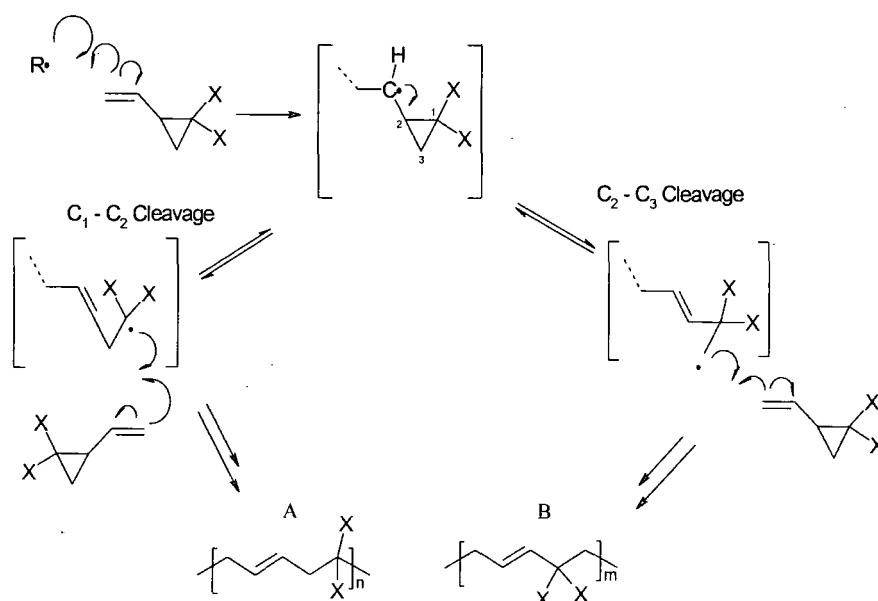


Figure 2.3 General RROP mechanism of the disubstituted VCP monomers

Thus, it was claimed that when the polymerisation of 1,1-difluoro-2-vinylcyclopropane was carried out at room temperature the polymer structure derived from the C₁-C₂ cleavage leading to repeat unit A, *Figure 2.4*, was the major component (91±1 %) in the polymer backbone, and the structure derived from the C₂-C₃ cleavage, B in *Figure 2.4*, was the minor component (9±1 %) of the structure.

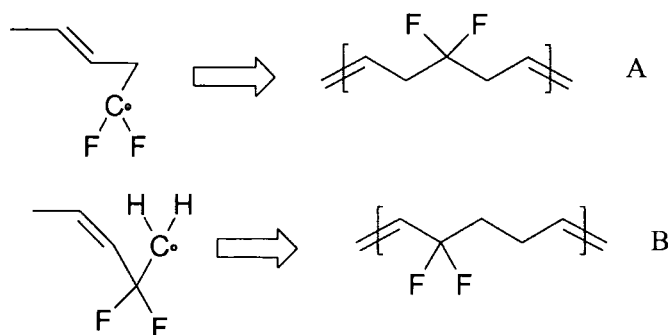


Figure 2.4 Scheme for the only two polymer structures considered in ref 37

Moreover, polymerisation at increased pressure resulted in an increased proportion of the structure derived from the C₂-C₃ cleavage up to an extent of 28 ±1 %, as well as some cross-linking. The identification of both structures in the polymer was based on an analysis of ¹⁹F nmr and IR spectra. The fluorine atoms in the two types of repeat unit structures shown in *Figure 2.4* have different environments, and two different signals were seen in the ¹⁹F nmr spectrum. In the ¹⁹F nmr spectrum shown in the earlier article,³⁷ which is consistent with the one obtained in the present work for the same polymer (See section 2.2 b), the two signals display unequal relative intensity. In the reported study the major signal at -94.1 ppm upfield with respect to CFC_l₃ was assigned to the fluorine atoms in the environment shown in *Figure 2.4* structure A, and the signal with lower intensity at -90.5 ppm was assigned to the minor structure B shown in *Figure 2.4*. These assignments were based on the assumption that the double bond reduces the screening of fluorine nuclei in the α-position, therefore the CF₂ pair from the structure B in *Figure 2.4* would appear downfield from the signal due to A. The assumptions concerning the screening effects of the double bond on difluoromethylene groups were based on the

observed ^{19}F nmr spectra of perfluorocyclopentene, which is an inappropriate model for this purpose and so these assignments can not be regarded as secure.

The analysis of the IR spectrum lead the Russian authors to postulate that the absence of bands at 1020 cm^{-1} (skeletal vibrations of a three-member ring) and 3090 cm^{-1} (bond stretching vibrations of CH_2 in the ring) observed in the spectrum of the monomer and the appearance of a strong band at 1680 cm^{-1} (bond-stretching vibrations of a double bond) indicated that only the structures A and B in *Figure 2.4* were present in the polymer backbone. Further, since $-\text{CH}=\text{CH}-$ stretching is usually relatively weak in symmetrically substituted double bonds they assumed that the structure A was not visible and that the band observed at 1680 cm^{-1} in the spectrum, which was relatively strong, involved a double bond vibration with a dipole moment change consistent with the minor isomer, i.e. structure B in *Figure 2.4*. This argument, depending on “relative strengths” of bands is also insecure in the absence of appropriate reference compounds.

In a related study carried out by Dolbier et. al.,⁴⁵ it is predicted that fluorine substitution in a cyclopropane ring produces a dramatic impact on the properties and behaviour with respect to radical ring opening. These predictions are based on a theoretical study using density functional theory calculations and revealed a lower energy barrier for the ring opening of the difluorocyclopropylcarbiny radical via $\text{C}_2\text{-C}_3$ cleavage, than for the $\text{C}_1\text{-C}_2$ ring-opening, i.e. the right hand side of the scheme shown in *Figure 2.3* will be favoured. The implication of this work is that the assignment of structure by the Russian workers may be wrong.

2.2 b) Results and discussions for the ring-opening polymerisation of 1,1-difluoro-2-vinylcyclopropane

2.2 b) (i) Monomer synthesis and characterisation

The monomer 1,1-difluoro-2-vinylcyclopropane was synthesized using the previously reported Buddrus methodology.³⁵ The scheme for the reaction is shown in *Figure 2.5*.

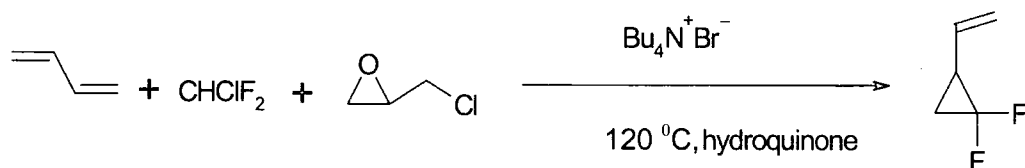


Figure 2.5 Synthesis of 1,1-difluoro-2-vinylcyclopropane

A colourless liquid product was obtained in 30 % yield with purity above 99 % as assessed by capillary gas chromatography; see section 2.7 for experimental details. Although this compound has been known since 1967 the detailed nmr spectroscopic characterisation has not been reported. The ^1H nmr spectrum is shown in *Figure 2.6*, the shifts and integrations are entirely consistent with the assigned structure, and taken with the gas chromatography result demonstrate that the monomer is pure; although it is, of course, a racemic mixture.

The vinyl hydrogens are readily assigned on the basis of the values of the J_{HH}^3 coupling constants, respectively 10.0 Hz (*cis*) and 16.4 Hz (*trans*), and the very small ~ 1.2 Hz vicinal HH coupling. The cyclopropyl hydrogens all occur as complex multiplets and display non-first order splittings, however a COSY spectrum (see Appendix AX1) identifies H_4 and we are only left with an unresolved ambiguity concerning H_5 and H_6 , see *Figure 2.7*.

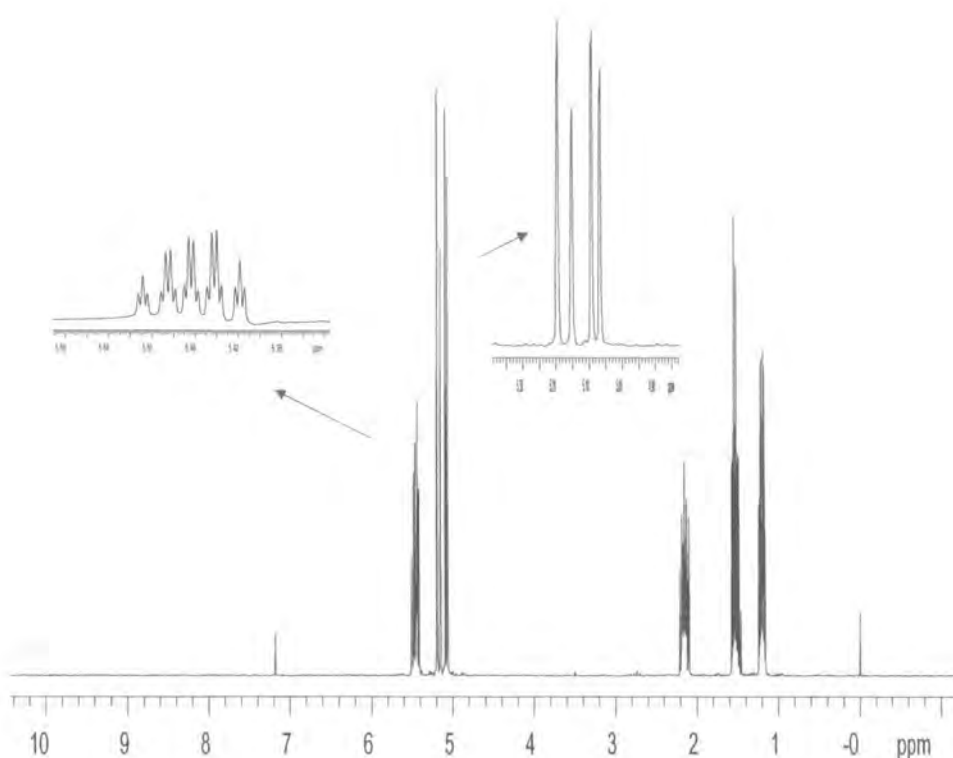


Figure 2.6 The ^1H nmr spectrum of 1,1-difluoro-2-vinylcyclopropane

In the ^{19}F nmr spectrum, (see Appendix AX2) the difluoromethylene shows a J_{FF} coupling of 156.8 Hz which is in expected range for a cyclopropyl CF_2 , one signal is further split into a triplet of doublets $J^3_{\text{HF}} = 12.79$ Hz and 3.0 Hz and the other into a doublet of doublets $J^3_{\text{HF}} = 12.79$ Hz and 4.51 Hz; in both signals the larger J_{HF} splitting has a value which is in the normal range for a three bond *syn* HF coupling in a cyclopropyl,⁴⁶ and the smaller signal is consistent with a three bond *anti* HF coupling. The signal at -141.61 ppm is assigned as F_7 on the basis of the 12.79 Hz triplet from H_4 and H_6 coupling and F_8 at -128.62 ppm on the basis of the 12.79 Hz doublet due to H_5 . The assigned coupling constants in Hz are shown in Figure 2.7.

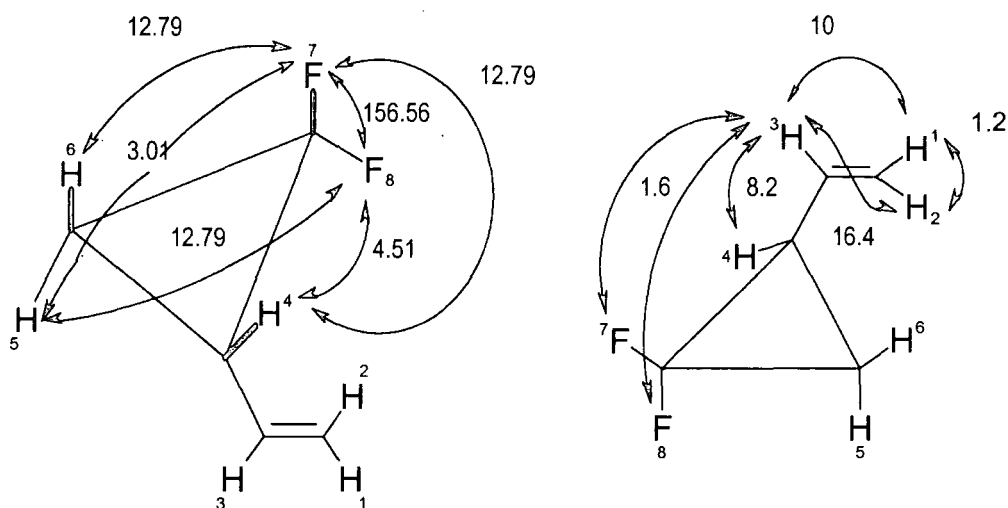


Figure 2.7 Observed coupling constants of 1,1-difluoro-2-vinylcyclopropane

In the ^{13}C nmr spectrum (see Appendix AX3) the CF_2 carbon appears as a doublet of doublets, $J^1_{\text{C-F}} = 287.6$ and 284.6 Hz, due to the slightly different fluorine environments. The $J^1_{\text{C-F}}$ values are in the normal range expected for the fluorosubstituted carbons of a cyclopropyl.⁴⁶ The two other carbons in the ring occur at lower field, the ring carbon substituted with the vinyl group at 26.7 ppm displays a doublet of doublets, $J^2_{\text{C-F}} = 12.3$ and 11.6 Hz, and the unsubstituted carbon appears at 12.7 ppm as a triplet, although it well may be an unresolved doublet of doublets, with a $J^2_{\text{C-F}} = 10.8$ Hz. The methine carbon of the vinyl group at 131.50 ppm displays a doublet of doublets with couplings $J^3_{\text{C-F}} = 4.6$ and 1.5 Hz, and the methylene vinyl carbon is seen as a singlet at 117.6 ppm.

A possible rationalisation for the mechanism of the reaction is shown in Figure 2.8, where the carbene is generated from a carbanion intermediate.

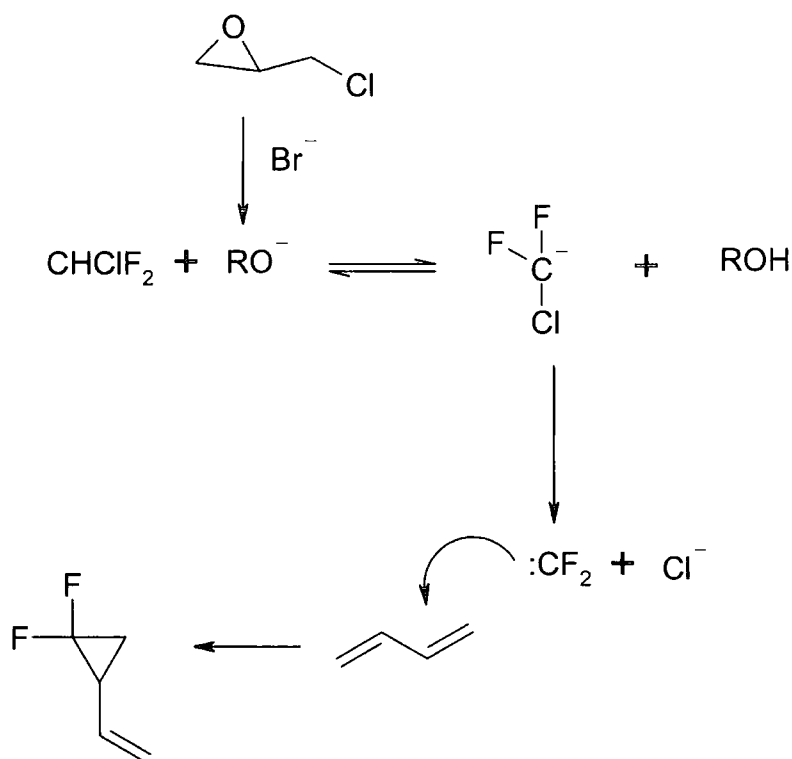


Figure 2.8 Hypothetical reaction mechanism

The epoxide, which is used in large excess, reacts with bromide to give an alkoxide, which is able to extract a proton from the chlorodifluoromethane. The resulting chlorinated anion loses a chloride ion to generate the carbene. The use of the epoxide as solvent and reagent ensures that the process occurs under non-aqueous conditions.

2.2 b) (ii) Polymerisation of 1,1-difluoro-2-vinylcyclopropane. Results and discussions

The polymerisation of 1,1-difluoro-2-vinylcyclopropane was carried out in neat monomer in an oxygen-free atmosphere with AIBN (0.75 mole %) as radical initiator. The colourless liquid was stirred at 50 °C for 5 days, becoming viscous by the end of the process. The product polymer was precipitated in cold methanol to give a white powder in low yield (15 %). The material was soluble in benzene.

The possible structures reported for the ring opening polymerisation of vinyl cyclopropanes applied to the 1,1-difluoro-2-vinylcyclopropane system are shown in *Figure 2.9*.²¹⁻²⁴

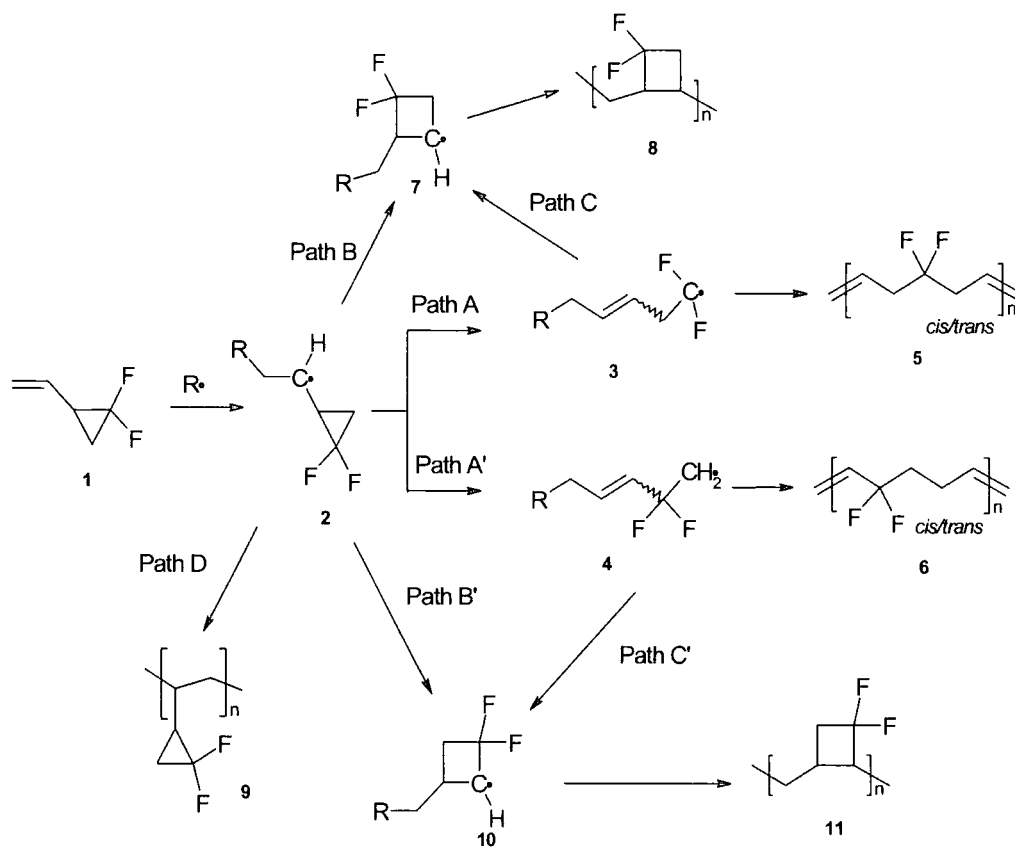
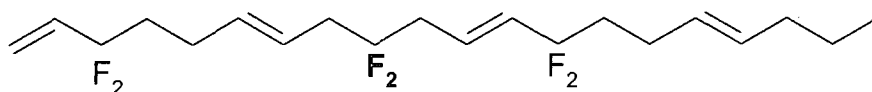


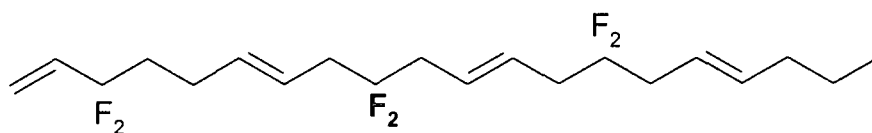
Figure 2.9 Possible structures for the product of RROP of 1,1-difluoro-2-vinylcyclopropane

In the ^{19}F nmr spectrum of the product, see *Figure 2.10*, signals with different relative intensities are observed, consistent with different structural features. The major signal (91%) is seen at -96.11 ppm with respect to CFCl_3 . This is a fairly broad signal in which a 12.4 Hz splitting can be seen and has a low intensity multiplet next to it at -96.36 ppm. The other signal with significant intensity occurs at -92.02 ppm (9%) and appears as a quartet with an observed coupling constant $J = 15.43$ Hz. This peak also has an adjacent low intensity multiplet at -91.8 ppm. Two other small peaks are seen at -87.7 and -88.2 ppm ($\sim 0.4\%$). As will emerge from the author's analysis of the ^{13}C and ^1H spectra of the polymer, the major structural feature (91%) is assigned to structure 6 (*Figure 2.4*) and the minor structural feature to structure 5. The

other low intensity peaks in the ^{19}F nmr spectrum might be indicative of minor contributions of structures such as 8, 9 and 11 in *Figure 2.9*; however the cyclopropyl unit (9) can be ruled out as it would be expected in the region -120 to -150 ppm and the cyclobutane units (8 and 11) also seem unlikely on the basis of shift.⁴⁶ The very small signals adjacent to the main signals are probably due to sequence effects in the distribution of repeat units. For an all *trans* vinylene polymer, the repeat units are either symmetrical (S, minor) or unsymmetrical (U, major). If the incorporation is statistical the most probable situation for the minor repeat unit is in the sequence USU, that is we assign the signal at -92.02 ppm to the structure below.



The occurrence of two of the minor S units together has a probability of 0.01 if the incorporation is statistical and the minor peak at -91.8 ppm is about 1/10 th of the intensity of the peak at -92.02 ppm and can be assigned to the USS sequence, below.



On this basis it would appear that the incorporation of the two different repeat units appears to be statistical. A similar analysis cannot be applied to the larger peak with its adjacent peak because of overlapped signals. The very small peaks at -87.7 and -88.2 ppm remain unassigned and may be structural defects arising from dehydrofluorination or chain ends. Thus, the current ^{19}F nmr spectrum of this polymer is in broad agreement with that reported in the earlier Russian work,³⁷ apart from a discrepancy of about 2 ppm in the chemical shift assignment and the extra low intensity signals identified in this work. The differences can be attributed to improvements in equipment during the last 30 years and different referencing procedures.

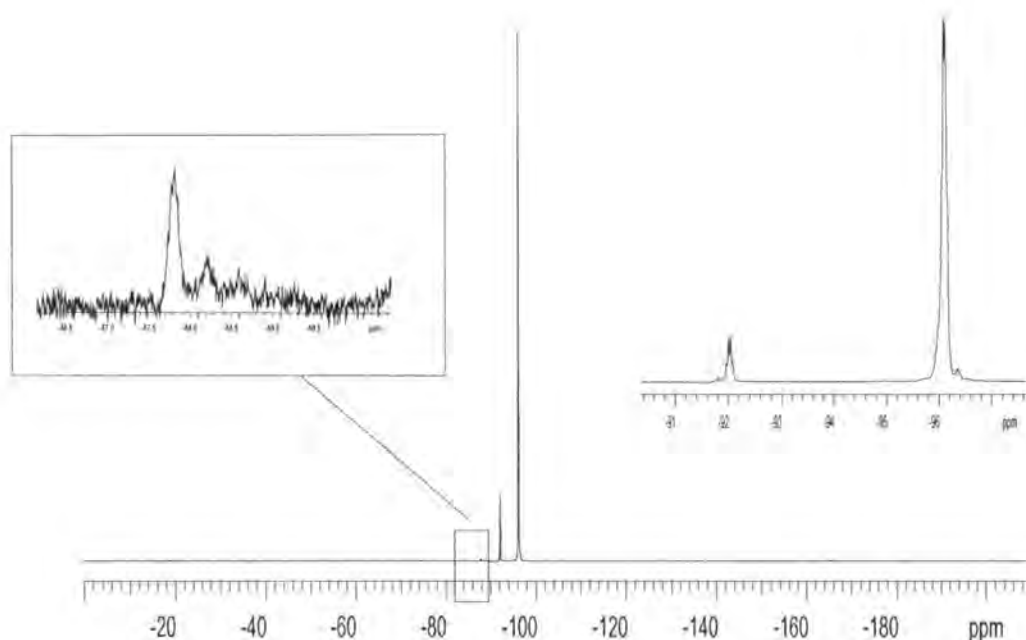


Figure 2.10 The ^{19}F nmr spectrum of poly(1,1-difluoro-2-vinylcyclopropane)

In the ^1H nmr spectrum shown in Figure 2.11 the bulk of the signal intensity is contained in four major signals, which are all fairly broad. These are two vinylic signals and two methylene signals and this is only consistent with structure (6) in Figure 2.9, being the major structural feature, where the unsymmetrical repeat unit generates these four different environments for the hydrogens. The two signals observed in the vinyl region have different intensity, and this suggests a possible overlapping with the signal of the vinylic hydrogens from the symmetrical structure (5) shown in Figure 2.9. The signal at 5.2 ppm possesses a higher relative intensity, the difference in intensity between these vinylic signals leads to a major:minor structural composition ratio of 88:12 compared to the ratio 91:1 obtained from the analysis of the ^{19}F nmr spectrum, which is within the experimental error of the method. The smaller signal at 2.44 ppm, was assigned to the allylic protons in the symmetrical structure (5), but the overlapping with neighbouring signals does not allow an accurate integration. The narrow lines at ca 0.5 and 0.7 ppm are probably due to contaminants in the nmr solvent.

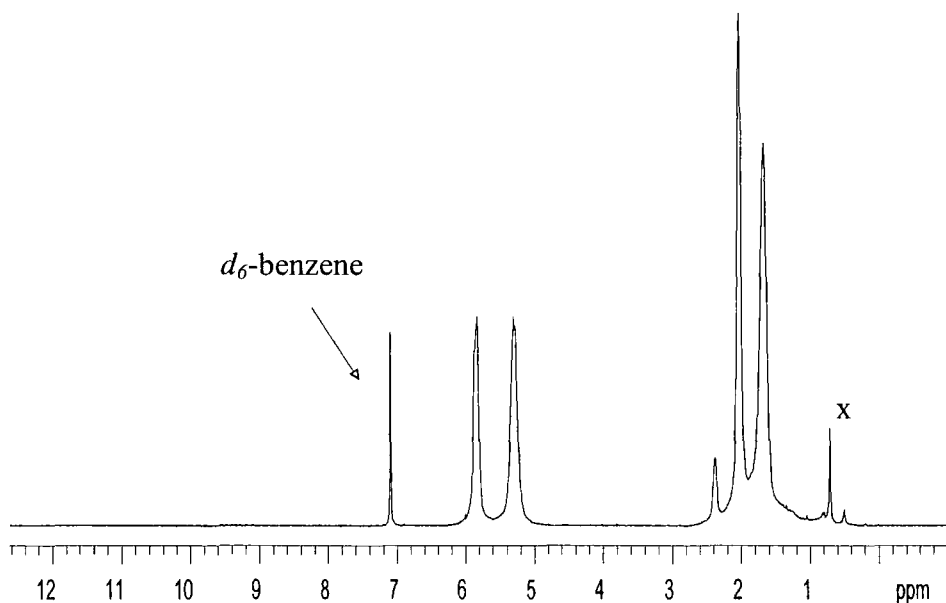


Figure 2.11 The ^1H nmr spectrum of poly(1,1-difluoro-2-vinylcyclopropane)

Analysis of the ^{13}C nmr spectrum was conclusive in assigning the major structural features of the polymer. In the spectrum, shown in Figures 2.12 and 2.13, four major and a minor signal are observed. The minor signal at 120.99 ppm is a triplet ($J_{\text{C-F}}^1 = 238.9$ Hz) arises from the CF_2 unit. Two major signals are observed in the vinyl region at 125.9 and 134.3 ppm, both are resolved into triplets and therefore coupled with the CF_2 , the different coupling constants, respectively $J_{\text{C-F}}^2 = 26.1$ Hz and $J_{\text{C-F}}^3 = 8.7$ Hz, are only consistent with the unsymmetrical repeat unit and the observed coupling constants are in the expected range.⁴⁶ The methylene region of the spectrum shows two major signals, which again is only consistent with an unsymmetrical repeat unit, one of them is a triplet $J_{\text{C-F}}^2 = 26.90$ Hz at 36.2 ppm and the other repeat unit is a singlet at 24.86 ppm. The signal of the methylene carbons of the symmetrical repeat unit (5) appears at 37.1 ppm as triplet with a $J_{\text{C-F}}^2 = 27.0$ Hz, the signal for the vinyl carbons in this minor structure is found as a broad multiplet at 136.22 ppm, and the signals of the CF_2 carbon appear as a very weak triplet at 122.1 ppm ($J_{\text{C-F}}^1 = 239$ Hz).

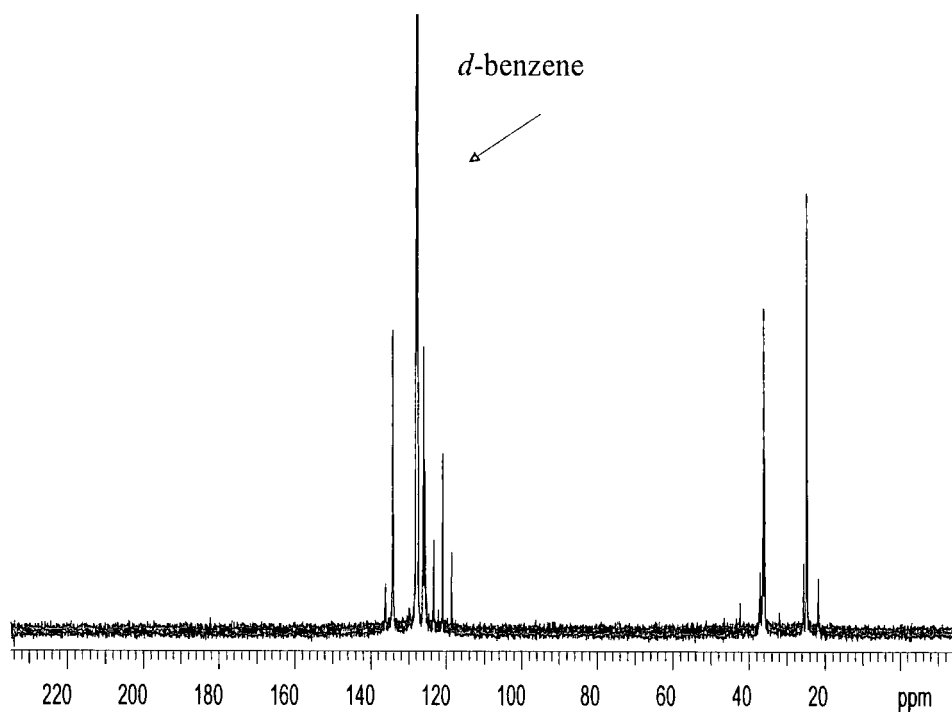


Figure 2.12 The ^{13}C nmr of poly(1,1-difluoro-2-vinylcyclopropane)

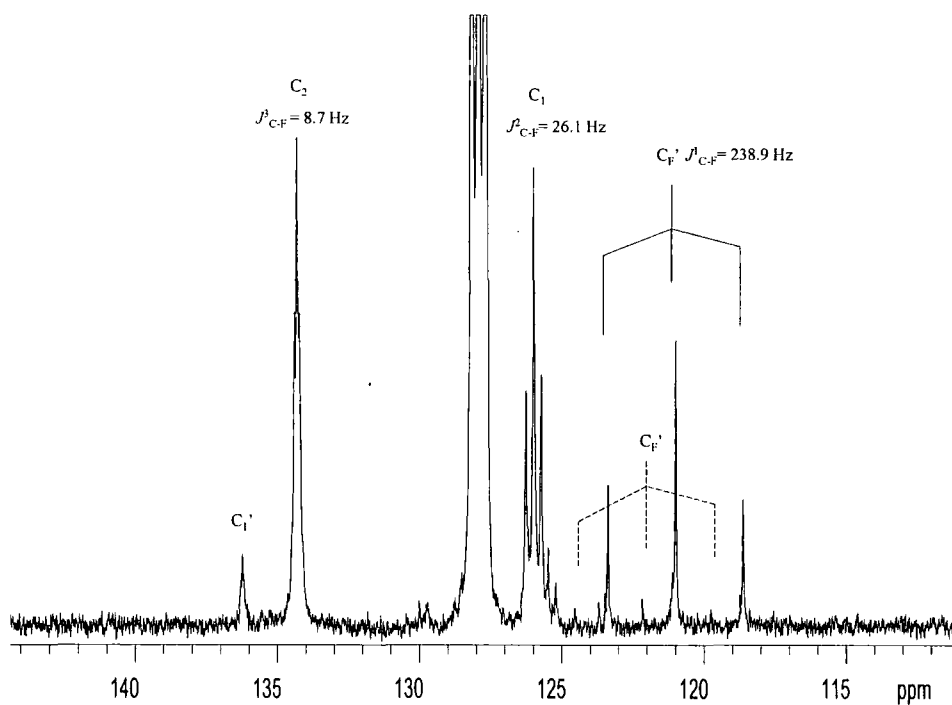
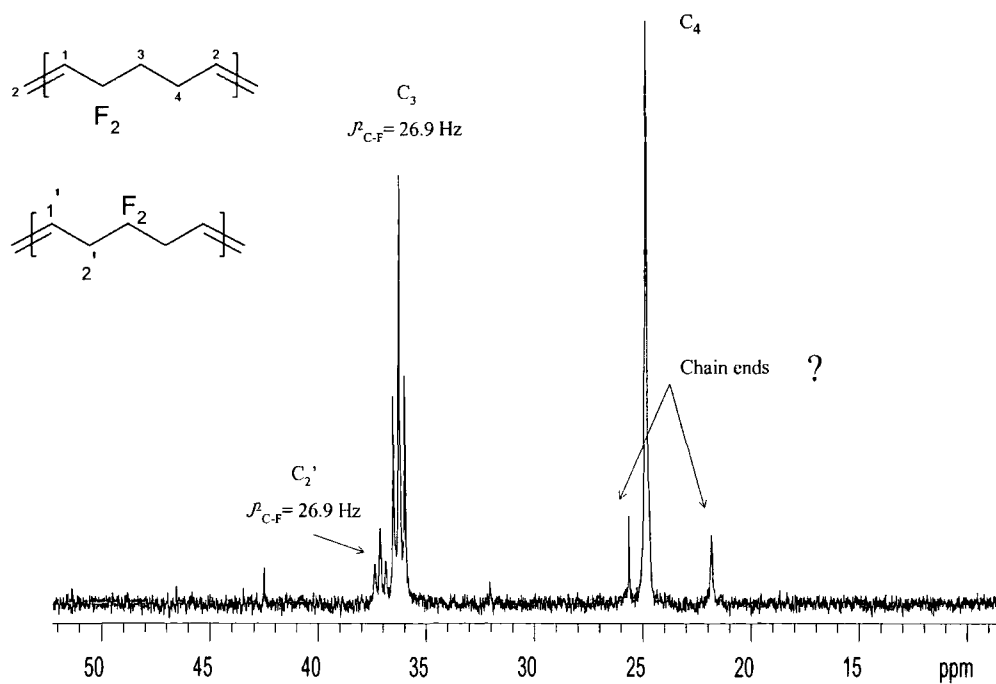


Figure 2.13 The expanded ^{13}C nmr spectrum of the unsaturated region (above) and vinyl region (below)

The relative simplicity of the nmr spectra implies that the vinylenes are all *cis* or *trans* but does not allow an assignment. The nature of the double bonds in the polymer structure was determined by IR spectroscopy (see Appendix AX4). The band at 971 cm^{-1} is characteristic of the out-of-plane bending mode for the C-H of *trans* double bonds, whereas the characteristic band for the *cis* double bonds, expected between $730\text{-}675\text{ cm}^{-1}$ does not appear. The absorption band for -CH=CH- stretching appears at 1684 cm^{-1} in agreement with earlier work,³⁷ in a relatively low intensity which is normal in *trans* double bonds. The C-F stretching vibration appears as a sharp strong band in the IR spectrum in the fingerprint region at 1384 cm^{-1} .

The polymer displays a T_g of $+55.6\text{ }^{\circ}\text{C}$ (DSC) and GPC gives $M_w = 59.600$, $M_n = 33.500$, with a $\text{PDI} = 1.78$, versus polystyrene calibration. This molecular weight obtained is higher than those from RROP of VCP monomers bearing chloride or bromide groups ($M_w \sim 1000$),²⁰ however, it is substantially lower than values reported for RROP of VCP monomers bearing ester or cyano groups ($M_w > 100,000$).²³ The TGA analysis indicated that less than 0.5 % of the mass is lost at $300\text{ }^{\circ}\text{C}$ (10°C per min, in N_2), which indicates a relatively high stability for this fluorinated polymer. The elemental analysis was consistent with the assigned structure.

2.2 c) Conclusions

The assignments reported in this thesis for the structure of poly(1,1-difluoro-2-vinylcyclopropane) were in agreement with the theoretical calculations reported by Dolbier et. al.,⁴⁵ and are in disagreement with the structure reported previously by the Russian authors.³⁷ This work establishes that the RROP of 1,1-difluoro-2-vinylcyclopropane proceeds mainly via cleavage of the C-C bond opposite the CF_2 unit in the ring to give mainly (ca 90%) the unsymmetrical repeat unit shown in *Figure 2.14*.

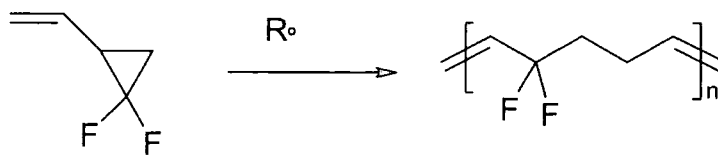


Figure 2.14 Main structure of the polymer in a 1,4-addition

The structure shown in *Figure 2.15* constitutes ca 10% of the polymer structure and detailed analysis of the ^{19}F nmr spectrum leads to the conclusion that the repeat units are statistically incorporated.

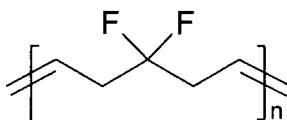


Figure 2.15 Minor structure in the polymer

The adopted route works and it is potentially useful, but the material obtained is not appropriate for the requirements of this project as the T_g for this material is above room temperature and consequently it does not meet the requirements for an electrostrictive elastomer. Therefore a synthetic modification to the monomer was needed and the approach selected was to incorporate an n-alkyl chain in order to induce the internal plasticisation.

2.3 Approaches to alkyl substituted and partially fluorinated poly(pentenylene)s

2.3 a) Introduction

In order to obtain a hydrophobic low T_g polymer the generalised route shown in *Figure 2.16*, which is an extension of that described in section 2.2 was chosen.

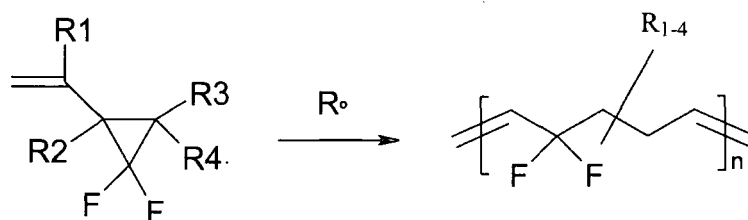
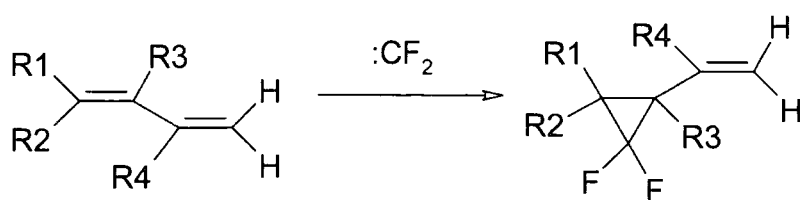


Figure 2.16 Target monomer and polymer

The approach was to consider the variation of R_1 to R_4 from H to alkyl to make alkyl substituted vinyl cyclopropane monomers. Dolbier's earlier work had established that alkyl substitution increases the yield in the cyclopropanation by addition of difluorocarbene.³⁴ Thus, the yield of the 1,1-difluorocyclopropyl products from addition to simple olefins increases in the order:

propene < isobutene < 2-methyl-2-butene < 2,3-dimethyl-2-butene.

Conversions of the highly alkylated alkenes reaching as high as 98 %, based on ^{19}F nmr analysis before purification, were reported; whereas, the mono substituted alkene gave a significantly lower conversion, of the order of 5-10 % before purification. Therefore, the use of alkyl substituted 1,3-butadiene units seemed attractive since it would allow the inclusion of an alkyl substituent which could act as an internal plasticising group and also enhance the reactivity towards carbene addition, as shown in *Figure 2.17*.



R_1 to R_4 being H, Me, n-alkyl

Figure 2.17 Hypothetical difluorocarbene addition to substituted butadiene substrates

Thus, in competition experiments with a molecule with two alkene groups, the difluorocarbene added predominantly to the more substituted double bond.³⁴ For the purposes of this work we aimed to make alkyl substituted 1,3-butadienes and then react the substituted double bonds with difluorocarbene or a fluoroalkyl carbene to give the required fluorinated vinyl cyclopropane monomer. This approach would allow the production of alkyl substituted partially fluorinated poly(pentenylene)s and the nature of the alkyl groups was expected to allow the tailoring of the glass transition temperature by internal plasticisation. The difluorocarbene methodology chosen was the one described by Dolbier,³⁴ as the Buddrus method³⁵ used in the previous section required the use of chlorodifluoromethane, the carbene source, whose production and commercialisation is discontinued in the EU and US due to its potential environmental hazard, and consequently its use as a reagent on any significant scale would require elaborate recovering and recycling procedures.

A possible alternative synthetic route, see *Figure 2.18* based on difluorocarbene addition to an α,β -unsaturated ketone or aldehyde, followed by Wittig-Horner methylenation of the carbonyl group was tried and rejected because the deactivating effect of the electronwithdrawing carbonyl group inhibited the difluorocarbene addition to the double bond.

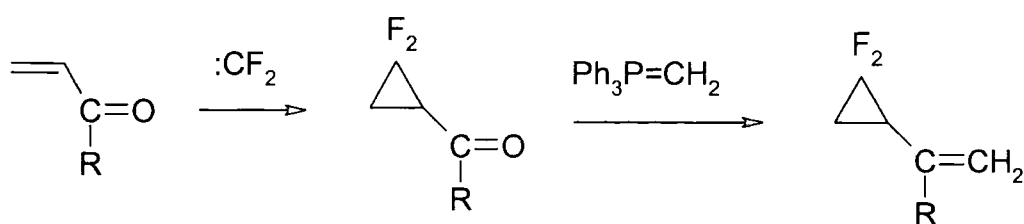


Figure 2.18 Unsuccessful alternative route

2.3 b) Synthesis and characterisation of alkyl substituted dienes

2.3 b) (i) Introduction

The synthetic routes chosen were selected on the basis of the accessibility of starting materials, the ease of synthesis and purification, and the estimation of whether the difluorocarbene would add at the double bond to give a useful monomer.

2.3 b) (ii) Synthesis of 4-methyl-1,3-undecadiene

The first substituted butadiene synthesis involved the application of the Wittig reaction, starting from the commercially available products shown in the Figure 2.19. It was thought that the substituted vinylene would display higher selectivity towards the difluorocarbene addition in the next step and that the polymer produced from the resultant monomer with a main chain carbon bearing both a methyl and a heptyl group would display a low T_g .

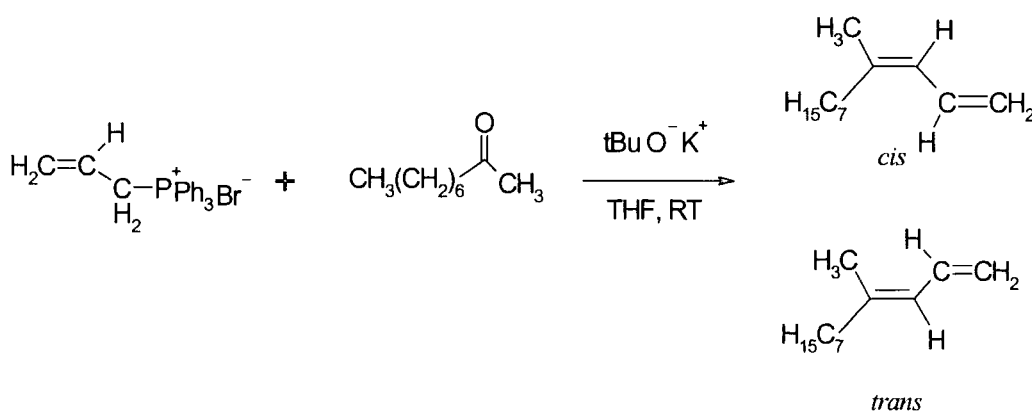


Figure 2.19 Proposed reaction scheme for substituted butadiene synthesis

This synthesis gave a colourless liquid product in very low yield (6.5%), which was resolved into two peaks of different retention time and different relative intensities by capillary gc, $t_R = 11.41$ min (rel. int. 38%) and $t_R = 11.66$ min (rel. int. 62 %) accounting for 98% of the material, see section 2.7 for experimental details. The shifts and integrations in the ^1H nmr spectrum (see Appendix AX5) are entirely consistent with the assigned structure. The hydrogens in the CH_2 near the double bond in the alkyl chain display two triplets with different intensities at 1.96 ppm (major signal) and 2.08 ppm (minor signal) with the same coupling $J_{\text{H-H}} = 8$ Hz, which is in the normal range expected.⁴⁶ It is known that these methylene hydrogens attached at a *cis* double bond appear at higher fields than their *trans* equivalents,⁴⁶ and based on this assumption the product was obtained as a 38:62 mixture of the *cis* and *trans* isomers respectively. The terminal vinyl hydrogens at 5 and 4.9 ppm also display two doublets of unequal intensity for each hydrogen due to overlapping signals from the *cis* and *trans* mixture of isomers, in the peak at 5 ppm the splitting was 17 Hz due to the J_{HH}^3 *trans* coupling with the methine hydrogen, while in the peak at 4.9 ppm the J_{HH}^3 *cis* coupling of 10.5 Hz was seen. In the ^{13}C nmr spectrum (see Appendix AX6) four major and four minor signals are observed in the vinyl region, they are displayed in pairs of unequal intensity and are attributed to the *trans* and *cis* isomers respectively. In the saturated carbon region of the ^{13}C nmr spectrum there are sets of overlapping peaks in a roughly 2:1 intensity ratio consistent with the assigned *cis:trans* isomer distribution. The gas chromatography-mass spectroscopy (gc-MS) record displayed two product peaks with different retention times t_R (minor intensity) 11.41 min and t_R (major intensity) 11.66 min and with the same molecular weight (M^+ 166), which were assigned to *cis* and *trans* structures respectively.

The low conversion in the Wittig reaction when ketones are involved is believed to be due to stereoelectronic inhibition effects. The formation of the intermediate betaine and oxaphosphetone species, in the general mechanism shown in Figure 2.20, is not favoured when long alkyl chains or bulky substituents are present in the carbonyl compound, and is favoured when stabilizing α -substitutes such as ester or cyano groups are present.⁴⁷

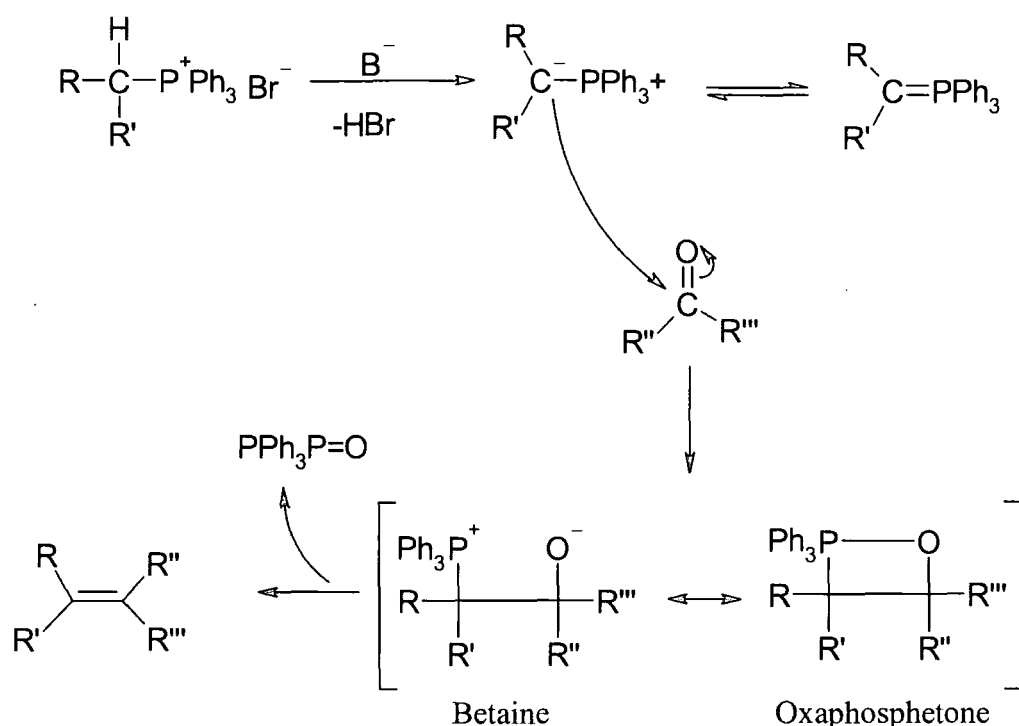


Figure 2.20 Wittig reaction mechanism

Due to the low yields obtained this synthetic route was abandoned and the difluorocarbene addition to 4-methyl-1,3-undecadiene was not investigated.

2.3 b) (iii) Synthesis of 3,4-dimethyl-1,3-tridecadiene

The scheme for the next reaction carried out using the commercially available 2-undecanone and vinyl methyl ketone is shown in Figure 2.21. This methodology, known as the McMurry coupling reaction, is based on the titanium induced coupling of two ketone substrates, and it was investigated because it was hoped that a tetrasubstituted alkene would increase the selectivity in the cyclopropanation reaction.³⁴ Thus, the addition of the difluorocarbene to the internal double bond in the next step would give a single product.

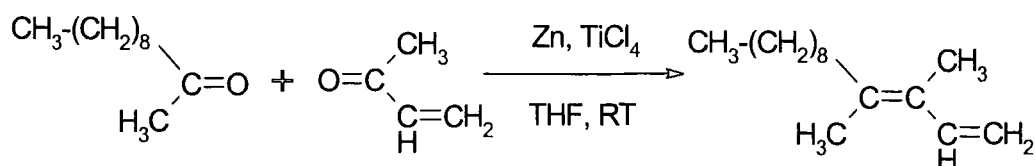


Figure 2.21 The McMurry coupling reaction between 2-undecanone and vinyl methyl ketone

In the recorded gc-MS chromatogram of the product obtained from the McMurry coupling, two well-resolved peaks were visible, and each peak was resolved into two peaks of very similar retention volume. These two products were the desired diene, 3,4-dimethyl-1,3-tridecadiene (M^+208) and the expected higher molecular weight symmetrical alkene product $\text{C}_{22}\text{H}_{44}$ (M^+308), see Figure 2.22. The 3,4-dimethyl-1,2,3-hexatriene which was expected to be formed by dimerisation of methyl vinyl ketone was apparently lost during the work-up. The resolution of both product peaks into two isomer peaks was ascribed to formation of *cis* and *trans* isomers in each case.

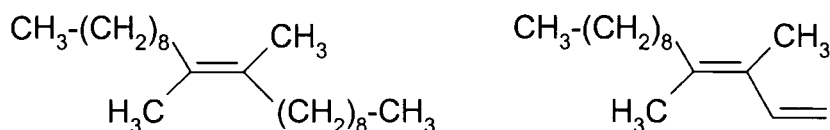


Figure 2.22 *trans*-Isomers of the products obtained from the McMurry coupling reaction

The 3,4-dimethyl-1,3-tridecadiene was obtained as a pure product by fractional vacuum distillation in a very low yield (3%) and assessed by capillary gc, where two peaks, arising from *cis* and *trans* isomers, were observed with $t_R = 14.90$ min and $t_R = 15.09$ min and with relative intensities of 1 and 1.1 respectively. See section 2.7 for experimental details. The vinyl hydrogens are readily assigned in the ^1H nmr spectrum (see Appendix AX7) on the basis of the values of the J_{HH} coupling constants, respectively $J^3_{\text{HH}} = 10.8$ Hz (*cis*) and $J^3_{\text{HH}} = 17.25$ Hz (*trans*), the vicinal HH coupling was not resolved in the spectrum but the terminal vinyl hydrogens which are *trans* to the substituted double bond occur at slightly different chemical shifts for the two isomers so that this peak appears as a triplet rather than a doublet. Two overlapping triplets

with similar intensity at approximately 2.1 ppm are assigned to the CH₂ hydrogens in the alkyl chain near the double bond in *cis* and *trans* isomers. The signals of the hydrogens in the CH₃ groups also overlap at 1.7 ppm, and the observation of more than two signals confirms the existence of a mixture of *cis* and *trans* internal double bonds in the product. The two other signals in the spectrum are assigned to the methylene hydrogens in the alkyl chain, the signal with high intensity at 1.2 ppm to the alkyl hydrogens and the signal resolved into a triplet at 0.8 ppm assigned to the hydrogens in the methyl end groups. The shifts and integrations of the signals in ¹H nmr spectrum are consistent with the assignment of the product as an approximately 50:50 mixture of *cis* and *trans* isomers. The ¹³C nmr spectrum (see Appendix AX8) of the product is rather complex as some carbons are resolved into two signals due to the mixture of *cis* and *trans* isomers whereas some are coincident. The vinyl carbons are resolved into eight signals, four for each isomer, and there are 16 signals in total in the saturated region of the spectrum, when a maximum of 22 (11 for each isomer) might be expected, although the similarity of the structures would lead to several coincident signals. In the gc-MS record the two peaks showed the molecular ion expected for the diene adduct (M⁺=208), and based on the previous analysis of the gc-MS record for 4-methyl-1,3-undecadiene, see section 2.3 b) (ii), where the *trans* isomer displays the longer retention time, it is suggested that the product is a 1:1.1 mixture of *cis* and *trans*-3,4-dimethyl-1,3-tridecadiene respectively.

The McMurry reaction has found extensive use in organic synthesis.⁴⁸⁻⁵⁶ Low valence titanium species are reported to induce coupling between ketones, the source of titanium is usually TiCl₃ or TiCl₄, and the Ti⁽⁰⁾ coupling reagent is generated electrochemically or by reaction with reducing agents. There is no general view as to which groups will or will not interfere with McMurry coupling, and only in the case of a diaryl ketones has it been demonstrated that cross coupling is favoured and occurs in acceptable yields (>50%). The relatively poor yields obtained in this work are in agreement with the Literature.⁵²

In the accepted reaction mechanism the coupling of the two-carbonyl compounds takes place in two steps.⁵³ The first is a carbon-carbon bond-forming step which is followed by deoxygenation. The first step is a pinacol

forming reaction where the reduced form of titanium, $\text{Ti}^{(0)}$, donates one electron to the ketones to generate the ketyl anion radicals that dimerise, *Figure 2.23*.⁵⁶

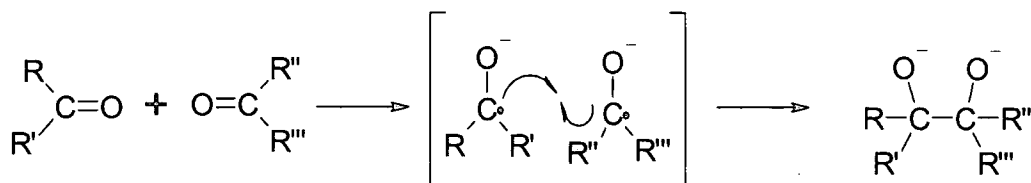


Figure 2.23 Dimerisation step

It is not really known how the second step, namely the deoxygenation step occurs. A hypothesis for the mechanism involves coordination of the diol to the surface of a heterogeneous titanium metal particle. Cleavage of the carbon-oxygen bonds then occurs, yielding the olefin and the oxide coated titanium surface, as shown in *Figure 2.24*. It has been shown that the two C-O bonds do not break at the same time and that a mixture of *cis*- and *trans*-alkenes is produced starting from a diol of known stereochemistry.⁵¹

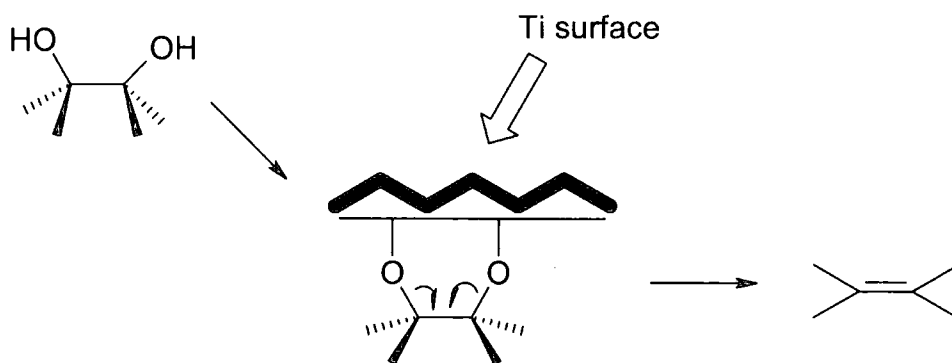


Figure 2.24 Hypothetical mechanism of the McMurry's reaction

The success of the McMurry reaction is highly dependent on the quantity of the $\text{Ti}^{(0)}$ inducing species created and the solvent used.⁵⁷

Zinc was used as the reducing agent in this work, although many other metals could be used, zinc is less hazardous and cheap, and it allowed its use in excess. The high cost of TiCl_3 also encouraged the use of TiCl_4 as a source of the $\text{Ti}^{(0)}$ species. In order to drive the reaction to the desired product an excess of the lower boiling point carbonyl compound was used due to easier separation

of it and its unwanted dimer. However, despite the variety of conditions investigated, less than 5% of the required diene product was obtained in all cases. Due to the low yields obtained and the complexity of handling titanates this synthetic route was abandoned and the difluorocarbene addition to 3,4-dimethyl-1,3-undecadiene was not investigated.

2.3 b) (iv) Synthesis of 1,3-undecadiene

This reaction was carried out next because it offered the possibility to obtain a suitable diene in an optimum yield, the scheme for the synthesis of 1,3-undecadiene, is shown in Figure 2.25. The starting materials, *trans*-2-decenal and methyl triphenylphosphonium bromide are commercially available, and the Horner-Wittig reactions of aldehydes are reported to proceed in good yield.⁴⁷

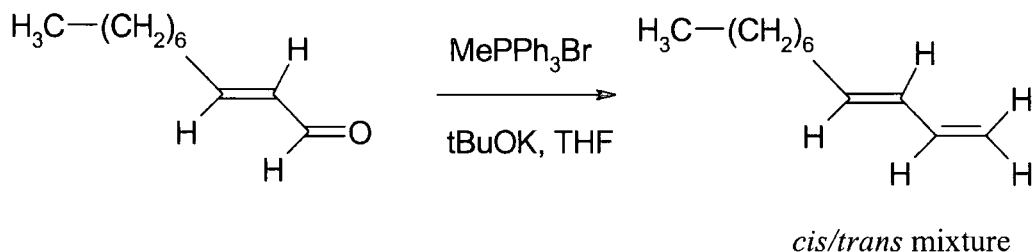


Figure 2.25 Synthesis of 1,3-undecadiene

A colourless liquid product was obtained in 80% yield with purity above 98 % as assessed by capillary gas chromatography; see section 2.7 for experimental details. Product analysis by ¹H and ¹³C nmr spectroscopy (see Appendix AX9 and AX10 and Experimental section), were consistent with the assigned structure. The nature of the internal double bond was determined by the relatively large coupling constant $J_{\text{HH}}^3 = 15.3$ Hz, in the range of typical *trans* double bonds.⁴⁶ Also in the ¹³C nmr spectrum there are only four signals for the vinyl carbons, which is consistent with only one double bond configuration, *trans* in this case.

Analysis of the IR spectrum (see Appendix AX11) confirms the assignment with a strong band at 1001 cm⁻¹ assigned to a conjugated *trans*

double bond, and the absence of the bands between 730-675 cm^{-1} the region characteristic of *cis* double bonds. Analysis by gc-MS shows only one peak with the correct molecular ion (M^+152).

The mechanism for the Wittig reaction was discussed earlier in relation to the reaction between 2-nonanone and allyltriphenylphosphonium bromide. The present reaction was more favoured because the aldehyde, *trans*-2-decenal, and a methyl ylide were used, which resulted in lower steric repulsion in the reaction intermediate.

2.3 b) (v) Attempted synthesis of 2-alkyl-1,3-butadiene

The synthesis of the alkyl substituted butadiene substrate shown in *Figure 2.26* was investigated.

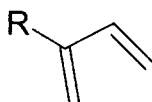


Figure 2.26 Butadiene substrate

This 2-alkyl substituted butadiene substrate was considered because both the products obtained from the difluorocarbene addition shown in *Figure 2.27* were considered to be suitable for polymerisation.

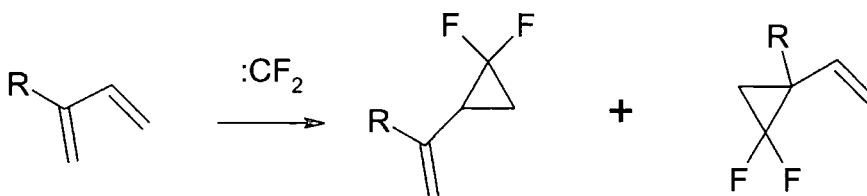


Figure 2.27 Difluorocarbene addition to the diene

Many routes have been reported for the synthesis of 2-substituted-1,3-dienes, *Figure 2.27*. Some of them involved a long sequence of reactions and low overall yields and were unattractive. For instance, the silicon based methodology, which involves the conversion of an aldehyde into α -silyl ketone by treatment with trimethylsilylmethylmagnesium chloride ($\text{Me}_3\text{SiCH}_2\text{MgCl}$) and rapid oxidation, followed by addition of vinylmagnesium

bromide at the carbonyl and elimination of trimethylsilylhydroxide.⁵⁸ The conversion of an olefin into an α,β -unsaturated bromomethylsulfone by addition of bromomethanesulfonylbromide ($\text{BrCH}_2\text{SO}_2\text{Br}$) followed by a base catalysed dehydrobromination and extrusion of SO_2 , was also considered see *Figure 2.28*.^{59,60}

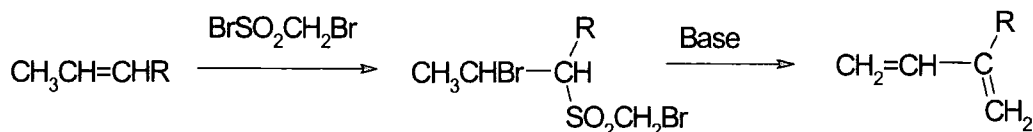


Figure 2.28 Possible route to 2-alkyl substituted 1,3-butadiene

The route selected was based on the synthesis of a suitable α -methylene alkyl ketone, followed by methylenation of the carbonyl group.^{47,61,62} The oxidation of a commercially available vinyl alcohol was the first step in the synthetic route investigated because it was an easy way to obtain an α -methylene ketone.

2.3 b) (vi) Synthesis of 1-octen-3-one

The synthesis scheme for the oxidation of the commercially available 1-octen-3-ol is shown in *Figure 2.29*. Most of the many accessible oxidizing agents for secondary alcohols use a transition metal in a high oxidation state, the Cr (VI) species being particularly effective, and many commercial reagents based on Cr (VI) are available.⁶³ Pyridinium dichromate (PDC) was chosen because of its low handling hazard reputation.

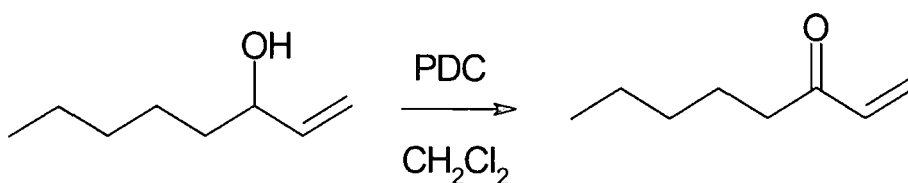


Figure 2.29 Synthesis of 1-octen-3-one

The product of the reaction was a colourless liquid obtained in 62 % yield with over 98 % purity as assessed by capillary gc. In the ^1H nmr spectrum (see

Appendix AX12) the shifts and integrations are entirely consistent with the assigned structure, the signal at 5.7 ppm is assigned to the vinyl hydrogen *trans* to the carbonyl, showing a *cis* coupling of $J_{\text{HH}}^3 = 9.8$ Hz and a vicinal HH coupling $J_{\text{HH}}^2 = 1.8$ Hz. The other vinyl hydrogen signals appear together as a non-first order multiplet. In the ^{13}C nmr spectrum (see Appendix AX13) the signal at 201.1 ppm is assigned to the C=O carbon, and the vinyl carbons appear at 136.7 ppm and 127.9 ppm in the spectrum, the 5 signals between 10 and 40 ppm are assigned to the 5 carbons of the alkyl chain. In the gc-MS record only one peak was observed ($t_{\text{R}} = 6.55$ min) and, although the molecular ion is not seen, the base peak at $m/z=55$ corresponds to $[\text{COCH}=\text{CH}_2]^+$. The IR spectrum (see Appendix AX14) of the product showed the disappearance of the strong O-H vibration above 3000 cm^{-1} and the appearance of a band at 1690 cm^{-1} assigned to the ketone C=O vibration mode.

2.3 b (vii) Attempted synthesis of 2-pentyl-1,3-butadiene

The next step was the methylenation of the ketone, the reaction is schematically shown in *Figure 2.30*, and was carried out in THF at room temperature to give a colourless liquid product after separation by column chromatography.

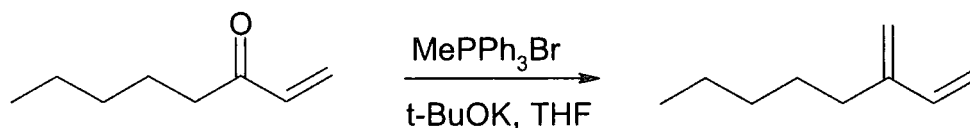


Figure 2.30 Methylenation step scheme

The analysis of the gc-MS record showed two peaks of different retention volume and intensities. The molecular weights obtained from the MS were 248 for each component of the product mixture, which suggested that the product of the reaction had dimerised via a Diels-Alder reaction, as shown in *Figure 2.31*.

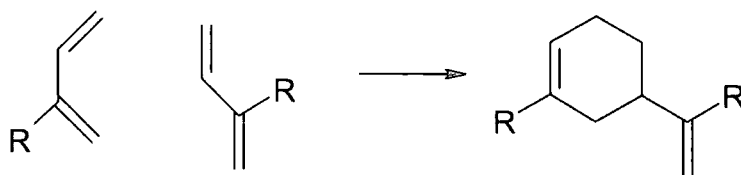


Figure 2.31 Hypothetical side reaction

This hypothesis was rejected because the [4+2] direct cycloaddition is inherently unlikely under room temperature conditions. An alternative hypothesis, is that the methyl vinyl ketone, which is a very good dienophile, scavenges the diene as it forms, the cycloaddition being faster than the methylenation. Methylenation on the carbonyl in the primary Diels-Alder adduct would then follow to give the substituted cyclohexene, as shown schematically in Figure 2.32.

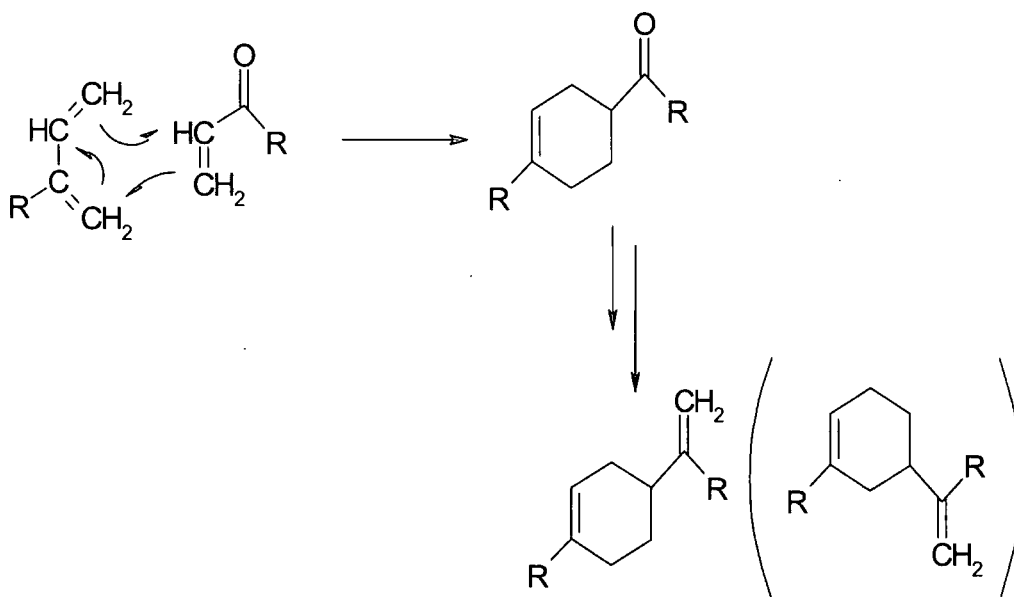


Figure 2.32 Hypothetical competitive reaction leading to undesired products

This result ruled out this route to alkyldienes and further analysis of the product of this reaction was not carried out.

As an attempt to avoid this competitive reaction, the experiment was carried out at lower temperatures (-10 to -15 $^{\circ}\text{C}$), nevertheless the same compounds were indicated on the gc-MS record, although a new compound in low concentration and shorter retention time was detected, which after gc-MS

analysis ($M^+=123$) was tentatively assigned to the desired diene ($M=124$), although it could not be conclusively identified and the yield was very low.

Although the Wittig reaction is the reaction of choice, many alternatives have been reported for the methylenation of carbonyls.⁶⁴⁻⁶⁸ Experiments were carried out in an attempt to accelerate the formation of the desired diene in competition with the possible cycloaddition reaction by using Oshima's methylenation,⁶⁸ the reaction is shown schematically in *Figure 2.33*.

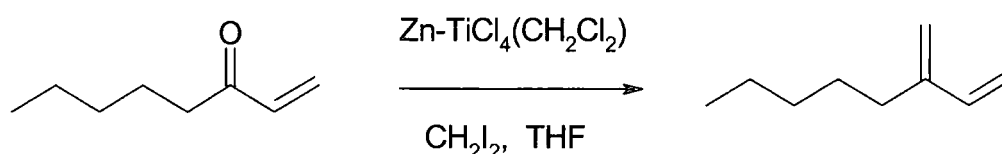


Figure 2.33 Oshima's methylenation synthesis scheme

The mechanism of the reaction has not been extensively studied although it is commonly assumed to be similar to the mechanism of the Tebbe reaction with a divalent form of a Zn-Ti complex as an intermediate.⁶⁹ This procedure also gave the mixture of the cyclo-adducts and the required 2-pentyl-1,3-butadiene was not detected. With hindsight this is not surprising since the reagent is a Lewis acid and the cyclo-adduct formation is catalyzed by Lewis acids.⁷⁰

2.3 b) (viii) Synthesis of 2-heptyl-1,3-butadiene

The methodologies based on organometallic chemistry deserved special attention in the author's search for a 2-alkyl-1,3-butadiene synthesis because of the high yields reported.⁷¹⁻⁷⁵ The main disadvantage of these methodologies is the expensive reagents required. However, the methodology reported by Renslo et. al., based on metallation of isoprene using a mixture of strong bases at low temperatures followed by reaction with an alkyl halide, offered a one step synthesis of the desired diene,⁷⁵ as shown schematically in *Figure 2.34*.

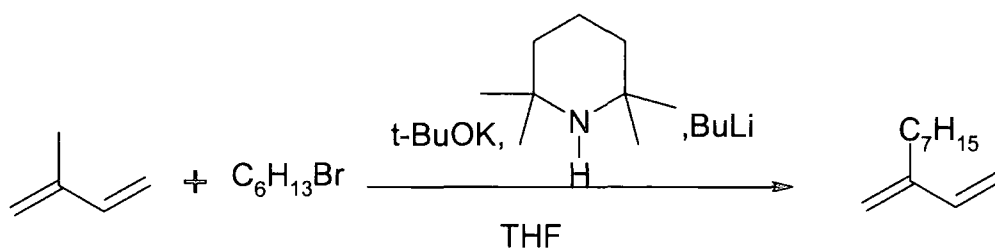


Figure 2.34 Scheme for the synthesis of 2-heptyl-1,3-butadiene

The product of the reaction, shown in Figure 2.34, was obtained as a colourless liquid in a 35 % yield and 99 % purity as assessed by capillary gas chromatography ($t_R = 9.64$ min), for experimental details see section 2.7. In the analysis of the ^1H nmr spectrum (see Appendix AX15) the shifts and integrations are entirely consistent with the assigned structure and taken with the gas chromatography result demonstrated that the product was pure. The hydrogens on the double bonds are readily assigned; the α,α substituted double bond signal appears at 4.90 ppm as a singlet, the signals of the vinyl group appear as doublets at 4.96 and 5.17 ppm and as doublet of doublets at 6.6 ppm, with coupling constants of $J^3_{\text{HH}}(\text{trans}) = 18$ Hz and $J^3_{\text{HH}}(\text{cis}) = 8.5$ Hz and a vicinal $J^2_{\text{HH}} \sim 0.5$ Hz partially resolved in the 4.96 and 5.17 ppm peaks. The ^{13}C nmr spectrum (see Appendix AX16) is consistent with the assigned structure with 4 signals in the vinyl and 7 in the saturated carbon region. In the IR spectrum (see Appendix AX17) bands are seen at 820 cm^{-1} , assigned to $\text{R}_2\text{C}=\text{CH}_2$, 950 cm^{-1} , assigned to $\text{RCH}=\text{CH}_2$, 1500 and 1590 cm^{-1} assigned to the diene stretching modes and are consistent with a 2-substituted diene.⁴⁶ The gc-MS detects one product only with the required molecular ion ($\text{M}^+ 152$).

The mechanism for this reaction involves a proton abstraction by base to create an anion, which acts as the nucleophile in a substitution on an alkyl bromide. The most acidic proton of the isoprene molecule is extracted by the strong bases, in this case a mixture of butyl lithium and potassium *tert*-butoxide, and the carbanion formed is stabilised by delocalisation, as shown in Figure 2.35.

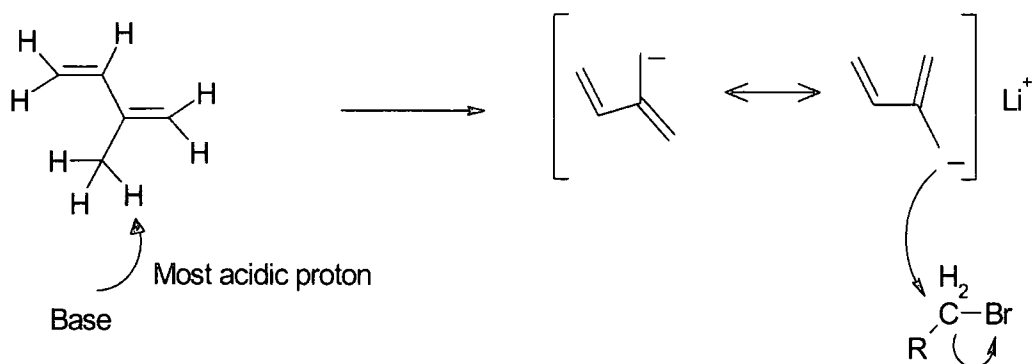


Figure 2.35 Scheme of mechanism for the metallation reaction

The isolation and purification process adopted was designed to prevent the possible oligomerisation of the diene, which required that high temperature conditions were avoided. The volatile products of the reaction were transferred from the crude product under vacuum (40°C , 4×10^{-2} mbar) and collected in a liquid nitrogen cooled trap. Analysis of the volatile fraction by gc-MS combined with ^1H and ^{13}C nmr spectroscopy identified it as a mixture of 2-heptyl-1,3-butadiene and hexylbromide. The isolation of the diene from this mixture was initially achieved by column chromatography (silica gel/hexane), however this process was considered very expensive in time and materials and unsuitable for large-scale reactions. A better procedure, based on static vacuum transfer of the lower boiling hexyl bromide monitored by ^1H nmr, proved successful, see experimental section 2.7.

2.4 Conversion of alkyl substituted buta-1,3-dienes to alkyl substituted vinyl difluorocyclopropane monomers

2.4 a) Introduction

As previously mentioned, the author aimed to prepare an alkyl substituted 1,1-difluoro-2-vinylcyclopropane suitable for RROP by an easy as possible route. The difluorocarbene addition experiments were carried out with the diene adducts shown below in *Figure 2.36*.

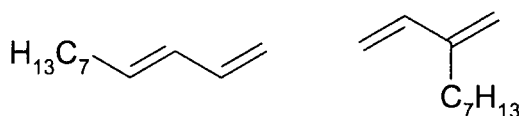


Figure 2.36 The diene adducts selected for the difluorocarbene addition

2.4 b) Difluorocarbene addition to *trans*-1,3-undecadiene

The scheme for the difluorocarbene addition to undeca-1,3-diene is shown in *Figure 2.37*, see the experimental section for details.

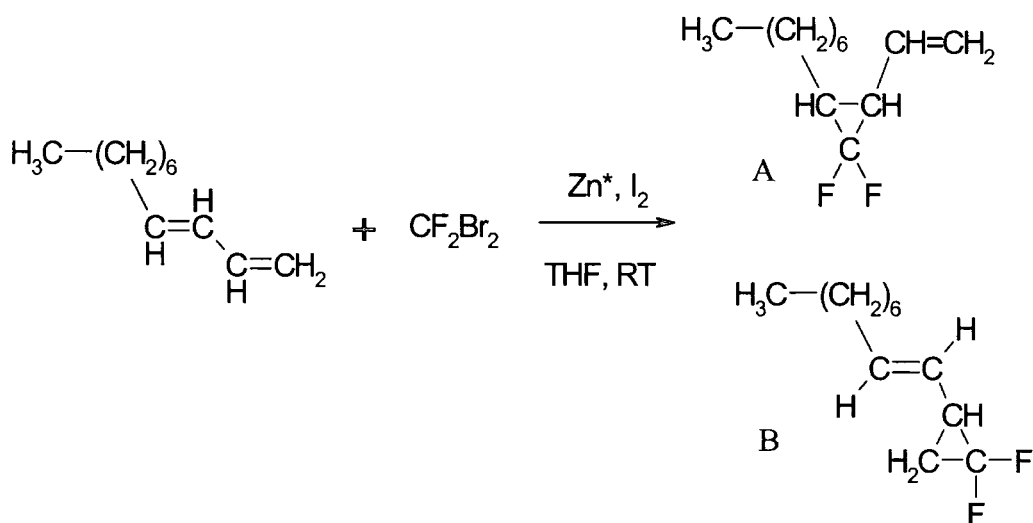


Figure 2.37 Scheme of addition of difluorocarbene to undeca-1,3-diene

The product obtained in a 20 % yield was a colourless liquid of 85% purity as assessed by capillary gc, which showed two peaks with relative

intensities of 6.9 % and 79.5 % and retention volumes of 11.15 and 12.24 min respectively.

In the ^{19}F nmr spectrum of the product, see *Figure 2.39* major ($J_{\text{FF}}^2 = 154.95$ Hz) and minor ($J_{\text{FF}}^2 = 155.24$ Hz) quartets are seen, which are in the range for cyclopropyl CF_2 units.

The multiplicity of the signals due to the coupling of each fluorine atom with the cyclopropyl hydrogens was used to assign the structures A or B in *Figure 2.37*. The doublet at -128.4 ppm of the major signal is further resolved into triplets with $J_{\text{HF}}^3 = 12.79$ Hz, and the doublet of the major signal at -141.8 ppm into doublets with $J_{\text{HF}}^3 = 12.79$ Hz. The doublets of the minor signals at -135.8 and -139.3 ppm are both resolved into doublets with $J_{\text{HF}}^3 = 13.73$ and 14.60 Hz respectively. The interpretation of these multiplicities is shown in *Figure 2.38* where large *syn* J_{HF}^3 couplings give rise to the observed multiplicities and the assignment given. The values are in agreement with the detailed analysis of the spectra of 1,1-difluoro-2-vinylcyclopropane given in section 2.2.

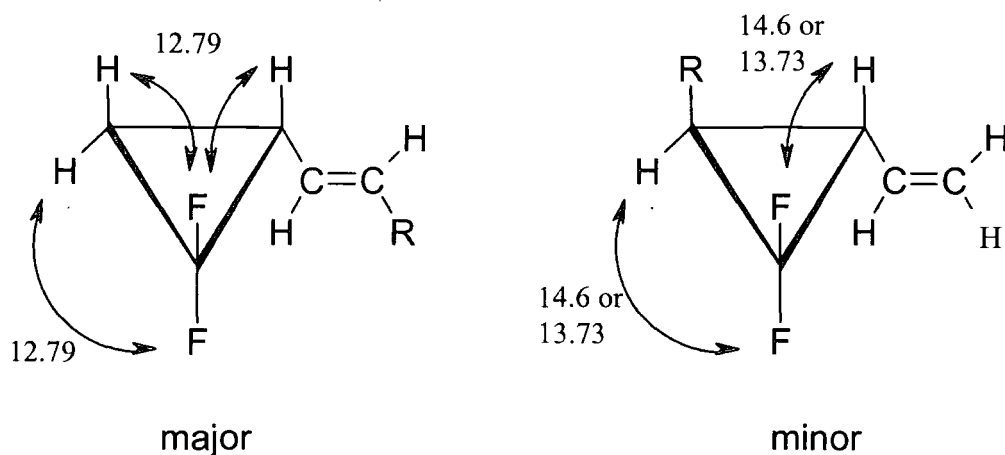


Figure 2.38 Rationalisation of observed multiplicities in the ^{19}F nmr spectrum of Compounds A and B, Figure 2.37

This result shows that, unexpectedly, the difluorocarbene addition takes place primarily at the unsubstituted double bond. It also demonstrates that in the minor product the initial *trans* conformation of the internal double bond in 1,3-undecadiene is preserved after the difluorocarbene addition.

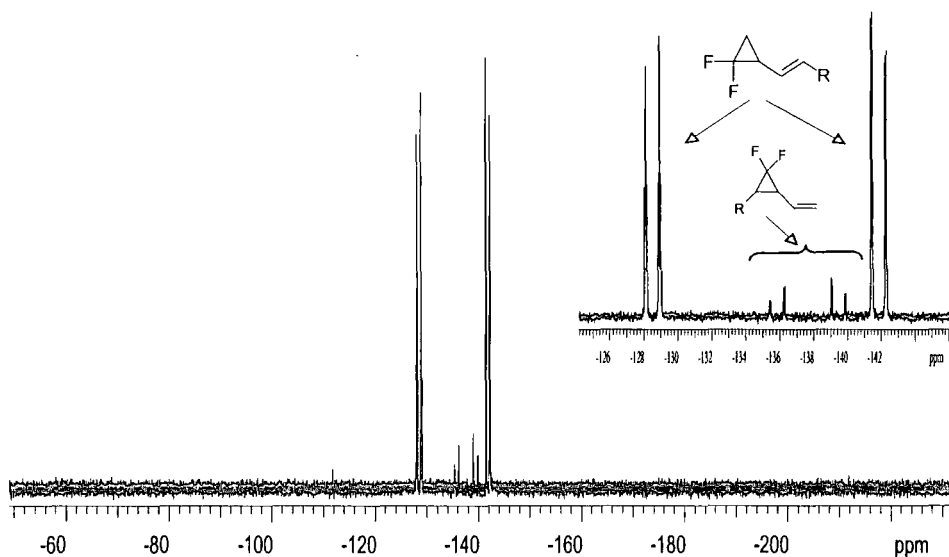


Figure 2.39 The ^{19}F nmr of the mixture of isomers from the difluorocarbene addition to *trans*-1,3-undecadiene

Integration of the ^{19}F nmr gives a 1:17 ratio for A:B, in Figure 2.37, which agrees approximately with the integration of the capillary gc peaks (1:12).

The hydrogens in the alkene region of the major isomer are readily assigned in the ^1H nmr spectrum shown in Figure 2.40. Two signals of equal intensity and different coupling patterns are seen in the vinyl region, which is consistent with the internal double bond of the major isomer being B in Figure 2.37. The signal at 5.58 ppm is a doublet of triplets and it is assigned to hydrogen attached at the double bond and vicinal with the alkyl chain, a coupling $\text{CH}=\text{CH}$ of 15.29 Hz indicates a *trans* double bond is present in the major isomer confirmed by the same large J_{HH}^3 coupling in the vinyl hydrogen at 5.1 ppm, which appears as a poorly resolved doublet of quartets (presumably because three couplings to nuclei in the cyclopropyl unit are fortuitously almost equivalent).

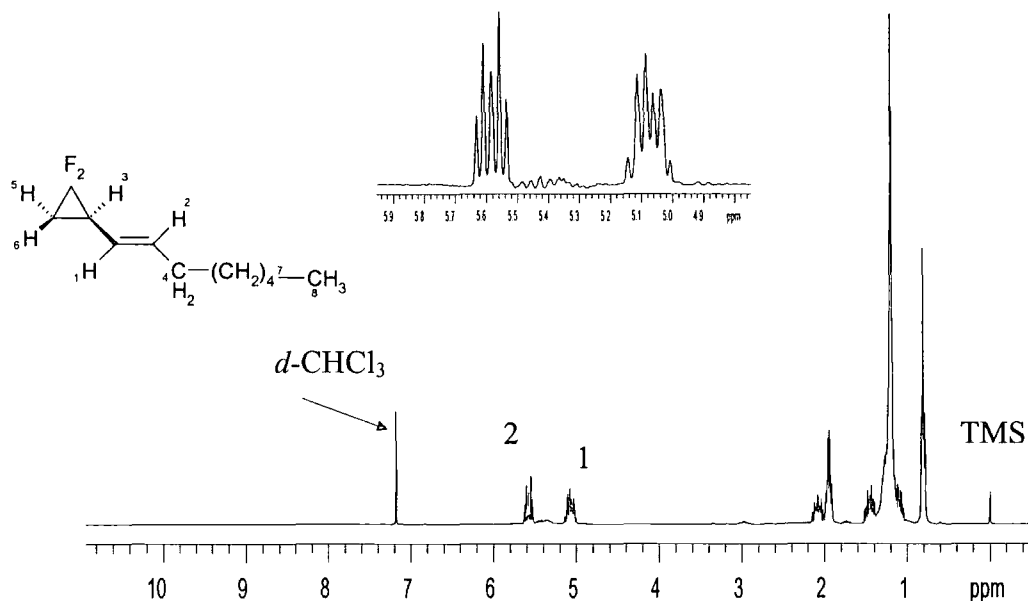


Figure 2.40 The ^1H nmr spectrum of the main isomer from the difluorocarbene addition to trans-1,3-undecadiene

Thus, based on the analysis of the gc and the ^{19}F nmr and ^1H nmr spectra it is demonstrated that the difluorocyclopropanation occurred primarily at the terminal monosubstituted double bond, in a 1,2-addition. The low proportion of the desired addition of the difluorocarbene at the internal double bond in the experiment with 1,3-undecadiene was a disappointment and made this synthetic route unattractive. Free-radical polymerisation experiments with the isolated mixture of both isomers were not successful. It was concluded that the monomer B (major component) in *Figure 2.37* was inhibited from undergoing radical polymerisation due to its highly hindered double bond.

2.4 c) Difluorocarbene addition to 2-heptyl-1,3-butadiene

The addition of the difluorocarbene to 2-heptyl-1,3-butadiene is shown schematically in *Figure 2.41*.

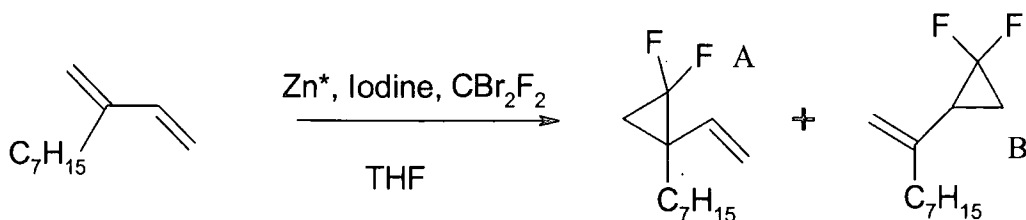


Figure 2.41 Difluorocarbene addition to 2-heptyl-1,3-butadiene

A colourless liquid product was obtained in 19 % yield with purity above 98 % as assessed by capillary gas chromatography, see Experimental section. A vacuum fractional distillation of a sample of 98 % pure material was carried out using Fisher-Spalthrohr™ Column (500 series) Distillation equipment to give a fraction of a mixture of two compounds, with the integrated gc areas of 99.51% and 0.39 %, the assignment of the minor component is discussed after that of the major one. See section 2.7 for experimental details.

The 1H nmr spectrum is shown in *Figure 2.42*, the shifts and integrations are entirely consistent with the structure A in *Figure 2.41*, and taken with the gas chromatography result demonstrate that the product is 99.5% pure; although it is, of course, a racemic mixture. The vinyl hydrogens are readily assigned on the basis of the values of the J^3_{HH} coupling constants, respectively 10.25 Hz (*cis*) and 17 Hz (*trans*), and the very small ~ 0.5 Hz vicinal HH coupling. The cyclopropyl hydrogens in A, *Figure 2.42*, both occur as complex multiplets at 1.1 ppm and 1.3 ppm and display non-first order splittings, with an unresolved ambiguity as to which signal is assigned to which hydrogen.

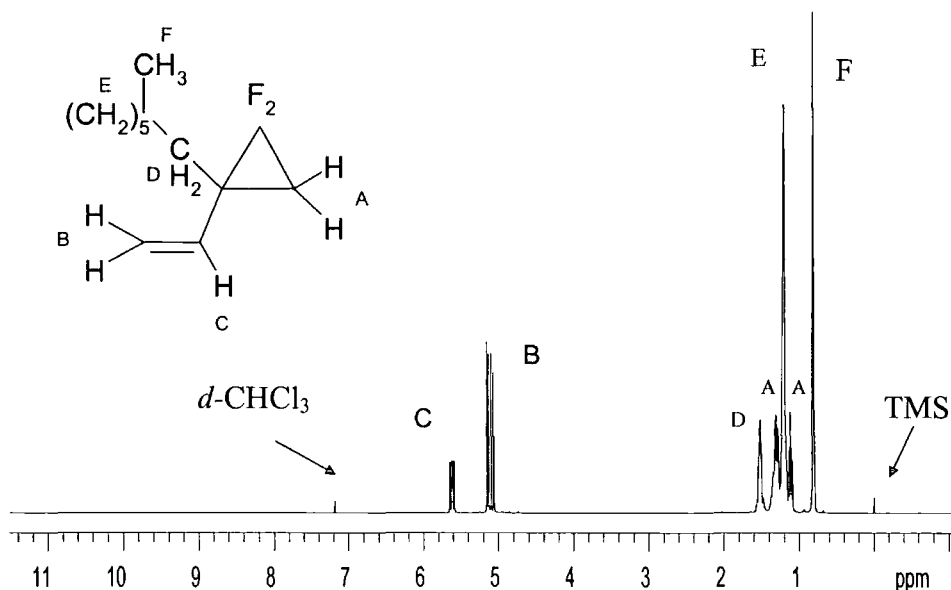


Figure 2.42 The ^1H nmr spectrum of 1,1-difluoro-2-heptyl-2-vinylcyclopropane

In the ^{19}F nmr spectrum the difluoromethylene shows a FF coupling constant $J_{\text{FF}} = 149.52$ Hz, which is in the expected range for a cyclopropyl CF_2 , one signal is further split into a doublet of doublets $J_{\text{HF}}^3 = 13.40$ and 4.23 Hz and the other into another doublet of doublets $J_{\text{HF}}^3 = 11.52$ Hz and 1.41 Hz; in both signals the larger J_{HF}^3 splitting has a value which is in the normal range for a three bond *syn* HF coupling in a cyclopropyl,⁴⁶ and the smaller signals are consistent with a three bond *anti* HF coupling. The signals appear at -135.73 ppm with the larger coupling constants and at -137.62 ppm with the smaller. It was suggested that the fluorine atom F₁ in Figure 2.43 is more shielded by the *trans* double bond than F₂, this hypothesis is confirmed by the analysis of 1,1-difluoro-2-vinylcyclopropane, see section 2.2, where the fluorine *trans* to the vinyl group, which is identified by the multiplicity of its signals (triplets $J_{\text{HF}}^3 = 12.79$ Hz), appears at lower frequency, and accordingly F₁ is assigned as shown in the ^{19}F nmr spectrum, Figure 2.43.

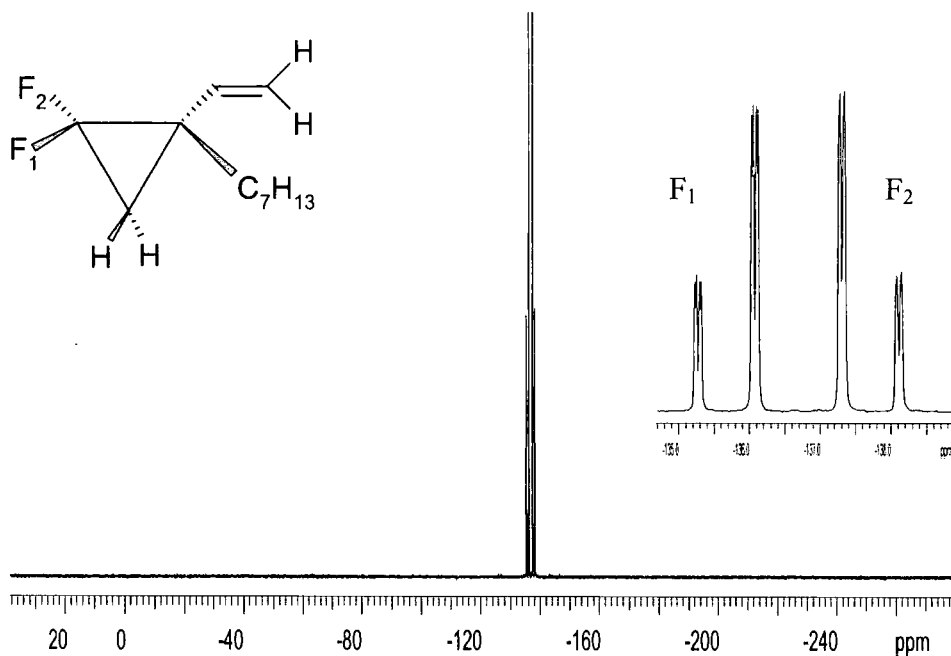


Figure 2.43 The ^{19}F nmr spectrum of 1,1-difluoro-2-heptyl-2-vinylcyclopropane with assignments for the signals

The assigned coupling constants in Hz are shown in Figure 2.44.

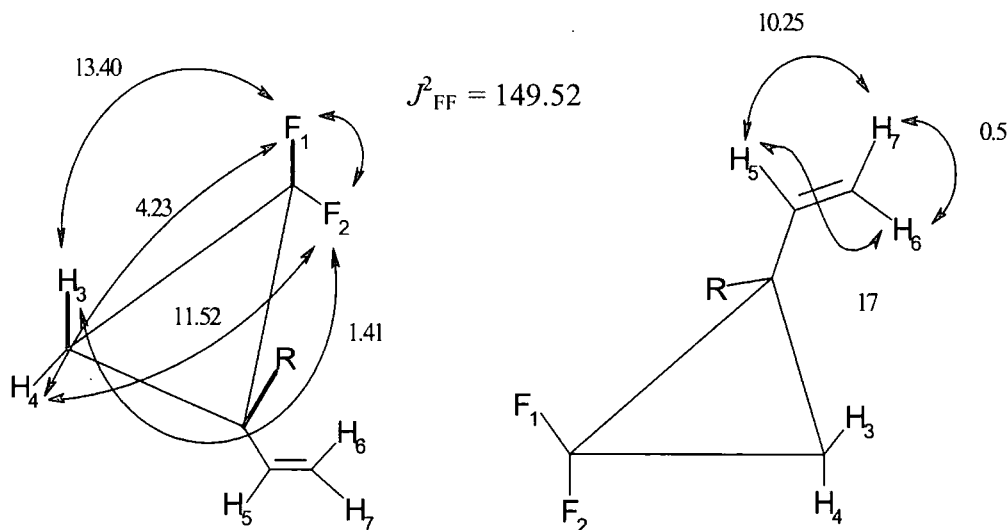


Figure 2.44 Observed coupling constants

In the ^{13}C nmr spectrum shown in Figure 2.45 and 2.46 the CF_2 carbon appears as a doublet of doublets at 115.38 ppm with two J^1_{CF} of 287.90 and

291.30 Hz as a consequence of the slightly different fluorine environments, the coupling constants and shifts are in the normal range expected for the fluorosubstituted carbons of a cyclopropyl.⁴⁶ The unsubstituted and vinyl substituted cyclopropyl carbons appear resolved into triplets at 33.26 ($J_{\text{CF}}^2 = 9.4$ Hz) and 21.79 ppm ($J_{\text{CF}}^2 = 10.9$ Hz). The methine carbon of the vinyl group appears at 133.9 ppm resolved in a doublet with a coupling constant $J_{\text{CF}}^3 = 2.9$ Hz. The carbons of the alkyl chain also displays a coupling $J_{\text{CF}}^3 = 3.5$ (C-7) and $J_{\text{CF}}^4 = 2.4$ Hz (C-6), see *Figure 2.46* and *2.47*.

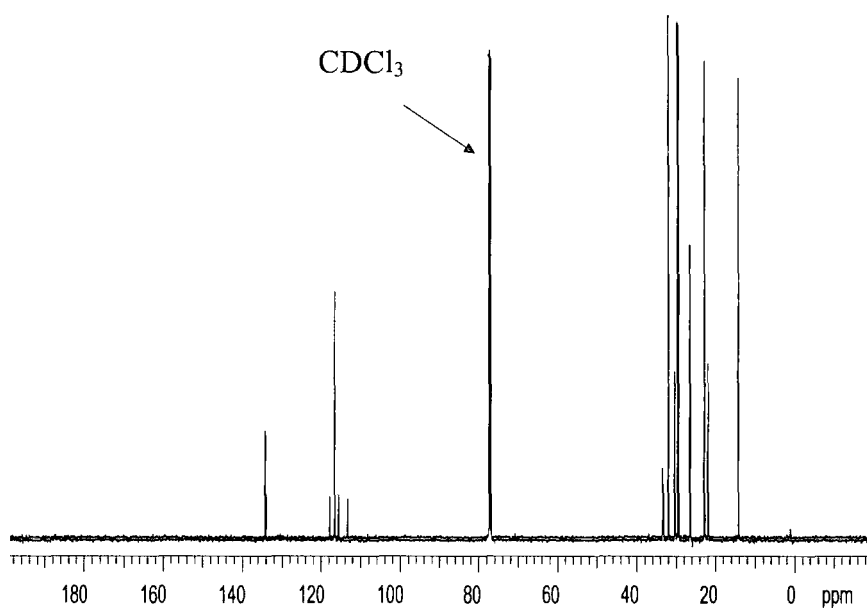


Figure 2.45 The ^{13}C nmr of 1,1-difluoro-2-heptyl-2-vinylcyclopropane

The expanded vinyl and allyl regions with assignments are shown in *Figure 2.46* and *Figure 2.47* respectively.

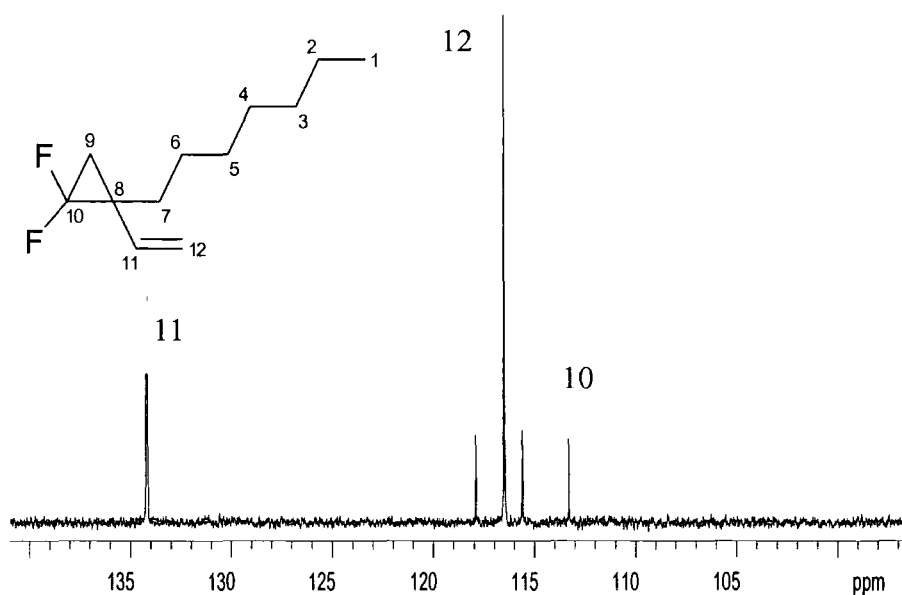


Figure 2.46 The expanded vinyl region in the ^{13}C nmr spectrum

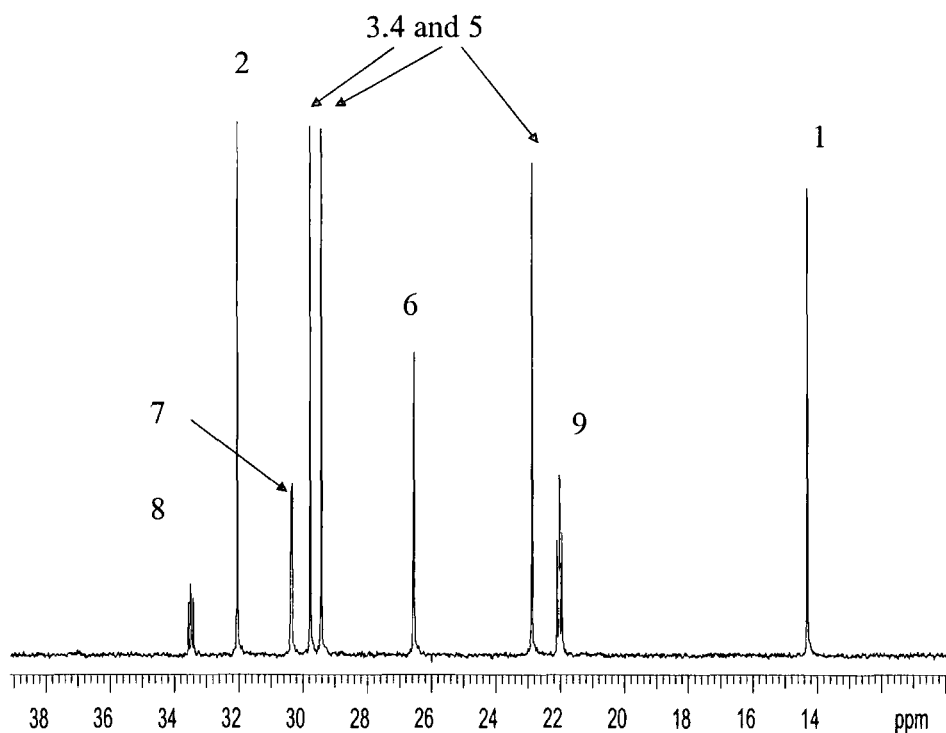


Figure 2.47 The expanded allyl region of the ^{13}C nmr spectrum

High-resolution distortionless-enhancement-through-polarisation-transfer (DEPT) spectroscopy differentiates between quaternary carbons, which are not

visible, CH₂ carbons which are seen as in a normal ¹³C nmr spectrum, and the CH and CH₃ carbons which are displayed inverted in the spectrum. Accordingly, in the DEPT spectrum for *1,1-difluoro-2-heptyl-2-vinylcyclopropane* shown below, *Figure 2.48*, the signals for the carbons (10) and (8) disappear and the signals for carbons (11) and (1) are inverted, compare *Figure 2.48* with *Figures 2.47* and *2.46*.

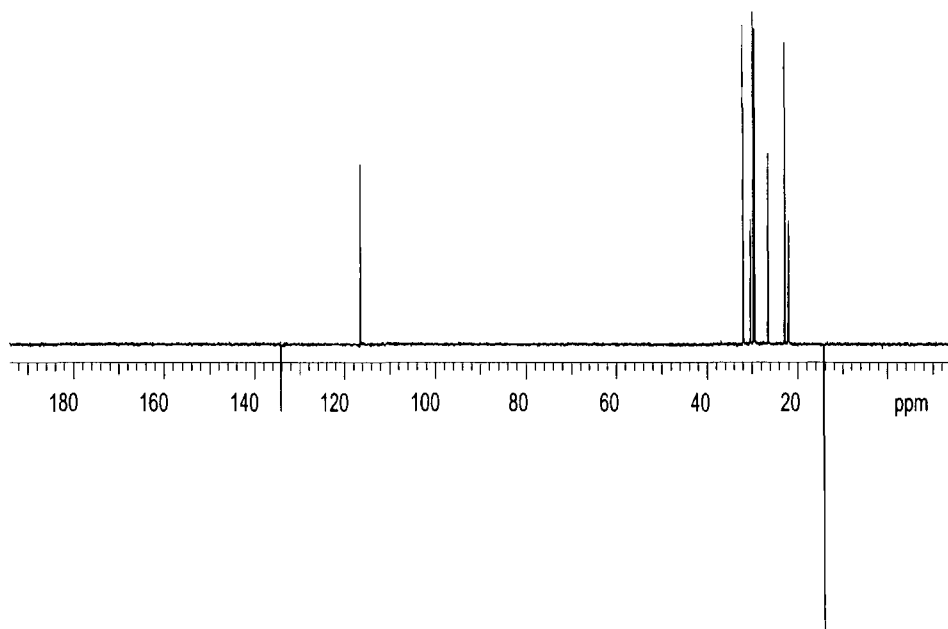


Figure 2.48 The DEPT spectrum of 1,1-difluoro-2-heptyl-2-vinylcyclopropane

In the IR spectrum (see Appendix AX18) the observation of the –CH=CH– stretching band at 1650 cm⁻¹ and the C-F vibration band at 1400 cm⁻¹ are consistent with the assigned structure.

The assignment of the minor peak observed in the capillary gc (0.37 %) was based on the analysis of the ¹⁹F nmr spectrum (see Appendix AX19) and gc-MS. The spectrum shows two doublets $J_{FF}^2 = 150.7$ Hz, the doublet at –126.6 ppm is resolved into triplets with $J_{HF}^3 = 10.9$ Hz, and that at –143.4 ppm into a doublet of doublets J_{HF}^3 (*syn*) = 12.6 Hz, J_{HF}^3 (*anti*) = 4.5 Hz.

The minor peak in the gc-MS possesses the same molecular ion (M⁺ 202) as the major peak, although the fragmentation pattern is different. This spectroscopic evidence suggested that the minor component was the isomer shown in *Figure 2.49*. Thus, the analysis shows that the product of reaction of

2-heptyl-1,3-butadiene with difluorocarbene is overwhelmingly Compound A in *Figure 2.41*, and the only other detected product is a trace of B. This is the result expected on the basis of Dolbier's work.³⁴

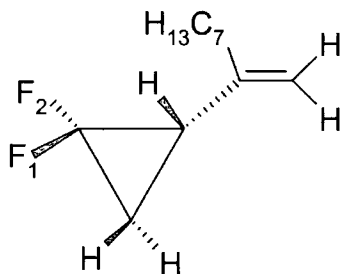


Figure 2.49 Minor isomer detected

2.4 d) Analysis of the results and conclusions

The mechanism of the difluorocarbene addition is not well established, it may be analogous to the Simmons-Smith carbene addition, where the carbene is believed to be transferred from the organometallic reagent to the double bond. Alternatively it may involve a free difluorocarbene.^{34,76-79}

In this work it appears that the carbene adds preferentially to the 1,2-double bond in 1,3-undecadiene and to the 1,2-double bond in 2-heptyl-1,3-butadiene. Thus, in the latter case there is an overwhelming preference for addition at the alkyl substituted double bond, whereas in the former case the unsubstituted double bond is preferred. Since the difluorocarbene is an electrophilic reagent we expect that reaction will occur at the most "electron rich" double bond, i.e. the alkylated one. In fact, a heptyl group at the terminal carbon of buta-1,3-diene results in attack at the least substituted double bond whereas attaching the same substituent at the middle carbon results in attack at the most substituted double bond. Clearly the factors controlling the outcome of this reaction arise from a subtle interplay of electronic and steric effects. Possibly the steric effects dominate because the heptyl at position 2 in butadiene hinders approach to both double bonds more or less equally and then the electronic factor takes over, but in 1,3-undecadiene the internal double bond is most sterically crowded and the bulky source of difluorocarbene attacks mainly at the sterically available terminal double bond.

2.5 Attempted polymerisation of 1,1-difluoro-2-heptyl-2-vinylcyclopropane.

Results and discussions

The polymerisation experiments were carried out in 99.9 % monomer under an oxygen-free nitrogen atmosphere using AIBN as a free radical initiator at 50 °C. None of the experiments gave a polymeric product. Oligomerisation occurred when a high concentration of the radical initiator (10-15 mole %) was used, experiments carried out with concentrations of the initiator below 10-mole % with respect to monomer did not give any conversion. In the best cases the conversion was only 16.5 % as estimated by integration of the ^{19}F nmr spectrum. The materials obtained were recovered as a white suspension by precipitation in cold methanol, and isolated by filtration using a cinter filter of low porosity. The material obtained, after drying in an oven at 50 °C overnight, was an extremely viscous white liquid (5%). The GPC analysis gave, in the best case, $M_n = 1740$, $M_w = 2210$, with a $\text{PDI} = 1.27$. The oligomers were partially soluble in methanol, which might explain the low yield obtained and the narrow polydispersity observed.

An attempt to effect polymerisation via gamma-ray irradiation of pure monomer, using a cobalt-60 source was carried out; however, even after four weeks of exposure no trace of polymer formation was observed.

The expected repeat units in the oligomer are shown in *Figure 2.50* and the analysis of the microstructure is based on the polymer obtained from 1,1-difluoro-2-vinylcyclopropane, see section 2.2.

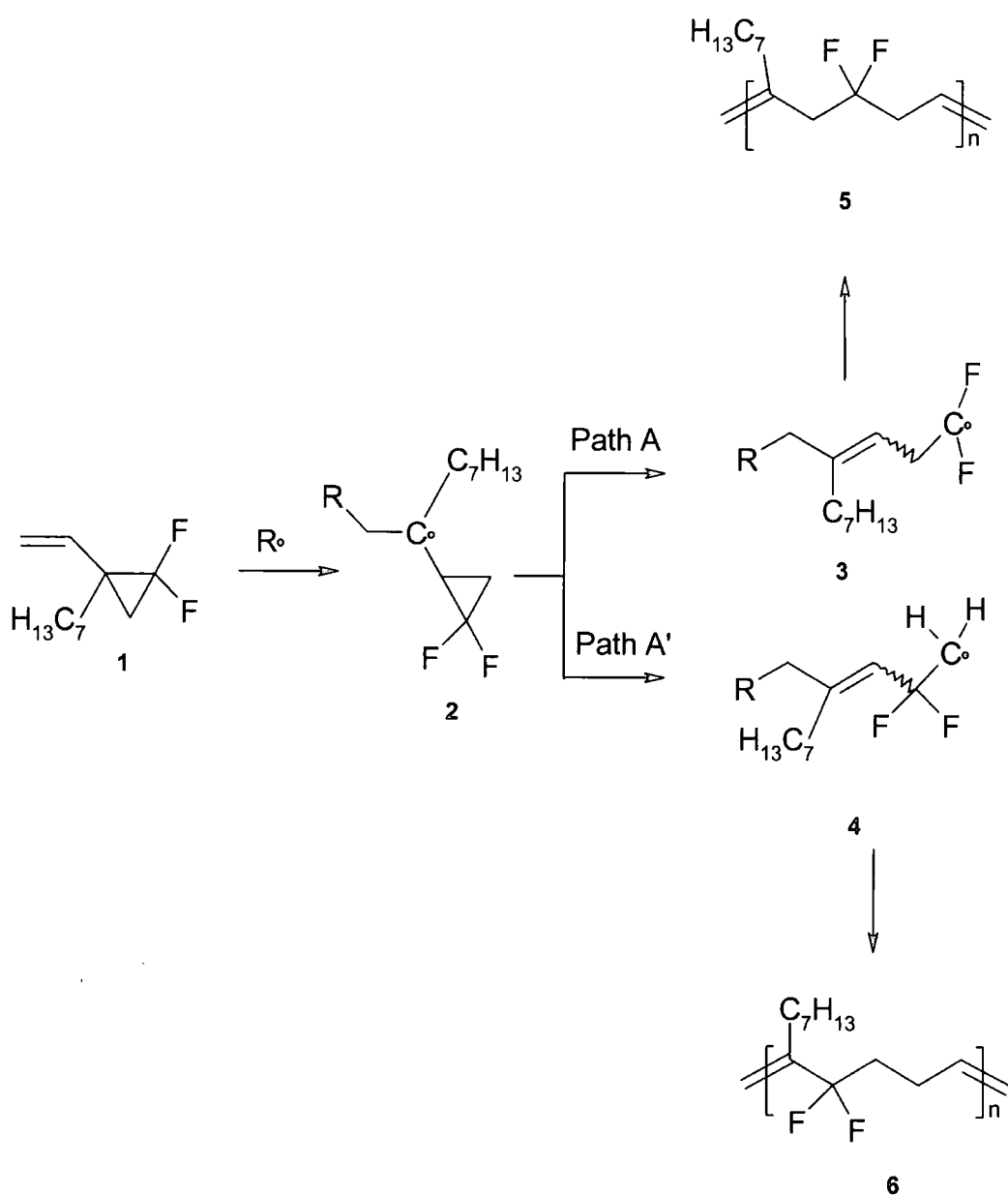


Figure 2.50 Main structures expected

The ^1H nmr spectrum of the oligomer obtained from RROP of 1,1-difluoro-2-heptyl-2-vinylcyclopropane with the assignments is shown in Figure 2.51.

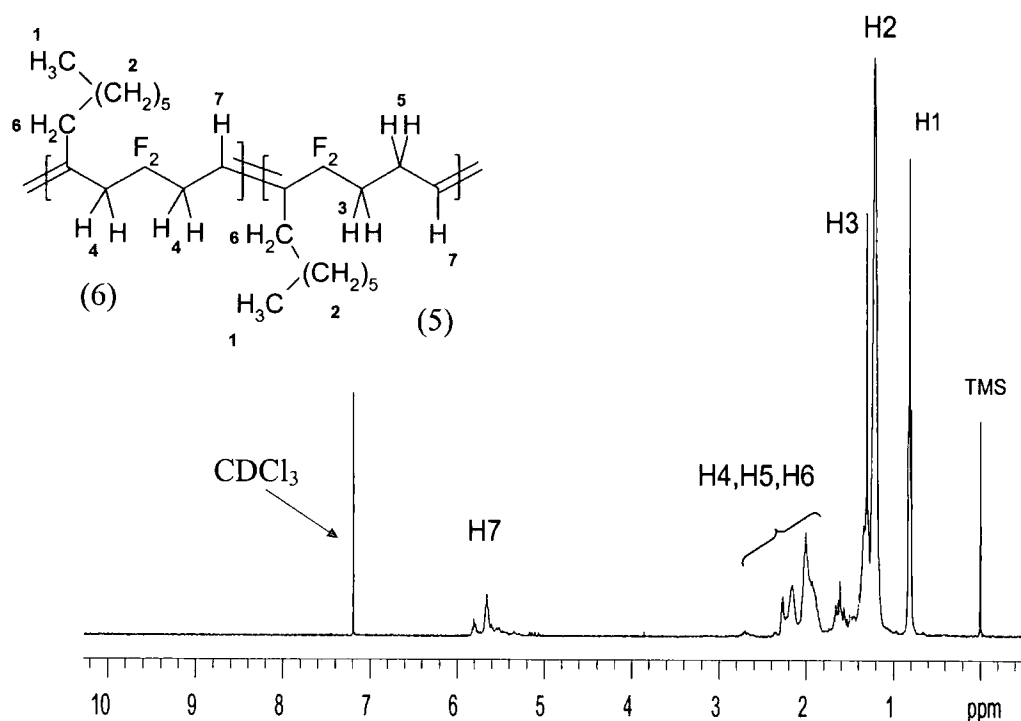


Figure 2.51 The ^1H nmr spectrum of the oligomer

The shifts and integrations of the signals in the ^1H nmr spectrum by analogy with poly(1,1-difluoro-2-vinylcyclopropane), Section 2.2 Figure 2.6 are readily assigned. There is some ambiguity in the assignment of the hydrogens H4, H5 and H6 which appear as a group of signals between 1.7 and 2.4 ppm, but the assignment of repeat unit (5), Figure 2.51 as the main feature is secure.

The ^{19}F mnr spectrum of the isolated oligomers and residual monomer are shown in Figures 2.52 and 2.53 respectively.

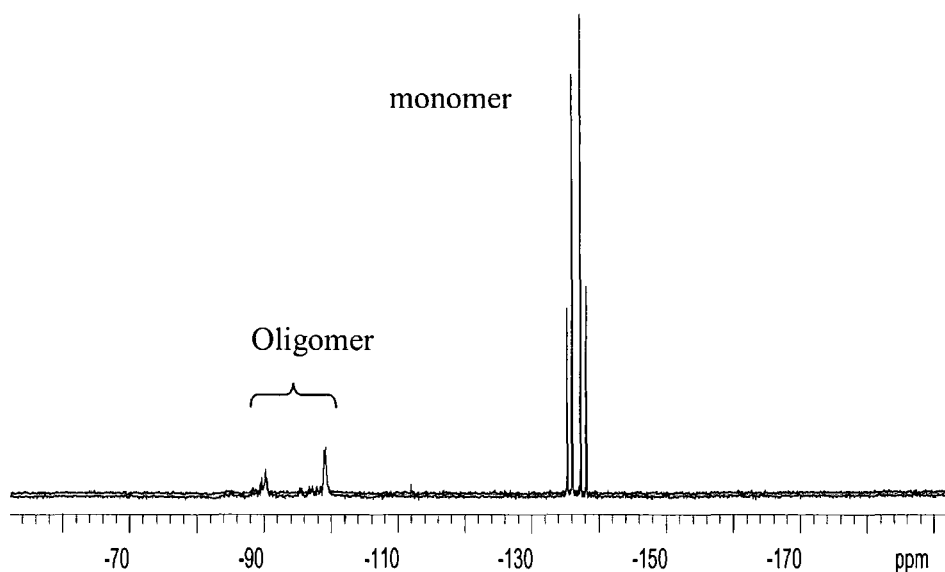


Figure 2.52 Raw product from the attempted RROP of 1,1-difluoro-2-heptyl-2-vinylcyclopropane

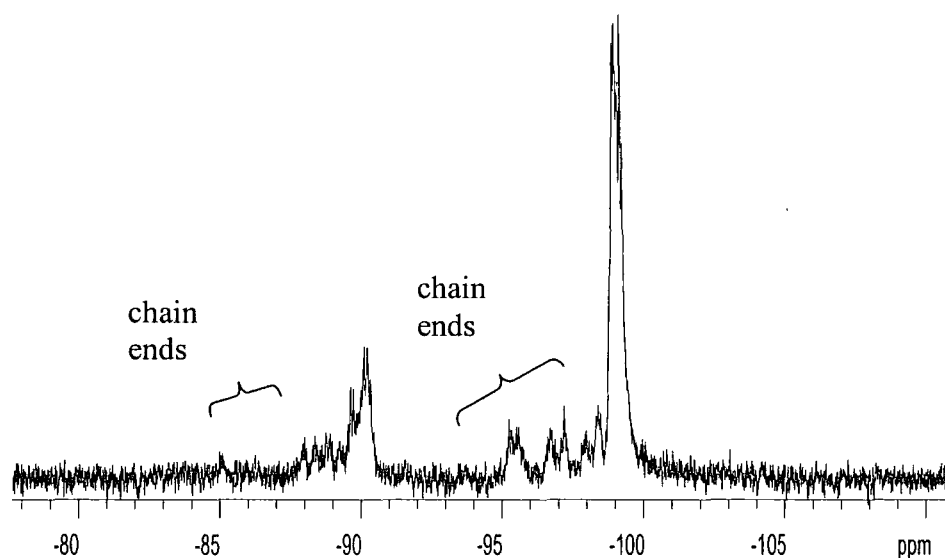


Figure 2.53 The ^{19}F nmr spectrum of the isolated oligomer

In analogy to poly(1,1-difluoro-2-vinylcyclopropane), the ^{19}F nmr spectrum of the material displays two main signals, and several minor signals which may result from repeat unit distribution and chain end effects. These two signals were assigned to the two types of repeat units formed via Path A'

(major) and Path A (minor), see *Figure 2.50*, in a 3:1 intensity ratio. Compared to the previously obtained poly(1,1-difluoro-2-vinylcyclopropane), it was observed that the proportion of the structure derived from the minor RROP pathway had increased remarkably, and it was concluded that this might be due to stereoelectronic effects produced by the alkyl side chain. However, the detailed investigation of this observation was outside of the scope of this work.

The compositions of poly(1,1-difluoro-2-vinylcyclopropane) and the oligomer obtained from 1,1-difluoro-2-heptyl-2-vinylcyclopropane are shown in *Figure 2.54*, with the approximate proportions of repeat units.

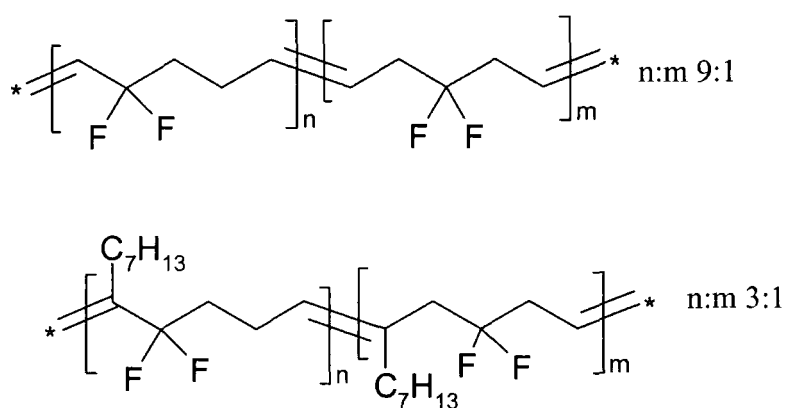


Figure 2.54 The structures and proportions of both materials

It was concluded that the presence of the n-alkyl side chain was likely to be the main reason for the failure of propagation in the RROP of 1,1-difluoro-2-heptyl-2-vinylcyclopropane. Thus, the high steric hindrance, which the long alkyl side chain produced on the vinyl moiety, probably increased the proportion of chain transfer reactions, giving early termination of the growing chains. At lower concentrations of radical initiator the ring-opening propagation was very unfavoured and no conversion was detected, whereas with an increased proportion of initiator radicals in the neat monomer the process was forced to occur if only up to a low conversion. This conclusion was in agreement with previous polymerisation studies of the methyl disubstituted VCPs monomers by Endo and Sanda, who showed a dramatic decrease in the molecular weights of the alkyl substituted polymers, as compared to the unsubstituted analogues.^{80,81} These earlier results are summarized in *Figure 2.55* and *2.56*.

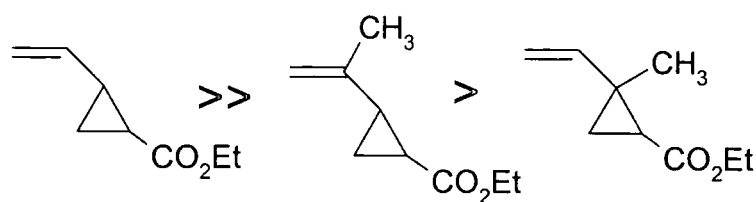


Figure 2.55 Schematic illustrating the relation between three nonomers and resultant molecular weights, decreasing from left to right, of the polymers investigated by Endo⁸⁰

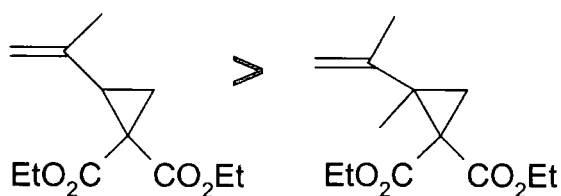


Figure 2.56 Schematic illustrating the relation between three nonomers and resultant molecular weights, decreasing from left to right, of the polymers investigated by Sanda and Endo⁸¹

The lower polymerisation rates of the alkyl-substituted monomers were explained in terms of increased steric hindrance produced by the methyl groups.

2.6 Attempted synthesis of 1,1-difluoro-3-butyl-2-vinylcyclopropane

2.6 a) Introduction

The previous experimental results suggested the possibility that the position of substitution of the alkyl side chain could play an important role in polymerisability in VCPs by RROP. Nevertheless, by decreasing the length of this alkyl side chain and distancing it from the vinyl moiety it was hoped to obtain a suitable monomer. The synthetic route designed is shown in *Figure 2.57*.

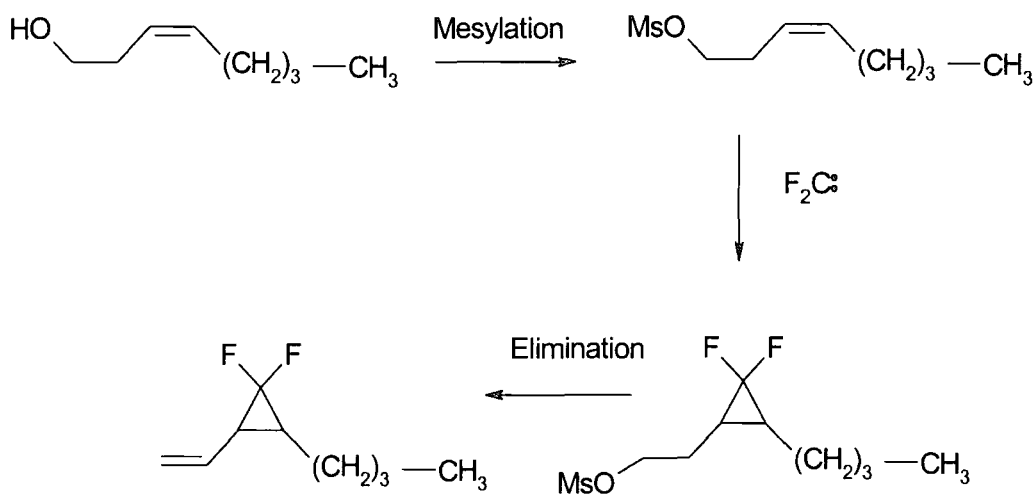


Figure 2.57 The proposed synthetic route to 1,1-difluoro-3-butyl-2-vinylcyclopropane

The starting material was commercially available, the difluorocarbene addition was understood so the transformation of the terminal alcohol into terminal double bond via sulfonate ester elimination,⁸² was the only new step. Since terminal alcohols do not undergo elimination via conventional acid treatment methodologies efficiently, due to side reactions such as ether formation and because the difluorocarbene species was likely to react with the alcohol,⁴⁷ the route chosen for this synthesis involved protecting group chemistry. The first step was mesylation of the alcohol, which was hoped to provide both a leaving group and a protecting group, followed by difluorocarbene addition at the double bond. In the last step a base-catalysed

elimination of the mesyl group leads to the alkene. The procedure in the last step is reported to give good yields for the direct transformations of terminal alcohols to terminal α -methyl olefins.⁸²⁻⁸⁴

2.6 b) Synthesis of *cis*-3-octen-1-mesylalcohol

The synthesis adopted involved the use of methanesulphonylchloride and pyridine with the commercially available *cis*-3-octen-1-ol, the scheme for the synthesis is shown in *Figure 2.58*.

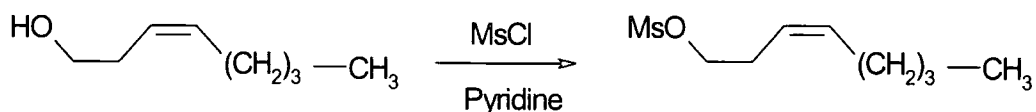


Figure 2.58 The mesylation of cis-3-octen-1-ol

The product obtained was as a colourless liquid in a 61.5 % yield and 98% purity as assessed by capillary gc. In the ^1H nmr spectrum (see Appendix AX20) the shifts and integrations are consistent with the assigned structure and taken with the gc results demonstrate that the product is pure. In the vinyl region of the ^1H nmr spectrum two signals of equal intensity are observed with a coupling constant $J_{\text{H-H}}^3 = 6.79$ Hz, which is in the expected range for *cis* double bonds and indicates that the nature of the double bond was preserved in the mesyl derivative. The signal at 2.9 ppm was assigned to the methyl of the mesyl group. In the ^{13}C nmr (see Appendix AX21) the methyl signal of the mesylate appears at 69 ppm, which is in the normal range expected for this signal. Two signals are observed in the alkene region and 6 signals downfield, which confirms the assigned structure. The IR spectrum (see Appendix 22) showed the disappearance of the band above 3000 cm^{-1} assigned to the $-\text{OH}$ band of the starting alcohol.

2.6 c) Attempted difluorocarbene addition to the *cis*-3-octen-1-mesylalcohol

The difluorocarbene addition to *cis*-3-octen-1-mesylalcohol was aimed to give the product shown in Figure 2.59.

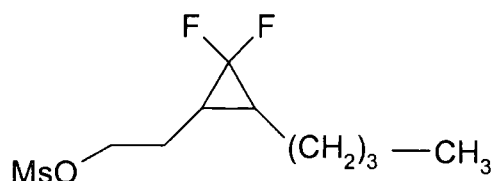


Figure 2.59 Attempted difluorinated molecule

After a partial purification of the product, a colourless liquid was obtained in a very low yield (3%) with 75 % purity as assessed by capillary gc. In the ^{19}F nmr spectrum of the impure sample signals associated with a 1,1-difluorocyclopropyl system were detected; however, in view of low conversion it was concluded that Dolbier's Zn-activated difluorocarbene addition methodology was not suitable for the hindered alkene substrate, *cis*-3-octen-1-mesylalcohol, and this synthetic route was abandoned.

2.7 Experimental procedures

2.7 a) General considerations

THF was obtained from a dry solvents purifying system or distilled over sodium metal. CH_2Cl_2 was distilled prior to use over calcium hydride and stored over 4A molecular sieves in a cool place. Isoprene was distilled at atmospheric pressure prior to use. Hexyl bromide was distilled under reduced pressure prior to use and stored over 4A molecular sieves. AIBN was recrystallised twice from ether or methanol and dried under vacuum. Toluene was distilled over sodium metal and stored with sodium wire in an oxygen free atmosphere. Pyridine was refluxed over NaOH pellets and distilled to a dry ampoule containing 4A molecular sieves. Butadiene (Aldrich, 99+% pure) was vacuum transferred prior to use from the storage cylinder polymerisation inhibitors. The rest of the reagents were used as supplied.

Infrared spectra were recorded on a Nicolet NEXUS FTIR spectrometer. The spectra were recorded between KBr discs. ^1H , ^{13}C and ^{19}F nmr spectra were recorded using Varian VXR 300, 400 and 500 nmr spectrometers and a Varian Gemini 200 nmr spectrometer. The solvents used were deuterated chloroform or deuterated benzene, ^1H and ^{13}C nmr used TMS as internal reference, and ^{19}F nmr spectra are referenced to CFCl_3 . Gas chromatography (gc) was recorded using a Hewlett-Packard (HP) 5890 series II fitted with a HP5 non-polar column (5% diphenyl, 95% dimethylsiloxane) capillary column; starting oven temperature 40°C , ramp $10^\circ\text{C min}^{-1}$ to 300°C ; flame ionisation detector. Gel permeation chromatography (GPC) was carried out in THF and DMF using a Knauer HPLC pump (model 64), Waters model R401 differential refractometer detector and 3 Plgel columns with pore sizes of 10^2 , 10^3 and 10^5 Å. The sample solutions were filtered through a Whatman WTP type 0.2- μm filters to remove any particles before injection onto the column. The columns were calibrated using Polymer Laboratories polystyrene standards (162-770 000amu).

2.7 b) Synthesis of 1,1-difluoro-2-vinylcyclopropane

1,3-Butadiene (11 g, 200 mmole) and CHClF_2 (26 g, 300 mmole) were vacuum transferred into a steel vessel containing 3-chloroepoxypropane (28 ml, 360 mmole), Bu_4NBr (0.2 g, 0.6 mmole), and hydroquinone (0.04 g, 0.34 mmole). The vessel was sealed under vacuum and heated to 120°C for 10 hours. The contents of the vessel were fractionally distilled (Vigreux column, 20 cm x 1cm) to give 1,1-difluoro-2-vinylcyclopropane (6.45 g, 30 % yield) as a colourless liquid (b.p. $52\text{--}53^\circ\text{C}$, literature³⁵ $51.5\text{--}52^\circ\text{C}$) (>99.9 % purity by capillary gc, $t_R = 5.45$ min). ^1H nmr (δ/ppm): 5.44 (1H, dddt, $J_{\text{H-H}}^3(\text{trans}) = 16.4\text{Hz}$, $J_{\text{H-H}}^3(\text{cis}) = 10\text{Hz}$, $J_{\text{H-H}}^3 = 8.2\text{ Hz}$, $J_{\text{H-F}}^4 = 1.6\text{ Hz}$, $\text{CH}=\text{CH}_2$); 5.17 (1H, dd, $J_{\text{H-H}}^3 = 16.4\text{Hz}$, $\text{trans CH}_2=\text{C-H}$); 5.08 (1H, dd, $J_{\text{H-H}}^3 = 10\text{Hz}$, $J_{\text{H-H}}^2(\text{vicinal}) \sim 1.2\text{Hz}$, $\text{cis CH}_2=\text{C-H}$); 2.21 (1H, m, $\text{CH-CH}=\text{CH}_2$); 1.52 (1H, m, C-ring); 1.21 (1H, m, C-ring). ^{19}F nmr (δ/ppm): -128.62 (1F, dtd, $J_{\text{F-F}}^2 = 156.56\text{Hz}$, $J_{\text{F-H}}^3 = 12.79, 12.79, 3.01\text{Hz}$); -141.65 (1F, dd, $J_{\text{F-F}}^2 = 156.56\text{Hz}$, $J_{\text{F-H}}^3 = 12.79, 4.51\text{Hz}$). ^{13}C nmr (δ/ppm): 131.5 (dd, $J_{\text{C-F}}^2 = 4.6, 1.5\text{Hz}$, $=\text{CH-}$); 117.6 (s, $\text{H}_2\text{C=}$); 113.5 (dd, $J_{\text{C-F}}^1 = 287.6, 284.6\text{Hz}$, C-F); 26.7 (dd, $J_{\text{C-F}}^2 = 12.3$ and 11.6Hz , CH ring); 12.7 (t, $J_{\text{C-F}}^2 = 10.8\text{Hz}$, CH_2 ring).

2.7 c) Polymerisation of 1,1-difluoro-2-vinylcyclopropane

Using the glove box, the initiator AIBN (0.012g, 0.07 mmol) was dissolved in the monomer (1g, 9.6 mmol) and transferred into an oxygen-free ampoule equipped with Young's Teflon vacuum tap and a magnetic stirrer. The sealed ampoule (nitrogen atmosphere) was taken out of the glove box and heated with stirring at 50°C for 5 days. The contents of the ampoule were recovered by precipitation into a 10-fold excess of cold methanol to give a white solid. The product was recovered by filtration and dried in a vacuum oven at 50°C overnight. The white solid was redissolved in the minimum quantity of benzene and reprecipitated using a 10-fold excess of methanol, recovered by filtration and dried in the vacuum oven to give poly(1,1-difluoro-2-vinylcyclopropane), (0.15 g, 15%). Found: C, 58.04; H, 5.83; F, 36 %;

(C₅H₆F₂)_n requires C, 57.69; H, 5.77; F, 36.54%. ¹H nmr (δ/ppm, S symmetrical, U unsymmetrical): 5.6-6 (bs, U, =CH-CF₂); 5-5.5 (bs, S and U, CH= overlapped); 2.3-2.5 (bs, S, CH₂-CF₂); 1.8-2.3 (bs, U, CH₂-CF₂); 1.2-2.2 (bs, U, CH₂-CH=); ¹⁹F nmr (δ/ppm (-1), Rel. Int. (%))(S symmetrical, U unsymmetrical): 87.7 (bm, <0.5); 88.2 (m, <0.5); 91.8 (q, <0.5); 92.02 (q, S, J_{H-F}³ = 15.43Hz, 8.8); 96.11 (q, U, J_{H-F}³ = 12.4Hz, 90.8); 96.36 (m, <0.5). ¹³C nmr (δ/ppm, S symmetrical, U unsymmetrical): 135.2 (bm, S, CH=); 134.3 (t, U, J_{C-F}³ = 8.7Hz, CH=C-CF₂); 125.9 (t, U, J_{C-F}² = 26.1Hz, CH=C-CF₂); 122.1 (t, S, J_{C-F}¹ = 239Hz, CF₂); 120.99 (t, U, J_{C-F}¹ = 238.9Hz, CF₂); 37.1 (t, S, J_{C-F}² = 27Hz, CH₂-CF₂); 36.26 (t, U, J_{C-F}² = 26.9Hz, CH₂-CF₂); 24.86 (s, U, CH₂-CH=).

2.7 d) Synthesis of 4-methyl-undeca-1,3-diene

Allyltriphenylphosphonium bromide (25 g, 65 mmol) and THF (150-ml) were placed in a 500-ml three-necked flask which was purged with dry oxygen-free nitrogen and equipped with a rubber septum, a solid addition funnel, a reflux condenser and magnetic stirrer. *tert*-BuO⁻K⁺ (9.20 g, 82 mmol) was added in small portions to the stirred suspension via the solids funnel. The resultant suspension was refluxed for one hour. The flask was cooled to room temperature and the reflux condenser was replaced by an addition funnel. 2-Nonanone (4.5 g, 33 mmol) in THF (100-ml) was added dropwise. The solution was stirred overnight at room temperature and the contents of the flask were poured into a saturated aqueous solution of NH₄Cl (150-ml), the aqueous layer was separated and extracted with ether, and the combined organic extracts were washed with brine, dried over anhydrous magnesium sulphate and concentrated under reduced pressure. The product was isolated from the crude mixture by column chromatography (silica gel, hexane) to give a 38:62 *cis*: *trans* mixture of 4-methyl-undeca-1,3-diene (350 mg, 6.5 % yield) as a colourless liquid (98 % pure on capillary gc, two peaks *t_R* (*cis*) = 11.66 min, *t_R* (*trans*) = 11.41 min). The ¹H nmr spectrum displayed sets of overlapping peaks which could be assigned as follows for the major *trans* isomer (δ/ppm): 6.6 (1H, m, RCH₃C=CH-CH=CH₂); 5.7 (1H, d, J_{HH}³ = 11Hz,

$\text{RCH}_3\text{C}=\text{CH}-\text{CH}=\text{CH}_2$); 5.0 (1H, d, $J_{\text{HH}}^3 = 17\text{Hz}$, $-\text{CH}=\text{CHH}$ *trans* HH coupling); 4.90 (1H, d, $J_{\text{HH}}^3 = 10.5\text{Hz}$, $=\text{CH}_2$); 1.96 (2H, t, $J_{\text{HH}}^3 = 8\text{Hz}$, $\text{RCH}_2-\text{C}(\text{CH}_3)=\text{CH}-$); 1.68 (3H, d, $J_{\text{HH}}^3 = 10\text{Hz}$, $\text{CH}_3-\text{CR}=\text{CH}-$); 1.34 (2H, m, $\text{RCH}_2-\text{CH}_2-\text{C}(\text{CH}_3)=\text{CH}-$); 1.2 (8H, s, $(\text{CH}_2)_6$); 0.8 (3H, t, CH_3-R); and for the minor *cis* isomer: 6.6 (1H, m, $\text{RCH}_3\text{C}=\text{CH}-\text{CH}=\text{CH}_2$); 5.7 (1H, d, $J_{\text{HH}}^3 = 11\text{Hz}$, $\text{RCH}_3\text{C}=\text{CH}-\text{CH}=\text{CH}_2$); 4.9 (1H, d, $J_{\text{HH}}^3 = 17\text{Hz}$, $=\text{CH}_2$); 4.8 (1H, d, $J_{\text{HH}}^3 = 10.5\text{Hz}$, $=\text{CH}_2$); 2.08 (2H, t, $J_{\text{HH}}^3 = 8\text{Hz}$, $\text{RCH}_2-\text{CH}=\text{CH}$); 1.68 (3H, d, $J_{\text{HH}}^3 = 10\text{Hz}$, $\text{CH}_3-\text{CR}=\text{CH}-$); 1.34 (2H, m, $\text{RCH}_2-\text{CH}_2-\text{C}(\text{CH}_3)=\text{CH}-$); 1.2 (8H, s, $(\text{CH}_2)_6$); 0.8 (3H, t, $J_{\text{HH}}^2 = 6.5\text{Hz}$, CH_3-R). The ^{13}C nmr spectrum displayed sets of overlapping peaks which could be assigned as follows for the major *trans* isomer (δ/ppm): 140.25 ($\text{C}=\text{CH}-\text{CH}=\text{CH}_2$); 133.70 ($\text{C}=\text{CH}-\text{CH}=\text{CH}_2$); 125.50 ($\text{C}=\text{CH}-\text{CH}=\text{CH}_2$); 114.56 ($\text{C}=\text{CH}-\text{CH}=\text{CH}_2$); 38.100 ($\text{C}-\text{CH}_3$); 32.906, 32.558, 29.767, 29.580, 29.481, 28.481, 28.057, 23.973, 22.924 *cis* and *trans* overlapped signals of $(\text{CH}_2)_6$; 16.796 ($\text{R}-\text{CH}_3$); and for the minor *cis* isomer: 140.59 ($\text{C}=\text{CH}-\text{CH}=\text{CH}_2$); 133.42 ($\text{C}=\text{CH}-\text{CH}=\text{CH}_2$); 126.30 ($\text{C}=\text{CH}-\text{CH}=\text{CH}_2$); 114.45 ($\text{C}=\text{CH}-\text{CH}=\text{CH}_2$); 40.104 ($\text{C}-\text{CH}_3$); 32.906, 32.558, 29.767, 29.580, 29.481, 28.481, 28.057, 23.973, 22.924, *cis* and *trans* overlapped signals of $(\text{CH}_2)_6$; 15.842 ($\text{R}-\text{CH}_3$); **GC-MS Peaks** (rel. int.) (*cis*-4-methyl-undeca-1,3-diene, $t_{\text{R}} = 11.41$ min): 166 (M^+ , 20), 123 (9), 95 (42), 79 (71), 67(82), 55 (36), 41 (100), 27 (38); (*trans*-4-methyl-undeca-1,3-diene, $t_{\text{R}} = 1.66$ min) 166 (M^+ , 22), 95 (46), 79 (75), 67(80), 55 (38), 41 (100), 29 (58).

2.7 e) Synthesis of 3,4-dimethyl-trideca-1,3-diene

Zinc powder (45 g, 688 mmol) and THF (700 ml) were placed in a 2-L three-necked flask which was purged with dry oxygen-free nitrogen and equipped with a reflux condenser, a solid addition funnel and a magnetic stirrer. The flask was cooled to 0°C , and titanium tetrachloride (38 ml, 344 mmol) was added dropwise to the stirred suspension using a syringe and the resulting black suspension was refluxed for 3 hours. The suspension was cooled to 0°C and a mixture of 2-undecanone (7.81 g, 46 mmol) and methyl vinyl ketone (12.86 g, 184 mmol) in THF (100 ml) was added. The suspension was refluxed and stirred for 12 h., cooled to room temperature, and poured into cold water

(800 ml). The aqueous layer was extracted with ether and the combined organic extracts were washed with brine, dried over anhydrous magnesium sulphate and rotary evaporated under reduced pressure. The crude product was fractional distilled under reduced pressure (4×10^{-1} mbar) to give *3,4-dimethyltrideca-1,3-diene* (287 mg, 3 % yield) as a colourless liquid. (98% purity by capillary gc, two peaks $t_R = 14.901$ min, 47.7 %, $t_R = 15.085$ min, 52.3 %) (b.p. $55^\circ\text{C}/4 \times 10^{-1}$ mbar). ^1H nmr (δ/ppm): 6.76 (1H, dd, *trans* $J_{\text{HH}}^3 = 17.25\text{Hz}$, *cis* $J_{\text{HH}}^3 = 10.8\text{Hz}$, $-\text{C}(\text{CH}_3)=\text{C}(\text{CH}_3)-\text{CH}=\text{CH}_2$); 5.0 (1H, d, *trans* $J_{\text{HH}}^3 = 17.25\text{Hz}$, $-\text{C}(\text{CH}_3)=\text{C}(\text{CH}_3)-\text{CH}=\text{CHH}$); 4.95 (1H, two doublets, *cis* $J_{\text{HH}}^3 = 9.75$ and 9.3Hz , from the *cis* and *trans* isomers, $-\text{CH}=\text{CHH}$); 2.1 (2H, 2t, $J_{\text{HH}}^2 = 6.8\text{Hz}$, overlapped *cis* and *trans* $\text{RCH}_2\text{C}=\text{C}$); 1.7 (6H, unresolved m, overlapped *cis* and *trans* $(\text{CH}_3)-\text{CR}=\text{C}(\text{CH}_3)-$); 1.2 (12H, s, overlapped *cis* and *trans* $(\text{CH}_2)_6$); 0.81 (3H, t, $J_{\text{HH}}^2 = 6.3\text{Hz}$, CH_3-R). ^{13}C nmr (δ/ppm): 135.17, 135.08, 135.0, 134.49 (overlapped *cis* and *trans* signals of $\text{RCH}=\text{C}(\text{CH}_3)-\text{CH}=\text{CH}_2$); 125.61 (*trans* signal of $\text{C}=\text{C}-\text{CH}=\text{CH}_2$); 125.61 (*cis* signal of $\text{C}=\text{C}-\text{CH}=\text{CH}_2$); 109.97 (*cis* signal of $\text{C}=\text{C}-\text{CH}=\text{CH}_2$); 109.67 (*trans* signal of $\text{C}=\text{C}-\text{CH}=\text{CH}_2$); 34.70, 33.14, 30.88, 28.78, 28.72, 28.61, 28.58, 28.32, 27.80, 27.10, 21.66, 19.01, 17.34, 13.09, 12.62, 12.21 (overlapped *cis* and *trans* signals of $3(\text{CH}_3)$ and $(\text{CH}_2)_8$). GC-MS (*cis-3,4-dimethyl-1,3-tridecadiene*, $t_R = 14.90$ min) (M^+ , 208) 109, 95, 81, 67, 55, 41, 29. (*trans-3,4-dimethyl-1,3-tridecadiene*, $t_R = 15.09$ min) (M^+ , 208), 109, 95, 81, 67, 55, 53, 43, 41, 39, 29, 27.

2.7 f) Synthesis of 1,3-undecadiene

Methyltriphenylphosphonium bromide (8 g, 22 mmol) and THF (150ml) were placed in an 250-ml three-necked flask which was purged with dry oxygen-free nitrogen equipped with a reflux condenser, a solid addition funnel, a pressure-equalizing addition funnel, and a magnetic stirrer. $t\text{-BuO}^-\text{K}^+$ (2.6 g, 23 mmol) was added in small portions to the stirred suspension via the addition funnel and the reaction mixture was refluxed for one hour. The suspension was cooled to room temperature and a solution of *trans*-2-decenal (3.1 g, 20 mmol) in THF (25ml) was added dropwise. The reaction mixture was stirred overnight

at room temperature and quenched with an aqueous 10 % NH_4Cl solution (200ml). The aqueous layer was extracted with diethyl ether and the combined organic fractions were washed with brine and dried over anhydrous magnesium sulphate. The solvent was rotary evaporated under reduced pressure and the crude product was purified by column chromatography (silica gel, hexane) to give *trans*-1,3-undecadiene (2.42 g, 79.6 % yield) as a colourless liquid. (98% purity on capillary gc, $t_R = 10.43$ min). Found C, 86.47; H, 13.32 %; $\text{C}_{11}\text{H}_{20}$ requires: C, 86.76; H, 13.23%. ^1H nmr (δ/ppm) 6.2 (1H, dt, *trans* $J_{\text{HH}}^3 = 17.1\text{Hz}$, $J_{\text{HH}}^3 = 10.2, 10.2\text{Hz}$, $-\text{CH}=\text{CH}-\text{CH}=\text{CH}_2$); 6.0 (1H, dd, *trans* $J_{\text{HH}}^3 = 15.3\text{Hz}$, *cis* $J_{\text{HH}}^3 = 10.5\text{Hz}$, $-\text{CH}=\text{CH}-\text{CH}=\text{CH}_2$); 5.7 (1H, dt, *trans* $J_{\text{HH}}^3 = 15.3\text{Hz}$, $J_{\text{HH}}^3 = 7.2\text{Hz}$, $-\text{CH}=\text{CH}-\text{CH}=\text{CH}_2$); 5.0 (1H, d, *trans* $J_{\text{HH}}^3 = 17.1\text{Hz}$, $-\text{CH}=\text{CH}-\text{CH}=\text{CH}_2$); 4.9 (1H, d, *cis* $J_{\text{HH}}^3 = 10.2\text{Hz}$, $-\text{CH}=\text{CH}-\text{CH}=\text{CH}_2$); 2.2 (2H, dt, $J_{\text{HH}}^3 = 7.2, 7.2\text{Hz}$, $\text{R}-\text{CH}_2-\text{CH}=\text{CH}-$); 1.7 (2H, m, $\text{R}-\text{CH}_2-\text{CH}_2-\text{CH}=\text{CH}-$); 1.2 (8H, s, $(\text{CH}_2)_4$); 0.8 (3H, t, $J_{\text{HH}}^2 = 6.49\text{Hz}$, CH_3-R). ^{13}C nmr (δ/ppm) 137.6, 135.8 ($=\text{CH}-\text{CH}=\text{CH}_2$); 131.0 ($\text{R}-\text{CH}=\text{CH}-\text{CH}=\text{CH}_2$); 114.7 ($=\text{CH}_2$); 32.7, 32.05, 29.43, 29.42, 29.41, 22.88 ($(\text{CH}_2)_6$); 14.3 (CH_3). IR (cm^{-1} , vibration modes): 889.25 ($=\text{CH}_2$), 1001.5 (C-H), 1458.8 (C-H), 1600 and 1650 ($-\text{CH}=\text{CH}-\text{CH}=\text{CH}_2$), 2925.9 (CH_3). MS Peaks (rel. int.): 152 (65, M^+), 124 (5), 109 (11), 95 (25), 81 (59), 77(11), 68 (80), 67 (100), 54 (61), 41 (93), 39 (58), 27 (29).

2.7 g) Synthesis of 1-octen-3-one

Pyridinium dichromate (53 g, 140 mmol) and CH_2Cl_2 (500 ml) were placed in a 1-L two-necked flask, which was purged with dry and oxygen-free nitrogen and equipped with a reflux condenser, a rubber septum and a magnetic stirrer. A solution of 1-octen-3-ol (12 g, 94 mmol) in CH_2Cl_2 (150 ml) was added, and the mixture was stirred at room temperature for three days, 72 h. The black solid was filtered and washed with 200 ml of ether. The filtrate was washed with 5% NaOH aqueous solution, 5% HCl aqueous solution, saturated brine solution and dried over anhydrous magnesium sulphate. The solvent was rotary evaporated under reduced pressure and the crude product was purified by fractional distillation under reduced pressure to give 1-octen-3-one (7.4 g, 62 %

yield) as a colourless liquid (b.p. 57⁰C, 56-60⁰C/16 mm, Lancaster Research Chemicals), (99 % purity by capillary gc, t_R = 6.55 min). Found: C, 75.48; H, 11.08 %; C₈H₁₄O requires C, 76.19; H, 11.11%. ¹H nmr (δ /ppm): 6.12 (2H, m 2^{on} order, *trans*-CH=CHH, and RCO-CH=CH₂); 5.7 (1H, dd, *cis* J_{HH} = 9.8Hz, vicinal J_{HH} = 1.8Hz); ¹³C nmr (δ /ppm): 201.09 (C=O); 136.72 (C=CH₂); 127.92 (C=CH₂); 39.71 (-CH₂-RC=O); 31.56, 23.83, 22.62 ((CH₂)₃); 14.041 (CH₃). IR (cm⁻¹): 1650 (C=C); 1690 (C=O); 2850 (CH₂ stretching); 2950 (C-H vibration band). MS Peaks: 111 (100), 97, 83, 70, 55, 41, 27.

2.7 h) First attempted synthesis of 2-pentyl-1,3-butadiene

Methyltriphenylphosphonium bromide (16 g, 44 mmol) and THF (250 ml) were placed in a 500-ml three-necked flask which was purged with dry and oxygen-free nitrogen and equipped with a reflux condenser, a rubber septum, a solid addition funnel, and a magnetic stirrer. *t*-BuOK (5.2 g, 46 mmol) was added in small portions to the stirred suspension via the addition funnel and was refluxed for 1 hour. After cooling the mixture to room temperature, a solution of 1-octen-3-one (5.6 g, 40 mmol) in THF 50 ml was added dropwise over 2-2.5 hours. The reaction was stirred at room temperature for 72 hours and quenched with saturated aqueous ammonium chloride (300 ml), extracted with ether, washed with brine and dried over anhydrous sodium sulphate. The solvent was evaporated under reduced pressure and the crude product was purified by column chromatography (silica gel, hexane) to give a mixture of two products detected by gc-MS both with M⁺ 248.

2.7 i) Second attempted synthesis of 2-pentyl-1,3-butadiene

Zn dust (1.2g, 18 mmol) in THF (200 ml) was placed in an oxygen-free 100 ml flask. Diiodomethane (0.80 ml, 10mmol) was added to the stirred solution via syringe. A TiCl₄ solution (1,0 M in dichloromethane, 2.0 ml) was added at 0⁰C and the resulting black mixture was stirred at room temperature for 1 h. A solution of 1-octen-3-one (0.25 g, 2.0 mmol) in THF (5ml) was added dropwise at room temperature and stirred for 2 h. The solution was diluted with ether (10ml) and the organic layer was washed with 1 M HCl

aqueous solution (20ml) and brine. The concentrated crude product was purified by column chromatography (silica gel/ hexane) to give a mixture of two products with the same molecular weight identified by gc-MS ($M^+=248$).

2.7 j) *Synthesis of 2-heptyl-1,3-butadiene*

A mixture of *t*-BuOK (50 g, 0.45 mol) and 2,2,6,6-tetramethylpiperidine (60 g, 0.45 mol) in THF (400 ml) was placed in a 2000-ml flask purged with dry oxygen-free nitrogen. The solution was cooled to $-65\text{ }^{\circ}\text{C}$ in an acetone/dry ice bath while *n*-BuLi solution (2.5 M in hexanes, 180 ml, 0.45 mol) was added using a syringe. The resulting orange solution was cooled to $-78\text{ }^{\circ}\text{C}$ while isoprene (40 g, 60 ml, 0.45 mol) was added dropwise using a syringe over 1h. The resulting red solution was stirred for 1 hour at $-78\text{ }^{\circ}\text{C}$ and a solution of 1-bromohexane (100 g, 0.60 mol) in THF (150 ml) was added using a syringe keeping the temperature below $-50\text{ }^{\circ}\text{C}$. The resulting yellow suspension was stirred at $-50\text{ }^{\circ}\text{C}$ for 2 hours. The cold bath was removed and when the stirred reaction mixture reached $0\text{ }^{\circ}\text{C}$ it was quenched with 400 ml of water. The aqueous layer was extracted with ether and the combined organic extracts were washed with 300 ml of 1N HCl solution, saturated brine solution and dried over MgSO_4 anhydrous. The solvent was removed by rotary evaporation under reduced pressure. The volatile components were separated from the crude reaction product by vacuum transfer (2×10^{-1} mbar) to give a mixture 60:20 of 2-heptyl-1,3-butadiene and the unreacted hexylbromide. The mixture was placed in a flask at 0°C equipped with a magnetic stirrer and glassware connected to a flask receiver cooled in liquid N_2 and the system was evacuated at partial static vacuum (4×10^{-1} mbar). The unreacted hexyl bromide (b.p. $154\text{--}158\text{ }^{\circ}\text{C}$) along with a fraction of the diene was trapped in the receiving flask. The remainder of the material in the first flask was monitored by ^1H nmr until no sign of the hexylbromide was observed (^1H nmr δ 3.5 ppm $\text{CH}_2\text{-Br}$). The pure 2-heptyl-1,3-butadiene was collected. The process was repeated three times. The collected fractions were combined to give 2-heptyl-1,3-butadiene (31.2 g, 34% yield) as a colourless liquid (99 % purity on capillary gc, $t_R = 9.64$ min). Found C, 86.07; H, 13.15 %; calculated for $\text{C}_{11}\text{H}_{20}$; C, 86.08; H,

13.16 %. ^1H nmr (δ/ppm): 6.6 (1H, dd, *trans* $J_{\text{HH}}^3 = 18\text{Hz}$, *cis* $J_{\text{HH}}^3 = 8.5\text{Hz}$, $-\text{CH}=\text{CH}-$); 5.17 (1H, dd, *trans* $J_{\text{HH}}^3 = 18\text{Hz}$, vicinal $J_{\text{HH}}^2 = 1.8\text{Hz}$, $-\text{CH}=\text{CHH}$); 4.96 (1H, dd, *cis* $J_{\text{HH}}^3 = 8.5\text{Hz}$, vicinal $J_{\text{HH}}^2 = 1.8\text{Hz}$, $\text{CH}=\text{CH}_2$); 4.90 (1H, s, $-\text{CR}=\text{CH}_2$); 2.1 (2H, t, $J_{\text{HH}}^3 = 7.5\text{Hz}$, $\text{R}-\text{CH}_2-\text{C}=\text{C}$); 1.4 (2H, s, $\text{R}-\text{CH}_2\text{CH}_2-\text{CH}=\text{CH}_2$); 1.24 (8H, s, $4\times(\text{CH}_2)$); 0.8 (3H, t, $J_{\text{HH}}^3 = 7\text{Hz}$). ^{13}C nmr (δ/ppm): 145.61 ($\text{C}=\text{C}$); 138.04 ($\text{CH}=\text{C}$); 114.43 ($=\text{CH}_2$); 111.99 ($=\text{CH}_2$); 30.87, 30.34, 28.60, 28.22, 27.17, 21.68 ($6(\text{CH}_2)$); 13.09 (CH_3). IR (cm^{-1}): 3020 and 2900 C-H stretching, 1590 and 1500 $-\text{CH}=\text{CH}-$ absorptions, 950 and 820 $\text{C}=\text{C}$ stretching. MS Peaks (rel. int.): M^+ 152 (0.75), 95 (34), 81 (52), 67 (100), 55 (49), 41 (93), 29 (30), 27 (30).

2.7 k) Difluorocarbene addition to undeca-1,3-diene

A suspension of zinc dust (1.45 g, 22.8 mmol) in THF (10 ml) was placed in a 100-ml three-necked flask, which was purged with dry oxygen-free nitrogen and equipped with a pressure equalizing addition funnel, a rubber septum, and a magnetic stirrer. Trimethylchlorosilane (1 ml) was added and the suspension was stirred for 20 min. 1,3-Undecadiene (0.9 g, 7.6 mmol) and a small crystal of iodine were added. The flask was placed in water bath and dibromodifluoromethane (6 g, 30 mmol) in THF (15 ml) was added dropwise over a period of 2 hours. The solution was stirred overnight at room temperature. The reaction mixture was poured into 100 ml of 10 % aqueous HCl. The aqueous layer was extracted with CH_2Cl_2 and the combined organic extracts were washed once with 10 % aqueous solution of Na_2HCO_3 and dried over anhydrous magnesium sulphate. The solution was concentrated by rotary evaporation under reduced pressure. The crude product was purified by column chromatography (silica gel, hexane) to give 1,1-difluoro-2'-nonenylcyclopropane and 1,1-difluoro-3-heptyl-2-vinylcyclopropane (0.52 g, 33.9 % yield) as a colourless liquid mixture (85.7 % purity of the mixture in gc) (major isomer integrates 79.5 % on gc, $t_{\text{R}}=12.24$ min; minor isomer integrates 6.9 % on gc $t_{\text{R}} = 11.15$ min). The ^1H nmr of the main isomer (δ/ppm): 5.4 (1H, dt, *trans* $J_{\text{HH}}^3 = 15.29\text{Hz}$, $J_{\text{HH}}^3 = 6.9\text{Hz}$, ring- $\text{CH}=\text{CH}-\text{R}$); 5.0 (1H, dt, *trans* $J_{\text{HH}}^3 = 15.29\text{Hz}$, $J_{\text{HF}}^4 = 8.1\text{Hz}$, ring- $\text{CH}=\text{CH}-$); 2.1 (1H, m,

CH(ring)-CH=CH-R); 1.9 (2H, dt, $J_{\text{HH}}^3 = 6.9\text{Hz}$, ring-CH=CH-CH₂-R); 1.44 (1H, m, CH ring); 1.2 (8H, s, 4(CH₂)); 1.12 (1H, m, CH ring); 0.8 (3H, t, $J_{\text{H-H}}^3 = 7.2\text{Hz}$). ¹⁹F nmr major (δ/ppm): -128.4 ppm (1F, dt, $J_{\text{F-F}}^2 = 154.95\text{Hz}$, $J_{\text{F-H}}^3 = 12.79\text{Hz}$); -141.8 ppm (1F, dd, $J_{\text{F-F}}^2 = 154.95\text{Hz}$, $J_{\text{F-H}}^3 = 12.79\text{Hz}$, $J_{\text{F-H}}^3 = 4.5\text{Hz}$). ¹⁹F nmr minor (δ/ppm): -135.8 ppm (1F, dd, $J_{\text{F-F}}^2 = 155.24\text{Hz}$, $J_{\text{F-H}}^3 = 14.60\text{Hz}$); 139.3 ppm (1F, dd, $J_{\text{F-F}}^2 = 155.24\text{Hz}$, $J_{\text{F-H}}^3 = 13.73\text{Hz}$); Ratio major/minor isomers on ¹⁹F nmr integration 17/1.

2.7 m) Synthesis of 1,1-difluoro-2-heptyl-2-vinylcyclopropane

A suspension of zinc dust (7.45 g, 0.114 mol) in THF (50 ml) was placed in an oxygen free 250-ml three-necked flask, which was purged with dry oxygen free nitrogen and equipped with a pressure equalizing addition funnel, a rubber septum, and a magnetic stirrer. Trimethylchlorosilane (10 ml) was added using a syringe and the suspension stirred for ½ hour. 2-heptyl-1,3-butadiene (6 g, 0.038mol) and a crystal of iodine were added. The flask was placed in a water bath at room temperature while dibromodifluoromethane (25 g, 0.12 mol) in THF (75 ml) was added slowly dropwise over a period of 3.5 hours. The water bath was removed and the reaction was stirred for 24 h at room temperature. The reaction mixture was quenched with 200 ml of 10 % aqueous HCl solution. The aqueous layer was extracted with CH₂Cl₂ and the combined organic extracts were washed with brine and dried over anhydrous MgSO₄. The solvent was evaporated under reduced pressure to give a pale yellow liquid. The crude product was fractional distilled under reduced pressure to give 1,1-difluoro-2-heptyl-2-vinylcyclopropane (1.5 g, 18.75 % yield) as colourless liquid (97 % purity on gc, $t_{\text{R}}=10.7$ min) (b.p 40⁰C, 0.8 mbar). The product was fractional distilled using a Fisher-Spalthror™ column (500-series) Distillator to give a 99.6:0.4 mixture of 1,1-difluoro-2-heptyl-2-vinylcyclopropane and 1,1-difluoro-2-(2'-nonenyl)cyclopropane respectively (0.15 g, 1.8 % yield) as a colourless liquid (99.9+% purity on capillary gc, major isomer $t_{\text{R}} = 10.85$ min, minor isomer $t_{\text{R}}=12.43$ min). (b.p. 35-37 ⁰C, 0.55 mm Hg); Found: C, 71.24; H, 9.94; F, 18.75 %; calculated for C₁₂H₂₀F₂: C, 71.25; H, 9.97; F, 18.78%. ¹H nmr (1,1-difluoro-2-heptyl-2-vinylcyclopropane, major isomer, δ/ppm): 5.6

(1H, dd, *trans* $J_{HH}^3 = 17.0\text{Hz}$, *cis* $J_{HH}^3 = 10.25\text{Hz}$, $-\text{CH}=\text{CH}_2$); 5.1 (1H, dd, *cis* $J_{HH}^3 = 10.25$, vicinal $J_{HH}^2 = 0.5\text{Hz}$, $-\text{CH}=\text{CHH}$); 5.0 (1H, dd, *trans* $J_{HH}^3 = 17.0\text{Hz}$, $-\text{CH}=\text{CHH}$); 1.5 (2H, m, $\text{R}-\text{CH}_2\text{-ring}$); 1.3 (1H, m, CH ring); 1.2 (10H, s, $5(\text{CH}_2)$); 1.1 (1H, m, CH ring); 0.81 (3H, t, $J_{HH}^3 = 7\text{Hz}$). **^{19}F nmr** (*1,1-difluoro-2-heptyl-2-vinylcyclopropane*, major isomer, δ/ppm): -135.73 (1F, ddd, $J_{F-F}^2 = 149.52\text{Hz}$; *syn* $J_{F-H}^3 = 13.40\text{Hz}$, *anti* $J_{F-H}^3 = 4.23\text{Hz}$); -137.62 (1F, ddd, *syn* $J_{F-F}^2 = 149.52\text{Hz}$, *syn* $J_{F-H}^3 = 11.52\text{Hz}$, *anti* $J_{F-H}^3 = 1.41\text{Hz}$). **^{19}F nmr** (*1,1-difluoro-2-isononenylcyclopropane*, minor isomer, δ/ppm): -126.6 (1F, dtd, $J_{F-F}^2 = 150.7\text{Hz}$, *syn* $J_{F-H}^3 = 10.9\text{Hz}$, *anti* $J_{F-H}^3 = 3.8\text{Hz}$); -143.4 ppm (1F, ddd, $J_{F-F}^2 = 150.7\text{Hz}$, *syn* $J_{F-H}^3 = 12.6\text{Hz}$, *anti* $J_{F-H}^3 = 4.5\text{Hz}$). **^{13}C nmr** (*1,1-difluoro-2-heptyl-2-vinylcyclopropane*, major isomer, δ/ppm): 133.9 (d, $J_{C-F}^3 = 2.9\text{Hz}$, $-\text{CH}=\text{CH}_2$); 116.2 (s, $-\text{CH}=\text{CH}_2$); 115.38 (dd, $J_{C-F}^1 = 287.90$, 291.30Hz , CF_2); 33.26 (t, $J_{C-F}^2 = 9.4\text{Hz}$, vinyl substituted cyclopropyl carbon); 31.8 (s, $\text{CH}_3\text{-CH}_2\text{-(CH}_2)_5\text{-}$); 30.1 (d, $J_{C-F}^3 = 3.5\text{Hz}$, $\text{R}-\text{CH}_2\text{-ring}$); 29.5 (s); 29.2 (s); 26.3 (d, $J_{C-F}^4 = 2.4\text{Hz}$, $\text{R}-\text{CH}_2\text{-CH}_2\text{-}$); 22.64 (s); 21.79 (t, $J_{C-F}^2 = 10.9\text{Hz}$, unsubstituted cyclopropyl carbon); 14.1 (s, $\text{R}-\text{CH}_3$). **IR**: 3049 cm^{-1} C-H stretch; 2980 cm^{-1} C-H stretch; 1650 cm^{-1} C=C stretch; 1400 cm^{-1} C-F bond; 990 cm^{-1} , 900 cm^{-1} out of plane C-H bend; 730 cm^{-1} methylene rock. **MS** (*1,1-difluoro-2-heptyl-2-vinylcyclopropane*, major isomer (rel. int.)): M^+ 202 (1), 198(10), 131 (21), 119(15.3), 118(89.8), 111(25.5), 109(27), 103(74.5), 97(71.3), 77 (54.12), 67(67), 55(81), 43(100), 41(100), 39 (82), 29(84), 27(85). **MS** (*1,1-difluoro-2-isononenylcyclopropane*, minor isomer) (rel. int.): M^+ 202 (1), 153 (5), 139(10), 112(22), 97(39), 77(27), 69(25), 56(40), 43(100), 41(50), 29(25), 27(18).

2.7 n) Attempted polymerisation of 1,1-difluoro-2-heptyl-2-vinylcyclopropane

The initiator AIBN (15 mole %) was dissolved in neat monomer in a dry ampule equipped with a magnetic stirrer and Young vacuum tap. The solution was freeze-thawed three times and the sealed ampule was heated at $50\text{ }^\circ\text{C}$ for 5 days with stirring. The reaction was monitored by ^{19}F nmr spectroscopy. The maximum conversion was 16.5 % by integration of the ^{19}F nmr spectrum. After 5 days of reaction the conversion remained constant and the contents of the

ampoule were precipitated in a 5-fold excess of cold methanol. The white precipitate was recovered by filtration (cinter filter porosity 3) and dried to give an extremely viscous white liquid (5% yield).

2.7 o) *Synthesis of 3-octen-1-mesylalcohol*

cis-3-Octen-1-ol (50g, 0.4mol) was placed in a 500 ml three-necked flask equipped with a calcium chloride guard tube, rubber septum, pressure equalizing addition funnel and a magnetic stirrer. The flask was cooled to 0°C and pyridine (180 ml) was added using a syringe. Methanesulphonylchloride (31 ml, 0.4 mol) was added dropwise using a syringe and the reaction mixture was stirred for 3 hour at 0 °C. The reaction mixture was quenched with water (100 ml) and the contents of the flask were poured into water (200 ml), the organic layer was separated and washed repeatedly with water and extracted with dichloromethane. The combined organic fractions were washed with an aqueous solution of HCl and dried over anhydrous magnesium sulphate. The solvent was rotary evaporated under reduced pressure and the crude product was fractionally distilled under vacuum to give *3-octen-1-mesylalcohol* (50.62 g, 61.5 % yield) as a colourless liquid (b.p. 80-90 °C, 10⁻¹ mbar) 99% purity on gc, *t_R*=15.95 min). Found C, 52.45; H, 8.75; calculated for C₉H₁₈O₃S C, 52.43; H, 8.74. ¹H nmr (δ/ppm): 5.5 (1H, dm, *cis* *J*_{HH}³ = 6.8Hz, RCH=CHR'); 5.3 (1H, dm, *cis* *J*_{HH}³ = 6.8Hz, RCH=CHR); 4.2 (2H, m, CH₂-SO₂CH₃); 2.9 (3H, t, *J*_{HH}⁵ = 2.4Hz, SO₂CH₃); 2.49 (2H, s, C=C-CH₂-CH₂SO₂); 2.05 (2H, s, R-CH₂-CH=CH); 1.3 (2H, m); 0.8 (3H, t, *J*_{HH}³ = 2.8Hz, CH₃-R). ¹³C nmr (δ/ppm): 134 (RCH=CHR'); 123 (RCH=CHR); 66 (-SO₂CH₃); 38, 32, 28 (2(-CH₂-CH=CH-) and -CH₂-O-SO₂); 27 (CH₃-CH₂-R); 14 (CH₃-R). IR (cm⁻¹): 2958 CH₃; 1355 and 1175 SO₂ bands. MS (rel. int.): M⁺ not seen, 110 (25), 95 (19), 81 (100), 79 (65), 67 (91), 54 (73), 41 (78), 29 (51).

Chapter 3

Synthesis of potentially
electrostrictive polymers via
ring-opening metathesis polymerisation
and copolymerisation of fluorinated
bicyclo[2.2.1]hept-2-ene monomers

3.1 Introduction

The work described in this chapter concerns the ring-opening metathesis polymerisation (ROMP) of partially fluorinated bicyclo[2.2.1]hept-2-ene monomers to give partially fluorinated poly(1,3-cyclopentylenevinylene)s. The generalised polymerisation scheme is shown in *Figure 3.1*, where the Rfs represent fluorine atoms or fluoroalkyl groups.

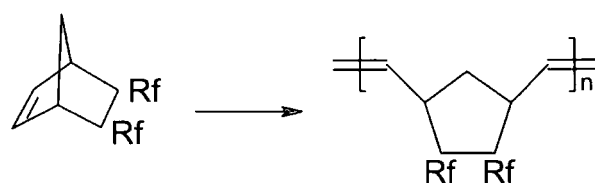


Figure 3.1 Generalised polymerisation scheme

The first syntheses of materials of this kind were carried out in Durham by Wilson.²⁶ The monomers were readily synthesised via Diels-Alder reaction of cyclopentadiene and fluorinated alkenes, as shown in *Figure 3.2*.

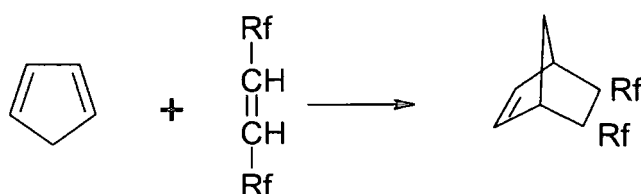


Figure 3.2 Generalised scheme for monomer synthesis²⁶

The reported polymers were obtained in good to excellent yields, however, due to the fluorine atom substitutions and the relatively bulky cyclopentane ring in the repeat units the T_g s obtained were above room temperature, thus a modification of monomers or polymers was required in this work in order to lower the T_g . The hydrogenation of the double bonds in these polymers was considered because it was expected that the transformation of the rigid double bonds into single bonds would increase the conformational mobility thereby increasing the flexibility of the polymer backbone. The generalised hydrogenation process for this type of polymer is shown

schematically in *Figure 3.3*.

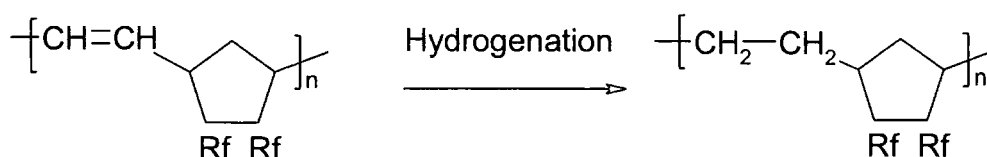


Figure 3.3 Hydrogenation of partially fluorinated poly(1,3-cyclopentenevinylene)s

Another alternative considered in order to obtain an elastomer was the copolymerisation with a co-monomer which could give a flexible repeat unit. The ROMP of cyclopentene, which gives flexible pentenylene repeat units, was selected for this purpose. The co-polymerisation of both monomers and hydrogenation of the double bonds in the resulting material was expected to give the targeted fluoroelastomer. The generalised synthetic route is shown in *Figure 3.4*.

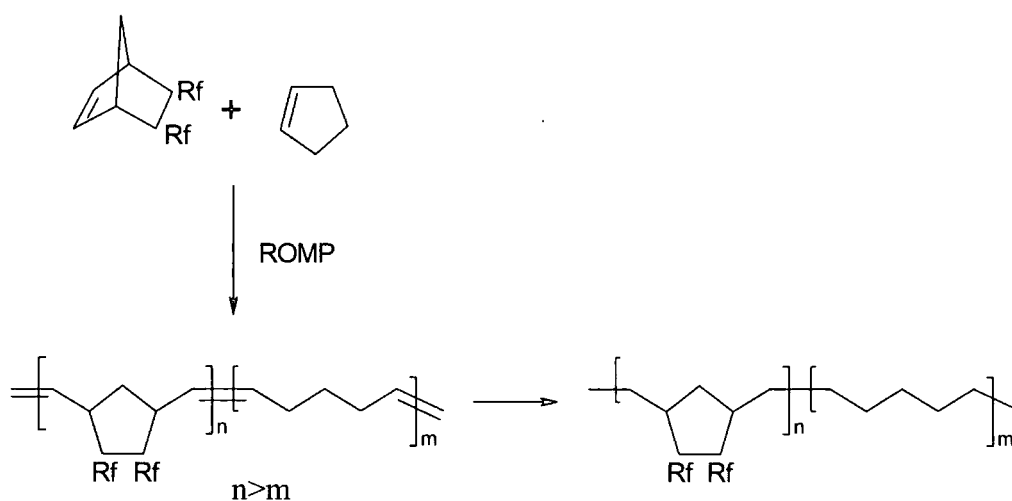


Figure 3.4 Generalised synthetic route to a potential electrostrictive elastomer

3.1 a) The Diels-Alder reaction

The Diels-Alder reaction involves the 1,4-addition of a *cis*-oriented conjugated diene, and a dienophile. This reaction is a very useful synthetic methodology for the preparation of six-membered rings, as shown in *Figure 3.5*

for the basic reaction between 1,3-butadiene and ethylene, because of the almost unlimited possibilities for variation of both diene and dienophile.



Figure 3.5 Scheme for the Diels-Alder reaction between butadiene and ethene

The Diels-Alder reaction may be divided into two extreme reaction types, firstly the normal Diels-Alder reaction in which dienes are activated by electron donating substituents, for example, $-\text{NMe}_2$, $-\text{OMe}$, $-\text{CH}_3$, and dienophiles which are activated by electron withdrawing substituents, for example $-\text{CN}$, $-\text{COOMe}$, $-\text{CHO}$, $-\text{NO}_2$. Secondly, the Diels-Alder reaction is Inverse-Electron Demand, in which the diene is activated by electron-withdrawing substituents and the dienophile by electron donating substituents. If both components in the reaction are either 'electron-rich' or 'electron poor' the reaction is generally sluggish or does not occur, in general the greater the difference in character the faster the reaction proceeds.⁴⁷

The fluorinated dienes are generally less active in the Diels-Alder reaction than their hydrocarbon equivalents, whereas fluorinated dienophiles are generally more reactive than their hydrocarbon equivalents.⁸⁵

3.1 b) Ring-opening metathesis polymerisation

As mentioned in the introduction to this work, the first citation of an olefin metathesis reaction catalysed by a transition metal was published in 1955.³¹ In that work the ring-opening metathesis polymerisation of bicyclo[2.2.1]hept-2-ene to give poly(1,3-cyclopentylenevinylene) was described. Since then the ROMP bicyclo[2.2.1]hept-2-ene substituted with nitrile, amide, imide, ester, pyridyl, acid anhydride, chlorine, bromine and fluorine units have been well established and numerous patents have been published concerning such reactions.^{86-88,94} The propagation mechanism in

ROMP has been the subject of intense research and the scheme, initially proposed by Herisson and Chauvin, see *Figure 3.6*, is now securely established.⁸⁹

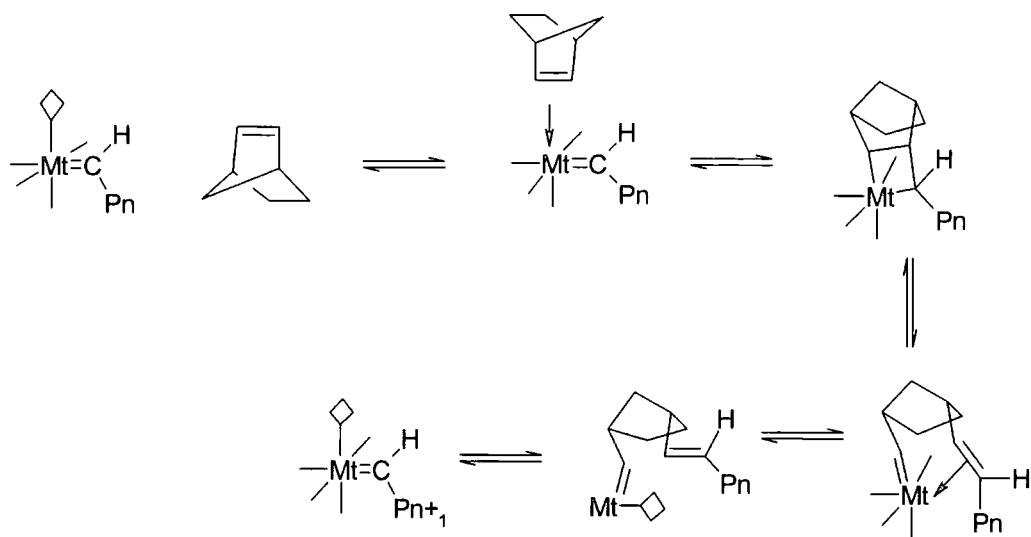


Figure 3.6 Proposed ROMP mechanism scheme by Herisson and Chauvin⁸⁹

The propagation reaction involves a transition metal carbene as the active chain end, which must possess a vacant coordination site. During the propagation the carbon-carbon double bond of the cycloalkene coordinates at this vacant site to form a metal π complex. This complexation step is followed by the formation of a metallacyclobutane intermediate that is usually unstable and cleaves to form a new metal carbene and a new carbon-carbon double bond that de-coordinates to regenerate the propagating metal carbene with a vacant coordination site. When 'classical initiators' are used, the metal carbene is formed from an organometallic reagent precursor, i.e. tungsten or molybdenum derivatives, which generally need activation by a co-catalyst, which can be an alkylating agent, such as tetramethyltin, or tetraphenyltin. The mechanism for the generation of a metal carbene from a transition metal halide and an alkylating agent is not well understood at present, however it is empirically established that a 2:1 molar ratio of alkylating agent to transition metal compound is generally optimal.⁹⁴

3.1 c) The hydrogenation of polymers

The hydrogenation of polymers is a practical methodology to generate new products with novel properties.⁹⁰ Polymer crystallinities tend to increase with increasing hydrogenation, but glass transition temperatures can either increase or decrease, depending upon the starting material. The saturated polymers are obtained from their unsaturated analogues by catalytic or noncatalytic processes, which differ in yield, selectivity, side reaction, and catalyst poisoning. In industry, hydrogenation is usually carried out using cobalt or nickel catalysts at elevated temperature and pressure, however these industrial methodologies were not suitable for the small-scale work reported here.

A common and convenient non-catalytic hydrogenation is based on the *in-situ* generation of diimide in a hot solvent. This process is shown schematically in Figure 3.7.

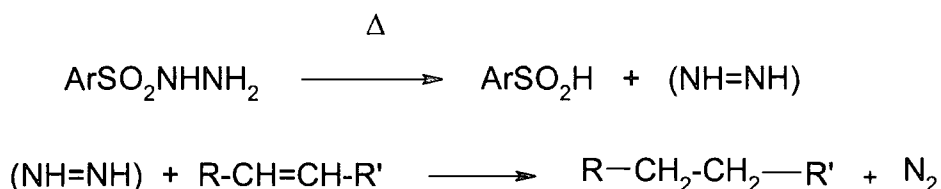


Figure 3.7 Non-catalytic hydrogenation mechanism

When *p*-toluensulfonylhydrazide is added to a solution of an unsaturated polymer at temperatures above 90 °C, diimide is generated, double bonds are reduced and *cis-trans* isomerisation of the remaining units is promoted. Attachment of hydrazide fragments to the polymer chains, which can be minimised by the addition of an antioxidant, depolymerisation and cyclisation are possible side reactions.

3.2 Study of the synthesis and hydrogenation of poly(5,5,6-trifluoro-6-trifluoromethyl-1,3-cyclopentylenevinylene)

3.2 a) Synthesis of 5,5,6-trifluoro-6-trifluoromethyl bicyclo[2.2.1]hept-2-ene

The monomer was synthesised from perfluoropropene and cyclopentadiene via a Diels-Alder reaction. The Diels-Alder addition reaction of an unsymmetrical substituted acyclic alkene to an unsubstituted cyclic diene leads to *endo* and *exo* isomers, as illustrated in Figure 3.8, for the reaction between perfluoropropene and cyclopentadiene.

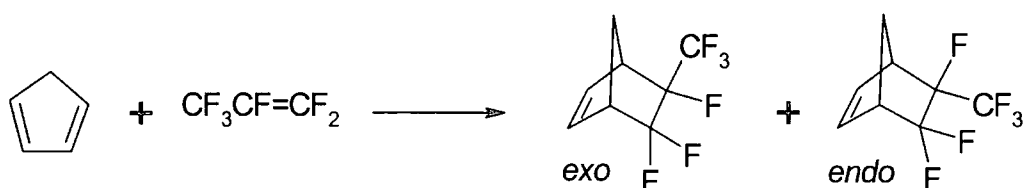


Figure 3.8 Synthesis scheme for the *exo* and *endo* mixture of 5,5,6-trifluoro-6-trifluoromethylbicyclo[2.2.1]hept-2-ene (I)

The starting materials were mixed and heated in a sealed Carius tube at 180°C for 3 days to give a colourless liquid (87 % yield) shown to be a mixture of two products in a 68:32 ratio by capillary gc, these two components accounting for over 99% of the material. See section 3.5 for experimental details. The products were fully characterised by analysis and spectroscopy. The gc-MS confirmed the molecular formulae of the products, M^+ 216, and both exhibited a base peak at m/e 66 (C_5H_6^+), arising from the retro Diels-Alder reaction of the parent ion, this fragmentation mode is characteristic of bicyclo[2.2.1]hept-2-enes.⁴⁷ The IR spectrum (see appendix AX23) showed the characteristic, vinylic C-H stretch (3080 cm^{-1} , weak), $-\text{CH}=\text{CH}-$ stretch (1716 cm^{-1} , weak) and C-F stretches ($1390\text{--}1000\text{ cm}^{-1}$, strong). The analysis of the ^{19}F nmr and ^1H nmr spectra (see appendix AX24 and AX25) were more complex than would be expected for a single component, however, they can be explained by the fact that the individual adducts are produced as mixtures of *endo* and *exo* isomers, the analysis of the ^{19}F nmr spectrum gave two sets of signals in a ratio 57:43, corresponding to the *exo* and *endo* isomers respectively.

The stereochemical assignment of these adducts were based on earlier work by Stone and Smart.^{26,91,92} The ^{13}C nmr spectrum (see appendix AX26) was analysed on the basis of the carbon-fluorine coupling constants, the carbon bearing one fluorine atom and the trifluoromethyl group appears as a doublet of multiplets at 95.4 ppm with a coupling constant of 209.2 Hz, the CF_2 carbon appears as two groups of doublets of doublet of doublets centred at 124.8 ppm, the observed coupling constants for the major isomer *exo* are $J^1_{\text{C-F}} = 272.3$ and 265.9 Hz and $J^2_{\text{C-F}} = 16.8$ Hz, but the couplings of the minor *endo* isomer could not be resolved. The trifluoromethyl carbons appear as two groups of quartets of doublets centred at 122.28 ppm and 121.88 ppm with C-F couplings $J^1_{\text{C-F}} = 283.5$ Hz and $J^2_{\text{C-F}} = 32.1$ Hz for the major signals corresponding to the *exo* isomer and $J^1_{\text{C-F}} = 282.6$ Hz and $J^2_{\text{C-F}} = 31.3$ Hz for the minor signals assigned to the *endo* isomer. The *exo* and *endo*-isomers co-distil and have similar gc retention volumes. No attempt to separate them was made, but since the objective is to make a low T_g material the copolymerisation of mixtures of *exo*- and *endo*-isomers might help this objective.

3.3 b) Ring-opening metathesis polymerisation of 5,5,6-trifluoro-6- trifluoromethylbicyclo[2.2.1]hept-2-ene

The scheme for the ROMP of 5,5,6-trifluoro-6-trifluoromethyl bicyclo[2.2.1]hept-2-ene is shown in Figure 3.9.

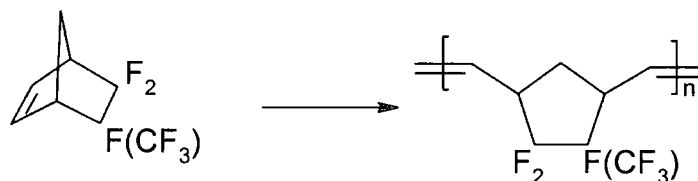


Figure 3.9 Scheme for ROMP of 5,5,6-trifluoro-6-trifluoromethylbicyclo[2.2.1]hept-2-ene (I)

Two different polymerisation experiments were carried out with monomer (I). Two types of initiator; namely, those derived from tungsten hexachloride and molybdenum pentachloride, by reaction with two equivalents of

tetraphenyltin were used. Toluene was used as a solvent and the experiments were carried out at room temperature.

The first polymerisation involved the use of the tungsten hexachloride derived initiator. In the experiment, a freshly made stock solution 0.01 M of WCl_6 (1 equivalent) in toluene was injected into an oxygen-free ampoule containing two equivalents of the co-catalyst. The blue-black mixture was vigorously stirred for approximately 10 minutes until the colour changed to dark-brown indicating that the metal carbene initiator had formed. 5,5,6-Trifluoro-6-trifluoromethylbicyclo[2.2.1]hept-2-ene (500 equivalents) was added and after approximately three hours swollen brown lumps of solid material were observed in the reaction vessel. The mixture was stirred for one hour more and then quenched by addition of few drops of methanol. The solid obtained was dissolved in the minimum amount of acetone and was precipitated in cold n-hexane to give poly(4,4,5-trifluoro-5-trifluoromethyl-1,3-cyclopentylenevinylene) (*Ia*) as a white powder in a 55 % mass recovery. The characterisation of this polymer is discussed later.

The second polymerisation carried out involved the use of the molybdenum pentachloride derived initiator. As in the previous polymerisation, a freshly made 0.01 M stock solution of MoCl_5 (1 equivalent) in toluene was injected into an ampoule containing two equivalents of the co-catalyst tetraphenyltin. After 5 minutes of vigorous stirring the colour of the solution changed from the initial dark-green to dark-brown, and 5,5,6-Trifluoro-6-trifluoromethylbicyclo[2.2.1]hept-2-ene (500 equivalents) was added. The solution was stirred for approximately 3 hours when it became progressively more viscous until the stirrer stopped. The reaction was quenched by addition of a few drops of methanol and the solid obtained was dissolved in the minimum amount of acetone and precipitated in cold n-hexane to give poly(4,4,5-trifluoro-5-trifluoromethyl-1,3-cyclopentylenevinylene) (*Ib*) as a white powder, and in a 30 % mass recovery. The characterisation of this polymer is discussed later.

3.2 c) Hydrogenation of poly(4,4,5-trifluoro-5-trifluoromethyl-1,3-cyclopentylenevinylene)

The hydrogenation scheme for the polymers (*Ia*) and (*Ib*) to give polymers (*IIa*) and (*IIb*) is shown schematically in Figure 3.10.

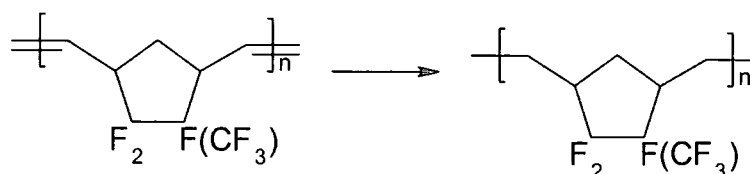


Figure 3.10 Scheme for the hydrogenation of polymer (*Ia*) and (*Ib*)

The materials were dissolved in 1,1,1-trifluorotoluene, which was a suitable high boiling point solvent for the polymers. *p*-Toluenesulphonylhydrazide was added in approximately 10 to 15 fold excess by weight in small aliquots at intervals of approximately 30 minutes, and the solution was refluxed at 110°C with stirring. Once the hydrogenation process was completed the contents of the flasks were poured into a 10 fold excess of methanol and stirred for 30 minutes to dissolve the residual biproduct ($\text{CH}_3\text{C}_6\text{H}_4\text{SO}_2\text{H}$) leaving a white precipitate, which was recovered by filtration, dissolved in toluene or acetone and reprecipitated in cold methanol to give the polymers (*IIa*) and (*IIb*).

The vinyl signal of the polymers between 5 and 6 ppm in the ^1H nmr spectra displayed very low intensity, the integration of the spectra of the new materials gives a percentage of hydrogenation of 83 % for polymer (*Ia*) and 95 % hydrogenation for polymer (*Ib*). The characterisation of these polymers is discussed below.

3.2 d) Structural characterisation of the polymers (Ia), (Ib), (IIa) and (IIb)

3.2 d) (i) Nmr spectroscopy

The microstructure of a wide range of partially fluorinated poly(1,3-cyclopentylenevinylene)s was previously investigated in Durham for polymers obtained from a variety of monomers and initiator.⁹³ Such polymers can be structurally characterised by elemental analysis, infrared (IR), ¹H nmr and ¹⁹F nmr spectroscopy, however the most valuable analytical probe to determine chain microstructure is ¹³C nmr spectroscopy.⁹⁴

The polymer repeat unit, shown in *Figure 3.12*, has eight different carbon environments.

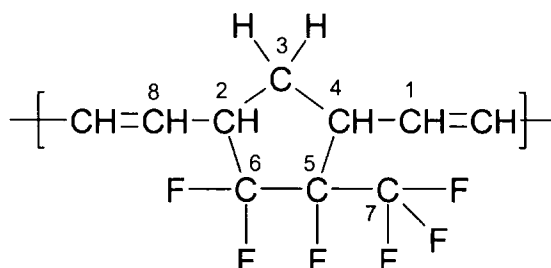


Figure 3.11 The carbon environments for the polymer (I)

Most of the classical initiators in ROMP are not well defined and probably contain different initiating species, this can give rise to a great variety of structures as a result of incorporating monomer residues in different configurations.⁹⁵ Moreover, monomer (I) exists as a mixture of *endo* and *exo* isomers both of which are racemic. On incorporation into the polymer chain the repeat unit has the structure shown in *Figure 3.11*, in which the vinylene unit can be *cis* or *trans*, the fluorinated cyclopentane unit can be incorporated in a head-tail, head-head or tail-tail fashion, the trifluoromethyl group can be *syn* or *anti* with respect to the adjacent vinylene carbons and the incorporated unit can be derived from an *R* or *S* monomer. This gives rise to an enormous range of possible structures and it is not surprising that in the past the nmr spectra of polymer (I) could not be disentangled in any great detail. However, since these polymers were first prepared high-resolution nmr has become available and

consequently more detailed assignment of the signals is possible and will be presented in this work.

Previous experience in the polymerisation of 5,5,6-trifluoro-6-trifluoromethyl[2.2.1]hept-2-ene indicated that the polymer (*Ib*) synthesised using the MoCl_5 derived initiating system displays mainly *trans* double bonds, and polymer (*Ia*) initiated using the WCl_6 derived catalyst gives a mixture of *cis* and *trans* double bonds.²⁶ Due to the complexity of the nmr spectra obtained from both polymers, it was decided to start the analysis with the marginally less complex ^{19}F nmr spectra, shown in *Figure 3.12*.

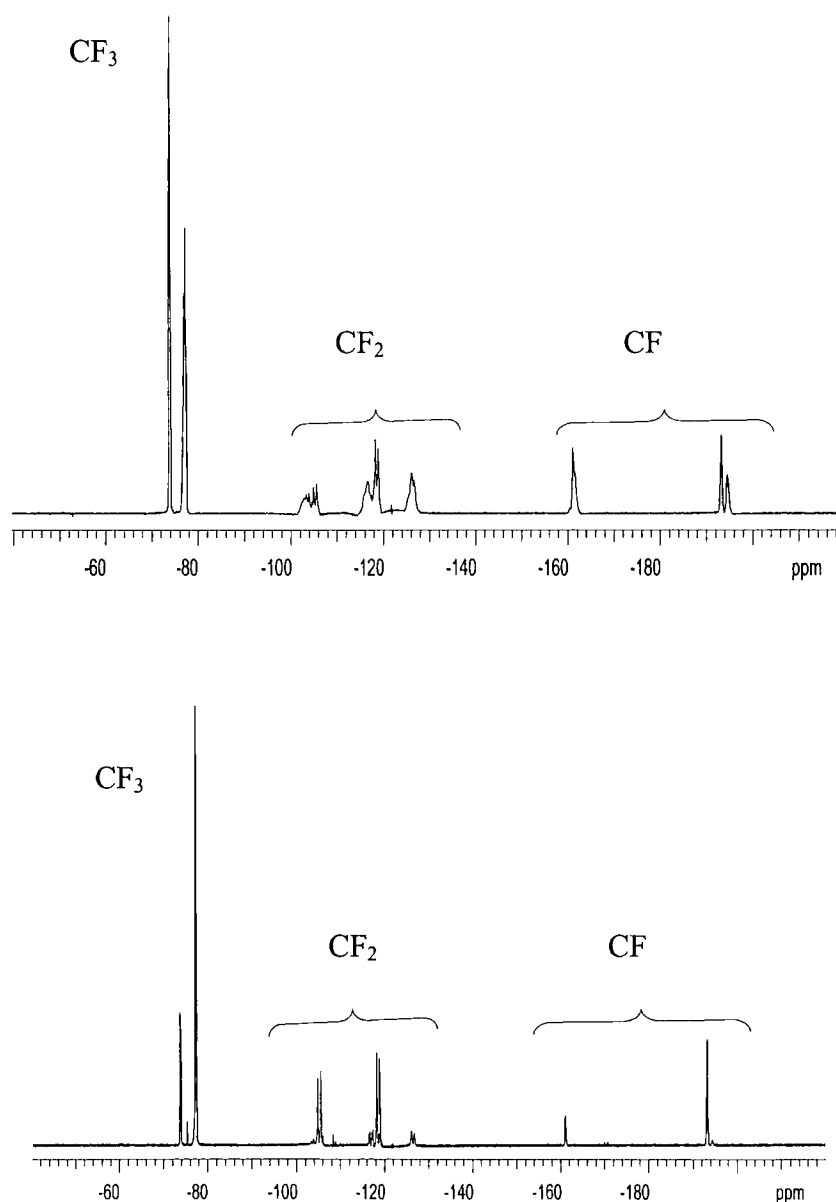


Figure 3.12 The ^{19}F nmr spectra of polymer (Ia) (above) and (Ib) (below)



Three sets of signals can be seen and assigned, those for $-\text{CF}_3$ occur between -70 and -80 ppm, those for the difluoromethylene group between -100 and -130 ppm and those for C-F units between -160 and -200 ppm see *Figure 3.12*. The signals for the trifluoromethyl groups in the spectrum of polymer (*Ib*) appear as two broad doublets displaying coupling with the adjacent fluorine atom. The smaller signal occurs at -77.2 ppm ($J_{\text{FF}}^2 = 50.4$ Hz) and the larger at -73.0 ppm ($J_{\text{FF}}^2 = 50.4$ Hz) with relative integrated intensities of 20:80 respectively. In case of the polymer (*Ia*) the signals of the trifluoromethylene groups appear in the spectrum as two broad multiplets at -73.8 and -77.2 ppm, with relative integrated intensities of 46:54 respectively.

From the integration of the relative intensities of the signals assigned to the fluorine atoms in the trifluoromethyl group, the relative proportions of the structures (*i*) and (*ii*) shown in *Figure 3.13* incorporated into the polymer can be determined, and hence the relative incorporation of *exo* and *endo* monomers from the monomer feed.

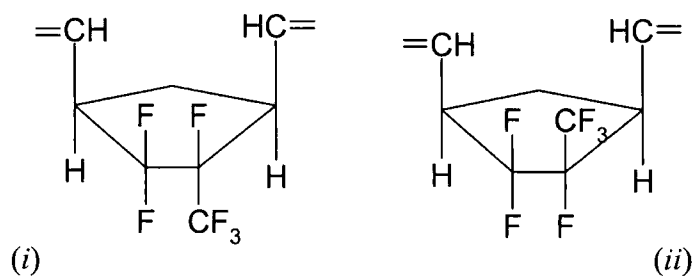
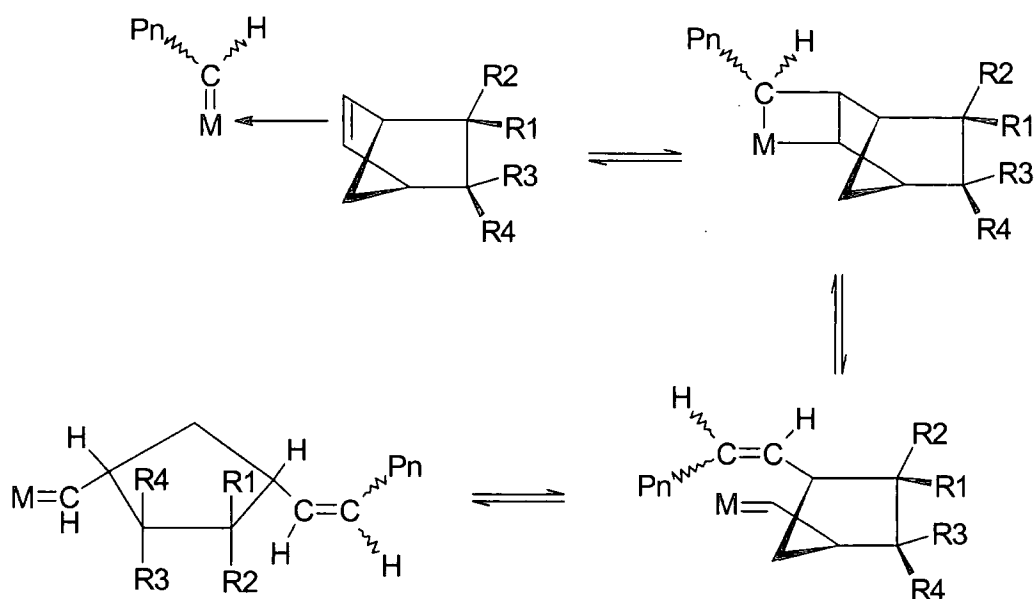


Figure 3.13 Polymer repeat unit structures

The mechanism and stereochemical regulation of ROMP of bicyclo[2.2.1]hept-2-enes has been the topic of detailed study over many years.⁹⁶⁻⁹⁹ It is generally accepted that for reactions of substituted bicyclo[2.2.1]hept-2-ene with transition carbene initiators approach to the double bond from the *exo*-direction is favoured. This gives rise to the mechanism depicted in *Figure 3.14*, where the metallocyclobutane formed initially opens to give a new propagating metallocarbene chain end after incorporating one monomer unit.



Pn is the polymer chain containing n monomeric units

Figure 3.14 Mechanism for the ring-opening polymerisation of substituted bicyclo[2.2.1]hept-2-ene

It has been proved by ozonolysis experiments that in poly(1,3-cyclopentylenevinylene) the cyclopentane ring has a *cis*-1,3-structure. From the mechanistic scheme shown in Figure 3.14 the *endo*-substituents R2 and R3 will be on the same side of the ring as the carbon-carbon double bond in the polymer chain. That is to say that the racemic monomer (\pm) *I-exo* gives the polymer structure shown in Figure 3.15-(i), and the monomer (\pm) *I-endo* gives the structure shown in Figure 3.15-(ii).

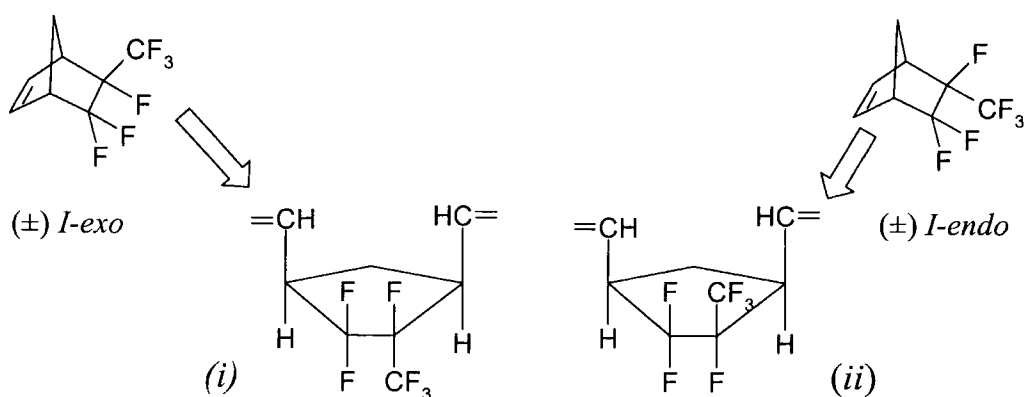


Figure 3.15 Polymer stereochemistry

Based on the previously established structural assignments,^{26,91,92} the integration of the signals from the trifluoromethyl group in the polymer (*Ia*) gives a 46:54 ratio for structures (*i*) and (*ii*) respectively, and the integration for polymer (*Ib*) gives a 20:80 ratio for the same pair of structures. The polymerisation started from a 43:57 mixture of *exo* and *endo* isomers respectively, so it can be said that under the experimental conditions employed, the $\text{WCl}_6/2\text{Ph}_4\text{Sn}$ initiator system does not discriminate significantly between *endo* and *exo* monomers. Whereas when using the less reactive $\text{MoCl}_5/2\text{Ph}_4\text{Sn}$ initiator system, the *endo* monomer was incorporated to a significantly greater extent.

The ^{19}F nmr spectrum of polymer (*Ib*) with mainly *trans* double bonds is much simpler to interpret than that of (*Ia*), the signals assigned to the difluoromethylene groups appear as two major group of signals at -104.5 ppm ($J_{\text{FF}}^2 = 250.3$ Hz) and -118.5 ppm ($J_{\text{FF}}^2 = 250.3$ Hz, $J_{\text{FF}}^3 = 58.7$ Hz). Minor signals were observed at -116.3 ppm ($J_{\text{FF}}^2 = 244.6$ Hz, $J_{\text{FF}}^3 = 76.1$ Hz) and -125.7 ppm ($J_{\text{FF}}^2 = 260.4$ Hz), the integration of both groups of signals gives a ratio of 21:79 which is consistent with that determined from the trifluoromethyl group integrations. The signals arising from the difluoromethylene group in the spectrum of polymer (*Ia*) have the same shift as those in polymer (*Ib*), although there is considerable overlapping and an accurate integration cannot be made. The signals from the CF group are well-resolved in both spectra and appear as three broad singlets with different intensities, the singlet at -193 ppm in both spectra is assigned to the repeat unit (*i*) in Figure 3.15, and when the relative intensities of these signals are compared with the sum of the other signals the incorporation ratio of *endo* and *exo* isomers obtained is entirely consistent with the previous determinations.

In the ^{13}C nmr spectrum of polymer (*Ib*), shown in Figures 3.16 and 3.17, the signals due to the trifluoromethyl carbon C7 are partially distinguished as a quartet of doublets at 122 ppm, with coupling constants $J_{\text{C-F}}^1 = 280.3$ Hz and $J_{\text{C-F}}^2 = 32.98$ Hz. An overlapped shoulder is observed in each signal, and this observation is attributed to the presence of the minor component structure (*i*) in Figure 3.15. In the signals assigned to the carbon C6, a doublet of doublet of doublets, is observed at 124.5 ppm with $J_{\text{C-F}}^1 = 269$ and 260 Hz and $J_{\text{C-F}}^2 = 33$ Hz, one part of this signal overlapping with the multiplet arising from

the vinyl carbons. The carbon C5 appears at 96.5 ppm as a doublet of multiplets with $J^1_{\text{C-F}} = 225$ Hz. The vinyl carbons C1 and C8 appear as a complex multiplet of signals between 127 and 132 ppm.

In the methylene region, shown in *Figure 3.17*, seven broad signals with different intensities are observed. The signals due to the methylene carbon C3 are readily assigned between 30 and 35 ppm, the major and minor signals at 32.6 and 31.3 ppm respectively are assigned to carbon C3 in a *trans-trans* sequence of double bonds, the integrated intensity ratio of these signals is 86:14 which, within experimental error, is consistent with the ratio of structures (i) and (ii), obtained from other signal integrations. A very small signal is also observed at 33.5 ppm as a multiplet, which is assigned to carbon C3 in a *cis/trans* sequence.⁹⁴ Although the integration is not accurate, this assignment leads to the conclusion that there is a 96:4 *trans:cis* ratio of double bonds in polymer (Ib). The four broad signals between 40 and 50 ppm appear as two major and two minor signals and are assigned to the allylic carbons C2 and C4 in *trans* vinylene sequences, the assignments are based on the multiplicities and intensities observed and the fact that allylic carbons adjacent to *trans* double bonds appear at lower frequency than their *cis* equivalents.⁴⁷ This leads to the conclusion that the signal at 47.8 ppm (triplet, $J^2_{\text{C-F}} = 24.2$ Hz) is assigned to carbon C2 and the doublet at 43.0 ppm ($J^2_{\text{C-F}} = 23.7$ Hz) is assigned to the carbon C4. The two minor signals at 46.6 ppm (doublet, $J^2_{\text{C-F}} = 23.7$ Hz) and 45.46 ppm (multiplet) were assigned to the C2 and C4 carbons in the minor component, structure (i) shown in *Figure 3.15*, and the integrated intensity ratios ca 20:80 correspond with the established incorporation ratio of the two repeat units. Finally, the low intensity signal observed at 38.48 ppm is assigned to carbon C4 in a *cis* vinylene sequence as will be confirmed from the analysis of the ^{13}C nmr spectrum of polymer (Ia).

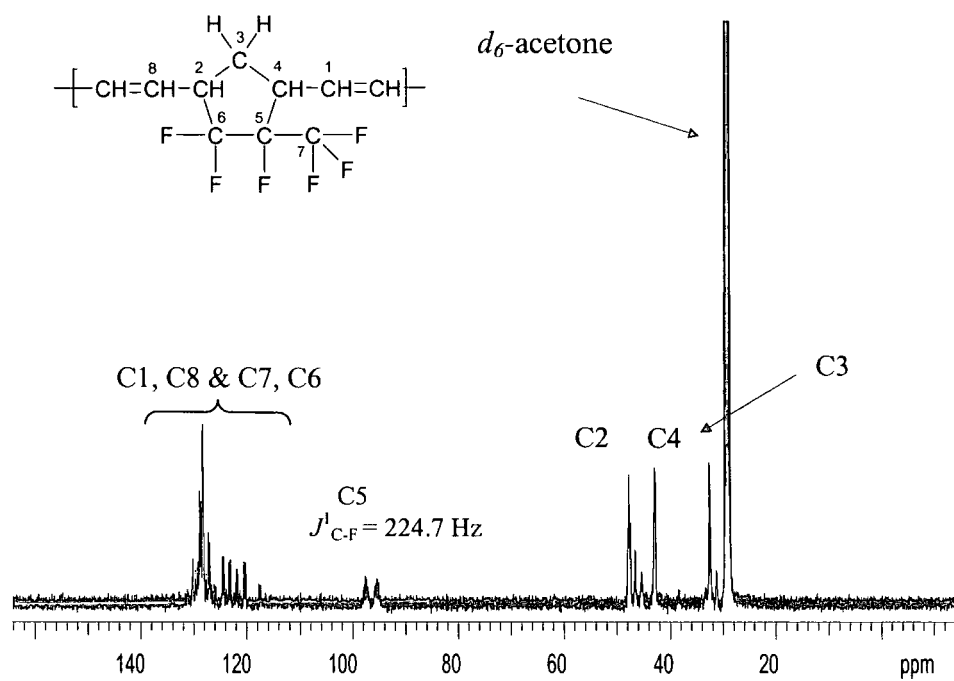


Figure 3.16 The ^{13}C nmr spectrum of polymer (Ib)

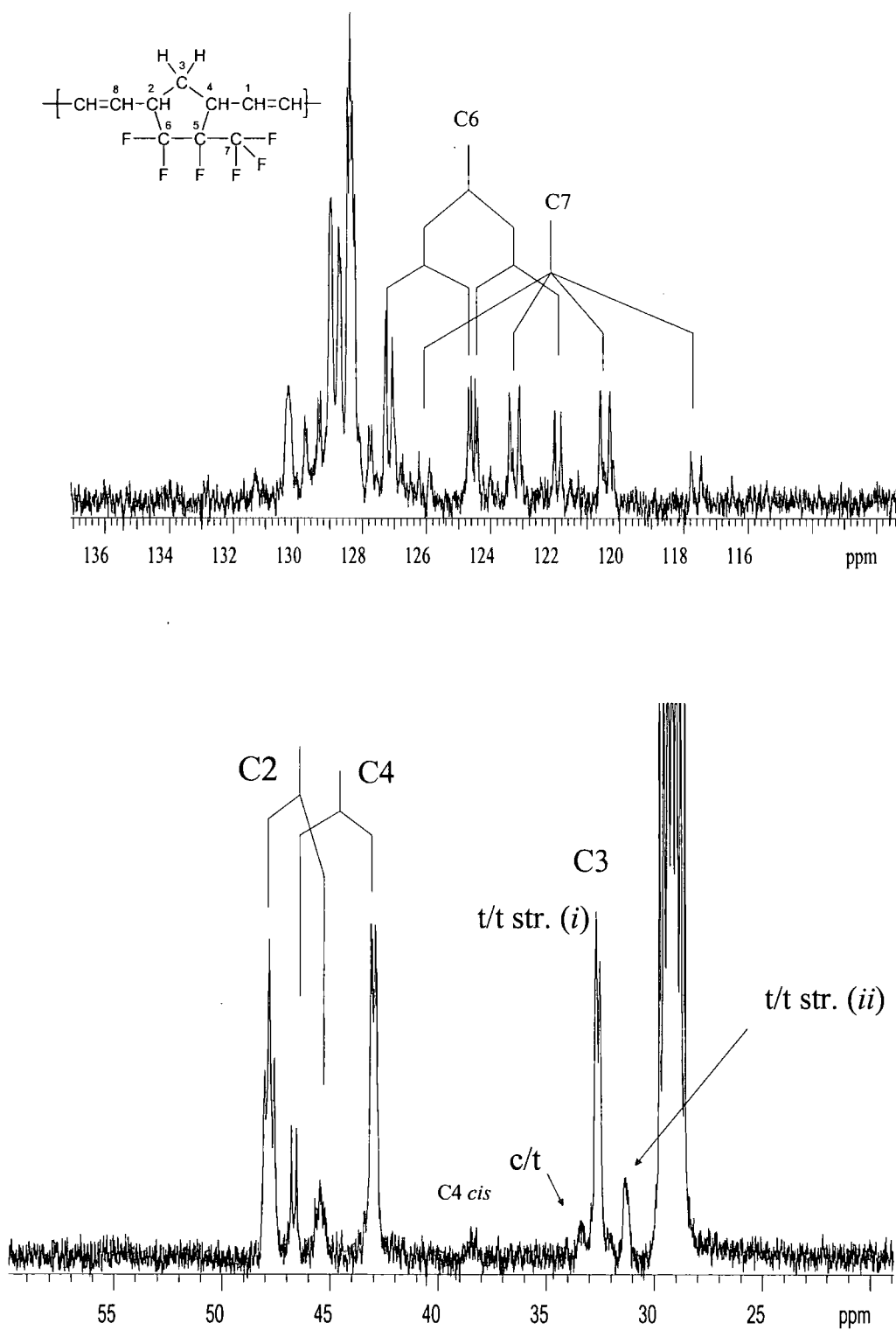


Figure 3.17 The expanded ^{13}C nmr spectrum of the vinyl region of polymer (Ib)(above) and the saturated region (below)

In the ^{13}C nmr spectrum of the polymer (*Ia*) shown in *Figure 3.18* and *3.19*, the signal of the CF_3 group, carbon C7 is partially resolved as a quartet of multiplets centred at 121.5 ppm with a coupling constant $J_{\text{C-F}}^1 = 285.8$ Hz, and the partially resolved signal of the carbon C6 appears to be a triplet of multiplets centred at 124.2 ppm with $J_{\text{C-F}}^1 = 271$ Hz. The signal of the carbon C5 appears at 98 ppm as a doublet of multiplets with $J_{\text{C-F}}^1 = 201.9$ Hz. The vinylic carbons C1 and C8 appear as a set of broad signals between 125 and 132 ppm. The methylene carbon C3 signal is much more complex than the analogous signal in the “all *trans*” polymer (*Ib*). Two groups of three signals are seen due to the existence of the different configurations of the trifluoromethyl group ((*i*) and (*ii*) in *Figure 3.15*), and different *cis:trans* vinylene sequences. The sets of three signals are attributed to the three possible *cis-cis*, *cis-trans* \equiv *trans-cis*, and *trans-trans* sequences for the carbon C3 nucleus in structures (*i*) and (*ii*); see assignments in *Figure 3.19*. The signals for the saturated carbons C2 and C4 appear between 36 and 50 ppm displaying eight broad signals (two overlapped) and based on the previous analysis of the ^{13}C nmr spectrum for polymer (*Ib*) the signals of carbons C2 and C4 in a *trans* vinylene sequence are assigned as depicted in *Figure 3.19*. The integration of the signals from carbon C2 at 45.5 and 48 ppm gives a 36:64 ratio for the incorporation of structures (*i*) arising from *exo*-monomer and (*ii*) from *endo*-monomer respectively, see *Figure 3.15*, and indicates an increased incorporation of structure (*i*) in *trans* vinylene sequences of polymer (*Ia*) compared to the 20:80 ratio in polymer (*Ib*). The other 4 signals are then assigned to the carbons C2 and C4 in a *cis* double bond environment, but the overlapping of the signals does not allow integration. Clearly from a simple comparison of the spectra of polymers (*Ia*) and (*Ib*), the former displays a much more complex microstructure than the latter, which is consistent with the higher reactivity and lower selectivity typically displayed by tungsten based initiators systems as compared to their molybdenum analogues.

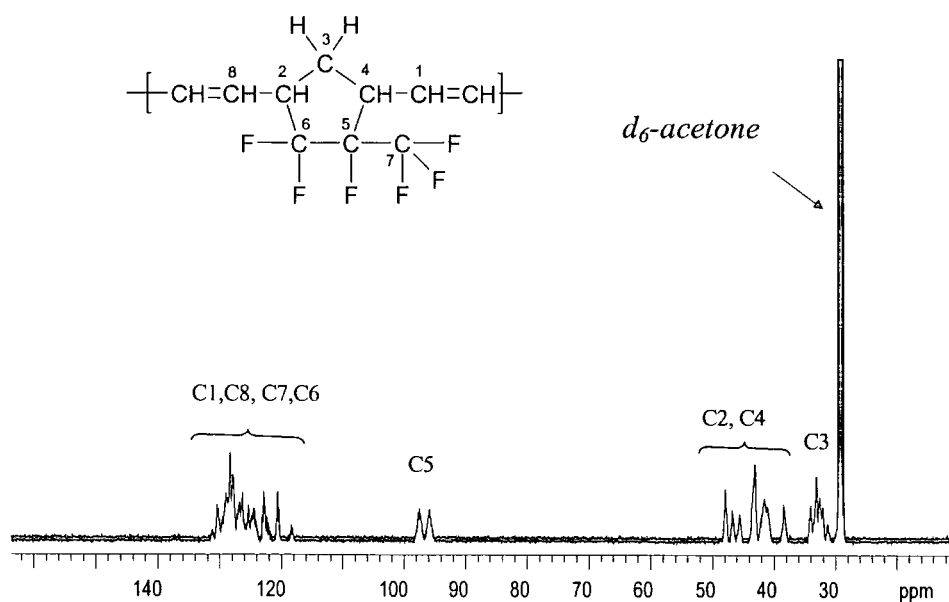


Figure 3.18 The ^{13}C nmr spectrum of polymer (Ia) with assignments

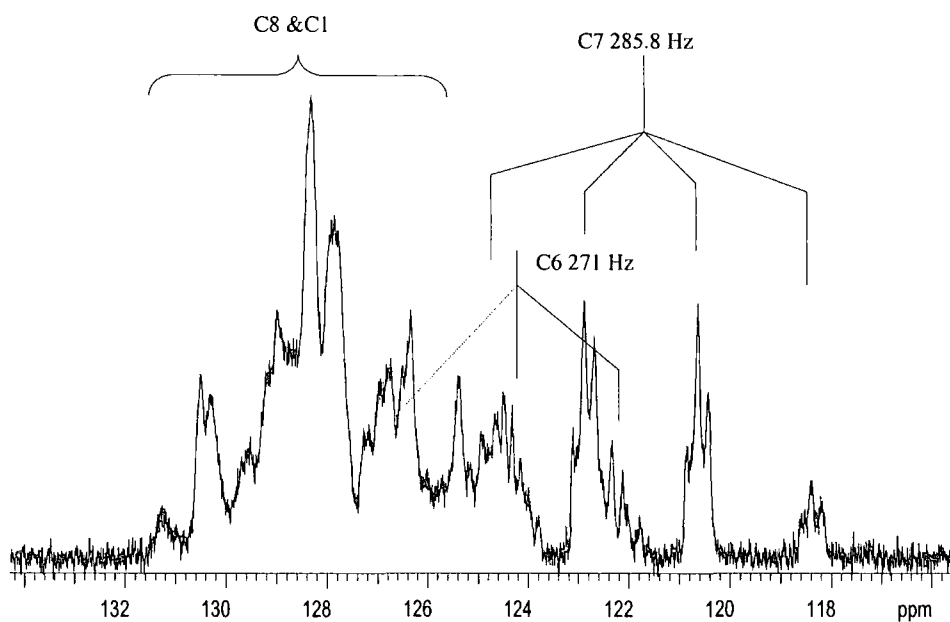
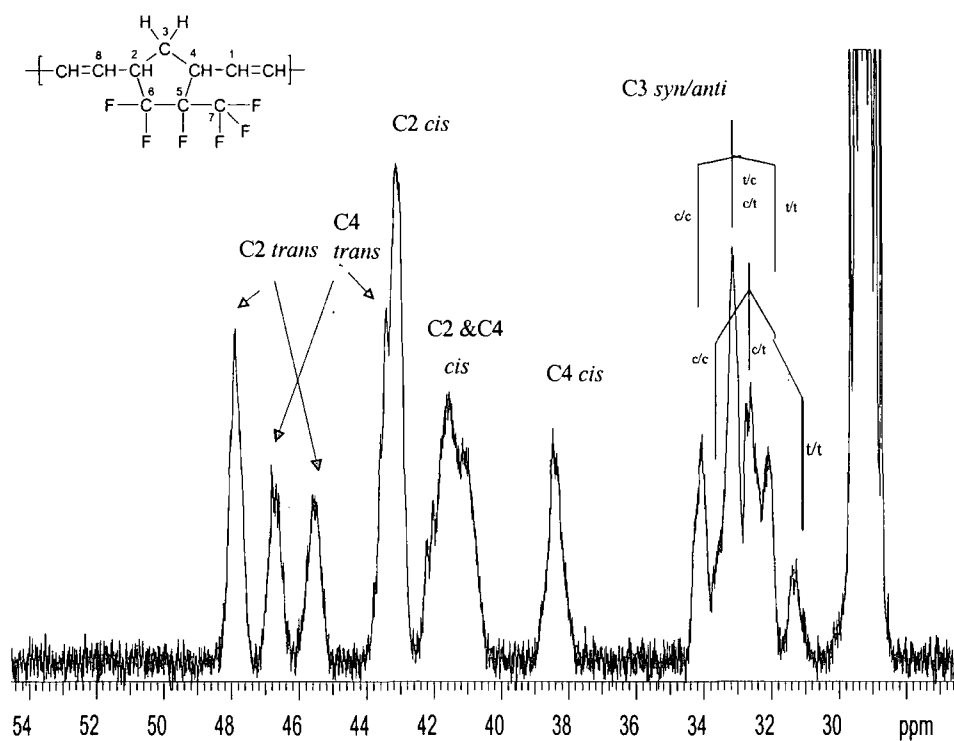


Figure 3.19 Assigned signals for the expanded ^{13}C nmr spectrum of polymer (Ia) in the saturated region (above) and the vinylic region (below)

The analysis of the ^1H nmr spectrum of polymers (*Ia*) and (*Ib*) differentiates three environments for the hydrogens, as shown in *Figure 3.20*.

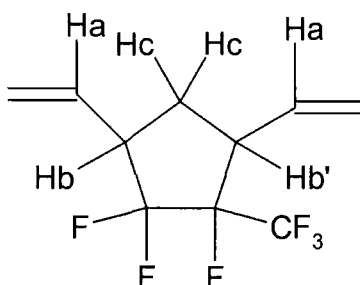


Figure 3.20 Hydrogen environments for polymer (I)

The ^1H nmr spectra for the polymers (*Ia*) and (*Ib*) are shown in *Figure 3.21* and *3.22* respectively.

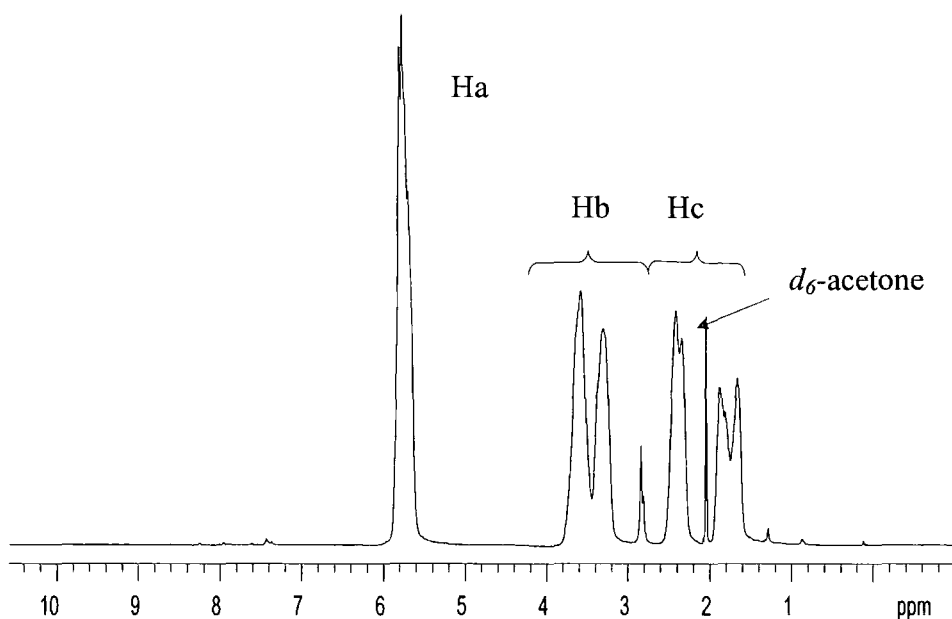


Figure 3.21 The ^1H nmr spectrum of polymer (Ia)

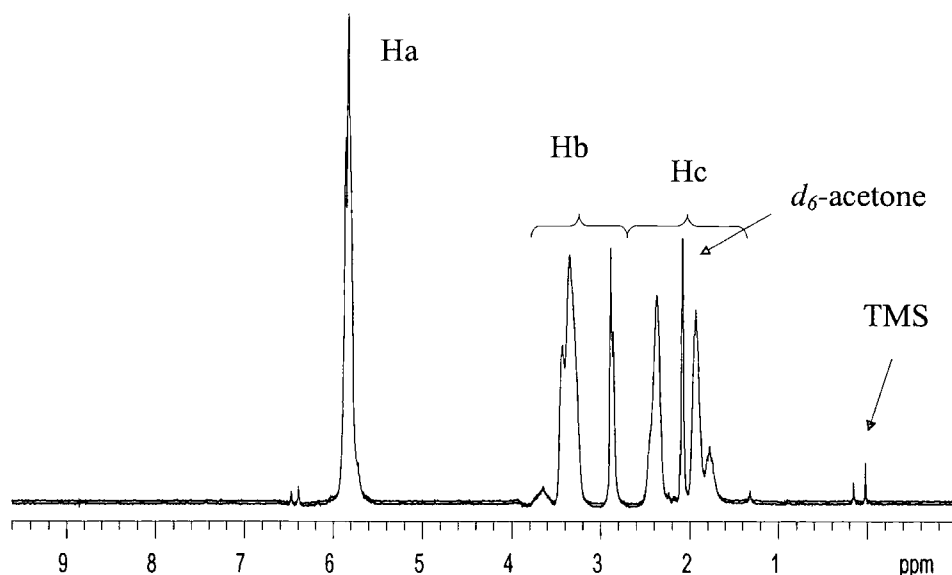


Figure 3.22 The ^1H nmr spectra of polymer (Ib)

The unresolved vinylic hydrogens Ha appeared at 5.9 ppm in both spectra. The hydrogens Hb or Hb' are assigned to the three signals between 2.5 and 4 ppm, and display different intensities in the different spectra. The spectrum of polymer (Ia) displays two broad signals at 3.34 ppm (43%), at 3.6 ppm (52%) and a sharp signal with low intensity at 2.8 ppm (5%). Whereas in the spectrum of polymer (Ib), the analogous signals are 6%, 70% and 24% of the intensity in this region. From earlier work,²⁶ we know that polymer (Ib) has predominantly *trans* vinylenes and we can assume that the signals at 3.34 and 2.8 ppm are associated with *trans* double bonds; the *cis:trans* ratio is determined from the relative intensities to be 52:48 for polymer (Ia) and 6:94 for polymer (Ib). A residual ambiguity concerning the detailed assignment of the sharp signals at 2.8 ppm remains unresolved.

The hydrogens Hc also display different signals in the ^1H nmr spectra for both polymers, which could arise from either *cis:trans* vinylene, head-head/head-tail or monomer isomer incorporation effects but there is not enough resolution to disentangle these effects.

The hydrogenation of polymers (Ia) and (Ib) was conveniently monitored by the disappearance of the signals assigned to the vinyl hydrogens Ha at 5.9 ppm. The signals in the saturated region of the spectrum (1 to 4 ppm) also

undergo change in the expected manner, the vinylene signals associated with (Ia) and (Ib) decrease in intensity and the new methylene signal appear. The spectra of polymers (IIa) and (IIb) are shown in Figures 3.23 and 3.24 respectively.

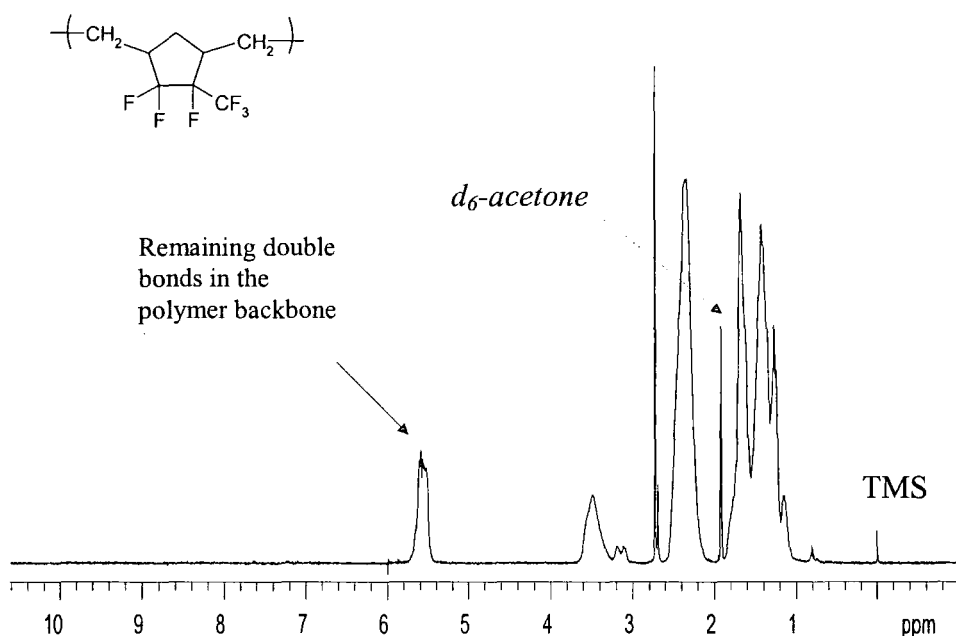


Figure 3.23 The ^1H nmr spectrum of polymer (IIa)

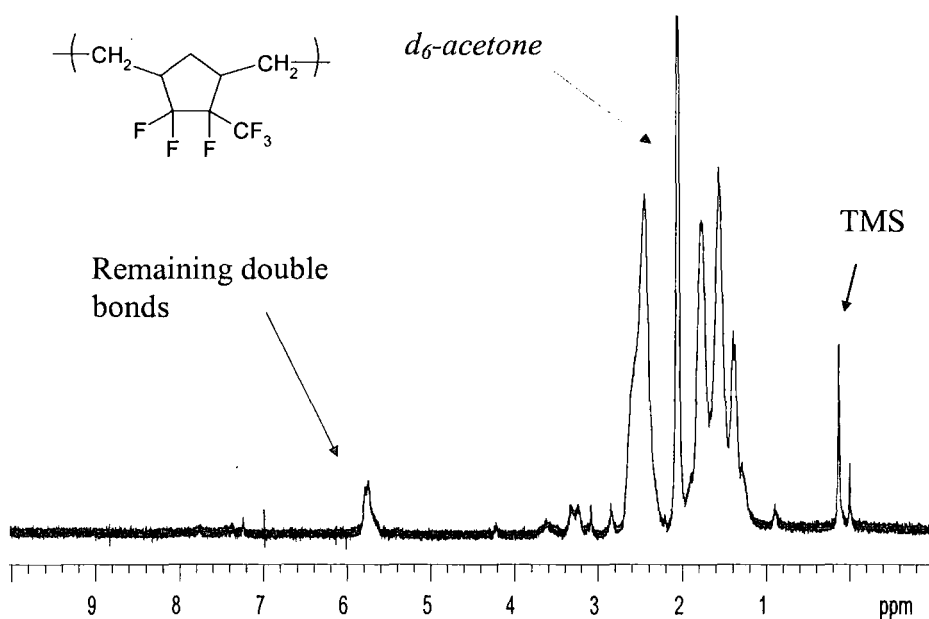


Figure 3.24 The ^1H nmr spectrum of polymer (IIb)

The relative intensities of the vinyl hydrogens at 5.9 ppm compared to the well-resolved signal centred at 2.5 ppm were used to calculate the extent of hydrogenation, giving values of 95 % and 83 % for polymers (*IIb*) and (*IIa*) respectively.

The hydrogenation of the polymers was also monitored by ^{13}C nmr spectroscopy. The partially hydrogenated polymers displayed new signals between 20 and 30 ppm assigned to the newly created CH_2 carbons, as well as decreased intensity of the signals from carbons C1 and C8 in the vinyl region as shown in *Figures 3.25* and *3.26* for polymers (*IIa*) and (*IIb*) respectively.

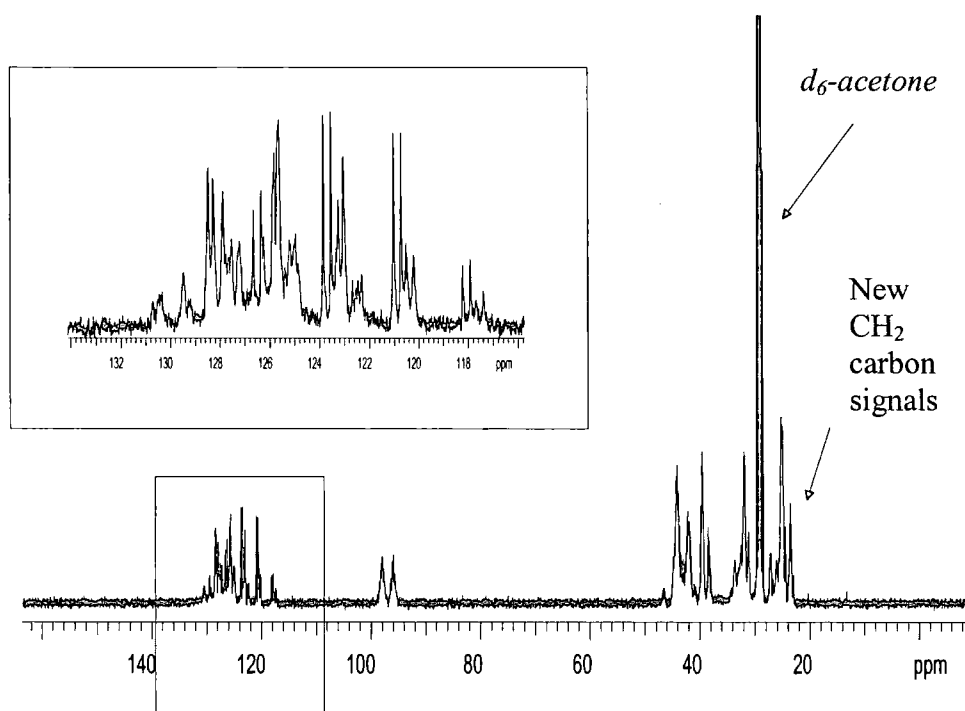


Figure 3.25 The ^{13}C nmr spectrum of polymer (IIa), cf Figure 3.19

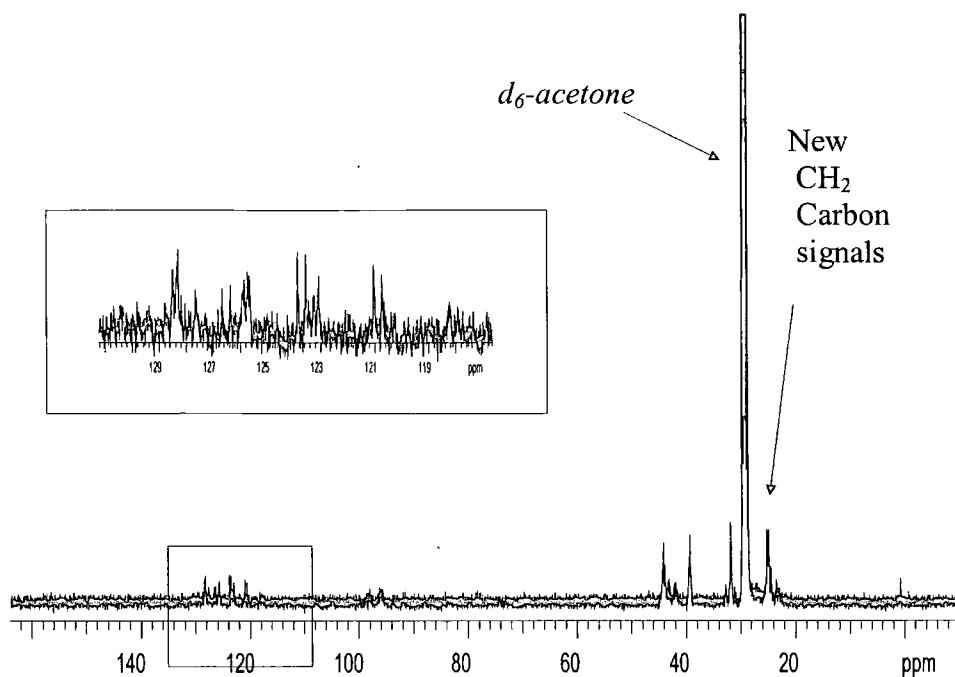


Figure 3.26 The ^{13}C nmr spectrum of polymer (IIb), cf Figure 3.17

3.2 d) (ii) Elemental analysis

The results of the elemental analysis for the polymers are shown in *Table 3.1*.

Polymers	C (%) (expected)	H (%) (expected)	F (%) (expected)
<i>Ia</i>	46.79 (44.4%)	2.60 (2.78%)	50.61 (52.78%)
<i>Ib</i>	45.78 (44.4%)	2.43 (2.78%)	52.11 (52.78%)
<i>IIa</i>	44.01 (44.04%)	3.37 (3.67%)	48.68 (52.29%)
<i>IIb</i>	44.10 (44.04%)	3.56 (3.67%)	51.76 (52.29%)

Table 3.1 Elemental analysis results

The percentages obtained are only moderately consistent with the expected values and suggests that there may be some contamination in some samples.

3.2 d) (iii) IR spectroscopy

The IR spectra of polymer (*Ia*) and polymer (*IIa*) are compared in *Figure 3.27*. In the spectrum for (*IIa*) there is an increased intensity and broadening of the signal at 2930 cm^{-1} associated with C-H stretching due to the increased

proportion of CH_2 groups. There is also a decreased intensity in the peaks associated with the $-\text{CH}=\text{CH}-$ out-of-plane bending mode bands between 600 and 900 cm^{-1} in the spectra of polymer (IIa).

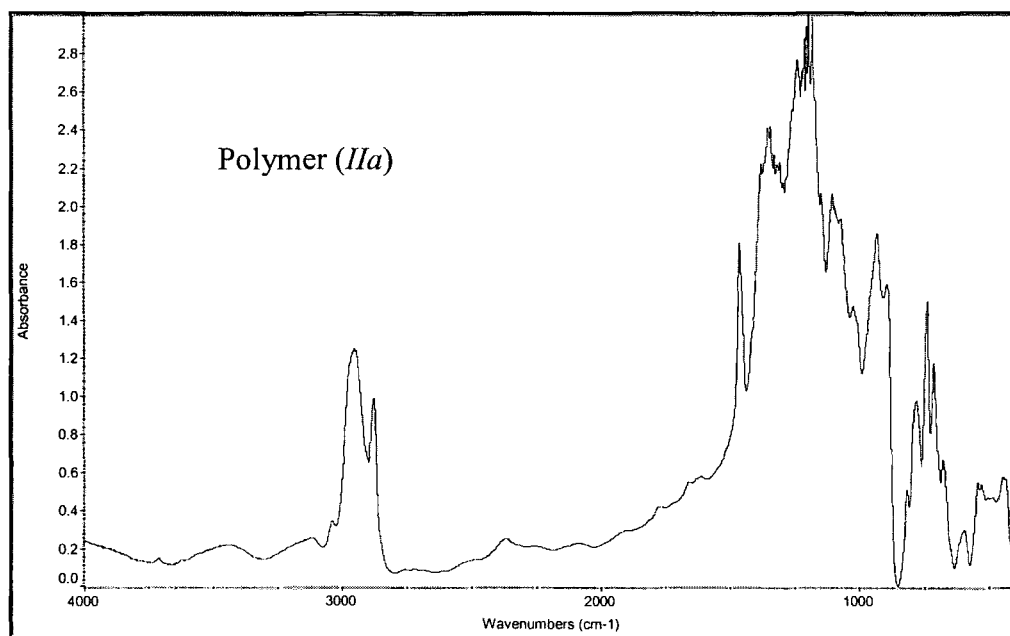
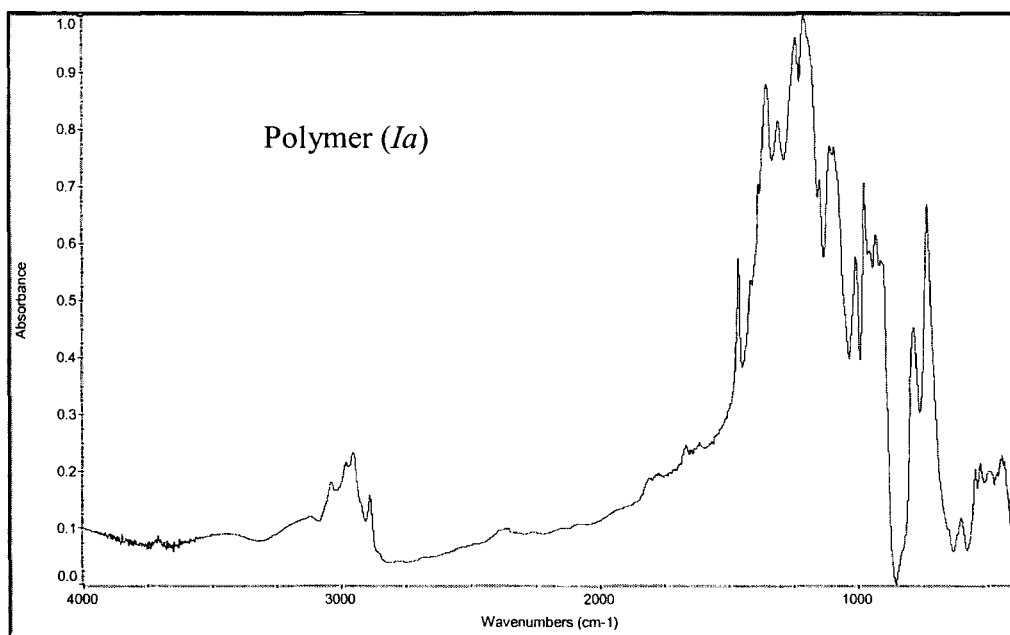


Figure 3.27 The IR spectra of polymer (Ia) above and (IIa) below

3.2 e) Physical characterisation of the polymers (Ia), (Ib), (IIa) and (IIb)

The polymers were characterised by GPC, DSC and TGA. The results from these experiments are shown in *Table 3.2*.

Polymer	T _g (DSC) (°C)	GPC			TGA % lost at 300 °C
		M _n	M _w	PDI	
<i>Ia</i>	161	154,000	240,000	1.6	<0.3
<i>Ib</i>	—				<0.4
<i>IIa</i>	125	172,000	479,000	2.8	9%
<i>IIb</i>	—				

Table 3.2 DSC, GPC and TGA analysis of the polymers

No glass transition process was observed in the DSC analysis of polymers (*Ib*) and (*IIb*). The GPC analysis shows a large polydispersity (PDI) for the polymers, which is common for materials produced using “classical” ROMP initiators. The GPC analyses were carried out in DMF, using a viscosity detector and calibration against polystyrene standards. A reduction in the thermal stability was observed for the saturated polymers as compared to their unsaturated precursors.

3.2 f) Conclusions

The experimental evidence demonstrated that the hydrogenation of the double bonds in this type of polymer could be achieved, and the resulting partially saturated polymers display a lower T_g than the precursors. However, the new materials were not elastomers at room temperature and were not suitable for the purposes of the project, so this aspect was not pursued in greater detail. The next ROMP study was concerned with the use of a monomer with lower fluorine content, which was expected to give a lower T_g polymer.²⁶

3.4 Study of the synthesis and hydrogenation of poly(5-trifluoromethyl-1,3-cyclopentylenevinylene)

3.3 a) Introduction

It was assumed that the more fluorine atoms or fluoroalkyl groups in the repeat unit the higher would be the T_g of the polymer. Therefore, the polymerisation and hydrogenation of 5-trifluoromethylbicyclo[2.2.1]hept-2-ene was undertaken. The primary ROMP product from this monomer was reported to have a T_g of 96 °C compared to 161 °C obtained for poly(4,4,5-trifluoro-5-trifluoromethyl-1,3-cyclopentylenevinylene).²⁶

3.3 b) Synthesis of 5-trifluoromethylbicyclo[2.2.1]hept-2-ene

5-Trifluoromethylbicyclo[2.2.1]hept-2-ene was synthesised from 1,1,1-trifluoropropane and cyclopentadiene in a Diels-Alder reaction. The scheme for the synthesis for the monomer (II) is shown in Figure 3.28.

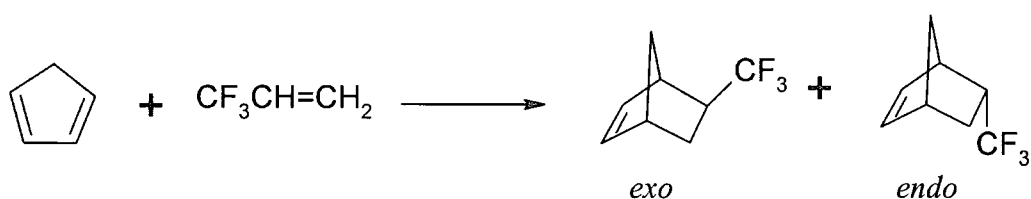


Figure 3.28 Synthesis scheme for 5-trifluoromethylbicyclo[2.2.1]hept-2-ene (II)

The starting materials were mixed and heated in a sealed Carius tube at 180 °C for 3 days, to give a colourless liquid product (52 % yield), see section 3.5 for the experimental details. The product was fully characterised by analysis and spectroscopy. The gc-MS confirmed the existence of two products with the same molecular formulae M^+ 162, and both exhibited a base peak at m/e 66 ($C_5H_6^+$), arising from the retro Diels–Alder reaction of the parent ion, this fragmentation mode is characteristic of bicyclo[2.2.1]hept-2-enes.⁴⁷ The IR spectrum (see Appendix AX27) showed the expected vinylic C–H stretch (3080

cm⁻¹, weak), -CH=CH- stretch (1690 cm⁻¹, weak) and C-F stretches (1390-1000 cm⁻¹, strong). The analysis of the ¹⁹F nmr spectrum (see Appendix AX28) showed two signals in the trifluoromethyl region revealing the presence of the *endo* and *exo* isomers.^{26,91,92} The signal at -66.3 ppm was the major component (62 %) and was assigned to the *exo* isomer displaying a coupling $J_{\text{H-F}}^2 = 9.78$ Hz. The minor component at -68.2 ppm (38 %) and $J_{\text{H-F}}^2 = 10.16$ Hz was assigned to the *endo* isomer. The ¹H nmr spectrum (see Appendix AX29) of the isomeric mixture was extremely complex and it can only be interpreted in the detail in the vinyl region. The ¹³C nmr spectrum (see Appendix AX30) was analysed on the basis of the carbon-fluorine coupling constants of the trifluoromethyl carbon, which appears as two low intensity quartets centred at 128.561 ppm and 128.06 ppm and $J_{\text{C-F}}^1 = 278$ and 277.6 Hz respectively, the spectrum however, was very complex and it could only be partially characterised. The spectroscopic characteristics were consistent with the literature.^{26,91,92}

3.3 c) Ring-opening metathesis polymerisation of 5-trifluoromethyl bicyclo[2.2.1]hept-2-ene

The ROMP experiment carried out is shown schematically in Figure 3.29.

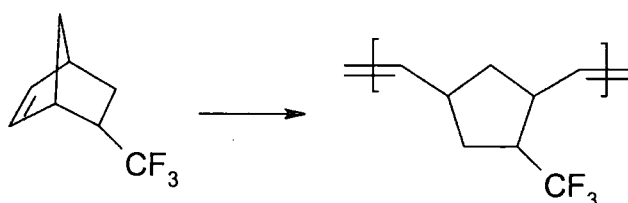


Figure 3.29 Polymerisation scheme for poly(5-trifluoromethylbicyclo[2.2.1]hept-2-ene(III))

The polymerisation was carried out at room temperature using the initiator derived from tungsten hexachloride (1 equivalent) in toluene using tetraphenyltin (2 equivalents) as a co-initiator. After the required activation time when the solution of the catalyst mixture became dark brown the monomer (500 equivalents) was injected into the reaction vessel. The dark brown solution

became gradually more viscous and the polymerisation was completed when the stirrer stopped. The contents of the ampoule were quenched with few drops of methanol, and the product was dissolved in acetone and precipitated in cold hexane to give a white solid (85 % yield). The characterisation of polymer (III) is discussed later.

3.3 d) Hydrogenation of poly(5-trifluoromethyl-1,3-cyclopentylenevinylene)

The hydrogenation of poly(5-trifluoromethyl-1,3-cyclopentylenevinylene) is shown schematically in *Figure 3.30*.

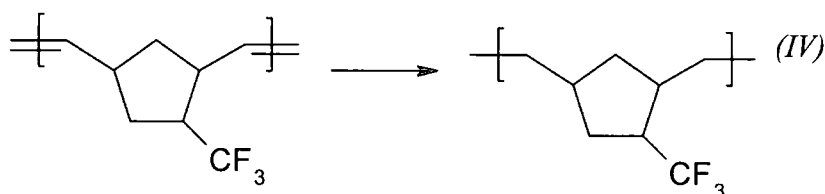


Figure 3.30 Hydrogenation scheme for polymer (III)

The hydrogenation of polymer (III) was practically complete. The resulting polymer (IV) was a white solid, which was precipitated in cold methanol and the T_g obtained by DSC analysis was 53.2°C .

The characterisation of the saturated polymer (IV) is discussed below.

3.3 e) Structural characterisation of the polymers (III) and (IV)

3.3 e) (i) Nmr spectroscopy

The carbon environments of polymer (III) in ^{13}C nmr spectroscopy are shown schematically in *Figure 3.31*, as a reminder to the reader.

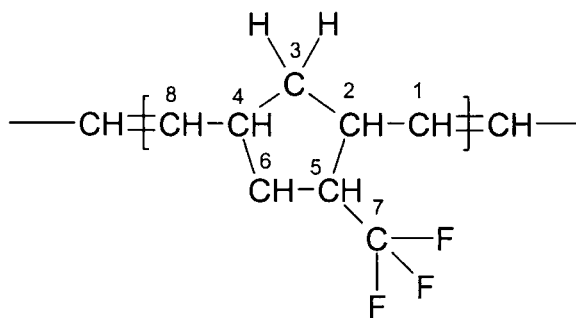


Figure 3.31 Carbon environments for polymer (III)

In the analysis of the ^{13}C nmr spectrum of polymer (III) two groups of signals are observed. The signals between 138 ppm and 120 ppm were assigned to the vinylenes carbons C1 and C8, and the trifluoromethyl carbon C7; the signals between 50 ppm and 30 ppm were assigned to the ring carbons (C2, C3, C4, C6 and C5). The ^{13}C nmr spectrum of polymer (III) is shown in *Figure 3.32*.

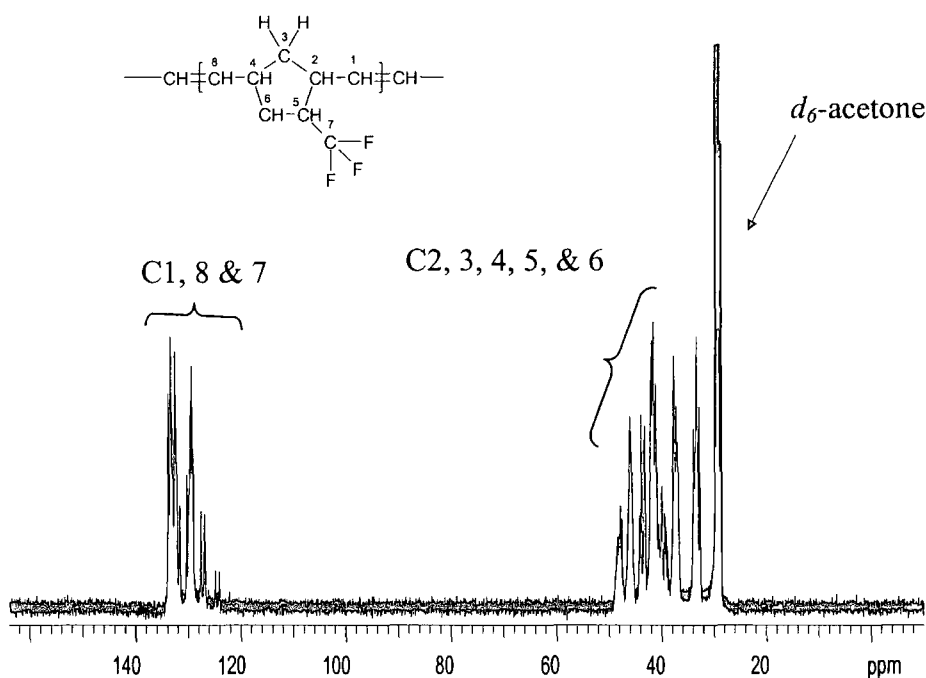


Figure 3.32 The ^{13}C nmr spectrum of polymer(III)

The resonance due to the carbon of the trifluoromethyl group is partially distinguished as two quartets centered at approximately 129 ppm with a $J_{\text{C-F}}^1 = 284.9$ Hz. The observation of two quartets was attributed to the incorporation of two different repeat units structures in the polymer backbone from the *endo* and *exo* monomers, and the discussion of this will follow from the analysis of the ^{19}F nmr spectrum. The remaining signals are assigned to the vinyl carbons C1 and C8, as previously studied and assigned in Durham.¹⁰⁰ Thus, in the case of polymerisation of a mixture *endo* and *exo* monomers we expect *cis* and *trans* double bonds in the polymer backbone, additionally two groups of signals are expected arising from *exo*- and *endo*-isomer incorporation consisting of two doublets for each of the C1 or C8 carbons which would give 16 signals in total. In the spectrum obtained two groups of signals are differentiated and the 16 signals are tentatively assigned as shown in Figure 3.33.

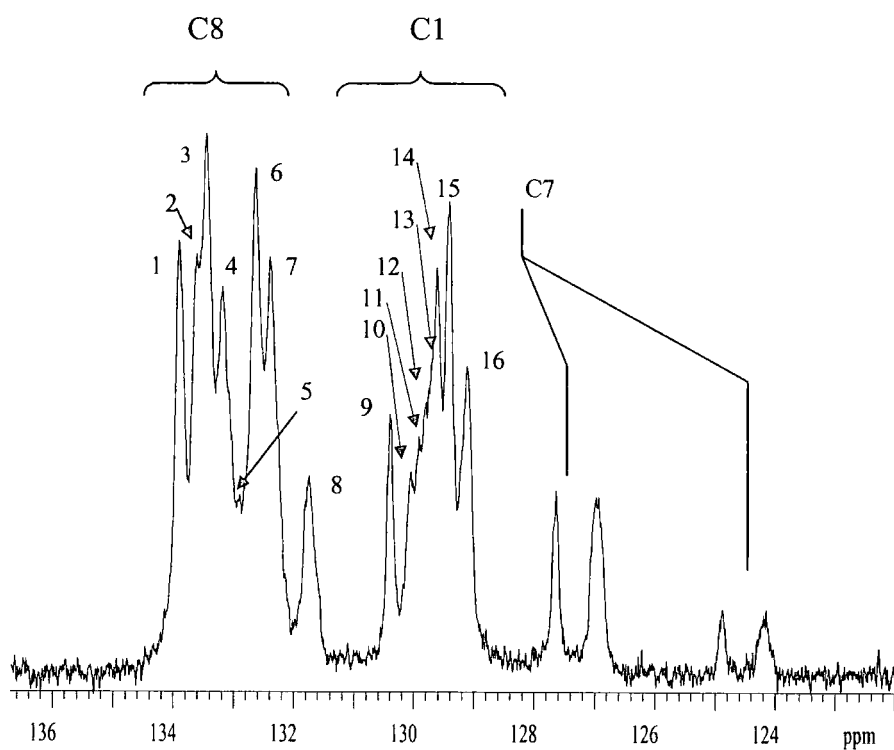


Figure 3.33 The expanded vinyl region of the ^{13}C nmr spectrum

The saturated region in the ^{13}C nmr spectrum with the assignments for the carbons, following the earlier work of Blackmore,¹⁰⁰ is shown in *Figure 3.34*.

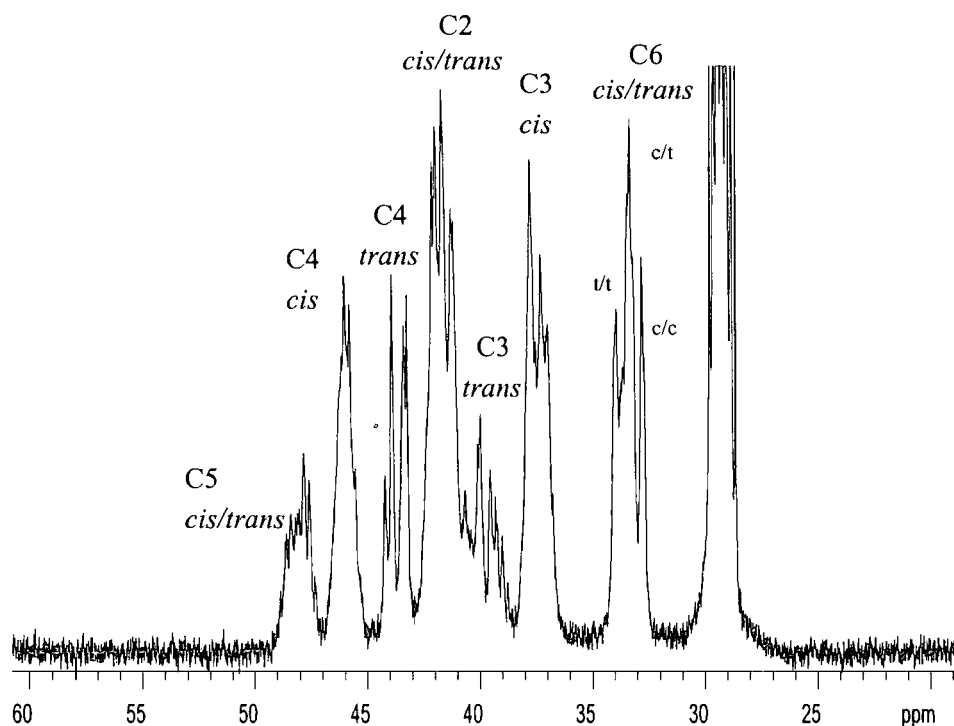


Figure 3.34 The expanded allyl region of the ^{13}C nmr spectrum of polymer (III)

The ^{19}F nmr spectra of polymers (III) and (IV) shown in Figures 3.36 and 3.37 respectively, displays two signals in the relative intensity ratio 63:37 assigned to the structures (i) and (ii) respectively in Figure 3.35. The situation is analogous to that previously discussed in section 2.2 for polymer (I).

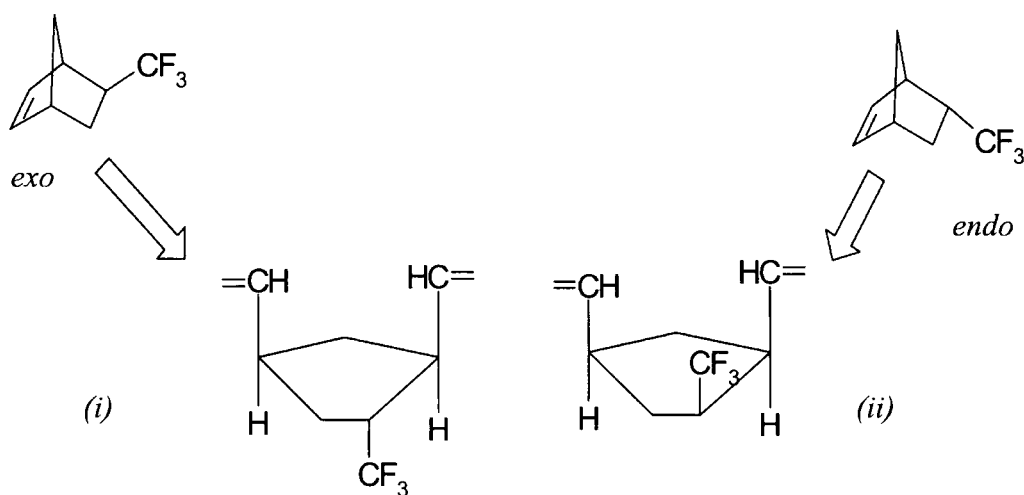


Figure 3.35 Polymer structures

As previously discussed for the ROMP of 5,5,6-trifluoro-6-trifluoromethylbicyclo[2.2.1]hept-2-ene monomer, the structure (i), which is the major structure in the polymer, is derived from the *exo* monomer and the structure (ii) from the *endo* monomer; since the initial monomer mixture had a 61:38 *exo:endo* ratio, it can be seen that, under the experimental conditions of the polymerisation, the $\text{WCl}_6/2\text{Ph}_4\text{Sn}$ initiator system does not discriminate between the *exo* and *endo* isomers of 5-trifluoromethylbicyclo[2.2.1]hept-2-ene.

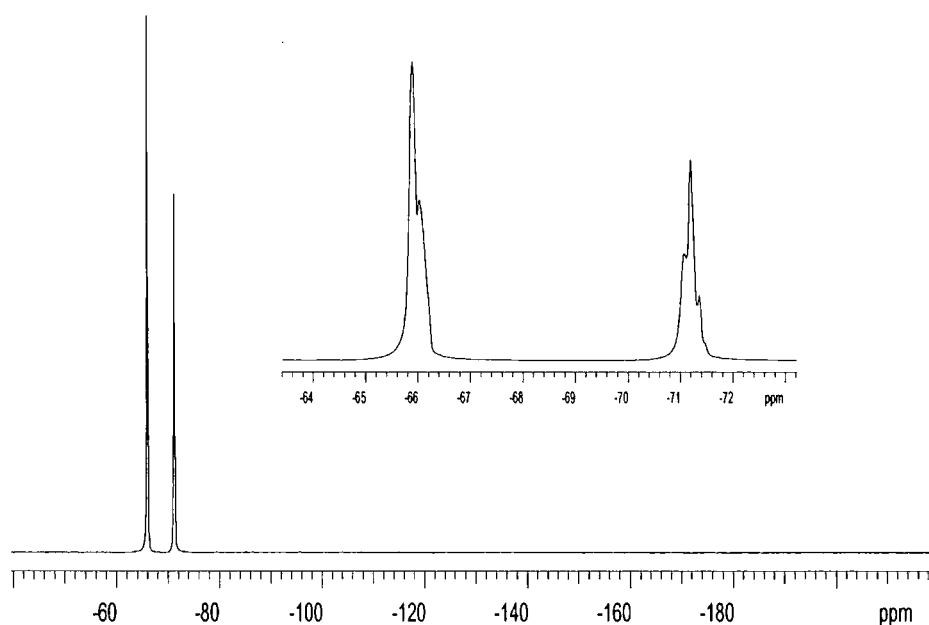


Figure 3.36 The ^{19}F nmr spectrum of polymer (III)

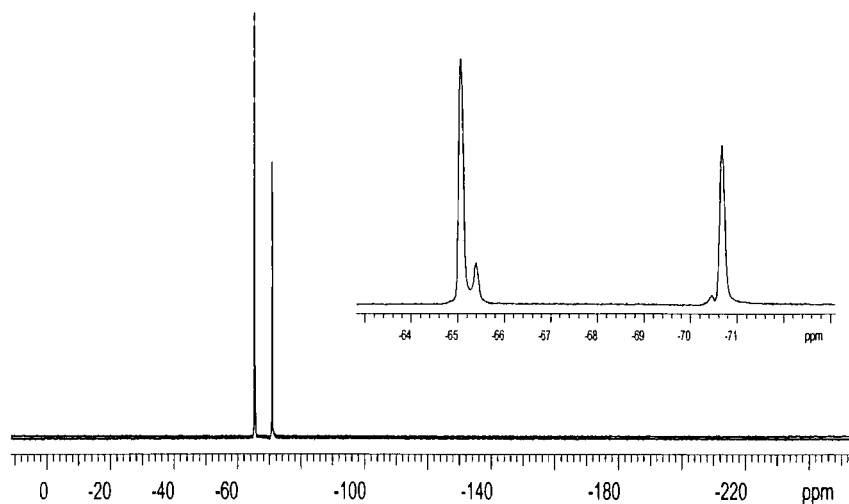


Figure 3.37 The ^{19}F nmr of the saturated polymer (IV)

Very similar relative intensities and shifts are observed in the analysis of the ^{19}F nmr spectrum for the saturated polymer (IV) compared to its unsaturated precursor (III), see Figure 3.36 and 3.37, however, the signals in the spectrum of the saturated polymer display small shoulders, which are tentatively assigned to H-H or T-T sequences of the fluoroalkyl groups, and if this assumption is correct the integration of the signals gives a minor proportion of H-H/T-T sequences in the polymer backbone, being ca 17% and 4% for the repeat units derived from the structures (i) and (ii) in Figure 3.35.

The analysis of the ^1H nmr spectrum of polymer (III), Figure 3.38, displays a complex multiplet at 5.5 ppm, attributed to the distribution of *cis* and *trans* double bond configurations along the backbone. The C_{sp^3} -H hydrogens, H_{bcd} , were assigned by analogy with earlier work.¹⁰⁰

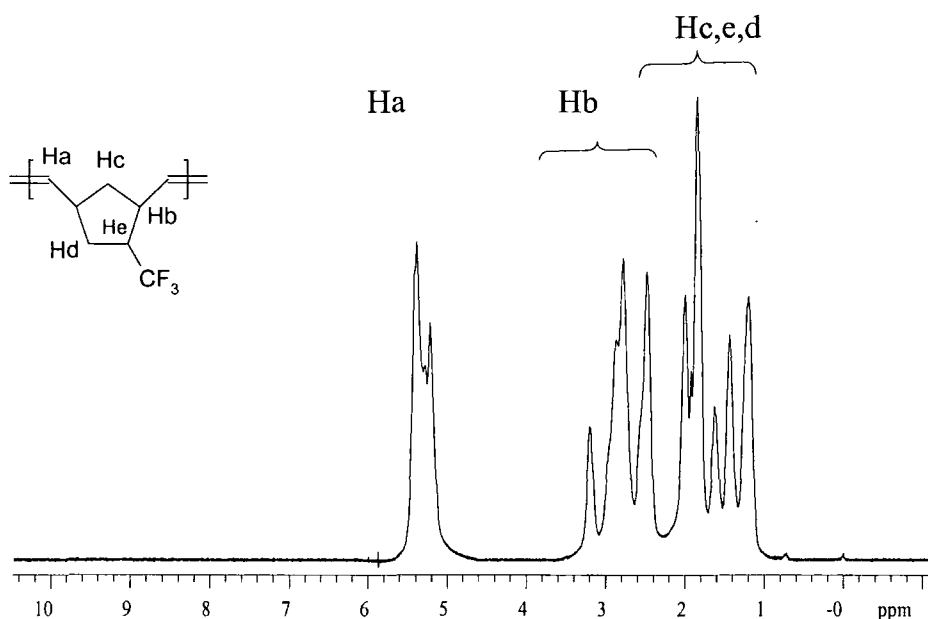


Figure 3.38 The ^1H nmr spectrum of polymer (III)

The analysis of the vinyl region in the ^1H nmr spectrum of the material obtained after the hydrogenation probes the extent of saturation of the double bonds in the polymer (IV), see Figure 3.39. Very low intensity signals are still observed between 5 and 6 ppm, suggesting the existence of traces of residual unsaturated double bonds in the polymer, but the amount is too small to measure reliably, probably less than 1%. It can be seen that the diimide hydrogenation of polymer (III) was much more efficient than the analogous

process with polymers (*Ia*) and (*Ib*). This observation may be a consequence of shielding of the double bonds in polymers (*Ia*) and (*Ib*) by the bulk of the substituents.

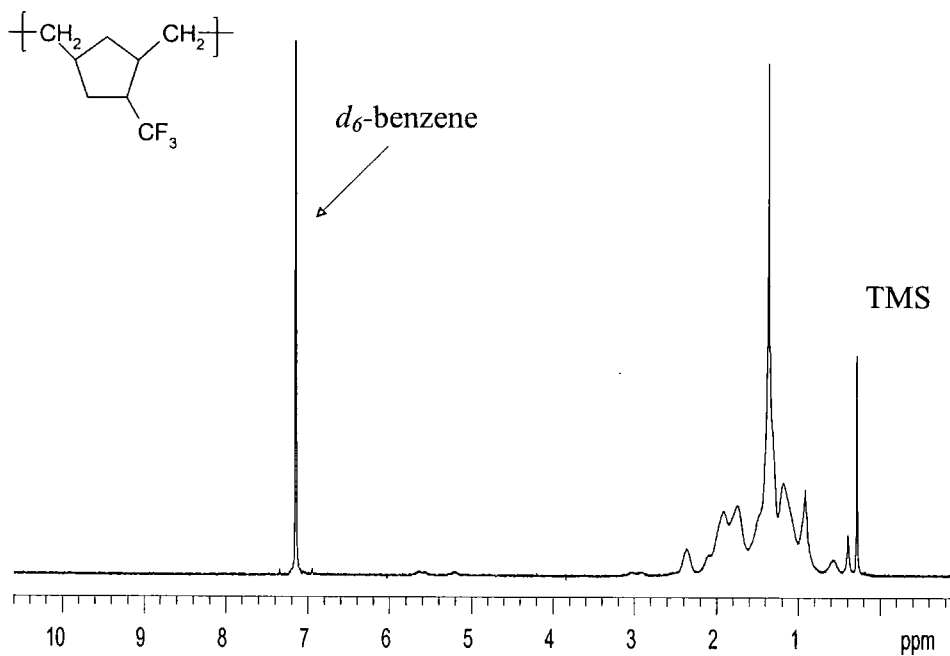


Figure 3.39 The ^1H nmr spectrum of saturated polymer (IV)

3.3 e) (ii) Elemental analysis

The results of the elemental analysis for polymers (III) and (IV) are shown in Table 3.3 and, although not perfect, are reasonably consistent with the assigned structures.

Polymer	%C (expected)	%H (expected)	%F (expected)
III	60.55 (59.26%)	5.54 (5.56%)	34.72 (35.18%)
IV	58.82 (58.84%)	7.34 (6.71%)	28.21 (34.77%)

Table 3.3 Elemental analysis

The results of the elemental analysis are consistent with the expected percentages for the polymers.

3.3 e) (iii) IR spectroscopy

The IR spectra of polymers (III) and (IV) are compared in Figure 3.40. The resolution is not good however the sharp signal at ca 1380 cm^{-1} is a characteristic fingerprint for the CF_3 unit. The spectra were recorded as dispersions of the powdered polymer in KBr and clearly some moisture contaminates the KBr discs. As would be expected the overall appearance of the two spectra are similar, but within the limitations of the poor resolution, the major changes are in the 1000 to 700 cm^{-1} region associated with vinylene out-of-plane C-H bending in polymer (III). The $-\text{CH}=\text{CH}-$ stretching mode in the polymers was too weak to be detected.

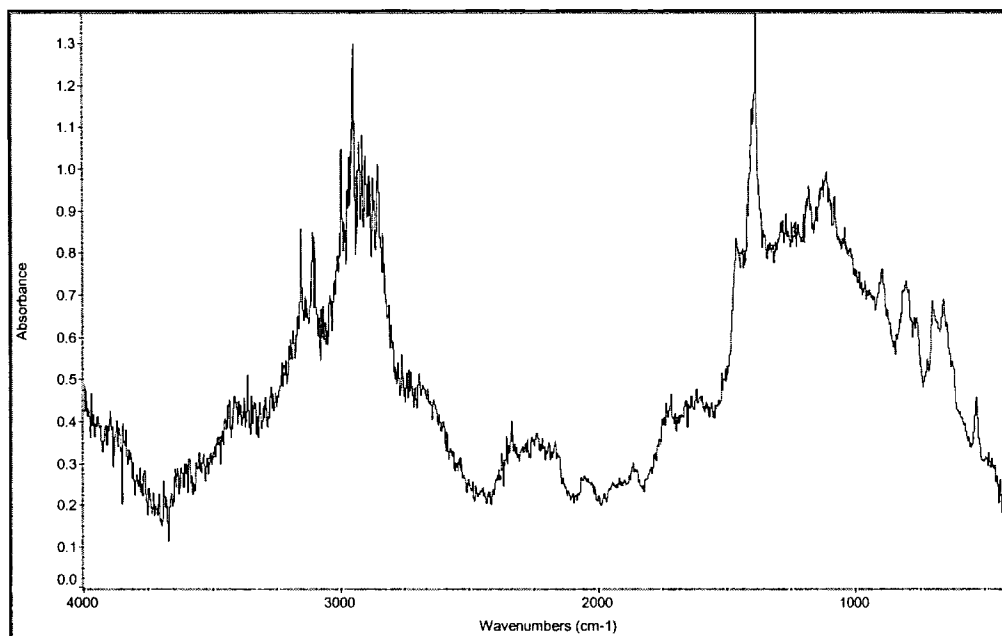
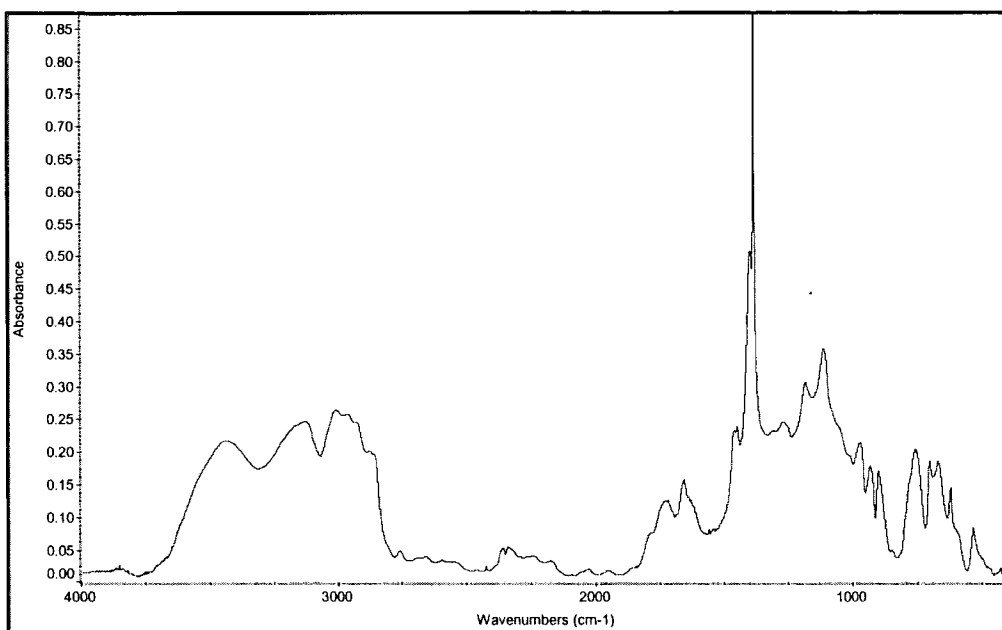


Figure 3.40 A comparison between IR spectra of polymer (III) above and polymer (IV) below

3.1 f) Physical characterisation of the polymers (III) and (IV)

The results of the DSC, GPC, and TGA for the synthesised polymers are shown in *Table 3.4*. We can see that as in the case of polymer (*Ia*) hydrogenation results in a significant reduction in T_g ; however, in this example hydrogenation has virtually no effect on thermal stability whereas in the earlier case the hydrogenated materials (*IIa*) and (*IIb*) appear to be less stable, possibly indicating that dehydrofluorination in polymer (*II*) is easier than in (*IV*).

Polymer	T_g	GPC			TGA
	(DSC) ($^{\circ}\text{C}$)	M_n	M_w	PDI	
<i>III</i>	+90	26,000	61,000	2.3	<1.2% at 300 $^{\circ}\text{C}$
<i>IV</i>	+53	-	-	-	2 % at 288 $^{\circ}\text{C}$

Table 3.4 Physical characterisation of polymers (III) and (IV)

Unfortunately the saturated polymer (*IV*) was insoluble in the common solvents used for the GPC analysis and its molecular weight remains unknown.

3.3 g) Conclusions

The hydrogenation of polymer (*III*) was successfully achieved, and the new material is a potentially useful polar polymer. Analysis by differential scanning calorimetry showed a T_g for polymer (*IV*) above room temperature, which made it unsuitable for our purposes. In an attempt to obtain a lower T_g material we next tried copolymerisations with cyclopentene since the homosubstituted norbornene approach seemed unlikely to succeed.

3.4 A study of the syntheses and hydrogenation of poly(5-trifluoromethyl bicyclo[2.2.1]hept-2-ene with cyclopentene and hydrogenation of the resulting polymers was adopted as an alternative approach to a material with low enough T_g and as high as possible fluorine content for our purposes. The synthetic route is shown in Figure 3.41.

3.4 a) Introduction

The combination of copolymerisation of 5-trifluoromethyl bicyclo[2.2.1]hept-2-ene with cyclopentene and hydrogenation of the resulting polymers was adopted as an alternative approach to a material with low enough T_g and as high as possible fluorine content for our purposes. The synthetic route is shown in Figure 3.41.

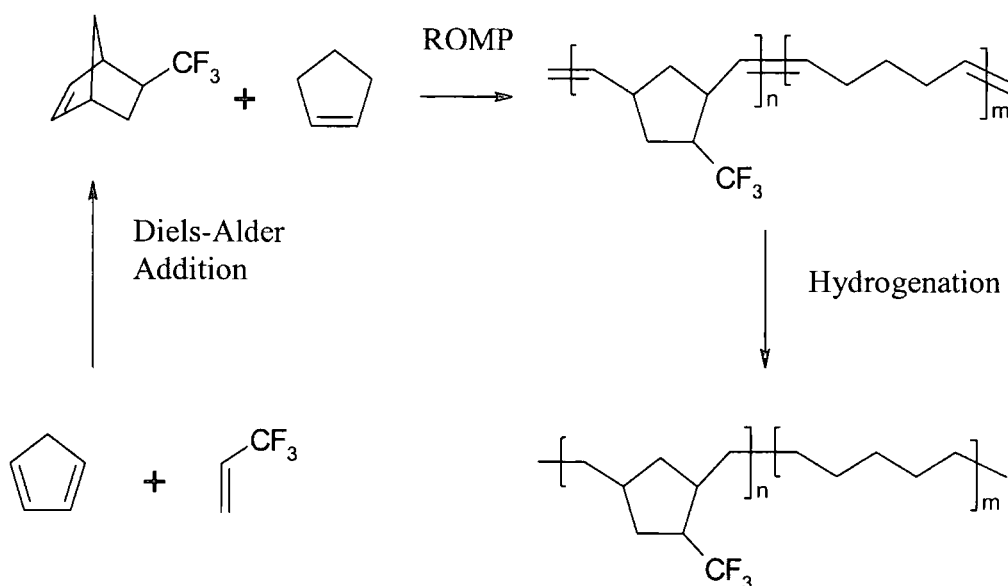


Figure 3.41 Synthetic route to low T_g copolymers

An initial investigation was carried out to determine how the inclusion of the co-monomer cyclopentene would affect the T_g of the new materials. The polymerisation experiments were carried out at room temperature with the $\text{WCl}_6/2\text{Ph}_4\text{Sn}$ initiator system in toluene, using a 500:1 monomer:tungsten ratio.

3.4 b) Copolymerisation experiments and results

The results of the copolymerisations carried out are recorded in *Table 3.5*. Two different batches of fluorinated monomer, having different *exo:endo* ratios were used.

Polymer	monomers ratio ^a	Yield (%)	Fluorine content (%)	Fluorinated repeat unit incorporated (mole-%)	T _g (DSC) (°C)
<i>V^b</i>	1:1	23	21.52	40	-7
<i>VI^b</i>	2:1	45	26.77	57	+8
<i>VII^c</i>	3:1	67	29.05	66	+42
<i>VIII^c</i>	4:1	72	31.45	78	+60
<i>IX*</i>	3:1	-	28.06	64	+12
<i>X*</i>	4:1	-	29.35	72	+36
<i>XI^c</i>	2.5:1	57	28.29	63	+20
<i>XII*</i>	2.5:1	-	26.99	60	-22

^aRatio of fluorinated bicyclo[2.2.1]hept-2-ene:cyclopentene

*Saturated polymers

^bFrom 62:38 *exo:endo* (±)-5-trifluoromethylbicyclo[2.2.1]hept-2-ene

^cFrom 74:26 *exo:endo* (±)-5-trifluoromethylbicyclo[2.2.1]hept-2-ene

Table 3.5 Co-polymers synthesised and hydrogenated

The feed stock composition was varied and the relative incorporation of monomers was calculated from the elemental analysis for fluorine. This was the only accessible method since there were no suitable distinct resonances in the

^1H nmr spectra of the copolymers and calculation of the degree of incorporation from the carbon elemental analyses gave unreliable results. For example, samples of polymers (V), (VI) and (VII), were computed as having 68, 72 and 70 mole-% of fluorinated monomer incorporation, that is the same with experimental error, which is intuitively unreasonable when the feed ratios were 1:1, 2:1 and 3:1 respectively and their T_g s varied from -7 to $+42$ $^{\circ}\text{C}$. In one case the calculation indicated over 100 % fluorinated monomer incorporation, which is ridiculous. We therefore abandoned the calculations based on the carbon elemental analyses. The polymerisations were initially carried out with a 1:1 and 2:1 ratio of monomers having a 62:38 ratio of *exo:endo* (\pm)-5-trifluoromethylbicyclo[2.2.1]hept-2-ene and cyclopentene, to give polymers (V) and (VI). The polymers were dissolved in acetone and precipitated in cold hexane to give, after drying, white rubbery materials.

The polymerisation yield decreased considerably when compared to the homopolymerisation of monomer (III), which gave 85% mass recovery, being 45 % for polymer (VI) and only 23 % for polymer (V). The DSC analysis of these two polymers indicated T_g s of -7 $^{\circ}\text{C}$ for polymer (V) with 40 mole-% of fluorinated monomer incorporation, and 8 $^{\circ}\text{C}$ for polymer (VI) with 57 mole-% of fluorinated monomer incorporation. This was encouraging and in the next phase of the work we attempted to maximise the fluorinated monomer content while producing a polymer which, after hydrogenation, would give a material with a T_g below room temperature. The optimised combination of both maximum molar percentage of fluorinated monomer incorporated and hydrogenation of the resulting polymers was investigated to obtain the targeted material.

The next copolymerisations were carried out with a batch of monomer (II) having a 79:21 *exo:endo* ratio. The monomer ratios, richer in the fluorinated adduct, were 3:1 and 4:1 for copolymers (VII) and (VIII) respectively. The polymerisation yields increased remarkably and the results of the elemental analysis indicated a 66 mole-% of fluorinated monomer incorporation for copolymer (VII) and 78-mole% for copolymer (VIII). The experimental evidence, obtained from the fluorine elemental analysis and from the material recovered, see Table 3.5, indicate that increasing the amount of fluorinated

monomer in the feed results in increased incorporation of the fluorinated repeat unit in the polymer backbone and increased mass recovery. When the feed composition is compared to the polymer composition there is a qualitative correlation, in that the richer the feed, the richer the polymer in fluorinated units; however, the correlation is not linear and the analysis can not be taken as better than qualitative. The double bonds in the polymers (VII) and (VIII) were hydrogenated and the analysis of the ^1H nmr spectra (see Appendix AX44 and AX47) of the resulting polymers (IX) and (X) showed the complete disappearance of the vinyl signal. A small reduction in the proportions of the incorporated fluorinated repeat unit was observed in the transformation of (VII) and (VIII) to (IX) and (X) respectively, this suggested the possibility that a non-hydrogenated fraction of the polymer backbone, or even a small proportion of homofluoropolymer, may have been lost during the recovery of the material. This would also explain the observed loss in weight of approximately 2 to 5 % for the recovered hydrogenated materials; however, this may be pushing the analysis too far since the effects are small and the compositional analysis is not very accurate.

The DSC analysis showed a T_g for the saturated polymer (IX) of 12 $^{\circ}\text{C}$ and 36 $^{\circ}\text{C}$ for the polymer (X) and this was not surprising as the increased incorporation of fluorinated units was expected to result in higher T_g s for those polymers. These polymers however, possessed too high T_g s for the purposes of the work and the next polymerisation was carried out with a 2.5:1 ratio to give polymer (XI), Table 3.5. The polymerisation yield of (XI) was again relatively low (45 %) and the percentage of the fluorinated repeat unit in the polymer backbone determined by elemental analysis was 63 mole-%. The complete hydrogenation of the double bonds in polymer (XI) was carried out to give (XII) and monitored by ^1H nmr and ^{13}C nmr spectroscopy (see Appendix AX49 and AX50) to give a white rubbery material with a T_g of -22°C . The fluorine elemental analysis for polymer (XII) indicated a 60 mole-% of the fluorinated repeat unit in the polymer backbone, which again shows a loss of fluorine content, when compared with its unsaturated analogue during the process of hydrogenation, although the effect is small.

3.4 c) Structural characterisation of the copolymers

3.4 c) (i) Nmr spectroscopy

The copolymer structure with the different carbon environments and the numbering system adopted is shown in *Figure 3.42*. A few, of the many, spectra accumulated during the analysis of the copolymers and their hydrogenation products are discussed in this section by way of illustration. The complete data are recorded in the Appendix.

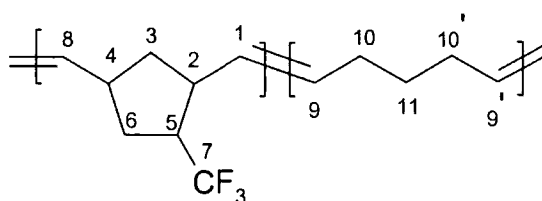


Figure 3.42 Carbon environments for the copolymers synthesised

The complexity of the structure shown in *Figure 3.42* is obvious, however, the spectroscopic data was compared with that for polymer (III) in order to simplify the assignments. The ¹³C nmr spectrum. The ¹³C nmr spectrum for the unsaturated polymer (VII) is shown in *Figure 3.43*, and its expanded vinylic and saturated region with partial assignments of the signals are shown in *Figures 3.44* and *3.45* respectively.

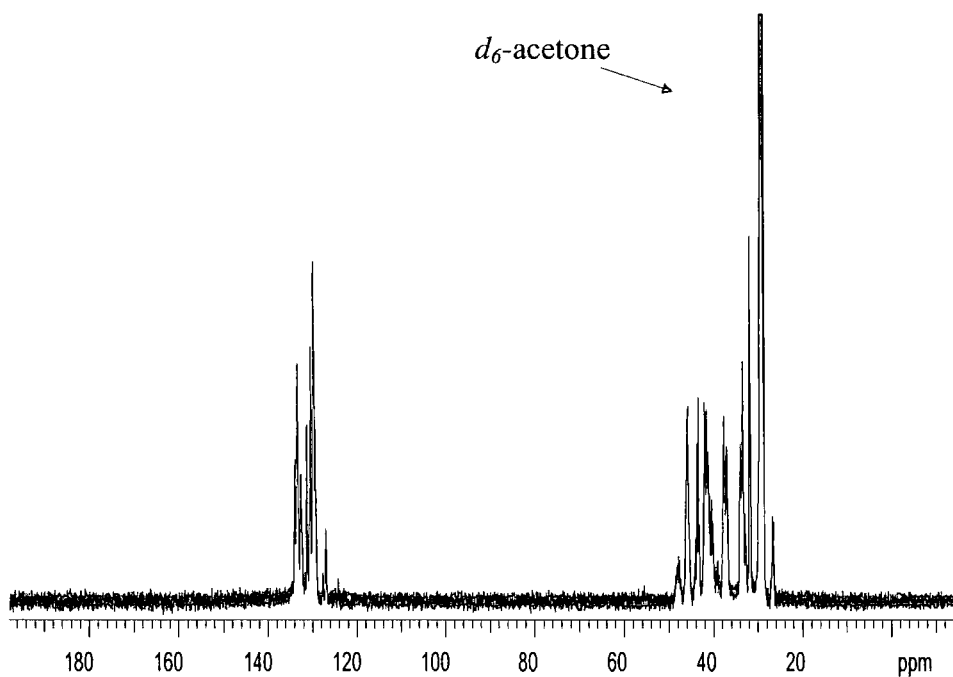


Figure 3.43 The ^{13}C nmr of the unsaturated polymer (VII)

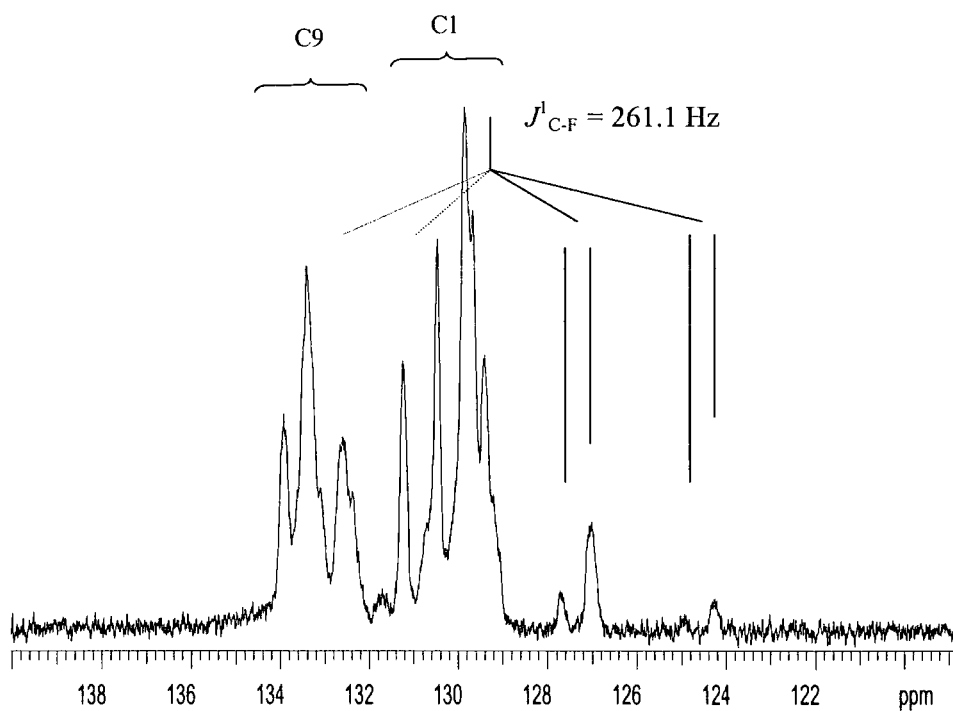


Figure 3.44 The expanded vinylic region in the ^{13}C nmr spectrum of polymer (VII)

The vinylic region of the ^{13}C nmr spectrum, *Figure 3.44*, was more complicated than that for polymer (*III*) with an increase in signal broadening and in the number of signals. The quartet for the carbon of the trifluoromethyl group is only partially resolved, two signals of the expected four can be seen and each occurs as two lines in the *exo:endo* ratio found in the monomer feed. This observation will be confirmed in the analysis of the ^{19}F nmr spectrum, see below. The saturated carbon region of the spectrum, *Figure 3.45*, was similar to that of polymer (*III*) with the addition of signals associated with pentenylene units.

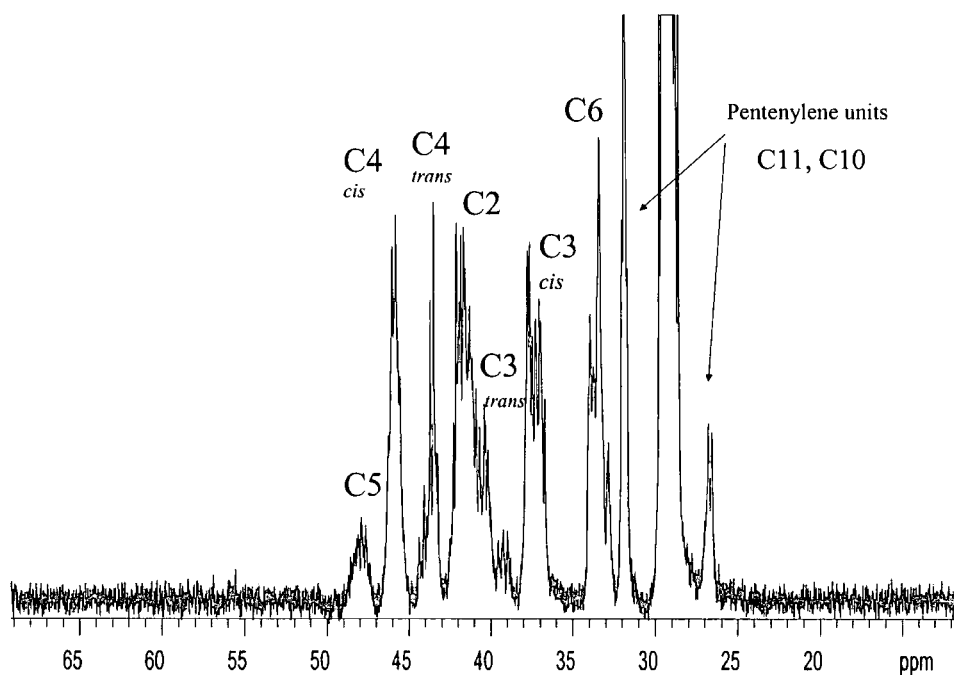


Figure 3.45 The expanded saturated region of the ^{13}C nmr spectrum of polymer (VII)

The ^{13}C nmr spectrum for the saturated copolymer (*VIII*) presents again a flat base line in the vinyl region, see *Figure 3.46*, the CF_3 carbon is visible but partially obscured by the solvent signal, see the expanded spectrum in *Figure 3.47*. The methylene region, shown in *Figure 3.46* displays an increased number of signals as compared to the hydrogenated fluorinated homopolymer, but the spectrum is too complicated, with too many overlapping peaks to allow

analysis of monomer distribution. This evidence confirms the formation of the copolymer and implies a random rather than a blocky distribution of repeat units, since the latter might be expected to give a simpler spectrum.

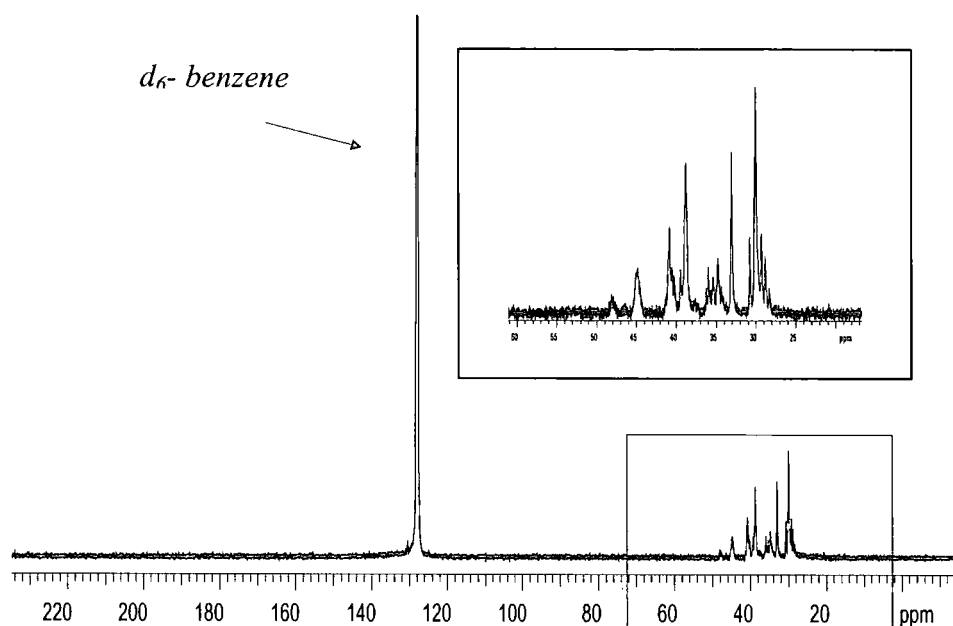


Figure 3.46 The ^{13}C nmr spectrum of polymer (VIII)

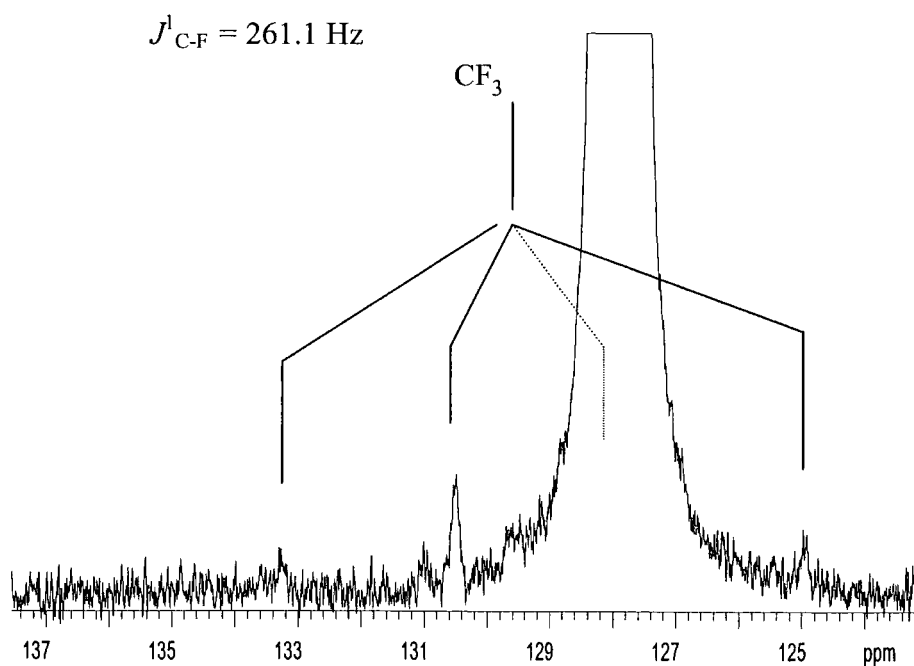


Figure 3.47 The ^{13}C nmr expanded vinyl region

The relative intensities of the expected signals in the ^{19}F nmr spectra were different in the copolymers depending on the different *exo:endo* ratios in the fluorinated monomer used as feed stock. The ^{19}F nmr spectra for the unsaturated polymers (V) (see Appendix AX31) and polymer (VI), see *Figure 3.48*, synthesised from 1:1 and 2:1 mixture of 62:38 *exo:endo* mixture of 5-trifluoromethylbicyclo[2.2.1]hept-2-ene and cyclopentene respectively display identical shifts and integrations of the expected two signals with relative intensities of 61:39, which indicates that the propagation proceeded without discrimination between monomer isomers. In the ^{19}F nmr spectra of the unsaturated polymers (VII), see *Figure 3.49* and (VIII) (see Appendix AX40) synthesised from 79:21/*exo:endo* ratio of 5-trifluoromethylbicyclo[2.2.1]hept-2-ene and cyclopentene, the integration of both signals displays a relative intensity of 80:20, which again indicates no discrimination between isomers during propagation.

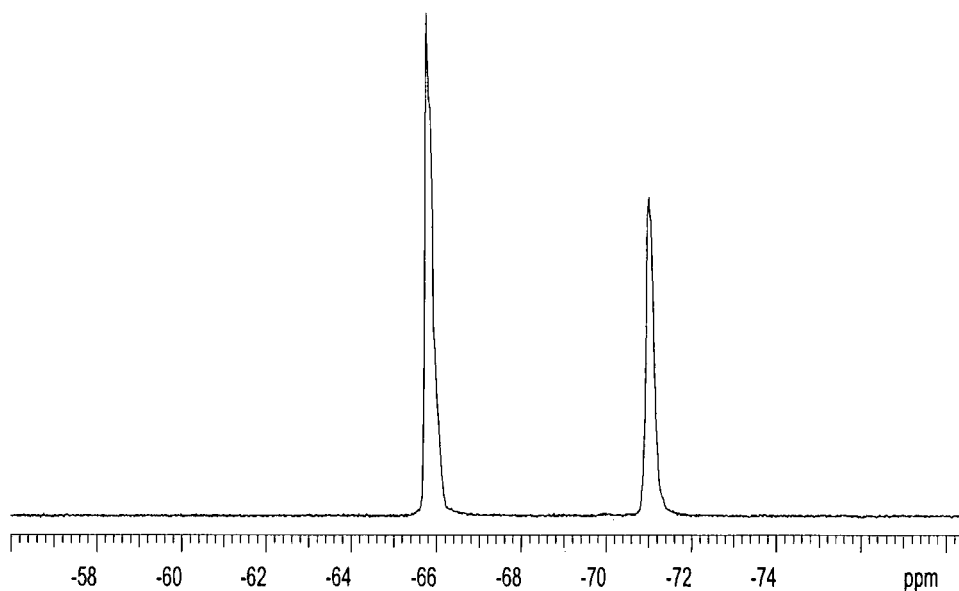


Figure 3.48 The ^{19}F nmr spectrum of copolymer (VI)

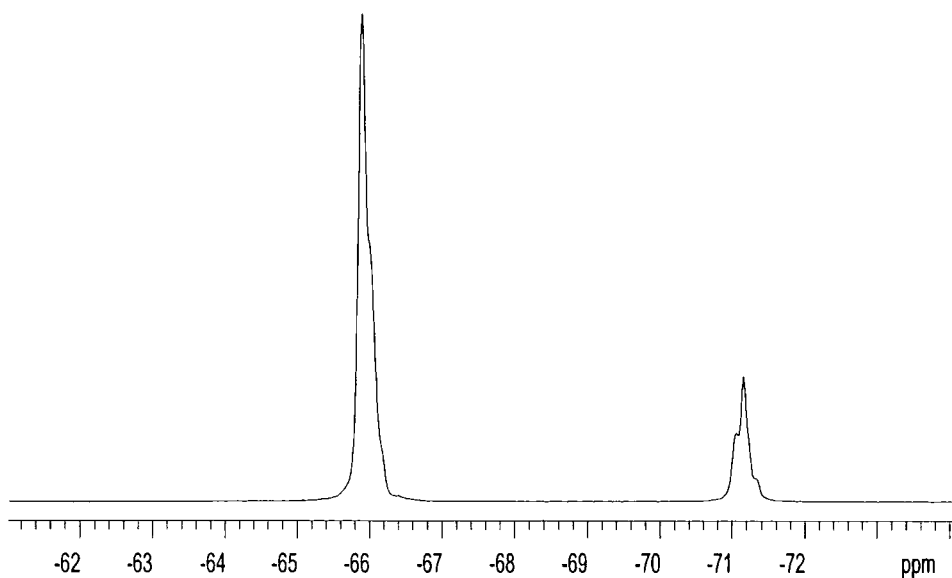


Figure 3.49 The ^{19}F nmr spectrum of copolymer (VII)

The ^{19}F nmr spectra of the hydrogenated polymers displayed chemical signal shifts and integrated intensities identical with their unsaturated analogues (See Appendix AX43 and AX46).

The ^1H nmr spectra of polymer (VII) recorded in d_6 -acetone and its saturated analogue polymer (IX) recorded in d_6 -benzene are compared in *Figure 3.50*. It is clear that the hydrogenation is complete within the detection sensitivity of high-resolution ^1H nmr.

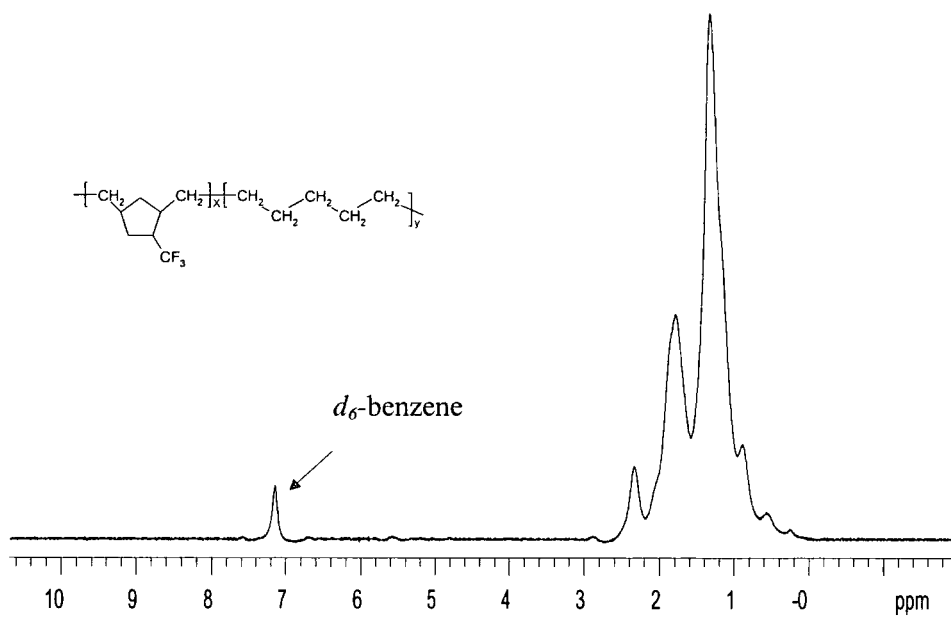
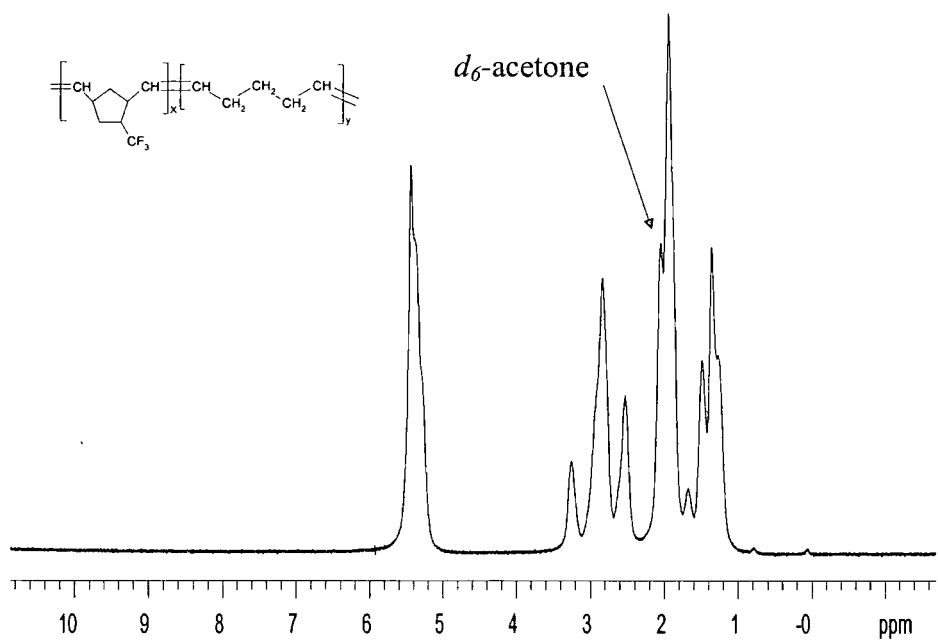


Figure 3.50 A comparison of the ^1H nmr spectra of polymers (VII) (above) and (IX) (below)

3.4 c) (ii) *Elemental analysis of the copolymers*

Elemental analysis is generally a useful tool in the characterisation of polymers. In this work, the fluorine content in the copolymers was used to determine the extent of incorporation of the fluorinated monomer into the copolymers and the results were qualitatively reasonable as discussed earlier. For the sake of completeness the carbon, hydrogen and fluorine analyses of the copolymers are recorded in *Table 3.6*. As already discussed the carbon analyses did not prove reliable for the determination of copolymer incorporation levels. The contrast in reliability between the carbon and fluorine analyses may be a function of the analytical methods used; thus, carbon analyses involve combustion analysis in a flow system and fluorinated materials are notoriously tricky when using this method, whereas fluorine analysis is conducted using potassium fusion in a sealed vessel and is inherently more likely to be reliable with these materials. This is unfortunate because our analysis of the copolymer composition has to depend on only one kind of measurement which means that discussion of small, albeit reproducible, effects (see text above in section 3.4 (b)) has to remain only as a provisional hypothesis.

Polymers	C (%)	H (%)	F (%)
<i>V</i>	64.11	7.24	21.52
<i>VI</i>	63.30	6.66	26.77
<i>VII</i>	63.65	6.53	29.05
<i>VIII</i>	59.09	6.02	31.45
<i>IX</i>	62.26	7.87	28.06
<i>X</i>	56.72	7.03	29.35
<i>XI</i>	-	-	28.29
<i>XII</i>	54.13	6.70	26.99

Table 3.5 Elemental analyses of the Polymers

3.4 d) Physical characterisation of the copolymers

The results obtained from the DSC, GPC and TGA analysis for the copolymers synthesised are shown in *Table 3.6*.

Polymer	DSC	GPC			TGA
	T _g (°C)	M _n	M _w	PDI	% loss at 300 °C
<i>V</i>	-7	-	-	-	0.5
<i>VI</i>	+8	-	-	-	1.3
<i>VII</i>	+42	138,00	152,000	1.1	<0.5
<i>VIII</i>	+60	116,000	189,000	1.6	0.5
<i>IX</i>	+12	65,000	125,000	1.9	<1
<i>X</i>	+36	102,000	123,000	1.2	<5
<i>XI</i>	+20	67,000	106,000	1.6	<0.5
<i>XII</i>	-22	-	-	-	<1

Table 3.6 Physical data of the polymers

From the obtained GPC data for polymers (*VII*), (*VIII*), (*IX*) and (*X*) we can see that hydrogenation has the effect of lowering the molecular weight which suggests that there is some fragmentation at the temperature of refluxing trifluorotoluene (102 °C). However, these GPC data have to be considered with some caution. The traces were recorded in DMF using PEO standards. Many of the samples were not completely soluble in DMF; in general the higher the fluorinated repeat unit content the more soluble the material. The GPC results are consistent with the processes described in that the materials are definitely polymers, but because the GPC obtained is not always representative of the whole sample, the deductions that can be made are not particularly secure. While the main conclusions; namely, that we have polymers and that during hydrogenation some degradation occurs are reasonable. However, the absolute values of M_n, M_w and polydispersity have to be treated with some caution; for

example, the low values observed for the polydispersity of polymers (VII) and (X) almost certainly arise from fractionation effects in dissolving and filtering the sample prior to analysis. The TGA analysis indicates no variation in the thermal stability of the copolymers after the hydrogenation process and that, if any of these materials proves to be useful, the working temperature range will be quite broad.

3.4 e) *Conclusions*

A series of polymers and copolymers were partially or completely hydrogenated to give new materials with new physical and chemical properties. The extent of hydrogenation was 85-95% for the homopolymers (Ia) and (Ib), and over 99 % for all the others. These saturated and partially saturated polymers showed lowered T_g values when compared with their unsaturated analogues. Partially fluorinated elastomers were achieved from copolymers from 5-trifluoromethylbicyclo[2.2.1]hept-2-ene and cyclopentene. The saturated copolymer (XII) with a T_g of -22°C and 27wt-% fluorine content (60 mole-% of fluorinated monomer) was selected as a potential electrostrictive material and a batch of a few grams was prepared for analysis to be carried out in the IRC Laboratories at the University of Leeds in the polymer physics research group of Prof. G.R. Davies.

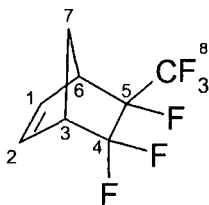
3.5 Experimental procedures

3.5 a) General considerations

Cyclopentadiene was freshly prepared by thermal cracking from dicyclopentadiene purchased from Koch-Light. Hexafluoropropene and 1,1,1-trifluoropropene were purchased from Bristol Organics Ltd., and used without further purification. Tetraphenyltin was purified by successive soxhlet extractions with toluene, dried under vacuum and stored in a glove box. Cyclopentene was distilled from CaH_2 and stored over phosphorous pentoxide. Tungstenhexachloride and molybdenum pentachloride (99.9+) were purchased from Aldrich, used without further purification and stored in the glove box. The different stock solutions were freshly prepared prior to use. Toluene was distilled from sodium and stored over molecular sieves. Trifluorotoluene was distilled prior to use and stored over molecular sieves. *p*-Toluenesulphonylhydrazide was dried under vacuum at room temperature overnight prior to use. All the polymers after precipitation and recovery by filtration were dried in a vacuum oven at 50 °C overnight.

3.5 b) Synthesis of 5,5,6-trifluoro-6-trifluoromethyl bicyclo[2.2.1]hept-2-ene

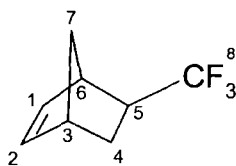
Freshly distilled cyclopentadiene (4.43 g, 5.5 ml, 67 mmol) was injected into an oxygen-free Carius tube containing hydroquinone (0.45g). Hexafluoropropene (21 g, 100 mmol) was vacuum transferred into the Carius tube, which was sealed under vacuum. The Carius tube was placed in a furnace at 180 °C for 72 hours. After "hot-spotting" to open the tube, the contents were flash distilled to give 5,5,6-trifluoro-6-trifluoromethylbicyclo[2.2.1]hept-2-ene as a colourless liquid mixture of *exo* and *endo* isomers (12.50g, 87 %) (b.p. = 140 °C; lit ¹⁰¹ 140-140.5 °C) capillary gc showed two peaks, $t_R = 4.68$ min, 67.5% *exo* adduct; $t_R = 4.76$ min 32.2 % *endo* adduct. Found: C, 44.6; H, 2.8; F, 52.8%; $\text{C}_8\text{H}_6\text{F}_6$ requires C, 44.5; H, 2.8; F, 52.7%.



^1H nmr: (*exo*; δ/ppm) 6.24 (2H, s, $-\text{CH}=\text{}$); 3.27 (2H, s, C-H); 2.30 (2H, s, $-\text{CH}_2-$); (*endo*; δ/ppm) 6.34 (2H, s, $-\text{CH}=\text{}$); 3.13 (2H, s, C-H); 2.05 (2H, s, $-\text{CH}_2-$). **^{19}F nmr:** (*exo*; δ/ppm): -169.5 (1F, q, $J_{\text{FF}} = 6.8\text{Hz}$, C-F); (2F, ABq, $J_{\text{FF}} = 237.85\text{Hz}$, $\delta_{\text{A}} = -109.07\text{ ppm}$, $J_{\text{FF}} = 12.79\text{Hz}$, $\delta_{\text{B}} = -108.23\text{ ppm}$, $J_{\text{FF}} = 5.26\text{Hz}$, $-\text{CF}_2-$); -76.01 (3F, dd, $J_{\text{FF}} = 13.17\text{Hz}$, $J_{\text{FF}} = 8.27\text{Hz}$, CF_3); (*endo*; δ/ppm): -170.3 ppm (1F, s, C-F); -107.9 (2F, d, $J_{\text{FF}} = 6.8\text{Hz}$); -74.7 (3F, td, 14.30 Hz and 6.7 Hz). **^{13}C nmr:** 135.9 (C2 *exo/endo*, dd, $J_{\text{C-F}} = 5.8$ and 1.4 Hz); 134.4 (C1 *exo*, d, $J_{\text{C-F}} = 22.5\text{Hz}$); 134.08 (C1 *endo*, d, $J_{\text{C-F}} = 7.9\text{Hz}$); 124.85 (C4 *endo*, ddd, $J_{\text{C-F}} = 272.3$ and 265.9Hz, $J_{\text{C-F}} = 16.8\text{ Hz}$); 124.7 (C4 *exo*, td, $J_{\text{C-F}} = 271.15$ and 265.9Hz, $J_{\text{C-F}} = 16.8\text{Hz}$); 121.8 (C8 *exo*, qd, $J_{\text{C-F}} = 283.2\text{ Hz}$, $J_{\text{C-F}} = 32.1\text{ Hz}$); 121.88 (C8 *endo*, qd, $J_{\text{C-F}} = 283.2\text{Hz}$, $J_{\text{C-F}} = 25.26\text{ Hz}$); 95.4 (C5 *exo/endo*, dm, $J_{\text{C-F}} = 209.3\text{ Hz}$); 49.01 and 48.825 (C3 *endo* or *exo*, two doublets with $J_{\text{C-F}} = 84\text{ Hz}$ and $J_{\text{C-F}} = 82\text{Hz}$ respectively); 48.82 (C3 *endo* or *exo*, t, $J_{\text{C-F}} = 88\text{ Hz}$); 47.6 (C6 *endo*, d, $J_{\text{C-F}} = 86\text{ Hz}$); 46.9 (C6 *exo*, d, $J_{\text{C-F}} = 78\text{ Hz}$); 44.8 (C7 *endo* or *exo*, s); 42.3 (C7 *endo* or *exo*, s); **IR:** C-H stretch 3080 cm^{-1} , $\text{CH}=\text{CH}$ stretch $1610\text{-}1631\text{ cm}^{-1}$, C-F stretches $1390\text{-}1000\text{ cm}^{-1}$. **MS:** $\text{M}^+ = 216$, ($\text{M}_{100\%}$, 66, retro Diels-Alder), 196, 176, 164, 144, 126, 94.

3.5 c) Synthesis of 5-trifluoromethylbicyclo[2.2.1]hept-2-ene

Freshly distilled cyclopentadiene (15 g, 67 mmol) and hydroquinone (0.45 g) were mixed in a Carius tube. 3,3,3-Trifluoropropene (6.43 g, 100 mmol) was introduced by vacuum transferred and the tube was sealed from the vacuum line and heated at 180°C for 72 hours. After opening by "hot-spotting" the contents of the tube were flash distilled to give a 62:38 mixture of the *exo* and *endo* isomers of 5-trifluoromethylbicyclo[2.2.1]hept-2-ene (II) (8.5 g, 52 % yield) as a colourless liquid. (b.p. = 118°C , lit.¹⁰² 119°C)



^1H nmr was complex with much overlapping of peaks (*exo*; vinyl hydrogens, δ/ppm): 6.21 (1H, m, $-\text{CH}=\text{}$, C2/C1); 6.19 (1H, s, $-\text{CH}=\text{}$, C1/C2); 2.00 (1H, m, CH_2 , C7); (*endo*; vinyl hydrogens, δ/ppm): 5.95 (2H, m, $=\text{CH}-$). **^{19}F nmr**: Two peaks at -68.28 ppm (1F, *endo* $J_{\text{F-H}}^3 = 9.78$ Hz) and -66.15 ppm (1F, *exo*, $J_{\text{F-H}}^3 = 10.16$ Hz). **^{13}C nmr** (δ/ppm): 138.2 (C1 *endo*); 137.62 (C2 *endo*); 136.45 (C1 *exo*); 131.93 (C2 *exo*); 128.56 (C8 *endo*, q, $J_{\text{C-F}}^1 = 278$ Hz); 128.1 (C8 *exo*, q, 277.6 Hz); 50.06, 46.2, 43.5, 43.3, 43.0, 42.7, 42.5, 42.2, 41.4 (C5, C6, C3, C4 *endo/exo*); 27.8 (C7 *exo*); 27.3 (C7 *endo*). **GC-MS EI+**: Two signals, identical MS (M^+ 162); 66 (100 % retro Diels-Alder, 93, 77, 51, 39, 27.

3.5 d) General procedure for ring-opening metathesis polymerisation

Ph_4Sn (2 equivalents) was placed in dry ampoule equipped with a magnetic stirrer and flushed with dry oxygen-free nitrogen. WCl_6 or MoCl_5 (0.01 M solution in toluene, 1 equivalent) was injected via a rubber seal. After the required activation time (10 to 15 minutes for the tungsten based catalyst, when the colour changed from blue-black to dark-brown and 5 minutes for the molybdenum based catalyst, colour changed from black-green to dark-brown), the monomer or mixture of monomers (500 equivalents) was injected and the solutions were stirred vigorously. The solutions became more viscous until the stirrer stopped. After quenching the reaction with a few drops of MeOH, the contents of the ampoule were poured in acetone and dissolved. The acetone solutions were partially rotary evaporated to give a viscous solution and the polymers were precipitated by dropwise addition to 5-fold excess of cold n-hexane, recovered by filtration and dried under vacuum.

3.5 d) General procedure for the hydrogenation of the polymers

The polymers were dissolved in trifluorotoluene (50 ml for 1 g of polymer) and placed in an oxygen-free three-necked flask equipped with a reflux condenser and a magnetic stirrer. *p*-Toluenesulphonylhydrazide (15 to 20 times weight of the polymer) was added in small aliquots at intervals of 30 minutes while the solution was stirred at reflux (102 °C). The mixture was cooled to room temperature and the contents of the flask were poured directly into a 10-fold excess of cold methanol and stirred for 30 minutes. The precipitated solid was recovered by filtration and dried in a vacuum oven at 50°C overnight. The products were re-dissolved in the minimum amount of acetone or benzene and re-precipitated in a 5-fold excess of cold methanol. The white solids obtained were recovered by filtration and dried in a vacuum oven at 50°C overnight to give the saturated or partially saturated polymers.

Possible future work

The author suggests that the synthesis and RROP of a monomer incorporating an alkyl side chain substituent, R, as shown in *Figure 4.1*, which was unsuccessfully attempted in the present work, is never the less worth further pursuit.

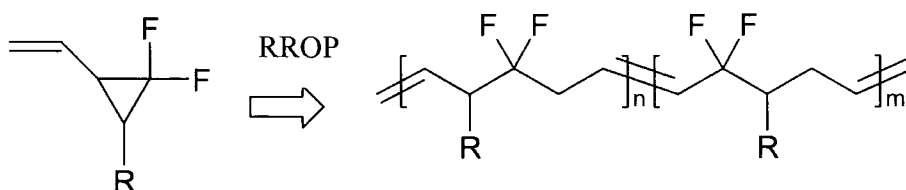


Figure 4.1 Proposed monomer and polymer structure

Also an increase in of the fluorine content in the monomer would increase the polarity of the resulting polymer and might improve the electrostrictive actuation, see *Figure 4.2*, for a suggested monomer modification.

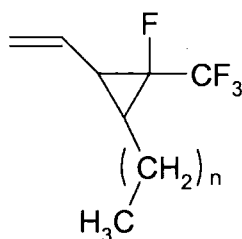


Figure 4.2 Target monomer

The monomers and polymers described above would require novel synthesis for which there are no literature precedents. However, the monomer shown in *Figure 4.3* has been previously made, although polymerisation studies have not been reported.¹⁰³

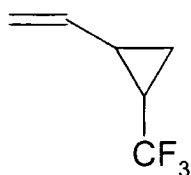


Figure 4.3 Plausible polymerisable monomer¹⁰³

It is suggested that the RROP of the monomer shown in Figure 4.3 might reasonably be expected to give the polymer shown in Figure 4.4 and that this polymer might have a lower T_g than 1,1-difluoro-2-vinylcyclopropane. As in this work, hydrogenation would be expected to give a further decrease in T_g .

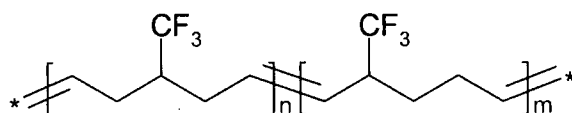


Figure 4.4 Suggested repeat units in the new polymer

The electrostrictive behaviour of the copolymer synthesised via ROMP of 5-trifluoromethylbicyclo[2.2.1]hept-2-ene and cyclopentene monomers shown in Figure 4.5, with an observed T_g of -22°C has yet to be investigated. In the case that a successful electrostrictive response is obtained, the conditions for the synthesis of such material should be optimised in order to obtain higher yields and/or molecular weights as required.

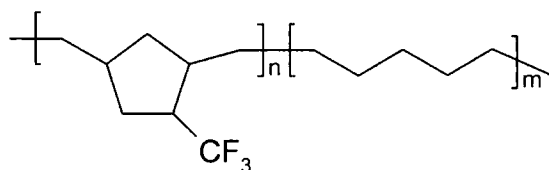


Figure 4.5 Potentially electrostrictive polymer synthesised

The degree of hydrogenation might be controlled so as to leave some residual unsaturation as potential cross-linking sites, which might give improved dimensional stability.

References

- ¹Cochlin, R.L., Ph.D. Thesis, University of Durham, (1998).
- ²Cady, W.D., 'Piezoelectricity', McGraw-Hill, New York, London (1964).
- ³Pelrine, R., Kornbluh, R., Joseph, J., *Materials Science & Engineering*, **C11**, 89-100 (2000).
- ⁴Pelrine, R., Kornbluh, R., Joseph, J., *Sensors & Actuators*, **A64**, 77-85 (1998).
- ⁵Bar-Cohen, Y., 'Electroactive polymer actuators (EAP) as artificial muscles. Reality, Potential and challenges' SPIE Press (2001).
- ⁶Nemoto, H., Hayashi, H., *J. Appl. Polym. Science*, **53**, 79-84 (1994).
- ⁷Schreyer, HB, Gebhart, N., Kim, K.J., *Biomacromolecules*, **4**, 642-647 (2000).
- ⁸Baughman, R., Kertesz, M., Sun, G.Y., Kurti, J., *Abstr. Pap. Amer. Chem. Soc.*, **22**, 218 (1999).
- ⁹Chattogalyay, D., Baughman, R., Zakhidov, A., *Abstr. Pap. Amer. Chem. Soc.*, 221 IECPart 1 (2001).
- ¹⁰Shahinpoor, M., Kwang, J., Kim, K.J., *Sensors and Actuators A*, **96**, 125-132 (2002).
- ¹¹Bar-Cohen, Y., Xue, T., Shahinpoor, J., Simpson O., Smith J., *Proceedings of SPIE's 5th Annual International on Smart Structures and Materials*, San Diego, (CA). 3324-32 (1998).
- ¹²Su, J., Zhang, Q.M., Wang, P.C., MacDiarmid, A.G., Wynne, K.J., *Polymers for advanced technologies*, **9**, 317-321 (1998).
- ¹³Xu, T.B., Cheng, Z.Y., Zhang, Q. M., Baughman, R. H., Cui, C., Zakhidov, A. A., Su, J., *J. Appl. Physics*, **88**, 404 (2000).
- ¹⁴Omote, K., Ohigashi, H., Koga, K., *J. Appl. Physics*, **81**, 2760 (1997).
- ¹⁵Buckley, S., Roland, C.M., *Appl. physics letters*, **78**, 29 (2001).
- ¹⁶Lehmann, W., Skupin, H., Tolksdorf, C., Gebhard, E., Zentel, R., Kruger, P., Losche, M., Kremer, F., *NATURE*, **410**, 447-450 (2001).
- ¹⁷Takahashi, T., Yamashita, I., Miyakama, T., *Bull. Chem. Soc. Japan*, **37**, 131-132 (1964).
- ¹⁸Takahashi, T., Yamashita, I., *Polym. Letters*, **3**, 251-5 (1965).
- ¹⁹Lishanskii et. al., *Polym. Science USSR* **A9**, 2138-48 (1965).
- ²⁰Takahashi, T., *J. Polym. Science A1*, **6**, 403-414 (1968).
- ²¹Ahm, K.D., *Polym. Letters*, **15**, 751-753 (1977).
- ²²Cho, I., Ahm, K.D., *J. Polym. Science*, **17**, 3169-3182 (1979).

- ²³Endo, T., Watanabe, M., Suga, K., Yokozama, T., *J. Polym. Science*, **A25**, 3039-3048 (1987).
- ²⁴Sanda, F., Takata, T., Endo, T., *Macromolecules*, **28**, 1346-1355 (1995).
- ²⁵Noels, F., *J. Organomet. Chem.*, **606**, 55-64 (2000).
- ²⁶Wilson B., Ph.D. thesis, University of Durham, (1978).
- ²⁷Banks, L., Bailey G.C., *Ind. Eng. Chem., Prod. Res. And Develop.*, **3**, 170 (1964).
- ²⁸Scott W., Calderon N., *J. Amer. Chem. Soc.*, **90**, 4133 (1968).
- ²⁹Wasserman R., Ben-Efram, D.A., Wolovsky R.J., *J. Amer. Chem. Soc.*, **90**, 3286 (1968).
- ³⁰Ivin, J., 'Olefin metathesis', Academic Press, New York (1983).
- ³¹Anderson, W., Merklings, N.G., *Chemical abstracts*, **50**, 3008 (1955).
- ³²Eleuterio, S., US Pat, 3074918 (1957).
- ³³Feast, W. J., Khosravi, E., *J. Fluorine Chem.*, **100**, 117-125 (1999).
- ³⁴Dolbier, W. R., Wojtowicz, H., Burholder, C. R., *J. Org. Chem.*, **55**, 5420-5422 (1990).
- ³⁵Weyerstahl, P., Klamann, D., Fligge, M., Finger, C., Nerdel, F., Buddrus, J., *Liebigs Ann. Chem.*, **710**, 17-35 (1967).
- ³⁶Gassen, K., Baasner, K.B., *J. Fluorine Chem.*, **49**, 127-139 (1990).
- ³⁷Zhulin, V.M., Gonikberg, M.G., Volchek, A.R., Nefedov, O.M., Shaahkov, A.S., *Vysokomol. Soedin., Ser. A*, **15**, 2258 (1973); *Chem. Abstr.*, **80**, 48457h (1973).
- ³⁸Seyferth, D., Hopper, S.P., *J. Org. Chem.*, **37**, 4070 (1972).
- ³⁹Burton, D.J., Nae, D.G., *J. Amer. Chem. Soc.*, **95**, 8467 (1973).
- ⁴⁰Tian, F., Dolbier, W.R., *Org. Letters*, **2**, 835-837 (2000).
- ⁴¹Moszner, N., Zeuner, F., Volkel, T., *Macromol. Chem. Physics*, **200**, 2173-2187 (1999).
- ⁴²Endo, T., Suga, K., *J. Polym. Science, Part-A-Polym. Chem.*, **27**, 1831-1842 (1989).
- ⁴³Sanda, F., Takata, T., Endo, T., *Macromolecules*, **26**, 1818-1824 (1993).
- ⁴⁴Sanda, F., Endo, T., *J. Polym. Science, Part A-Polym. Chem.*, **39**, 265-276 (2001).
- ⁴⁵Tian, F., Bartberger, M.D., Dolbier W.R., *J. Org. Chem.*, **64**, 540-546 (1999).

- ⁴⁶Williams, D.,H., Fleming, I., '*Spectroscopic methods in organic chemistry*', 5th ed., MacGraw-Hill (1995); Kalinowsky, H.O., Berger, S., Braun, S., '*Carbon-13 NMR Spectroscopy*', Wiley & Sons (1988); Berger, S., Braun, S., Kalinosky, H.O., '*NMR spectroscopy of the non-metallic elements*', Wiley & Sons (1997).
- ⁴⁷March, J., '*Advanced Organic Chemistry*', John Wiley & Sons, Inc., 839 (1992).
- ⁴⁸McMurry, J.E., Fleming, M.P., *J. Amer. Chem. Soc.*, **96**, 4708 (1974).
- ⁴⁹McMurry, J.E., Krepski, L.R., *J. Org. Chem.*, **41**, 3929 (1976).
- ⁵⁰Mukaiyama, T., Sato, T., Hanna J., *Chem. Letters*, 1041 (1973).
- ⁵¹McMurry, J.E., *Chem. Rev.*, **89**, 1513-1524 (1989).
- ⁵²Lenoir, L., *Synthesis*, **553**, (1977).
- ⁵³McMurry, J.E., *Acc. Chem. Res.*, **16**, 405-411 (1983).
- ⁵⁴Reddy, S.M., Duraisamy, M., Walborsky, H.M., *J. Org. Chem.*, **51**, 2361-2366 (1985).
- ⁵⁵Coe, P. L., Scriven, C.E., *J. Chem. Soc.-Perkin trans 1*, **15**, 475 (1986).
- ⁵⁶McMurry, J.E., Fleming, M.P., Kees, K. L., Krepski, L.R., *J. Organomet. Chem.*, **43**, 3255 (1978).
- ⁵⁷Fitjer, L., Quabeck,U., *Synthetic Communications*, **15**, 855-864 (1985).
- ⁵⁸Brown, P., Bonnert, R., Jenking, P., Lawrence, N., Selim, M., *J. Chem. Soc. Perkin trans 1*, **8**, 1893 (1991).
- ⁵⁹Block, E., Gebreyes, K., *Tetrahedron Letters*, **25**, 5469 (1984).
- ⁶⁰Block, E., Aslam, M., *J. Amer. Chem. Soc.*, **105**, 6164 (1983).
- ⁶¹Hibino, J., Okazoe, T., *Tetrahedron Letters*, **26**, 5570-5580 (1985).
- ⁶²Fiandanese, V., Marchese, G., Ronzini L., *Tetrahedron Letters*, **25**, 4805 (1984).
- ⁶³Corey, E.J., Schmidt, G., *Tetrahedron Letters*, **5**, 399-402 (1979).
- ⁶⁴Johnson, C.R., Tait, B.D., *J. Org. Chem.*, **52**, 281-283 (1987).
- ⁶⁵Hartne, F.W., Schwartz, J., *J. Amer. Chem. Soc.*, **103**, 4979-4981 (1981).
- ⁶⁶Eisch, J., Piotrowski, A., *Tetrahedron Letters*, **24**, 2043 (1983).
- ⁶⁷Takai, K., Hotta, Y., Oshima, K., Nozaki, H., *Tetrahedron Letters*, **27**, 2417 (1978).

- ⁶⁸Hibino, J., Okazoe, T., Takai, K., Nozaki, H., *Tetrahedron Letters*, **45**, 5579 (1985).
- ⁶⁹Reetz, M.T., '*Organotitanium reagents in Organic Synthesis*' Springer-Verlag, Berlin (1998).
- ⁷⁰Sauer, J., *Angew. Chem. Internat. Edit.*, **6**, 1 (1967).
- ⁷¹Dzhemilev, U., Ibragimov, A.G., *J. Org. Chem.*, **466**, 1-2 (1994).
- ⁷²Scott, F., *J. Organomet. Chem.*, **144**, 13-16 (1978).
- ⁷³Nunomoto, S., Kawakami, Y., Yamashita, Y., *J. Org. Chem.*, **48**, 1912 (1983).
- ⁷⁴Kawakami, Y., Toida, K., Ito, Y., *Macromolecules*, **26**, 1177 (1993).
- ⁷⁵Renslo, A., Danheiser, R., *J. Org. Chem.*, **22**, 7840-7850 (1998).
- ⁷⁶Simmons, H.E., Smith, R.D., *J. Amer. Chem. Soc.*, **80**, 5323 (1985).
- ⁷⁷Woodworth A., Skell C., *J. Amer. Chem. Soc.*, **79**, 2542 (1957).
- ⁷⁸Moss, R.A., Jones, M., '*carbenes*', John Wiley and Sons, New York, 1, 153-304 (1973)
- ⁷⁹Kirmse, W., Frey, H.M., Gaspar, P.P., Hammond, G.S., '*Carbene chemistry*', Academic Press, New York (1964)
- ⁸⁰Endo, T., Watanabe, M., Suga, K., Yokozawa, T., *J. Polym. Science, Part A-Polym. Chem.*, **25**, 3039 (1987).
- ⁸¹Sanda, F., Takata, T., Endo, T., *Macromolecules*, **28**, 1346 (1995).
- ⁸²Williams, R.M., Maruyama, L.K., *J. Org. Chem.*, **52**, 4044 (1987).
- ⁸³Hurdlick, P.F., Peterson, D., *Tetrahedron Letters*, 1133 (1974).
- ⁸⁴Hurdlick, P.F., Peterson, D., *J. Amer. Chem. Soc.*, **97**, 1464 (1975).
- ⁸⁵Perry, D.R.A., *Fluorine Chem. Revs.*, **1**, 253 (1967).
- ⁸⁶Streck, R., *Chem. Tech.*, 486 (1975).
- ⁸⁷Kaisha, K., Demande, Fr., **2**, 323, 709.
- ⁸⁸Demande, Fr., **2**, 298, 560.
- ⁸⁹Herisson, J.L., Chauvin, Y., *Makromol. Chem.*, **141**, 161 (1970).
- ⁹⁰Mark, H., Bikales, N., Overberger, C., Menges, G., '*Encyclopedia of Polymer Science and Engineering*, **7**, Schulz D. J., Wiley & Sons, 807-817 (1987).
- ⁹¹Bursics, A.R., Murray, M., Stone, F.G.A., *J. Organometal. Chem*, **111**, 31 (1976)
- ⁹²Smart, B.E., *J. Org. Chem.*, **38**, 2027 (1973)
- ⁹³Feast, W.J., Khosravi, E., *J. Fluorine Chem.*, **100**, 117-125 (1999).

- ⁹⁴Ivin, K.J., Mol, J.C., '*Olefin metathesis and metathesis polymerization*', Academic Press, London, (1997).
- ⁹⁵Alimunar, A.B., Edwards, J.H., Feast, W.J., Wilson, B., *Polymer*, **27**, 1281 (1986).
- ⁹⁶Ivin, K.J., Lavery, D.T., Rooney, J.J., *Makromol. Chem.*, **178**, 1545 (1977).
- ⁹⁷Ivin, K.J., Lavery, D.T., Rooney, J.J., *Recl. Trav. Chim. Pays Bas*, **96**, 54 (1977).
- ⁹⁸Ivin, K.J., Lavery, D.T., Rooney, J.J., *Makromol. Chem.*, **179**, 253 (1978).
- ⁹⁹Arnold, D.R., Trecker, D. J., Whipple, E.B., *J. Amer. Chem. Soc.*, **87**, 2596 (1965)
- ¹⁰⁰Blackmore, P.M., Feast, W.J., *Polymer*, **27**, 1296 (1986).
- ¹⁰¹Braedlin, H.P., Grindahl, G.A., Kim, Y.S., McBee, E.T., *J. Amer. Chem. Soc.*, **84**, 2112 (1962).
- ¹⁰²McBee, E.T., Hsu, C.G., Pierce, O.R., Roberts, C.W., *J. Amer. Chem. Soc.*, **77**, 915 (1955).
- ¹⁰³Dolbier, W.R., McClinton, M.A., *J. Fluorine. Chem.*, **70**, 249-253 (1995).

Appendix chapter 2

MG Miguel

Pulse Sequence: gCOSY

Solvent: CDCl₃

Ambient temperature

File: /data/m40207/31172425-05

Processed on "ircnmr"

Relax. delay 1.000 sec

Acq. time 0.140 sec

Width 3649.6 Hz

2D Width 3649.6 Hz

2 repetitions

256 increments

OBSERVE H1, 399.9694234 MHz

DATA PROCESSING

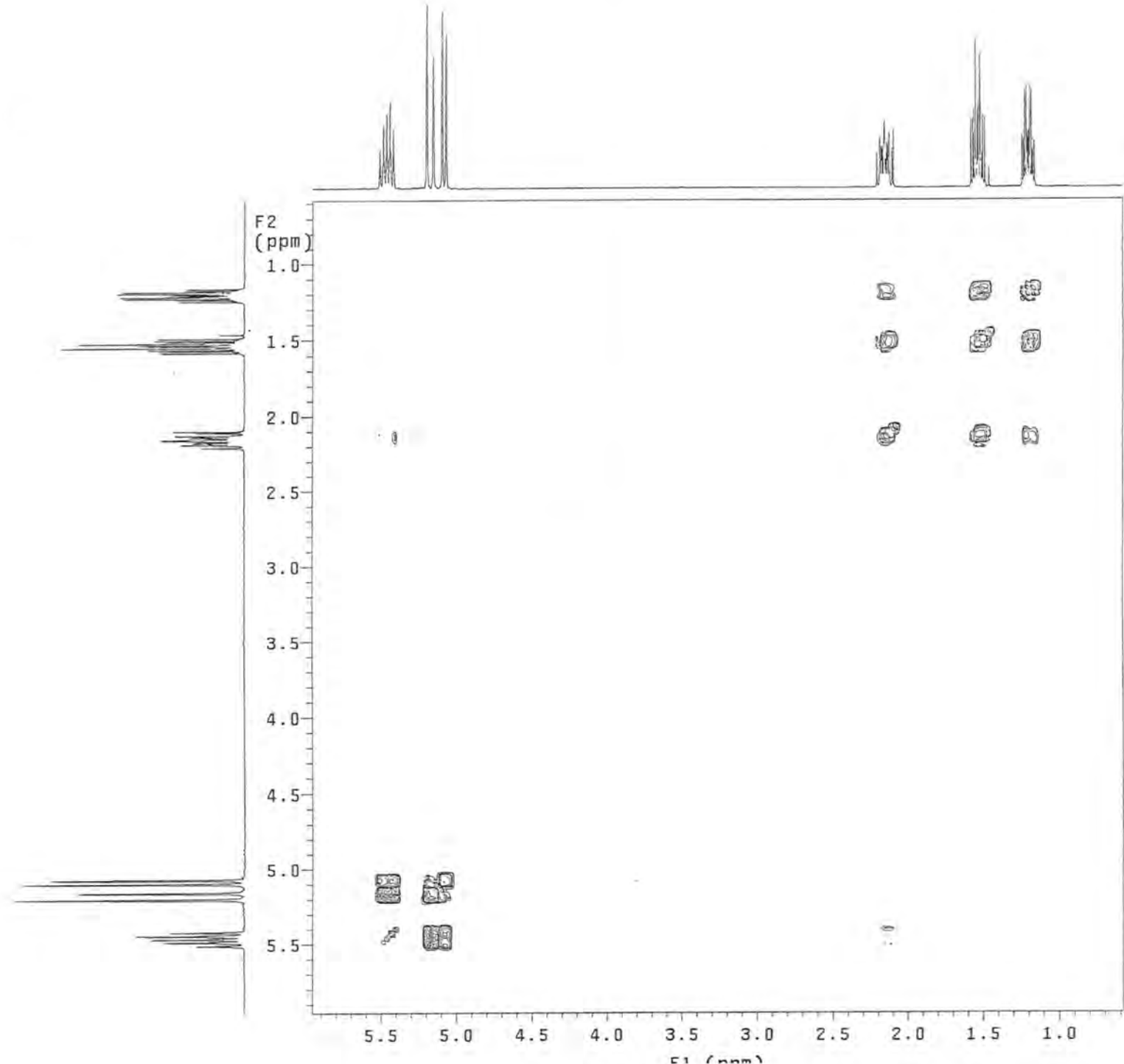
Sq. sine bell 0.070 sec

F1 DATA PROCESSING

Sq. sine bell 0.035 sec

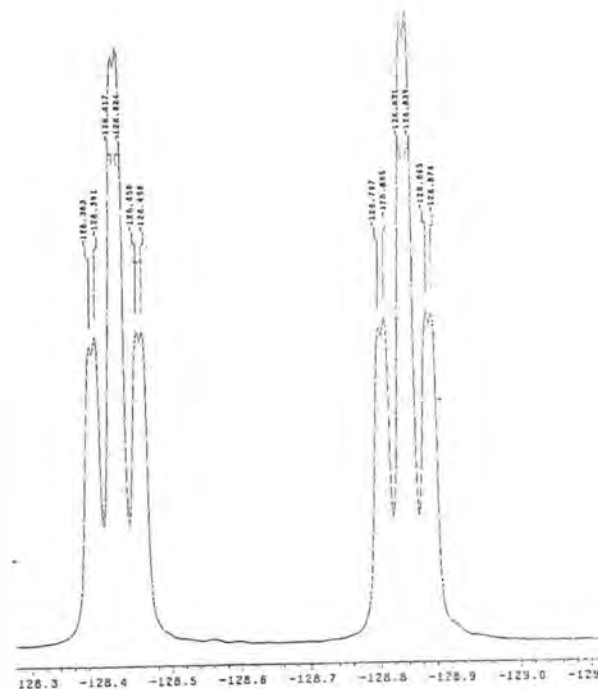
FT size 1024 x 1024

gCOSY spectrum of 1,1-difluoro-2-vinylcyclopropane



AX1


```
Relax. delay 1.000 sec
Pulse 35.0 degrees
Acq. time 0.600 sec
Width 100.0 kHz
16 repetitions
OBSERVE F19, 376.3473929 MHz
DATA PROCESSING
Line broadening 1.7 Hz
FT size 262144
Total time 0 min, 25 sec
```



¹⁹F-NMR spectrum of 1,1-difluoro-2-vinylcyclopropane

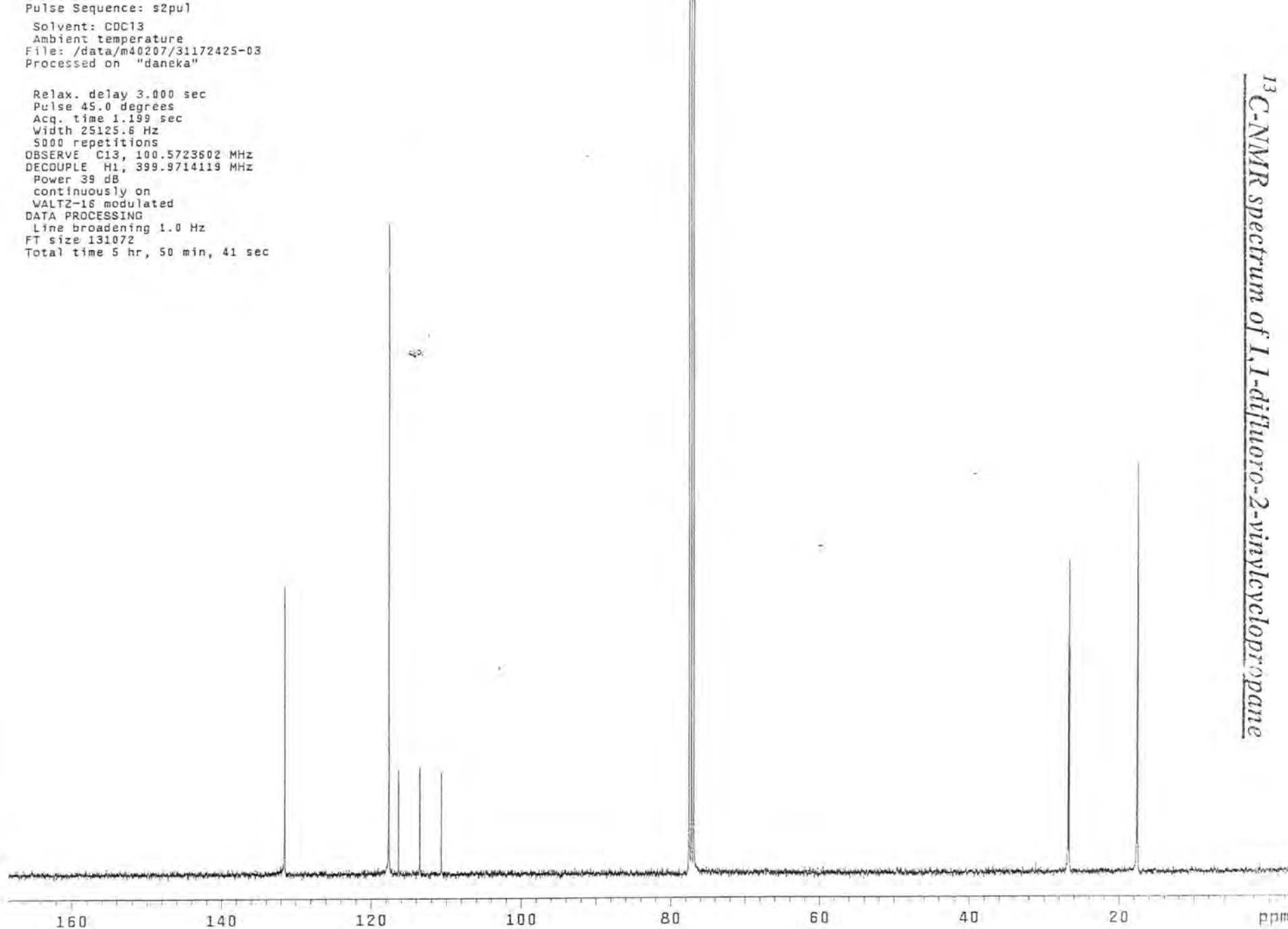
AXX2

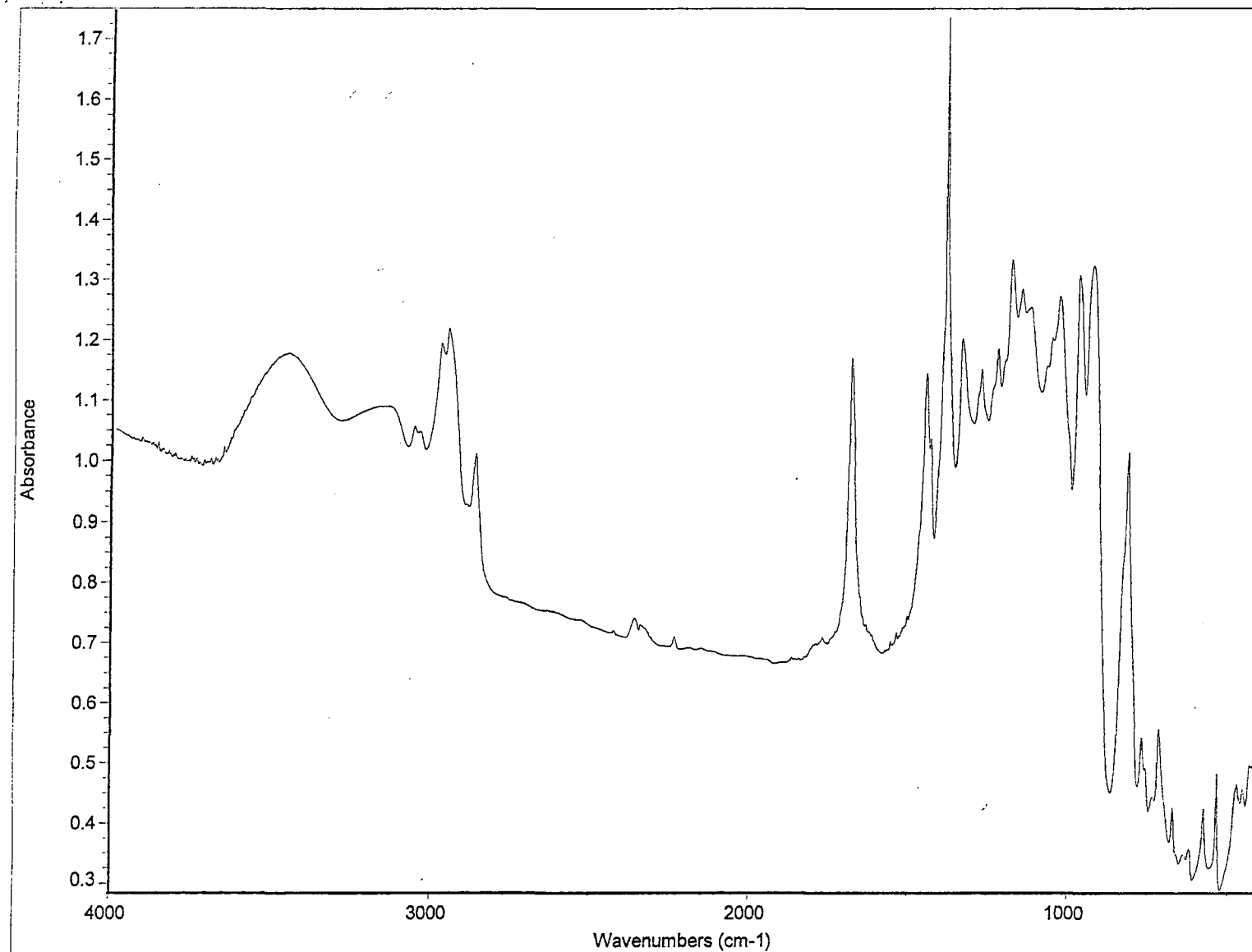
Pulse Sequence: s2pu1
Solvent: CDCl3
Ambient temperature
File: /data/m40207/31172425-03
Processed on "daneka"

Relax. delay 3.000 sec
Pulse 45.0 degrees
Acq. time 1.199 sec
Width 25125.6 Hz
5000 repetitions
OBSERVE C13, 100.5723602 MHz
DECOUPLE H1, 399.9714119 MHz
Power 39 dB
continuously on
WALTZ-16 modulated
DATA PROCESSING
Line broadening 1.0 Hz
FT size 131072
Total time 5 hr, 50 min, 41 sec

¹³C-NMR spectrum of 1,1-difluoro-2-vinylcyclopropane

AX3





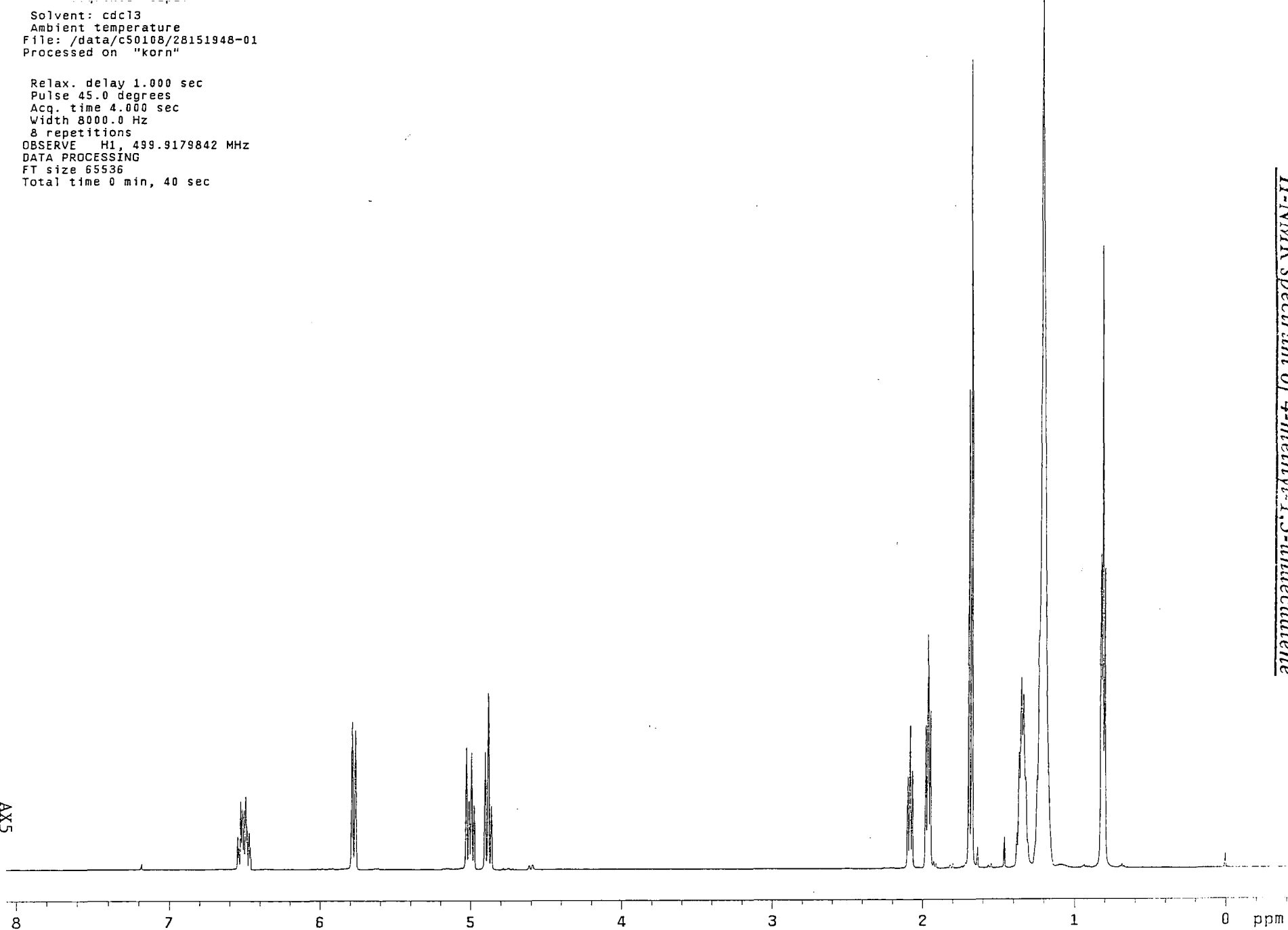
IR spectrum of poly(1,1-difluoro-2-vinylcyclopropane)

Solvent: cdc13
Ambient temperature
File: /data/c50108/28151948-01
Processed On "korn"

Relax. delay 1.000 sec
Pulse 45.0 degrees
Acq. time 4.000 sec
Width 8000.0 Hz
8 repetitions
OBSERVE H1, 499.9179842 MHz
DATA PROCESSING
FT size 65536
Total time 0 min, 40 sec

¹H-NMR spectrum of 4-methyl-1,3-undecadiene

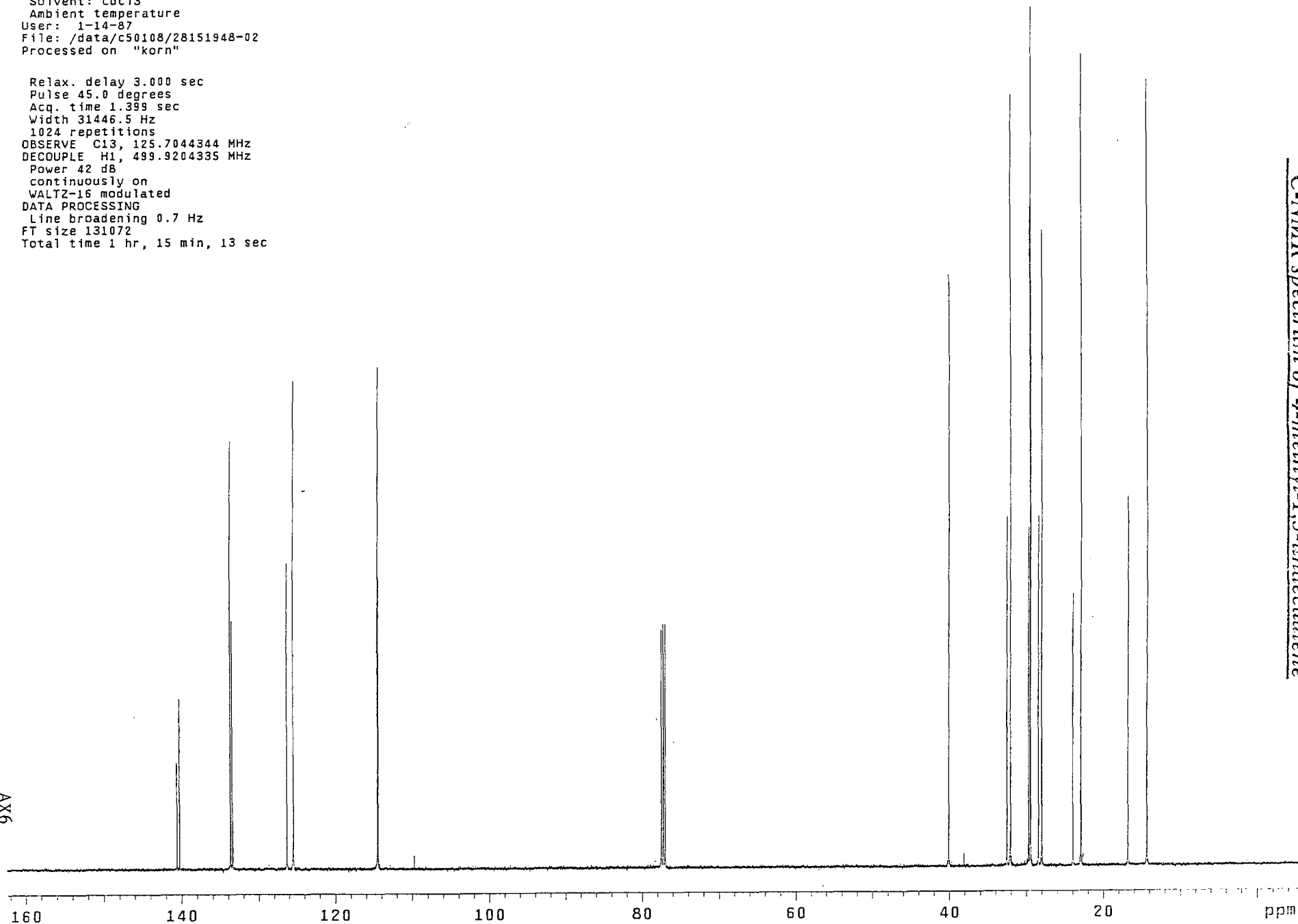
AX5



Solvent: cdc13
Ambient temperature
User: 1-14-87
File: /data/c50108/28151948-02
Processed on "korn"

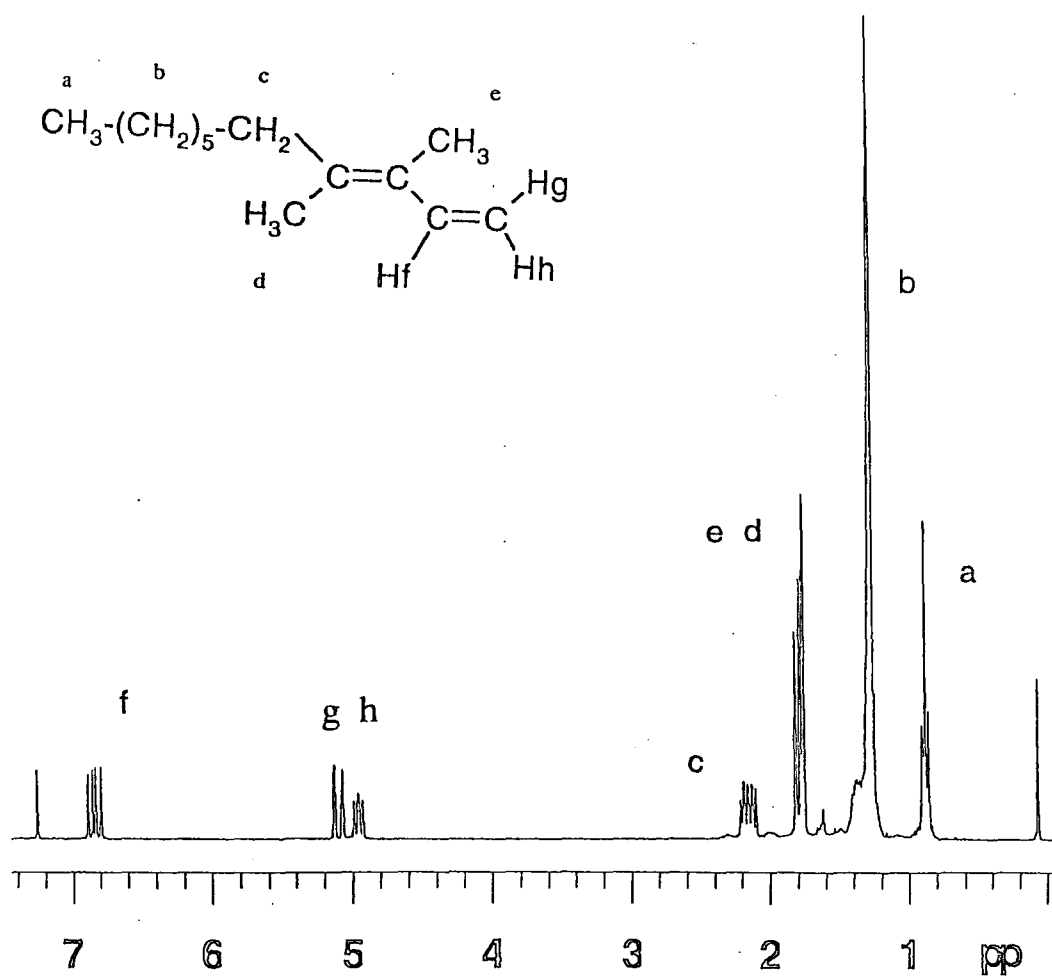
Relax. delay 3.000 sec
Pulse 45.0 degrees
Acq. time 1.399 sec
Width 31446.5 Hz
1024 repetitions
OBSERVE C13, 125.7044344 MHz
DECOUPLE H1, 499.9204335 MHz
Power 42 dB
continuously on
WALTZ-16 modulated
DATA PROCESSING
Line broadening 0.7 Hz
FT size 131072
Total time 1 hr, 15 min, 13 sec

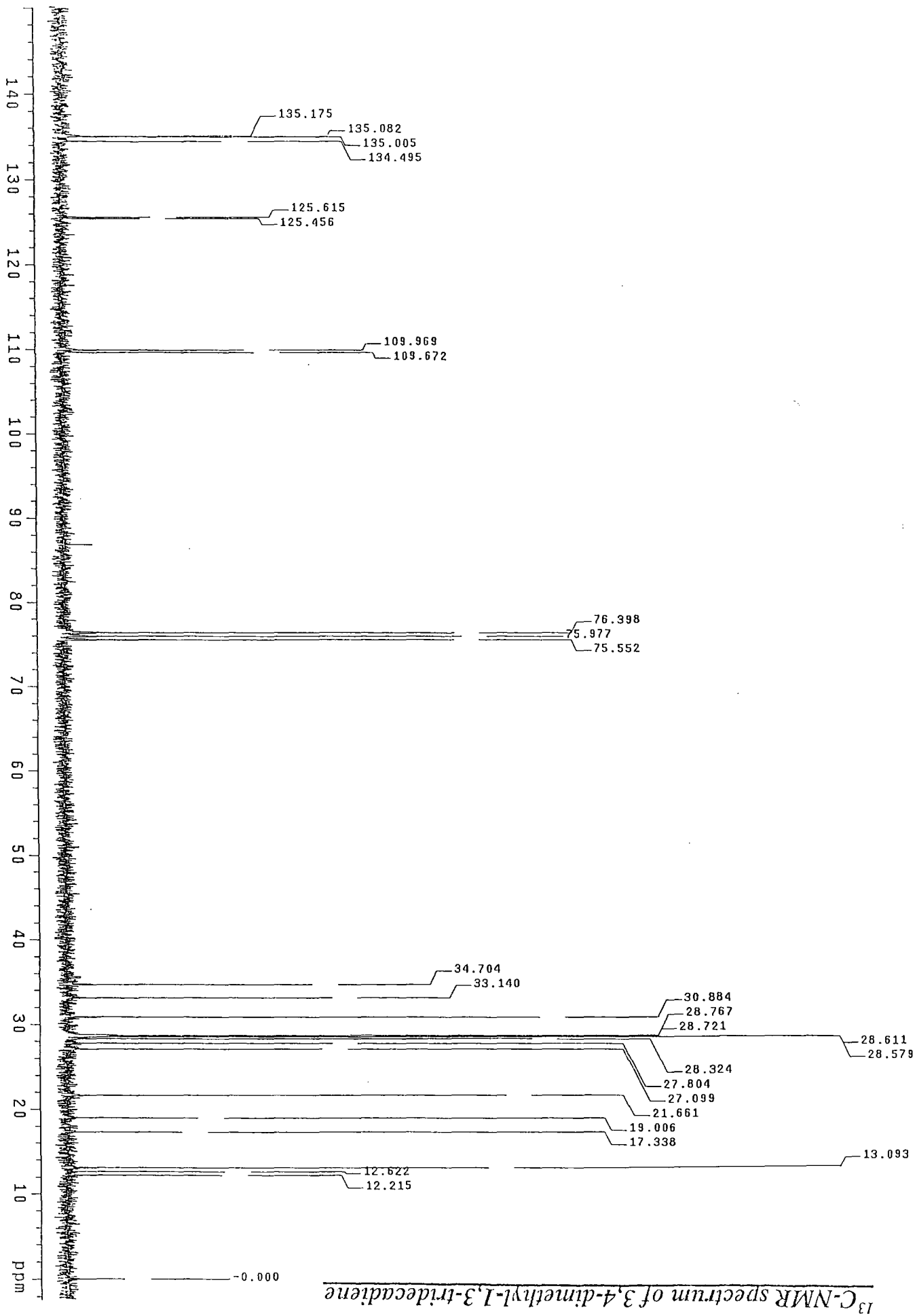
AX6

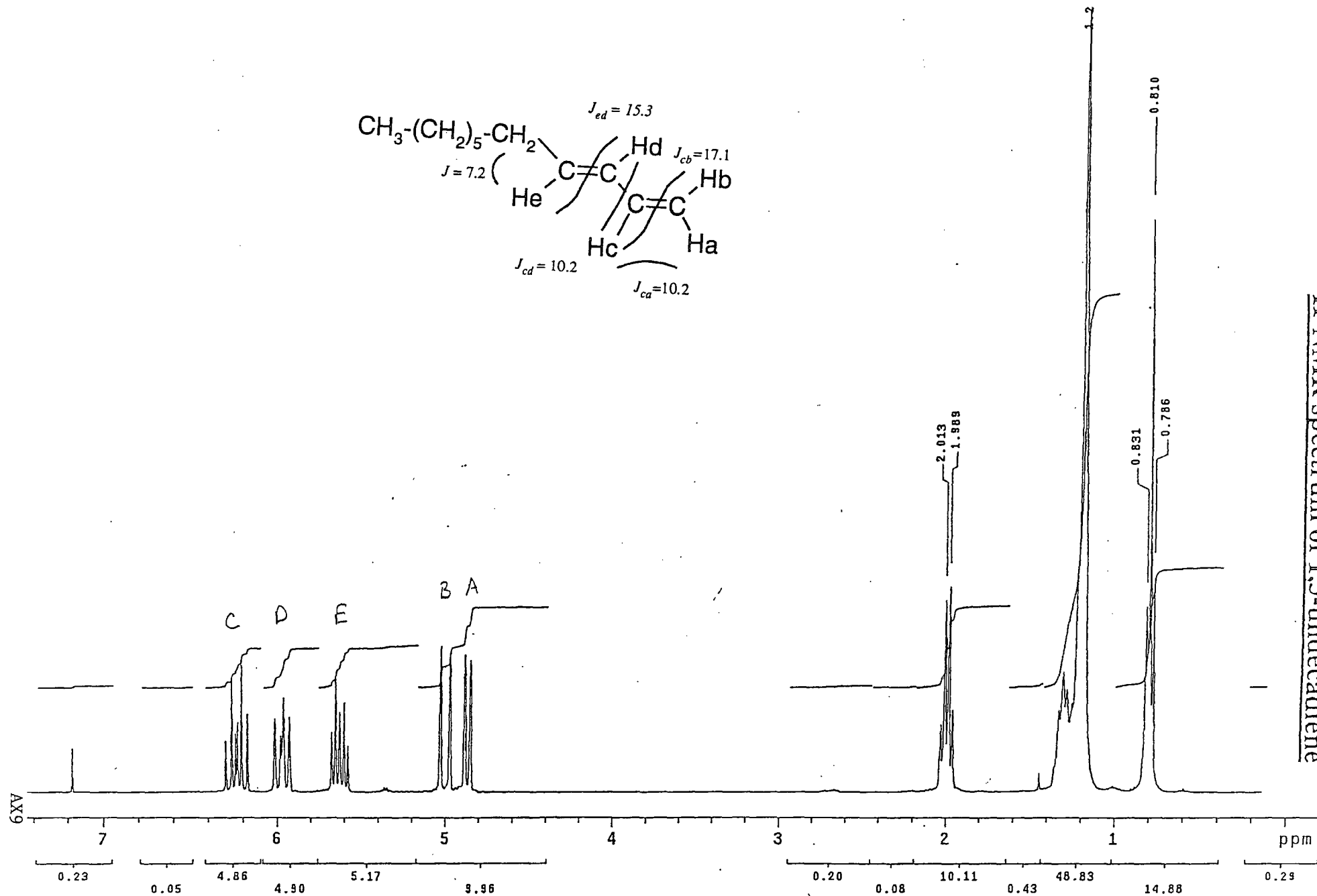


^{13}C -NMR spectrum of 4-methyl-1,3-undecadiene

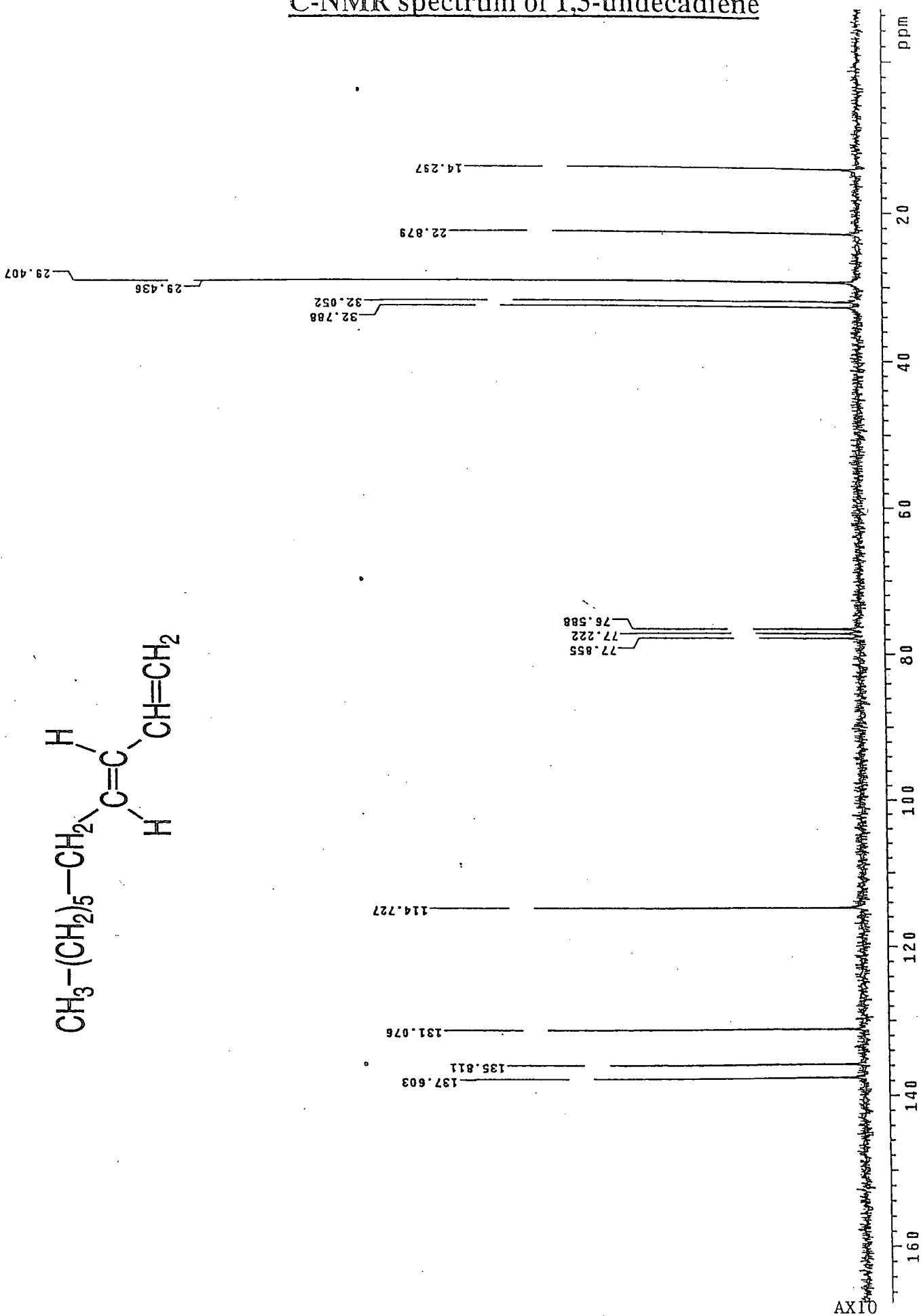
^1H -NMR spectrum of 3,4-dimethyl-1,3-tridecadiene.



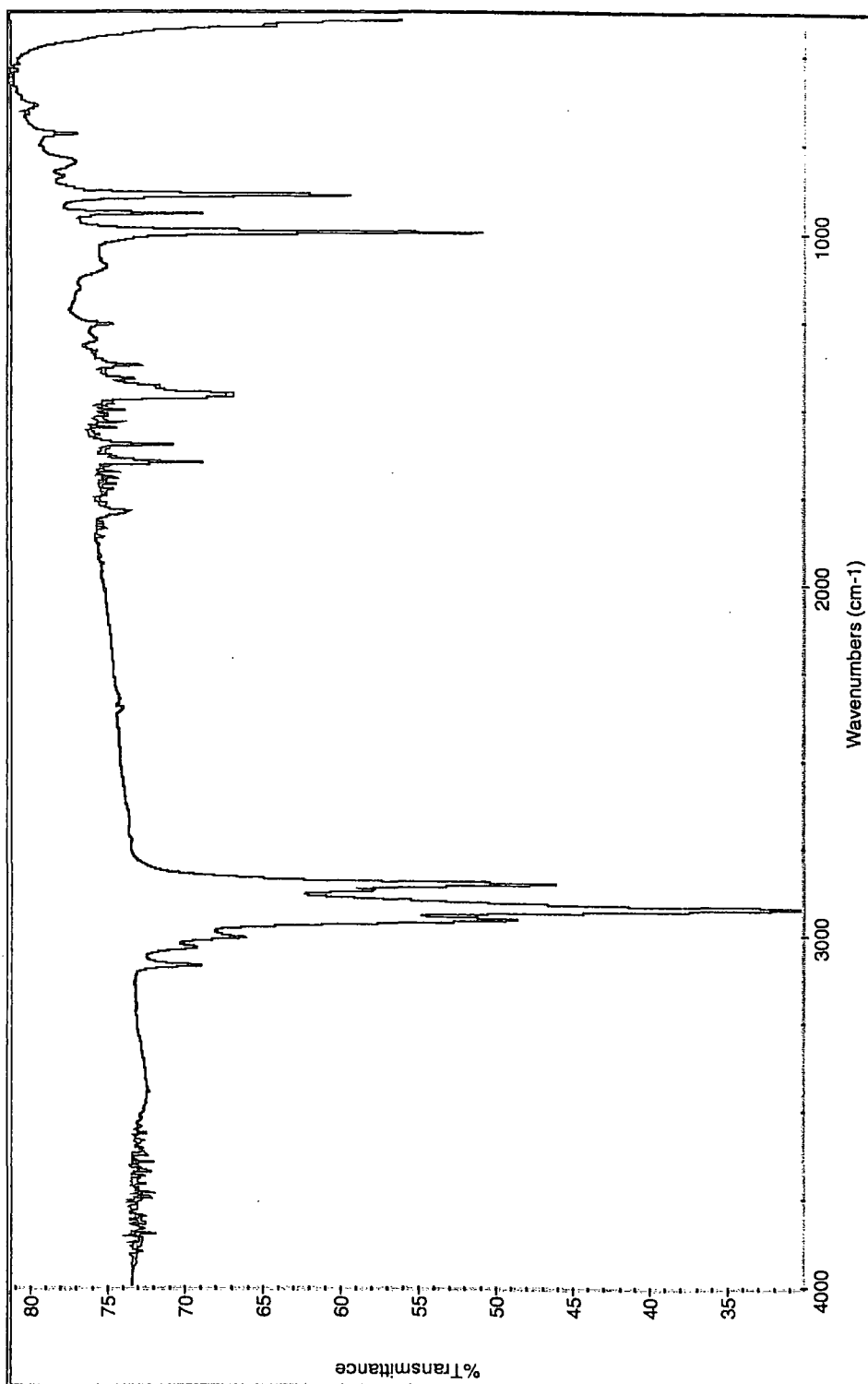




¹³C-NMR spectrum of 1,3-undecadiene



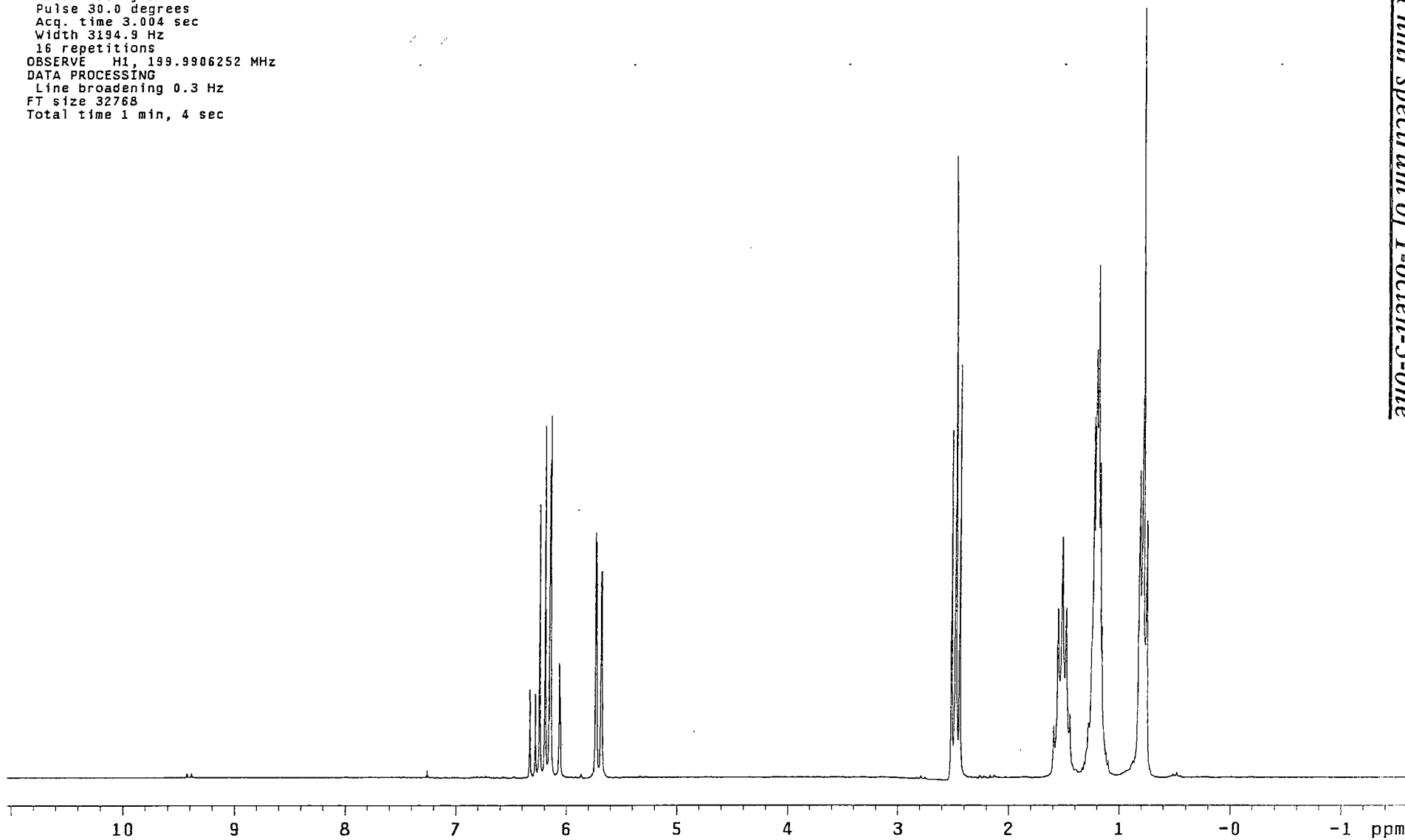
IR spectrum of undeca-1,3-diene



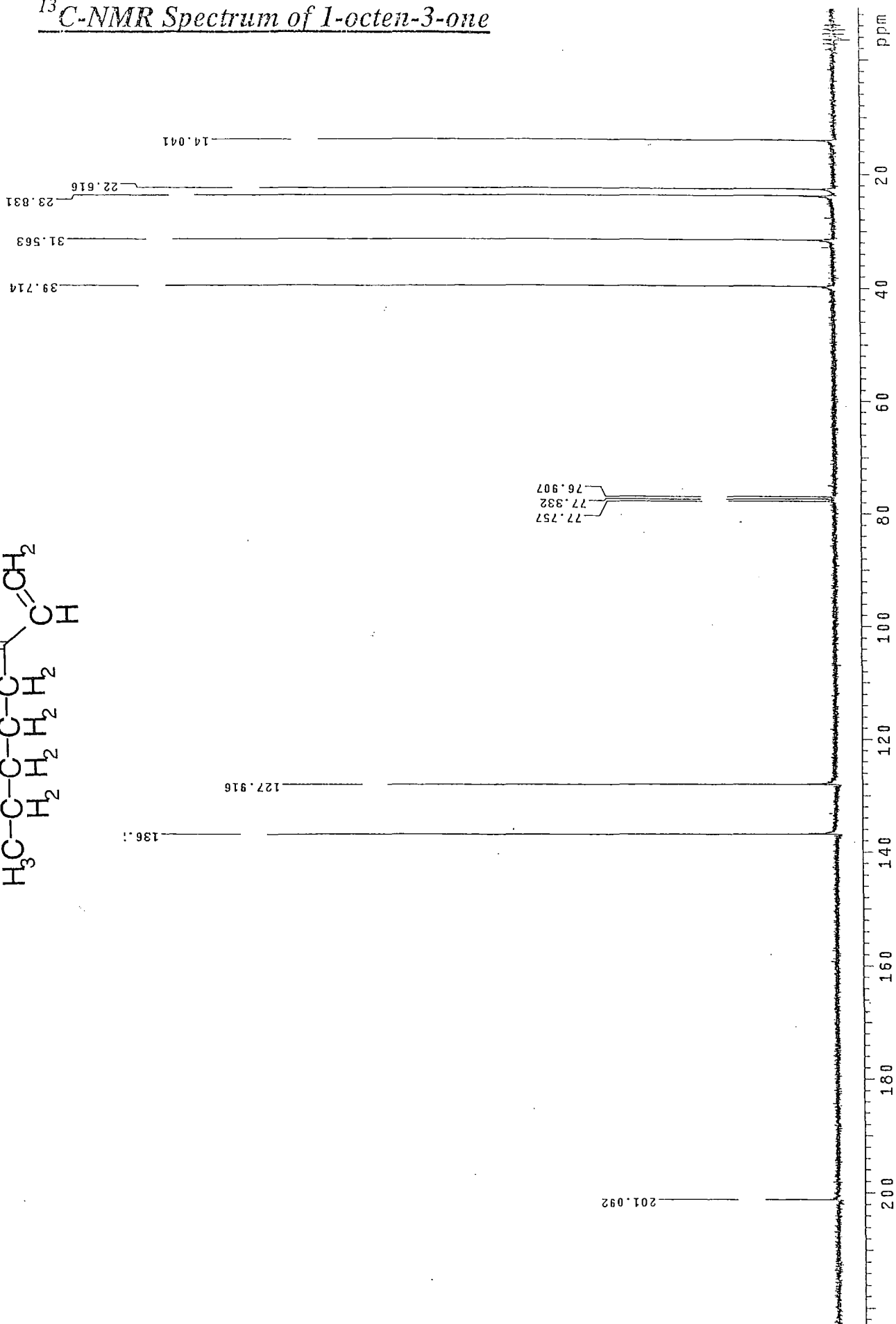
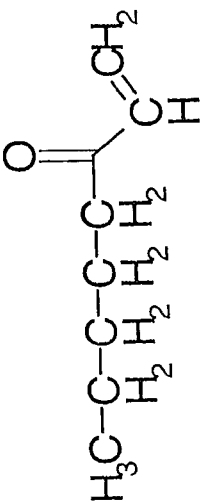
Pulse Sequence: s2pu1
Solvent: CDCl3
Ambient temperature
File: /data/tempdat/23181136
Processed on "korn"

Relax. delay 1.000 sec
Pulse 30.0 degrees
Acq. time 3.004 sec
Width 3194.9 Hz
16 repetitions
OBSERVE H1, 199.9906252 MHz
DATA PROCESSING
Line broadening 0.3 Hz
FT size 32768
Total time 1 min, 4 sec

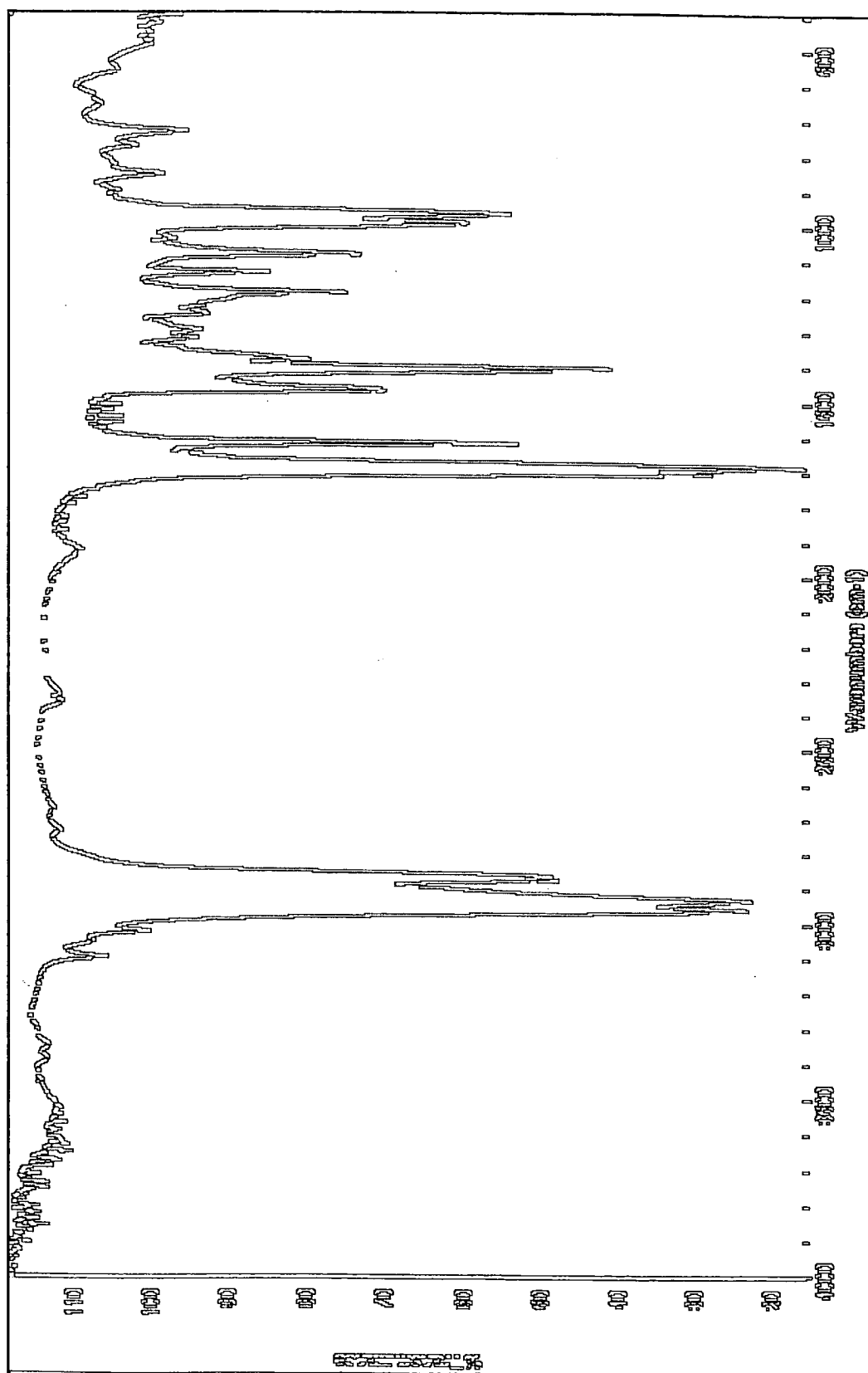
¹H nmr spectrum of 1-octen-3-one



¹³C-NMR Spectrum of 1-octen-3-one

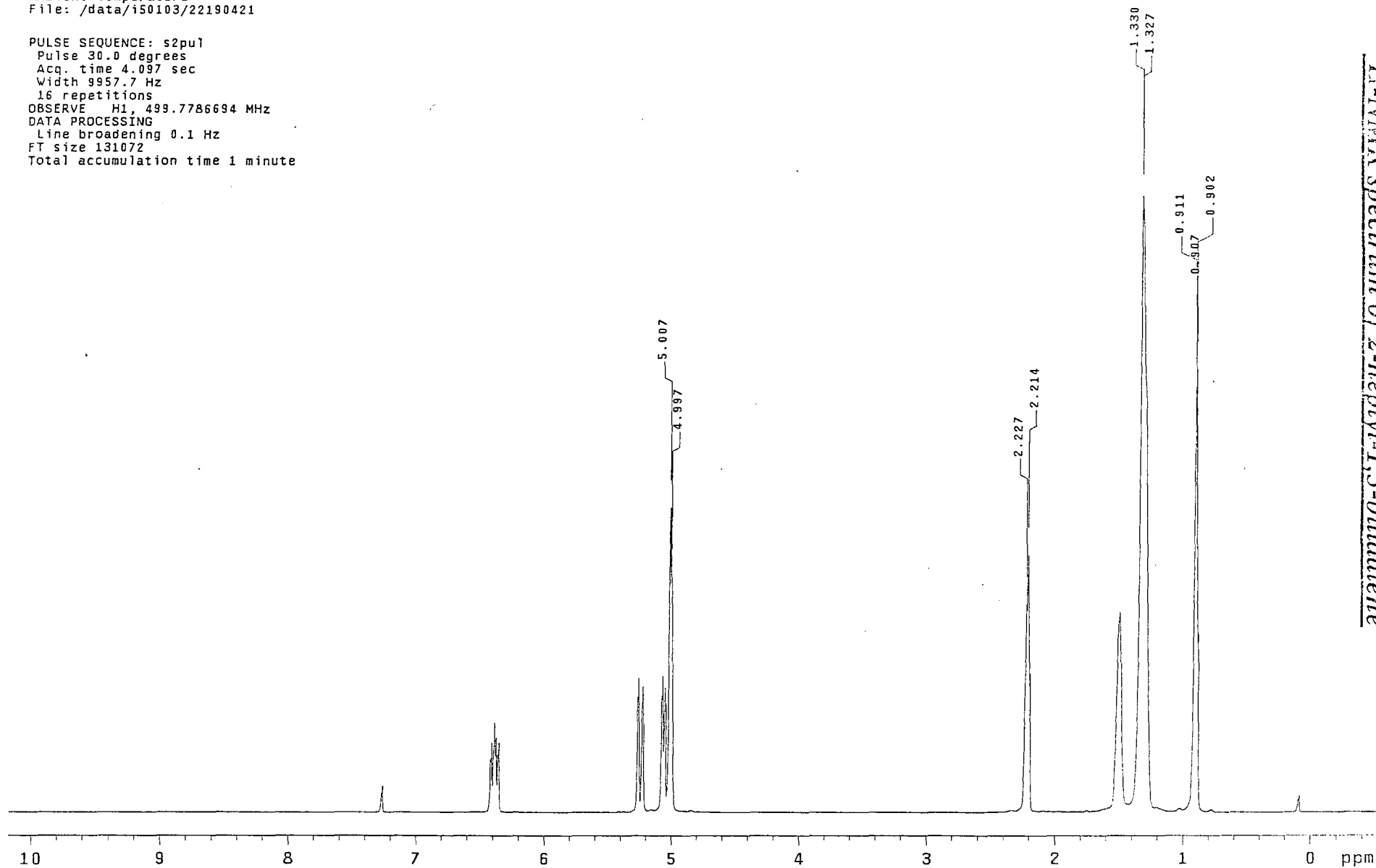


IR-Spectrum of 1-octen-3-one



Run on Mar 22 2001
Solvent: CDCl3
Ambient temperature
File: /data/i50103/22190421

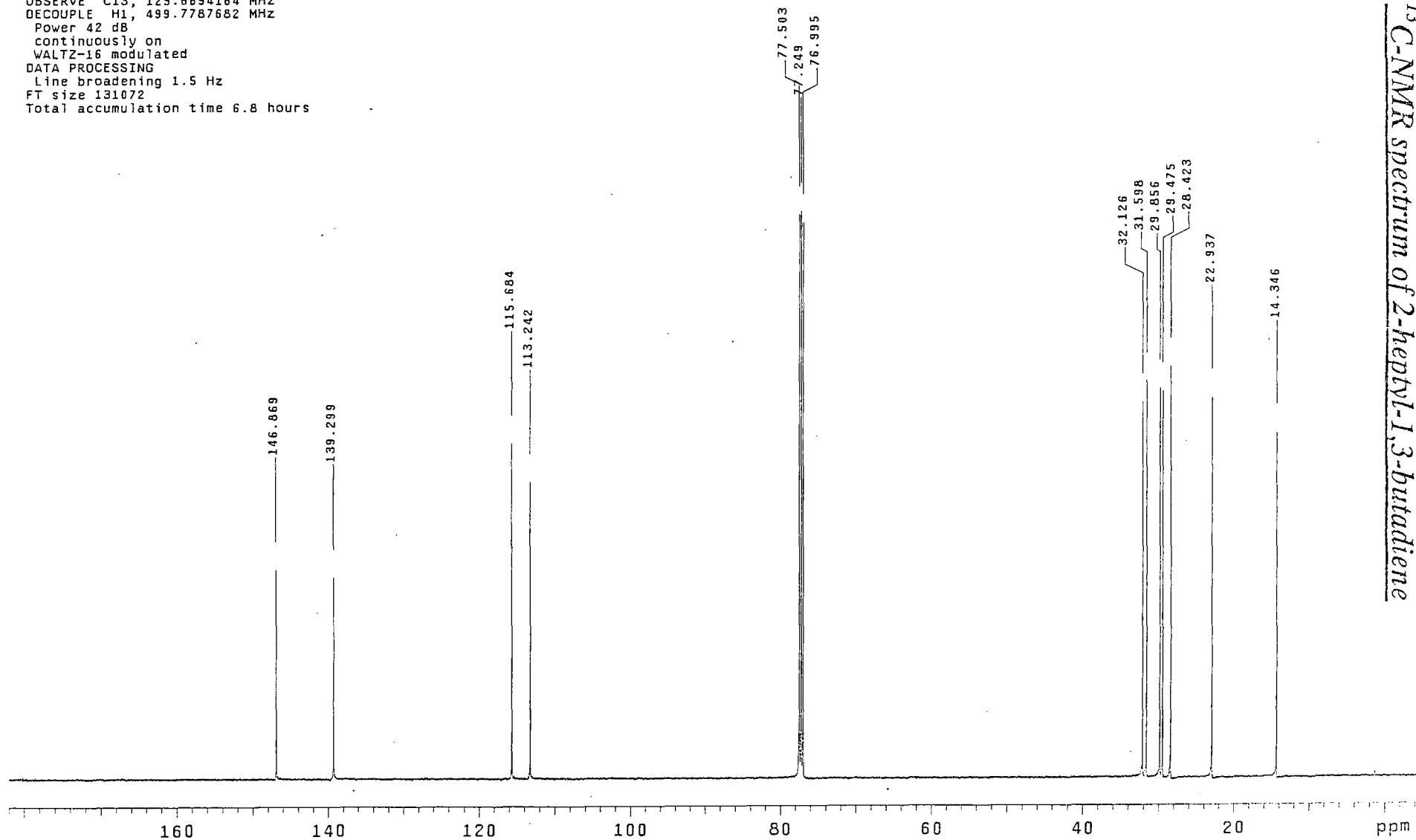
PULSE SEQUENCE: s2pu1
Pulse 30.0 degrees
Acq. time 4.097 sec
Width 9957.7 Hz
16 repetitions
OBSERVE H1, 499.7786694 MHz
DATA PROCESSING
Line broadening 0.1 Hz
FT size 131072
Total accumulation time 1 minute



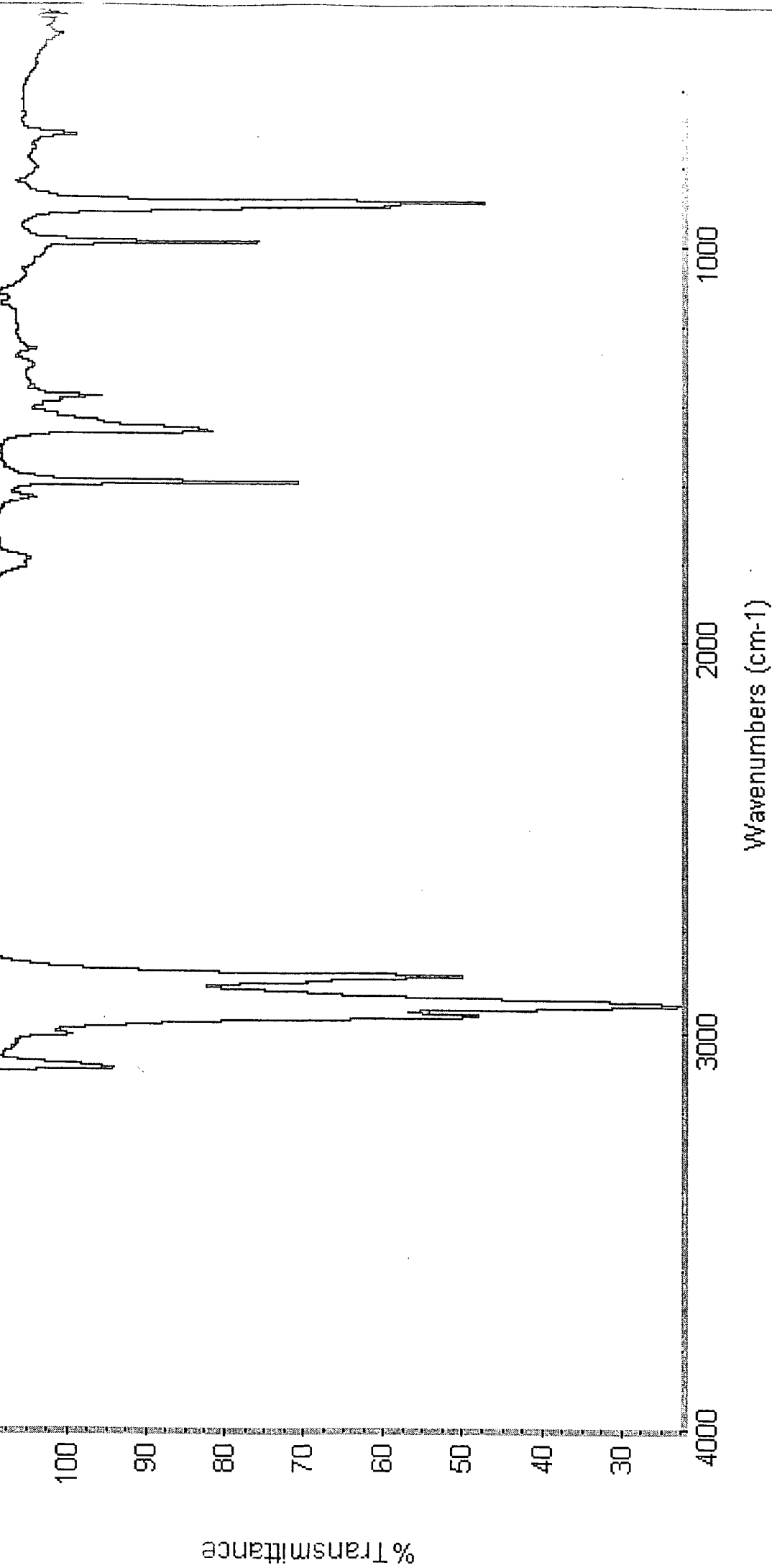
¹H-NMR spectrum of 2-heptyl-1,3-butadiene

Run on Mar 22 2001
Solvent: CDCl₃
Ambient temperature
User: 1-14-87
File: /data/i50103/23015903

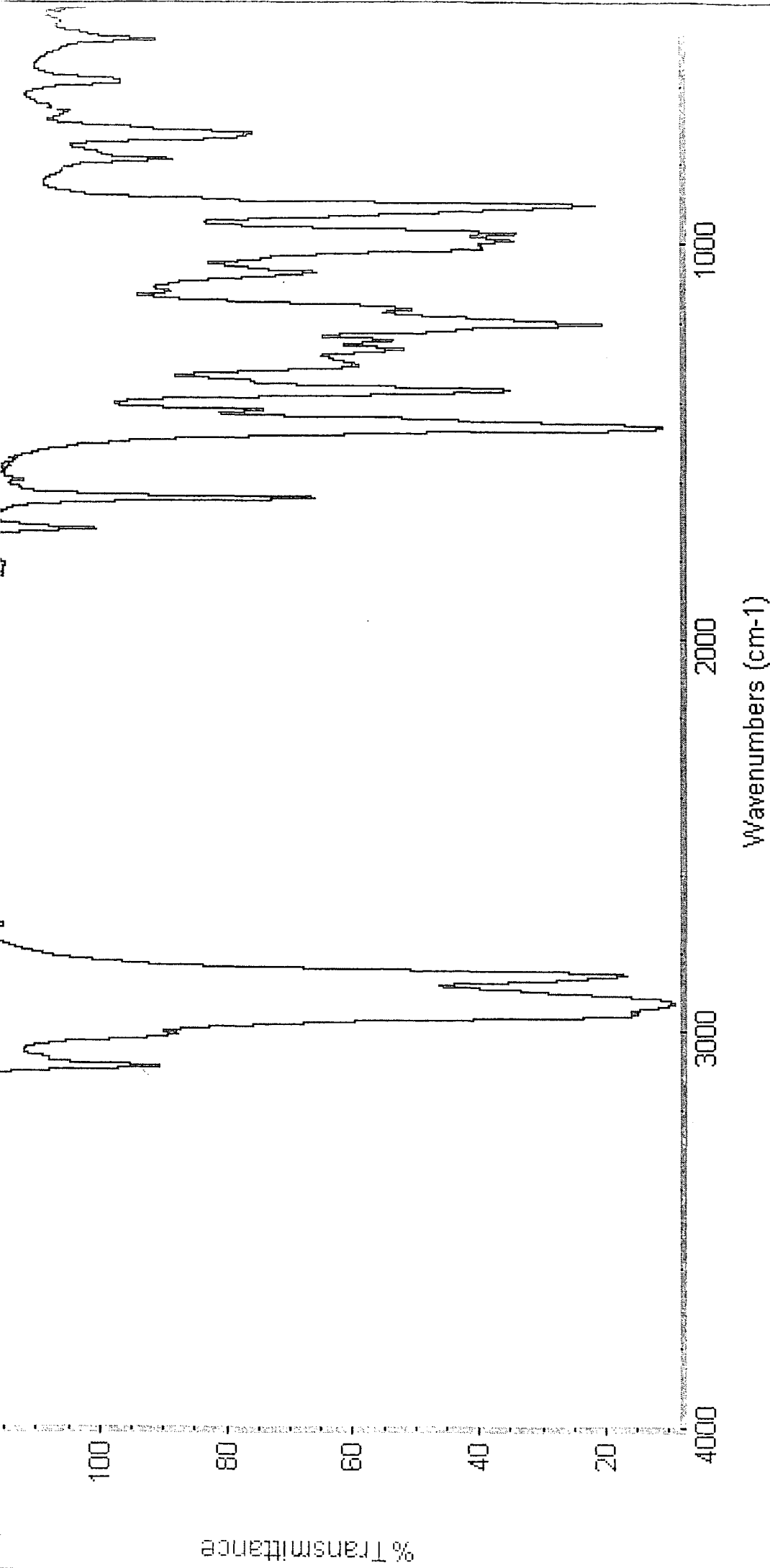
PULSE SEQUENCE: s2pu1
Relax. delay 2.000 sec
Pulse 30.0 degrees
Acq. time 1.002 sec
Width 32693.1 Hz
8192 repetitions
OBSERVE C13, 125.6694164 MHz
DECOUPLE H1, 499.7787682 MHz
Power 42 dB
continuously on
WALTZ-16 modulated
DATA PROCESSING
Line broadening 1.5 Hz
FT size 131072
Total accumulation time 6.8 hours



¹³C-NMR spectrum of 2-heptyl-1,3-butadiene



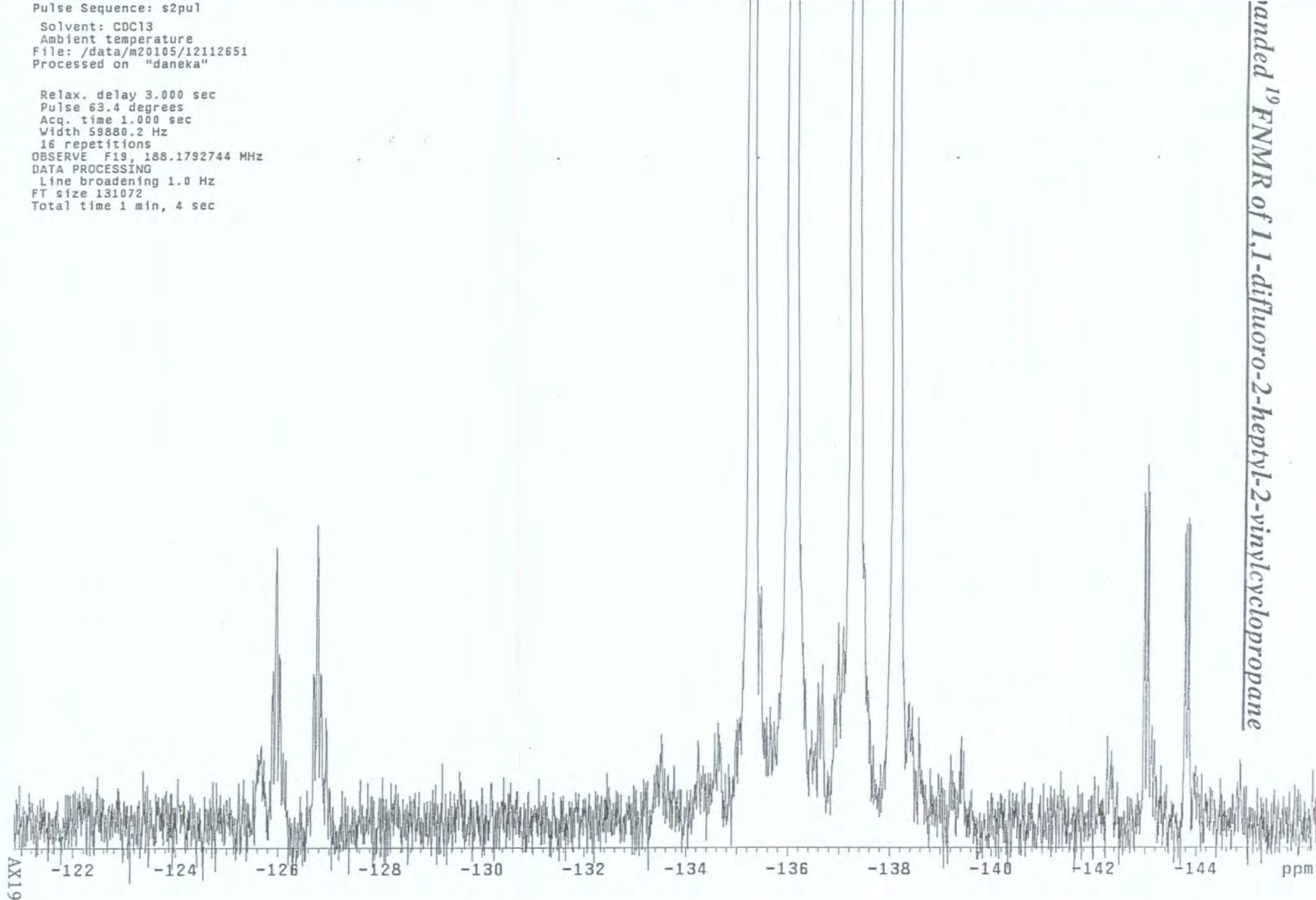
Infrared spectrum of 2-heptyl-1,3-butadiene



Infrared spectrum of 1,1-difluoro-2-heptyl-2-vinylcyclopropane

Pulse Sequence: s2pu1
Solvent: CDCl3
Ambient temperature
File: /data/m20105/12112651
Processed on "daneka"

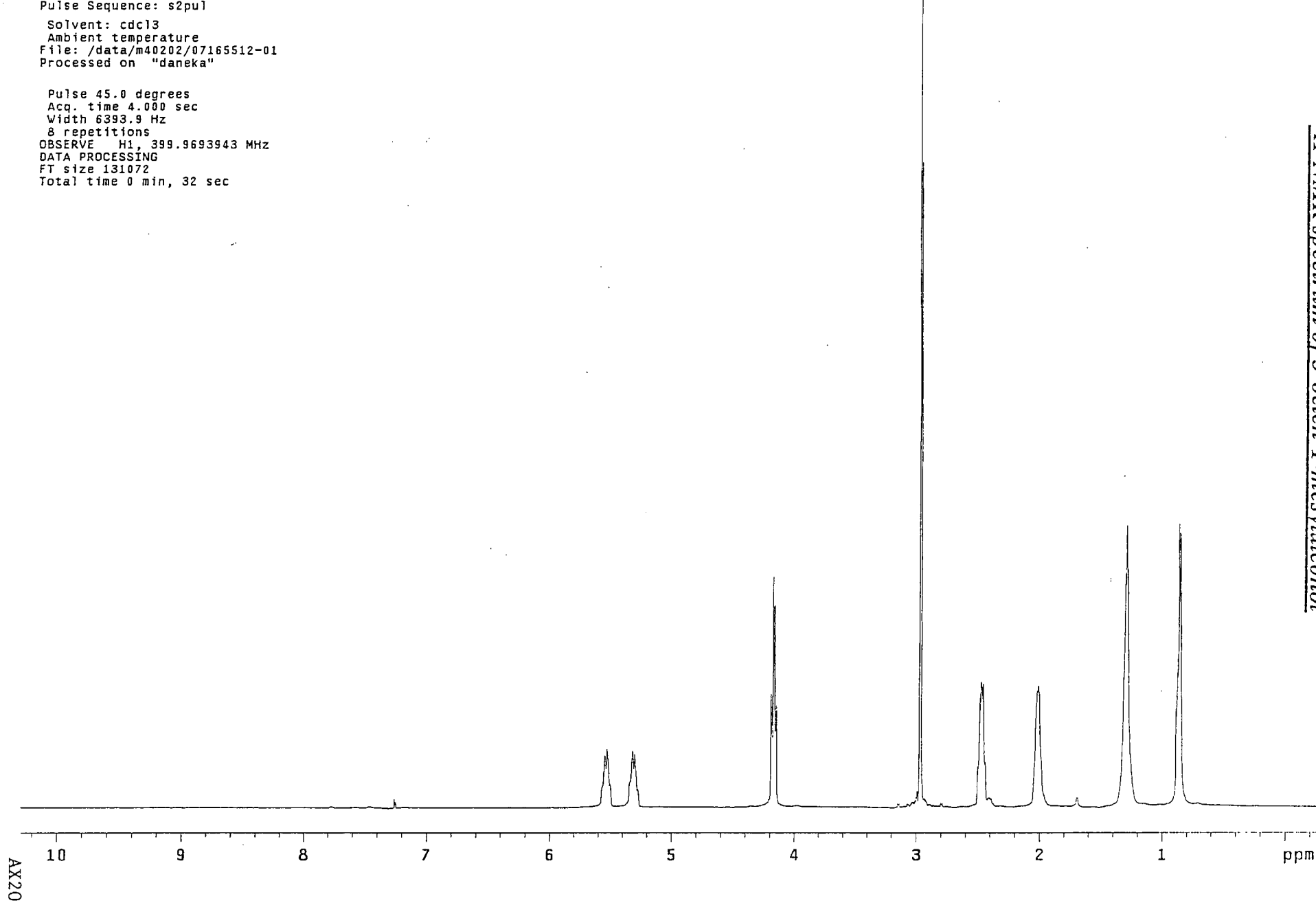
Relax. delay 3.000 sec
Pulse 63.4 degrees
Acq. time 1.000 sec
Width 59880.2 Hz
16 repetitions
OBSERVE F19, 188.1792744 MHz
DATA PROCESSING
Line broadening 1.0 Hz
FT size 131072
Total time 1 min, 4 sec



Pulse Sequence: s2pu1
Solvent: cdcl3
Ambient temperature
File: /data/m40202/07165512-01
Processed on "daneka"

Pulse 45.0 degrees
Acq. time 4.000 sec
Width 6393.9 Hz
8 repetitions
OBSERVE H1, 399.9693943 MHz
DATA PROCESSING
FT size 131072
Total time 0 min, 32 sec

¹H-NMR spectrum of 3-octen-1-methylalcohol

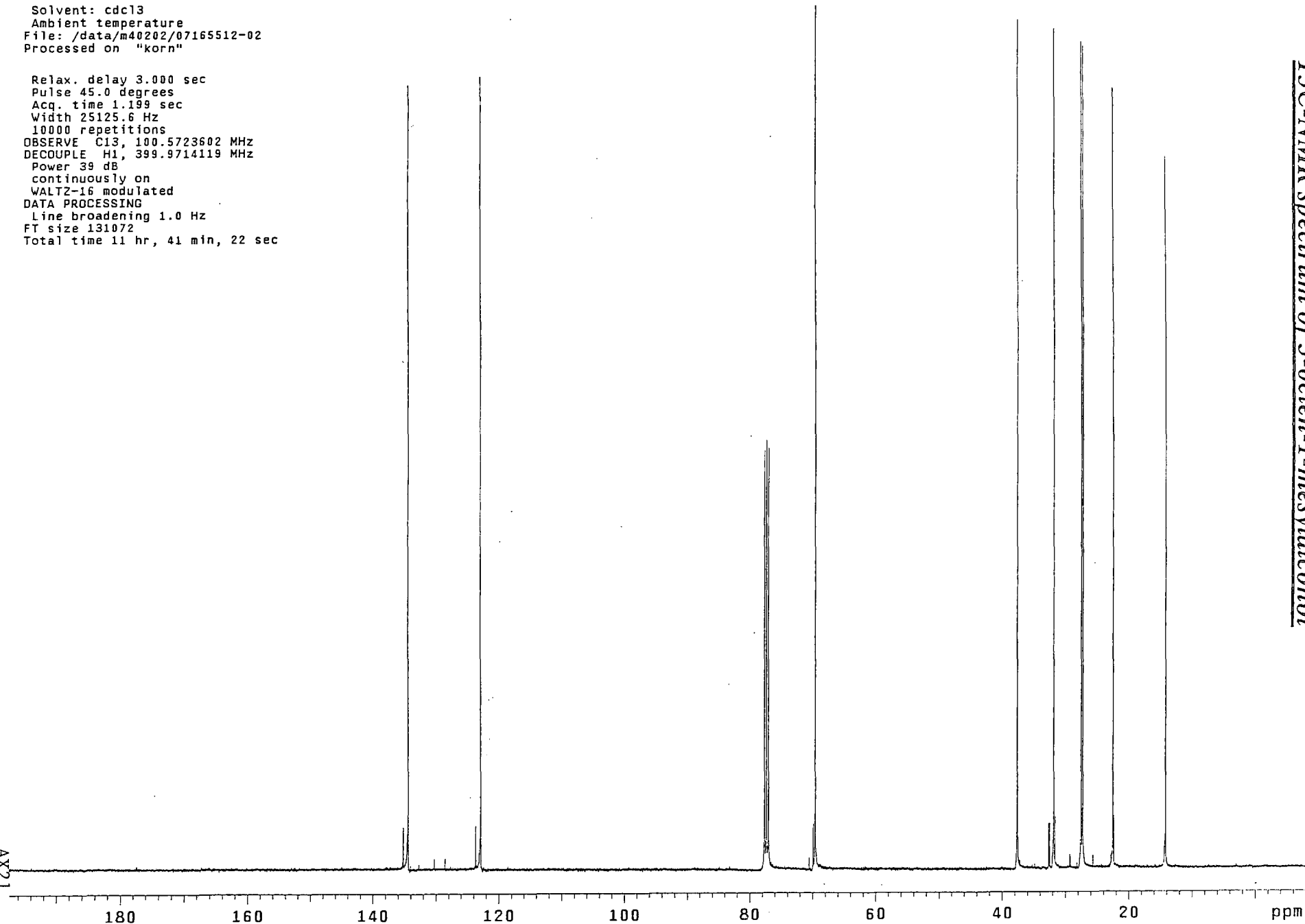


Pulse Sequence: szpu1
Solvent: cdcl3
Ambient temperature
File: /data/m40202/07165512-02
Processed on "korn"

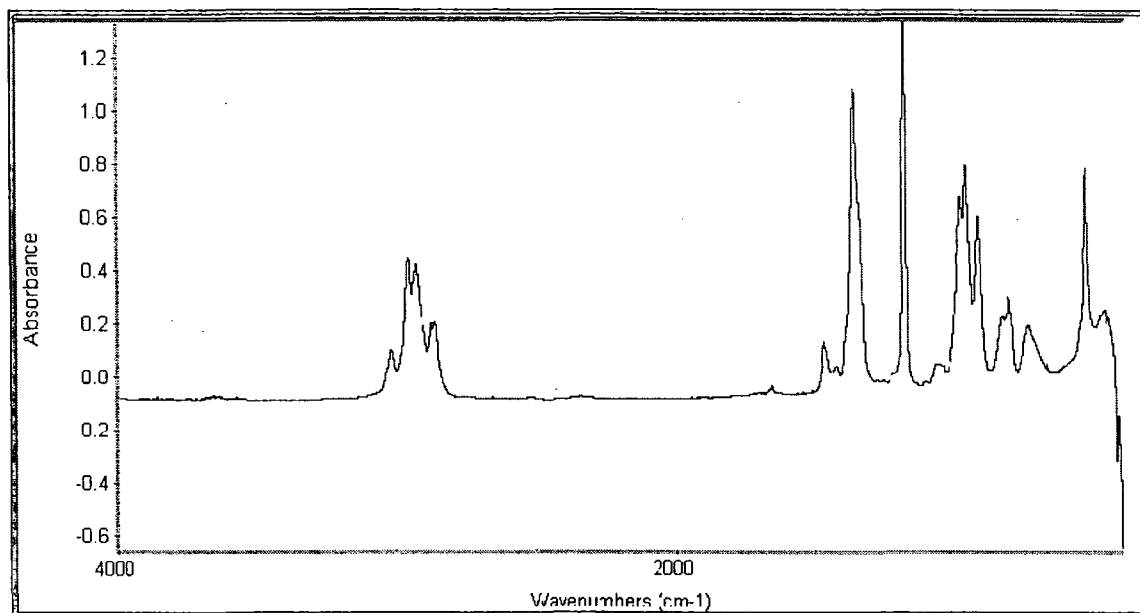
Relax. delay 3.000 sec
Pulse 45.0 degrees
Acq. time 1.199 sec
Width 25125.6 Hz
10000 repetitions
OBSERVE C13, 100.5723602 MHz
DECOUPLE H1, 399.9714119 MHz
Power 39 dB
continuously on
WALTZ-16 modulated
DATA PROCESSING
Line broadening 1.0 Hz
FT size 131072
Total time 11 hr, 41 min, 22 sec

¹³C-NMR spectrum of 3-octen-1-methylalcohol

AX21

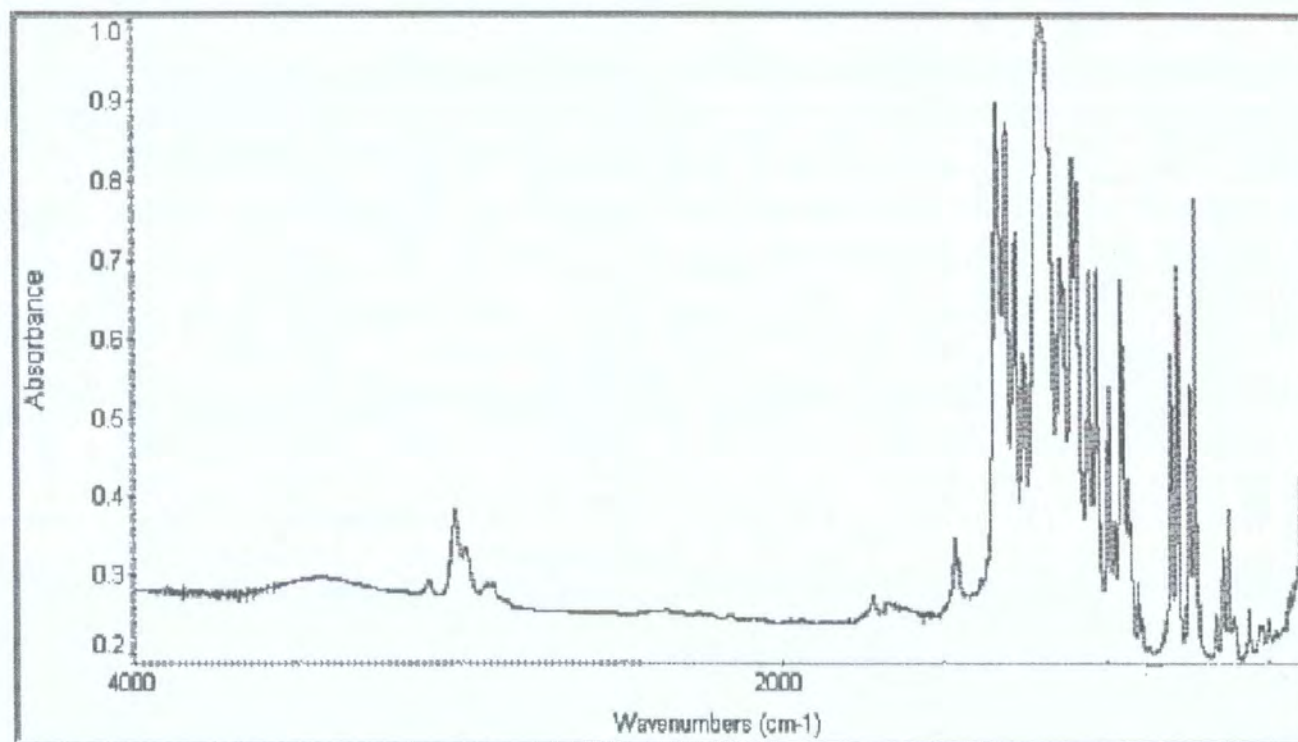


IR-FT spectrum of 3-octen-1-mesylalcohol



Appendix chapter 3

IR spectrum of 5,5,6-trifluoro-6-trifluoromethyl
bicyclo[2.2.1]hept-2-ene

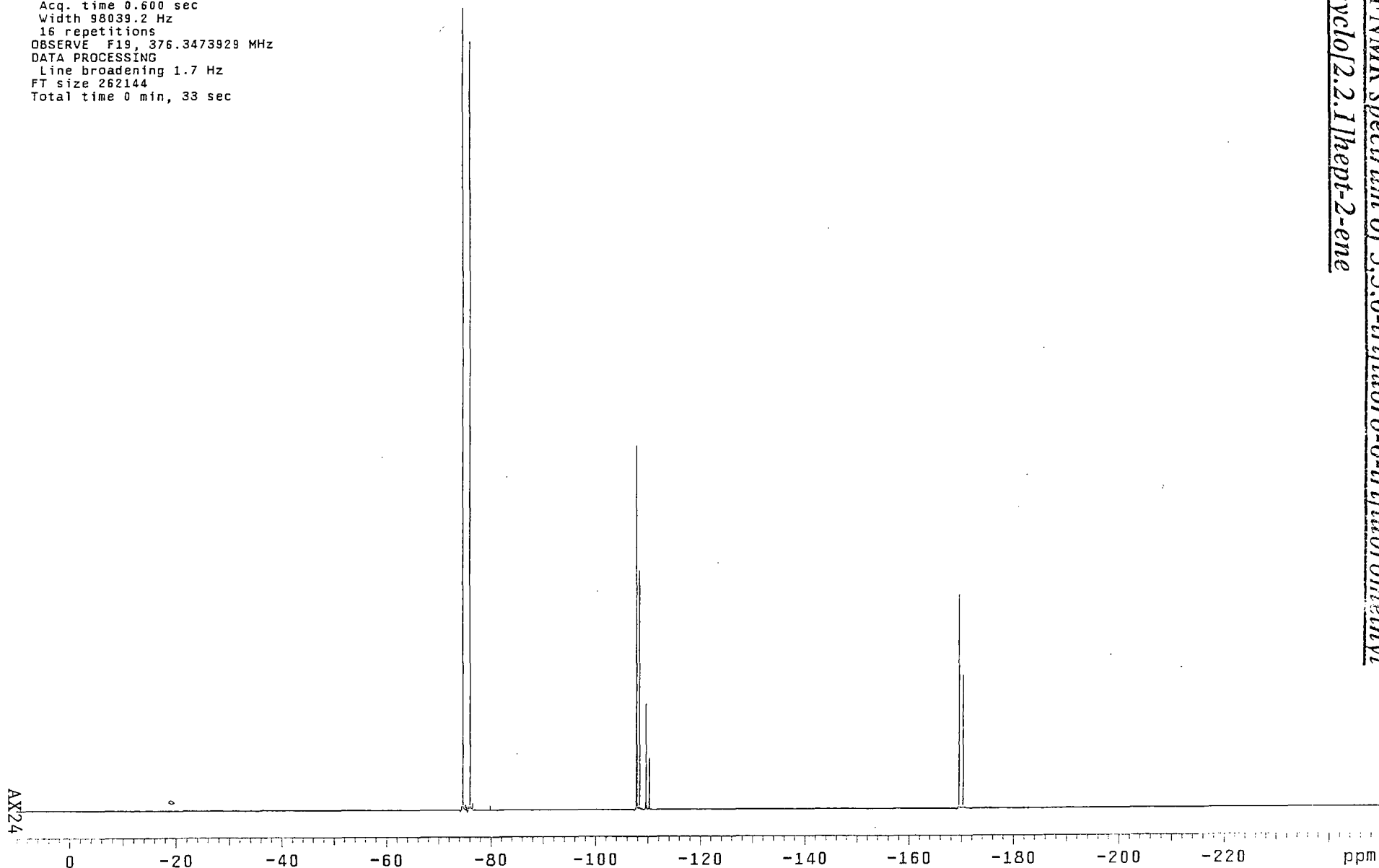


Pulse sequence: szpul
Solvent: cdcl3
Ambient temperature
File: /data/m40110/24152123-01
Processed on "daneka"

Relax. delay 1.500 sec
Pulse 30.0 degrees
Acq. time 0.600 sec
Width 98039.2 Hz
16 repetitions
OBSERVE F19, 376.3473929 MHz
DATA PROCESSING
Line broadening 1.7 Hz
FT size 262144
Total time 0 min, 33 sec

*19F NMR spectrum of 5,5,6-trifluoro-6-trifluoromethyl
bicyclo[2.2.1]hept-2-ene*

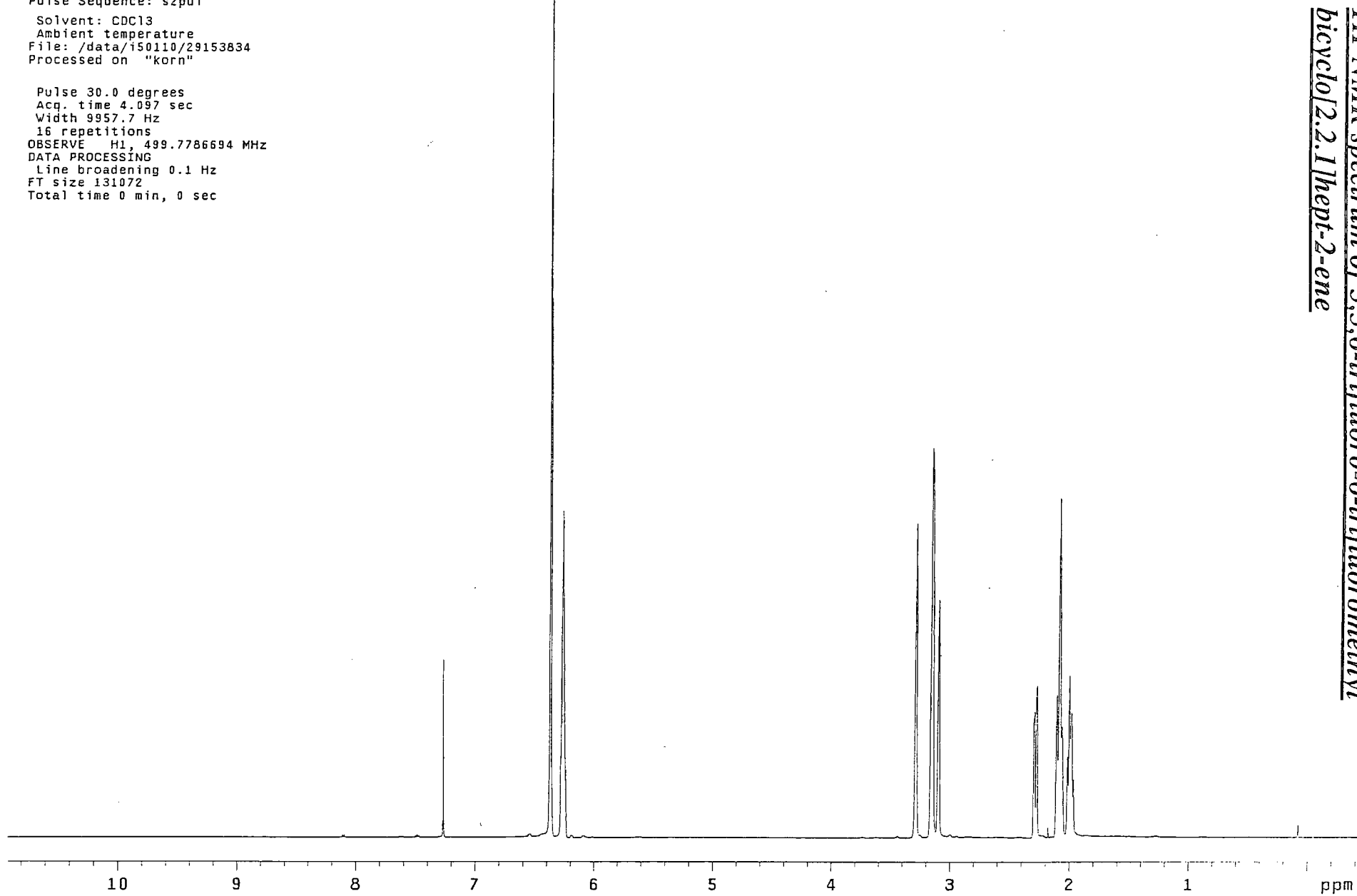
AX24



Pulse Sequence: szpu1
Solvent: CDCl3
Ambient temperature
File: /data/150110/29153834
Processed on "korn"

Pulse 30.0 degrees
Acq. time 4.097 sec
Width 9957.7 Hz
16 repetitions
OBSERVE H1, 499.7786694 MHz
DATA PROCESSING
Line broadening 0.1 Hz
FT size 131072
Total time 0 min, 0 sec

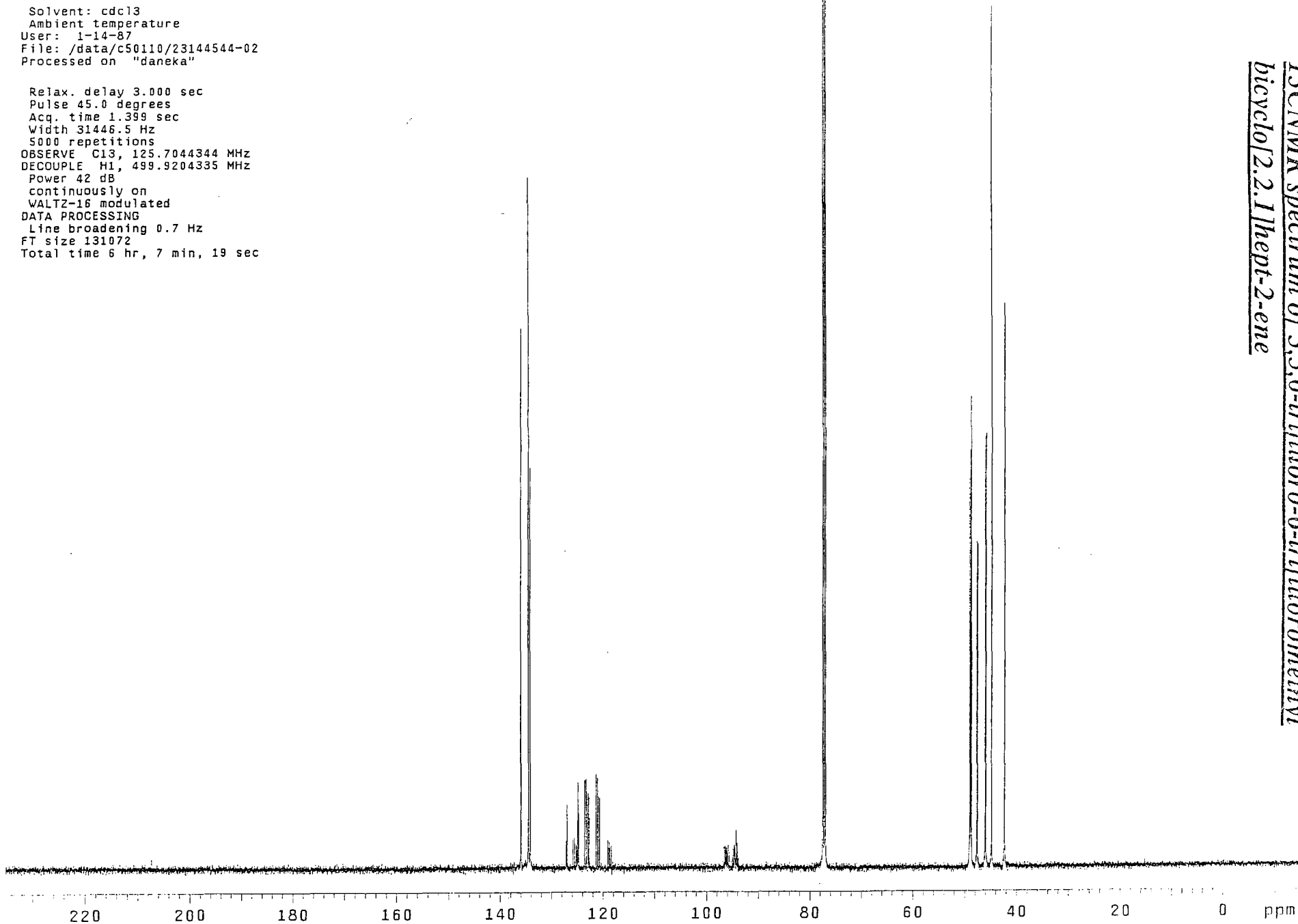
1H-NMR spectrum of 5,5,6-trifluoro-6-trifluoromethyl
bicyclo[2.2.1]hept-2-ene

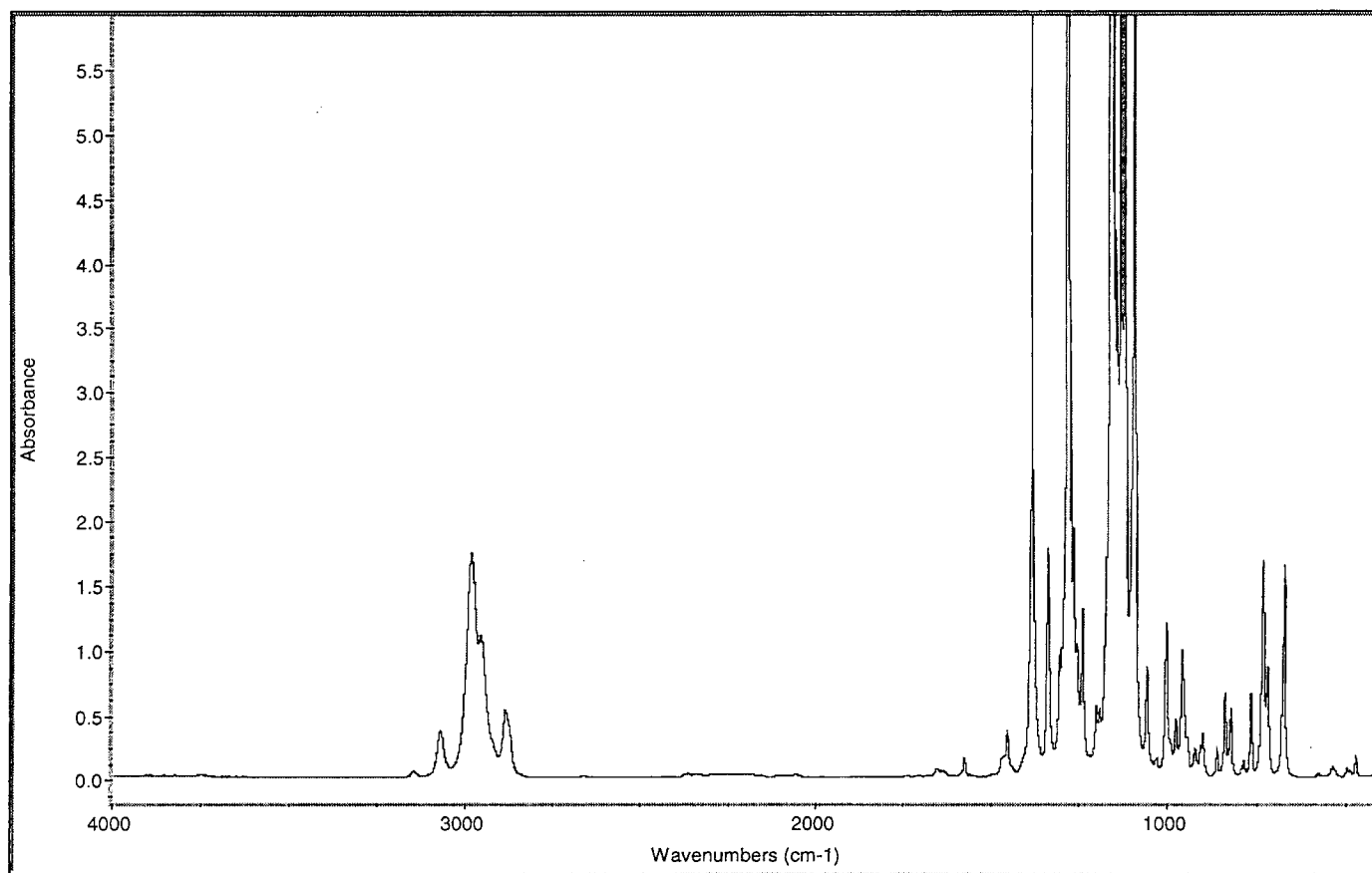


Pulse Sequence: s2pu1
Solvent: cdcl3
Ambient temperature
User: 1-14-87
File: /data/c50110/23144544-02
Processed on "daneka"

Relax. delay 3.000 sec
Pulse 45.0 degrees
Acq. time 1.399 sec
Width 31446.5 Hz
5000 repetitions
OBSERVE C13, 125.7044344 MHz
DECOUPLE H1, 499.9204335 MHz
Power 42 dB
continuously on
WALTZ-16 modulated
DATA PROCESSING
Line broadening 0.7 Hz
FT size 131072
Total time 6 hr, 7 min, 19 sec

*¹³CNMR spectrum of 5,5,6-trifluoro-6-trifluoromethyl
bicyclo[2.2.1]hept-2-ene*

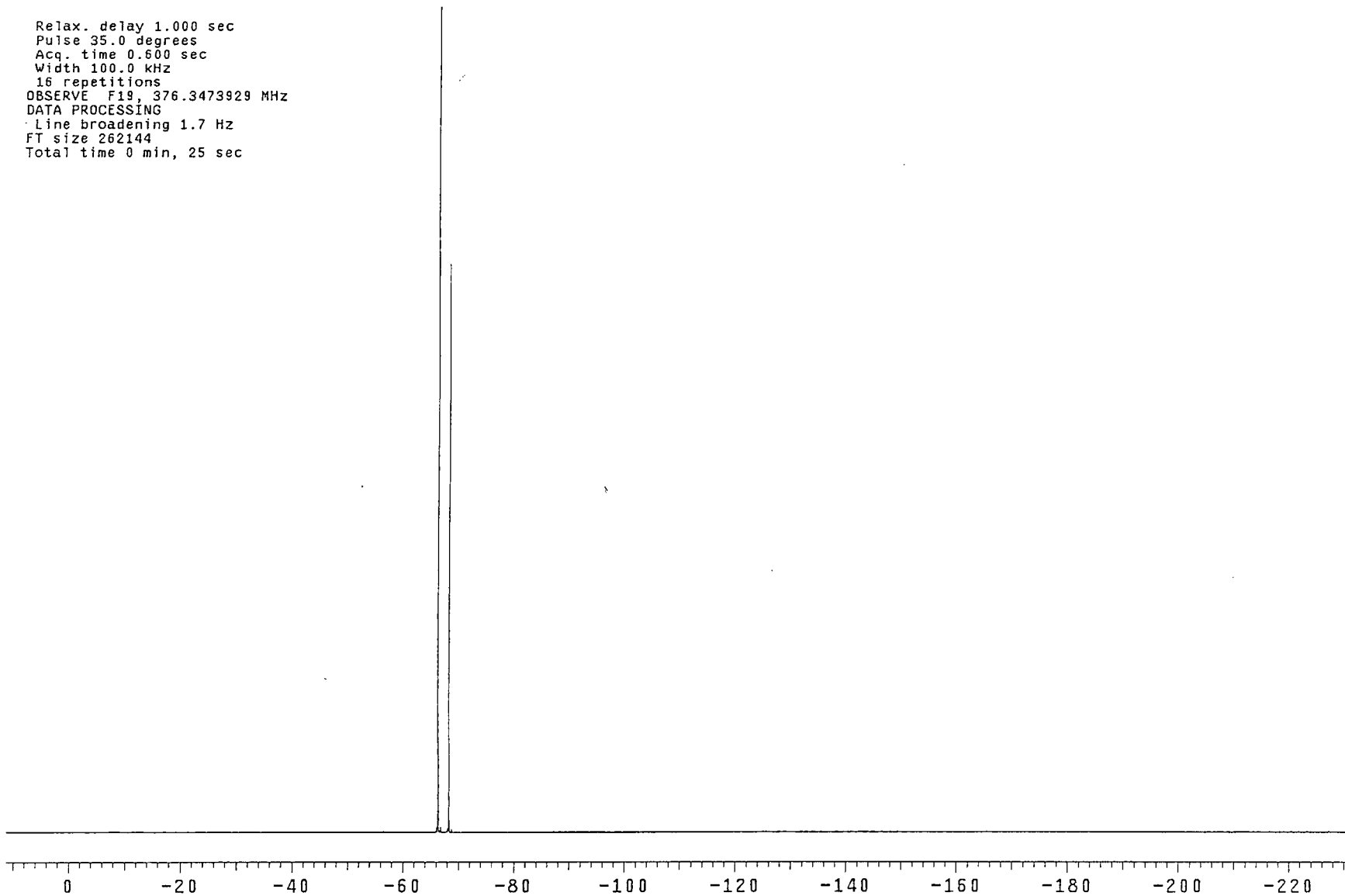




IR spectrum of 5-trifluoromethylbicyclo[2.2.1]hept-2-ene

Pulse Sequence: s2pu1
Solvent: cdc13
Ambient temperature
File: /data/m40207/02092120-03
Processed on "daneka"

Relax. delay 1.000 sec
Pulse 35.0 degrees
Acq. time 0.600 sec
Width 100.0 kHz
16 repetitions
OBSERVE F19, 376.3473929 MHz
DATA PROCESSING
Line broadening 1.7 Hz
FT size 262144
Total time 0 min, 25 sec

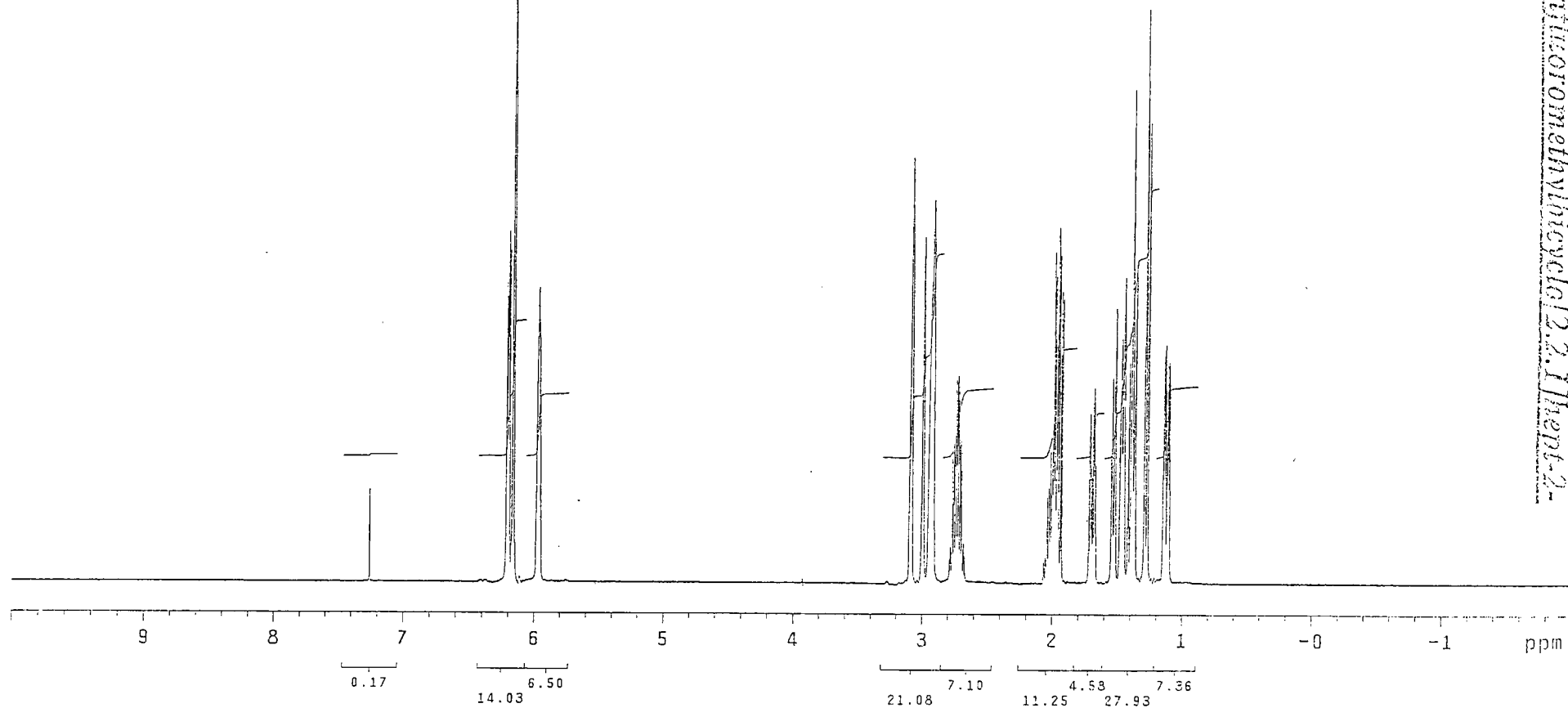


19F-NMR spectrum of 5-trifluoromethylbicyclo[2.2.1]hept-2-ene

File: /data/m40207/02092120-01
Pulse Sequence: s2pu1
Solvent: cdcl3
Ambient temperature
Sample #1
File: /data/m40207/02092120-01
Mercury-400BB "mudd"

Relax. delay 1.000 sec
Pulse 45.0 degrees
Acq. time 4.000 sec
Width 6393.9 Hz
8 repetitions
OBSERVE H1, 399.9693943 MHz
DATA PROCESSING
FT size 131072
Total time 0 min, 43 sec

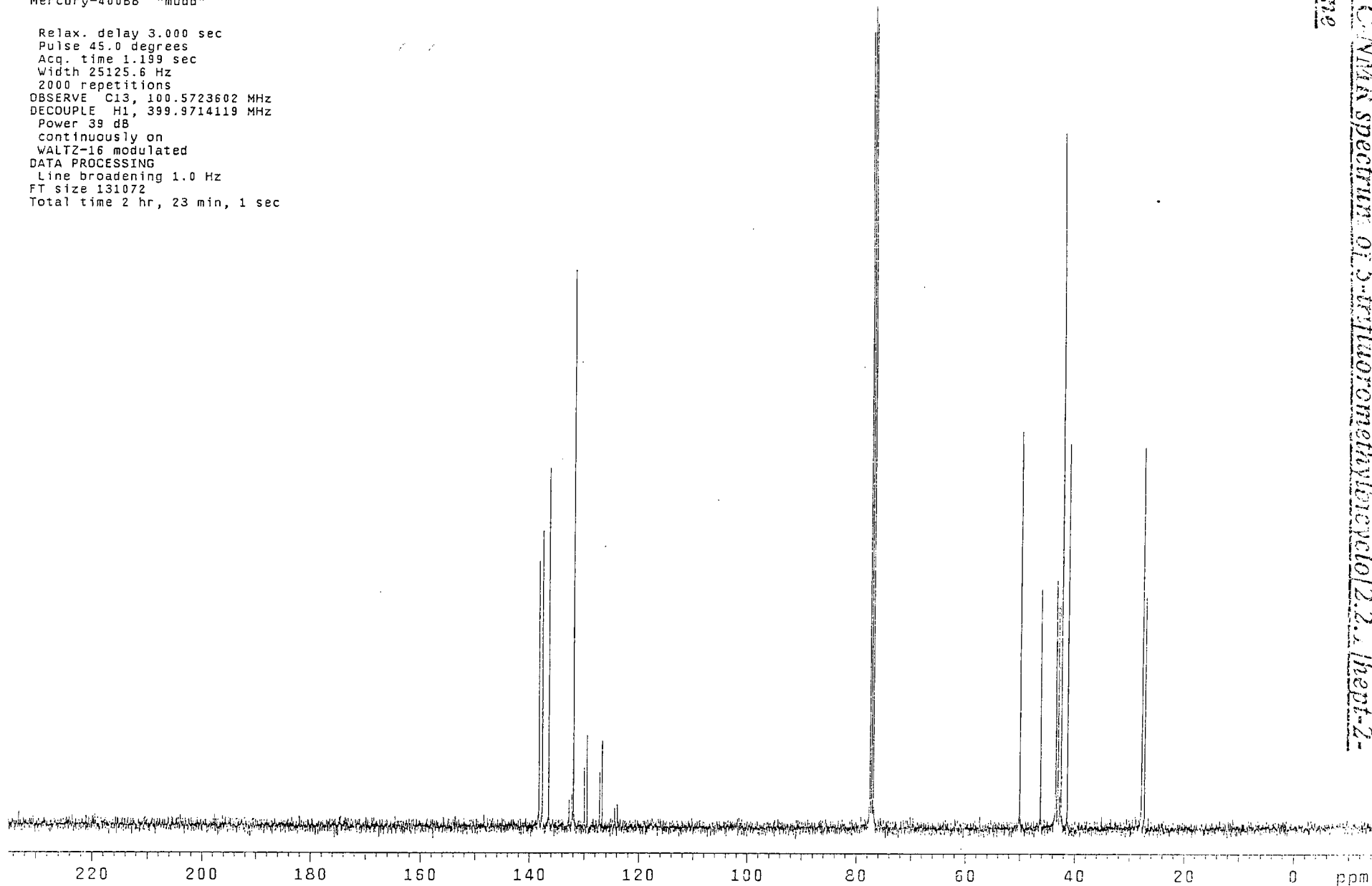
¹H-NMR spectrum of 5-(trifluoromethyl)bicyclo[2.2.1]hept-2-ene



File: /data/m40207/02092120-02
Pulse Sequence: s2pu1
Solvent: cdcl3
Ambient temperature
Sample #1
File: /data/m40207/02092120-02
Mercury-400BB "mudd"

Relax. delay 3.000 sec
Pulse 45.0 degrees
Acq. time 1.199 sec
Width 25125.6 Hz
2000 repetitions
OBSERVE C13, 100.5723602 MHz
DECOUPLE H1, 399.9714119 MHz
Power 39 dB
continuously on
WALTZ-16 modulated
DATA PROCESSING
Line broadening 1.0 Hz
FT size 131072
Total time 2 hr, 23 min, 1 sec

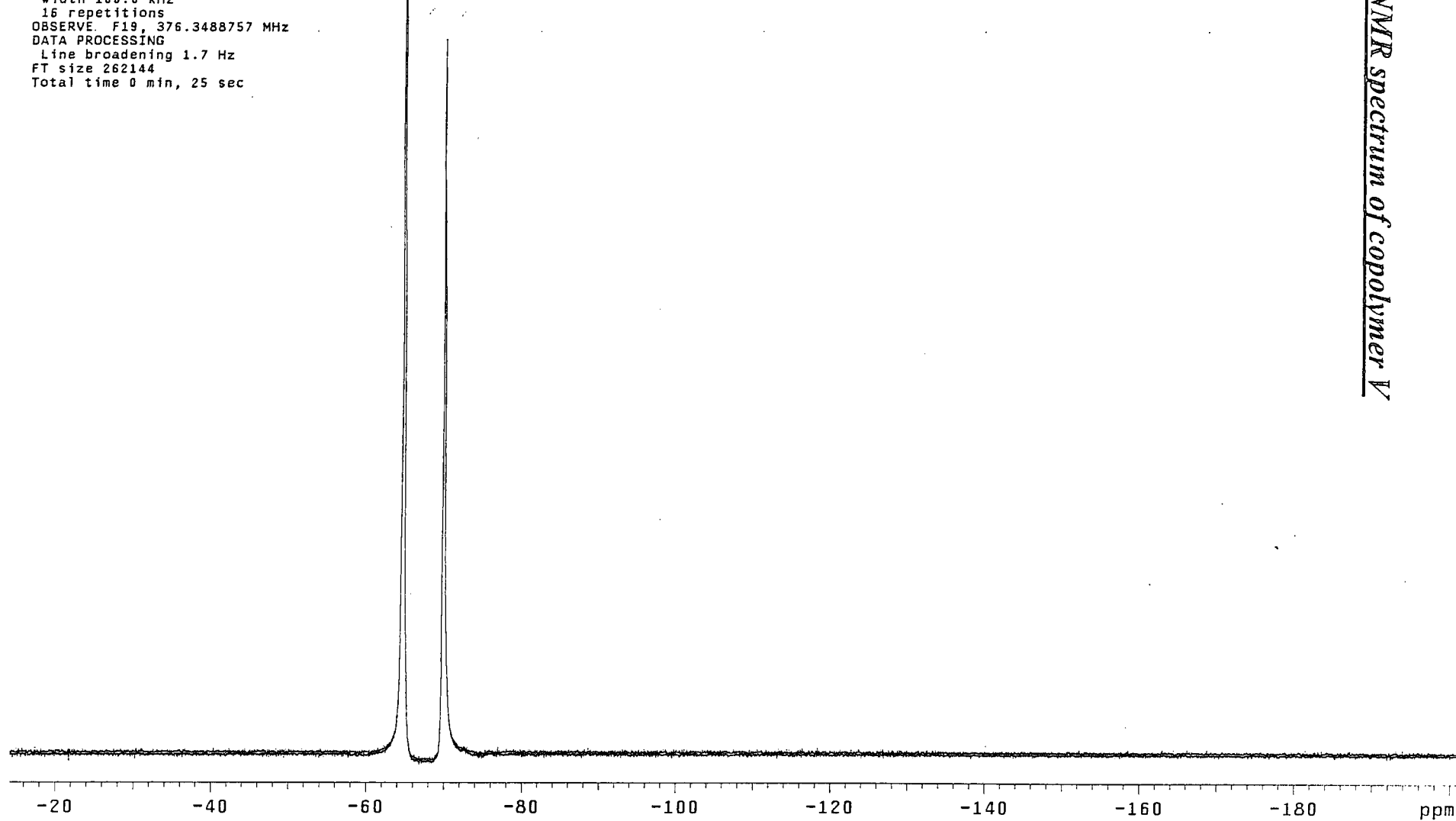
¹³C NMR spectrum of 5-trifluoromethylbicyclo[2.2.1]hept-2-ene



Pulse sequence: zgpg30
Solvent: CD300
Ambient temperature
File: /data/m40207/12171341-03
Processed on "daneka"

Relax. delay 1.000 sec
Pulse 35.0 degrees
Acq. time 0.600 sec
Width 100.0 kHz
16 repetitions
OBSERVE F19, 376.3488757 MHz
DATA PROCESSING
Line broadening 1.7 Hz
FT size 262144
Total time 0 min, 25 sec

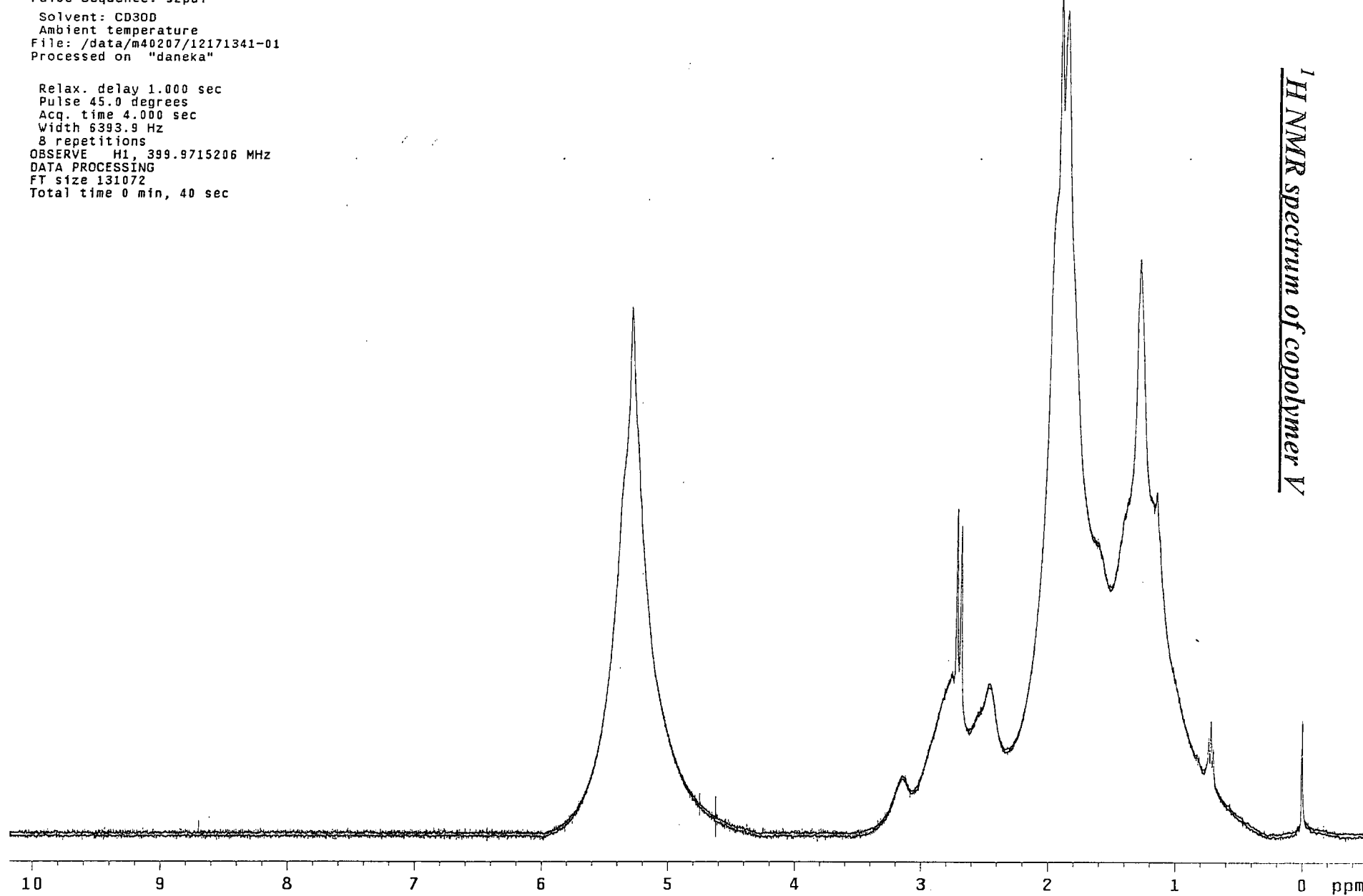
¹⁹F NMR spectrum of copolymer V



Device Sequence: 51201
Solvent: CD3OD
Ambient temperature
File: /data/m40207/12171341-01
Processed on "daneka"

Relax. delay 1.000 sec
Pulse 45.0 degrees
Acq. time 4.000 sec
Width 6393.9 Hz
8 repetitions
OBSERVE H1, 399.9715206 MHz
DATA PROCESSING
FT size 131072
Total time 0 min, 40 sec

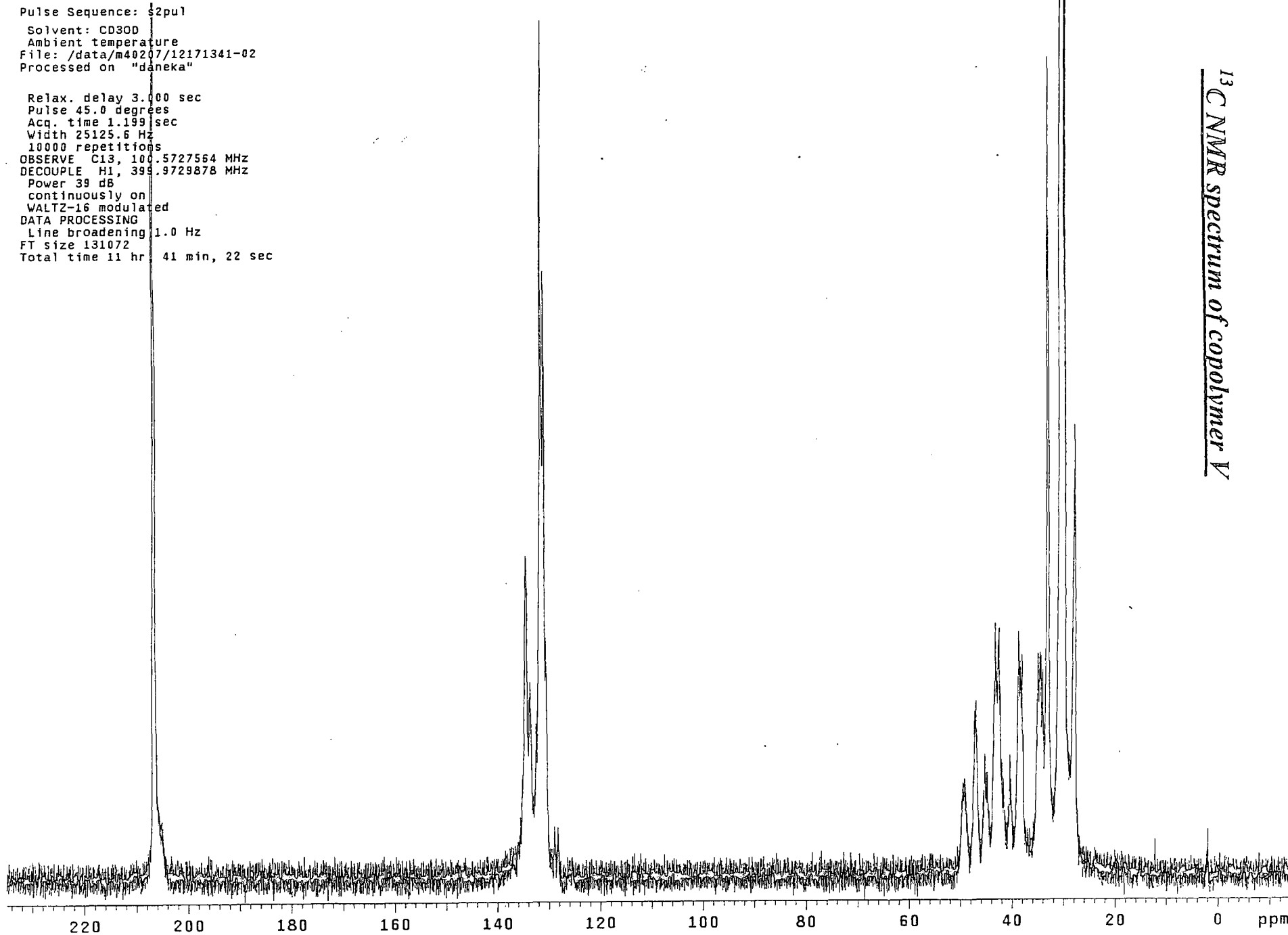
¹H NMR spectrum of copolymer V



Pulse Sequence: s2pu1
Solvent: CD3OD
Ambient temperature
File: /data/m40207/12171341-02
Processed on "daneka"

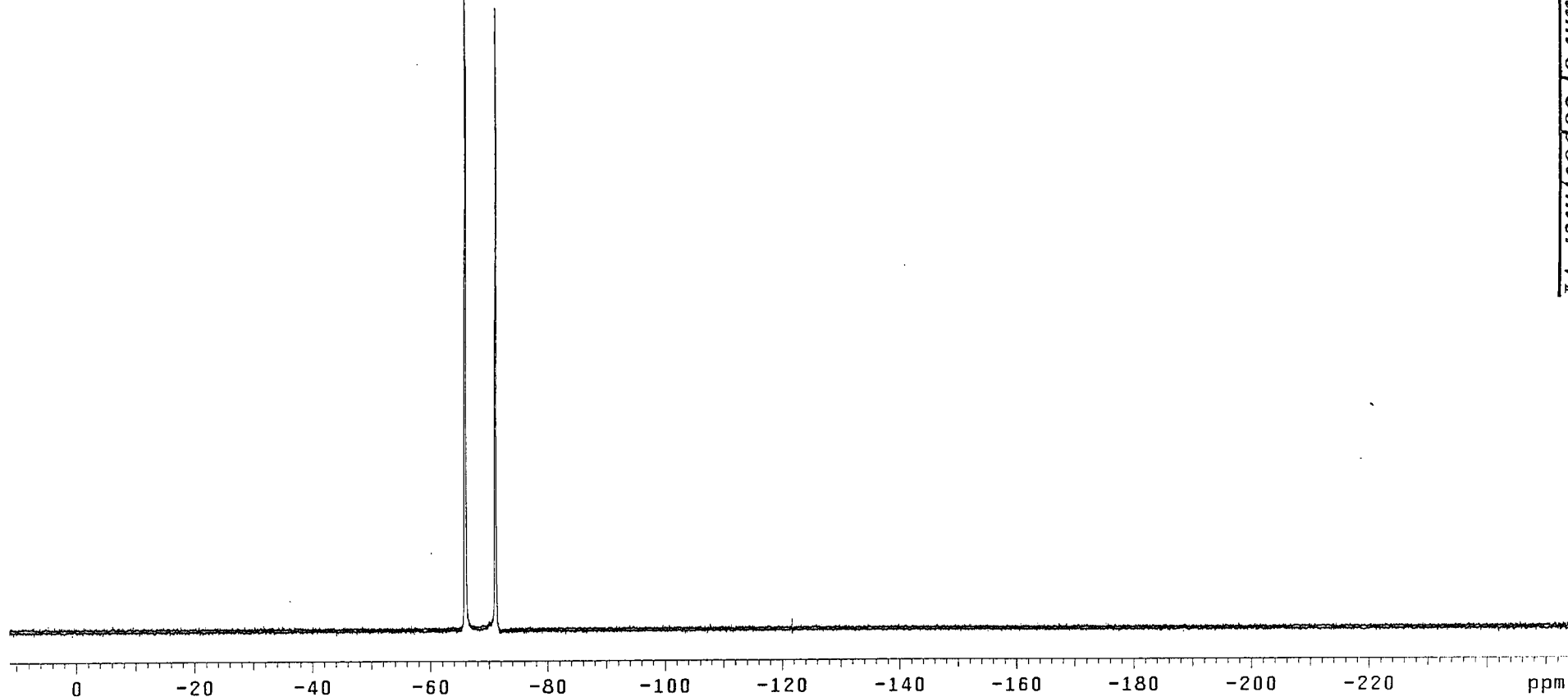
Relax. delay 3.000 sec
Pulse 45.0 degrees
Acq. time 1.199 sec
Width 25125.6 Hz
10000 repetitions
OBSERVE C13, 100.5727564 MHz
DECOUPLE H1, 399.9729878 MHz
Power 39 dB
continuously on
WALTZ-16 modulated
DATA PROCESSING
Line broadening 1.0 Hz
FT size 131072
Total time 11 hr 41 min, 22 sec

¹³C NMR spectrum of copolymer V



Pulse Sequence: s2pu1
Solvent: Acetone
Ambient temperature
File: /data/m40207/11094506-02
Processed on "daneka"

Relax. delay 1.000 sec
Pulse 35.0 degrees
Acq. time 0.600 sec
Width 100.0 kHz
16 repetitions
OBSERVE F19, 376.3493461 MHz.
DATA PROCESSING
Line broadening 1.7 Hz
FT size 262144
Total time 0 min, 25 sec

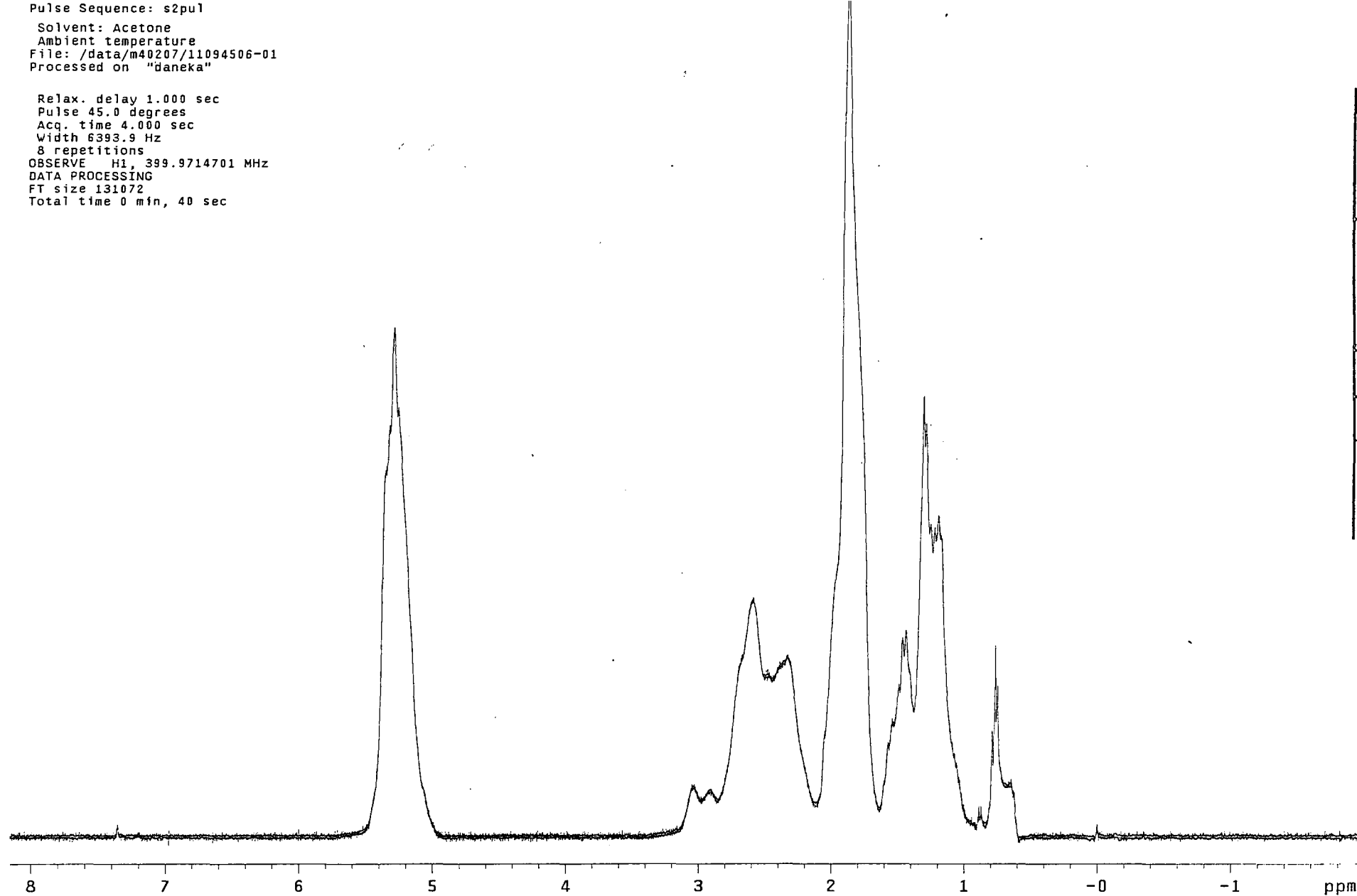


^{19}F NMR spectrum of copolymer VI

Pulse Sequence: s2pu1
Solvent: Acetone
Ambient temperature
File: /data/m40207/11094506-01
Processed on "daneka"

Relax. delay 1.000 sec
Pulse 45.0 degrees
Acq. time 4.000 sec
Width 6393.9 Hz
8 repetitions
OBSERVE H1, 399.9714701 MHz
DATA PROCESSING
FT size 131072
Total time 0 min, 40 sec

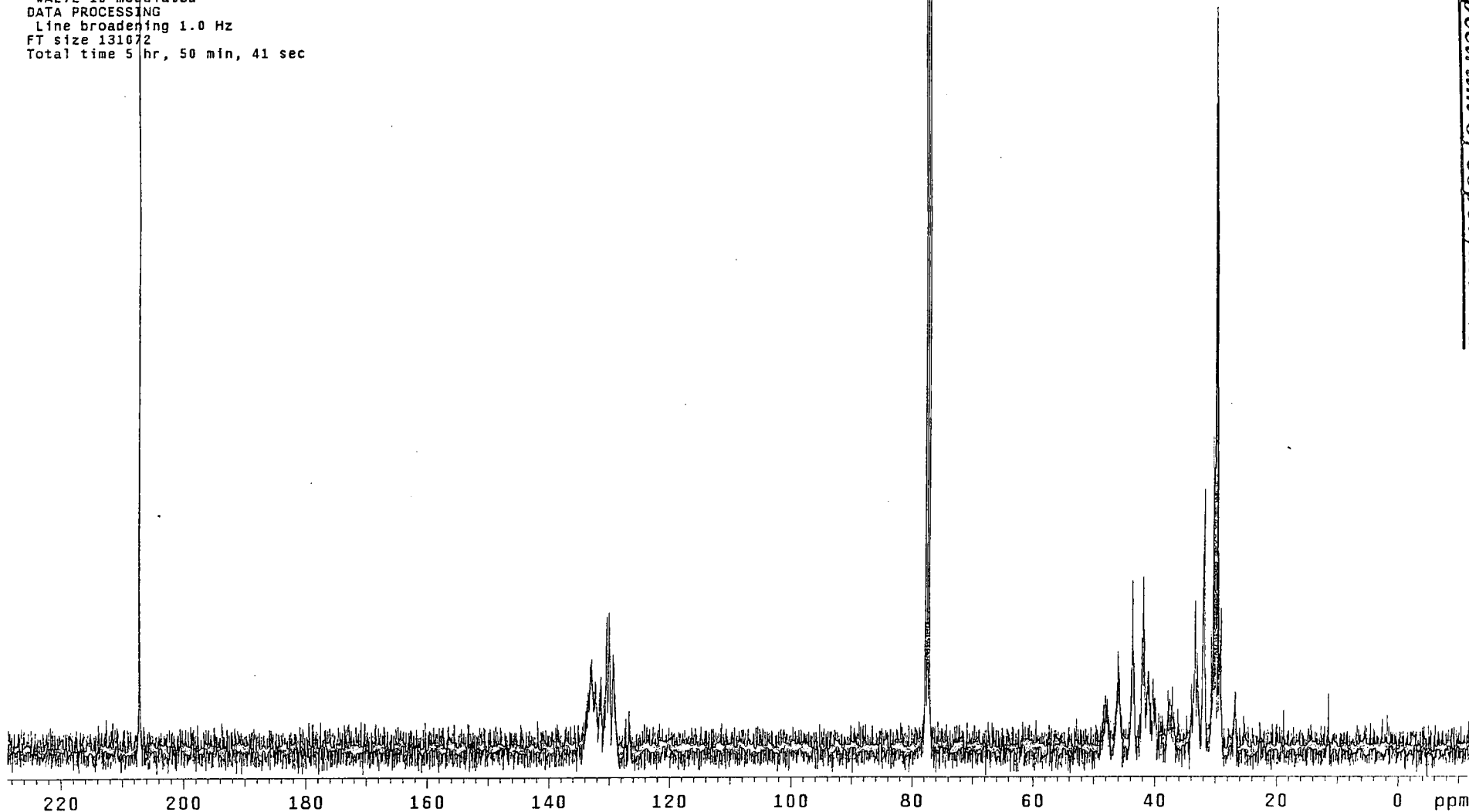
¹H NMR spectrum of copolymer VI



Pulse Sequence: s2pu1
Solvent: Acetone
Ambient temperature
File: /data/m40207/11172323-01
Processed on "daneka"

Relax. delay 3.000 sec
Pulse 45.0 degrees
Acq. time 1.199 sec
Width 25125.6 Hz
.5000 repetitions
OBSERVE C13, 100.5728822 MHz
DECOUPLE H1, 399.9734878 MHz
Power 39 dB
continuously on
WALTZ-16 modulated
DATA PROCESSING
Line broadening 1.0 Hz
FT size 131072
Total time 5 hr, 50 min, 41 sec

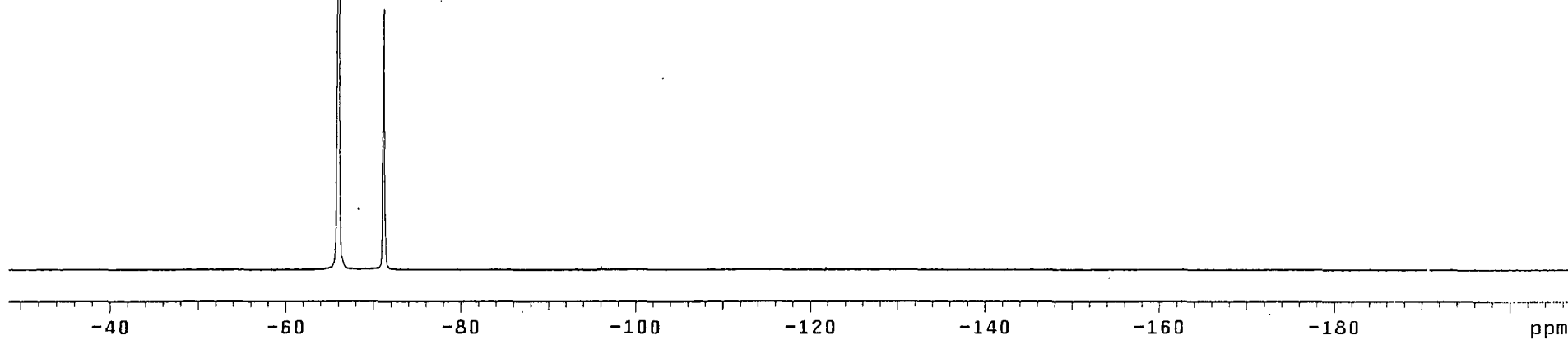
¹³C NMR spectrum of copolymer VI



Pulse Sequence: s2pu1
Solvent: Acetone
Ambient temperature
File: /data/m40208/23171845-03
Processed on "daneka"

Relax. delay 1.000 sec
Pulse 35.0 degrees
Acq. time 0.600 sec
Width 100.0 kHz
16 repetitions
OBSERVE F19, 376.3493461 MHz
DATA PROCESSING
Line broadening 1.7 Hz
FT size 262144
Total time 0 min, 25 sec

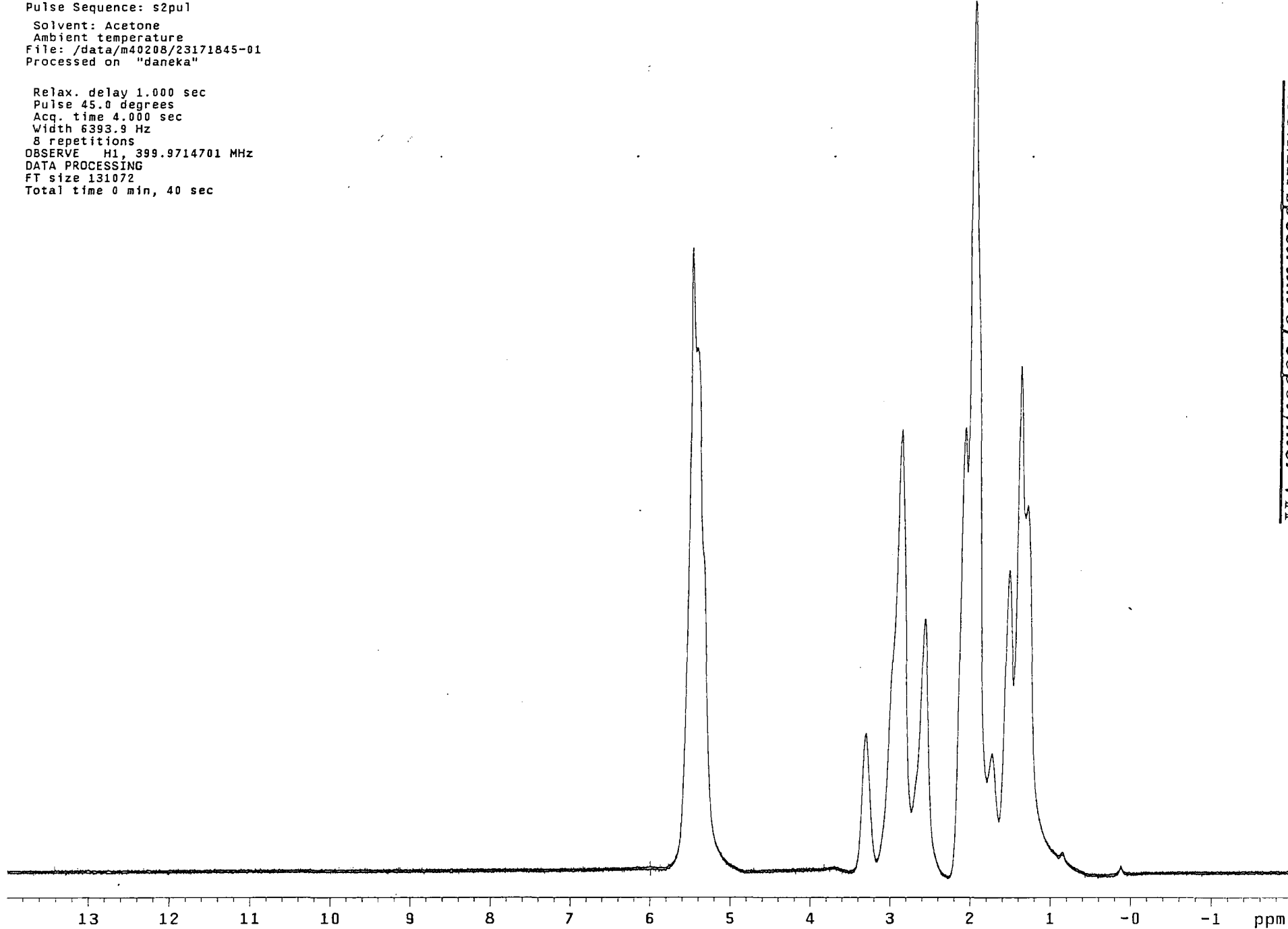
¹⁹F NMR spectrum of copolymer VII



Pulse Sequence: s2pul
Solvent: Acetone
Ambient temperature
File: /data/m40208/23171845-01
Processed on "daneka"

Relax. delay 1.000 sec
Pulse 45.0 degrees
Acq. time 4.000 sec
Width 6393.9 Hz
8 repetitions
OBSERVE H1, 399.9714701 MHz
DATA PROCESSING
FT size 131072
Total time 0 min, 40 sec

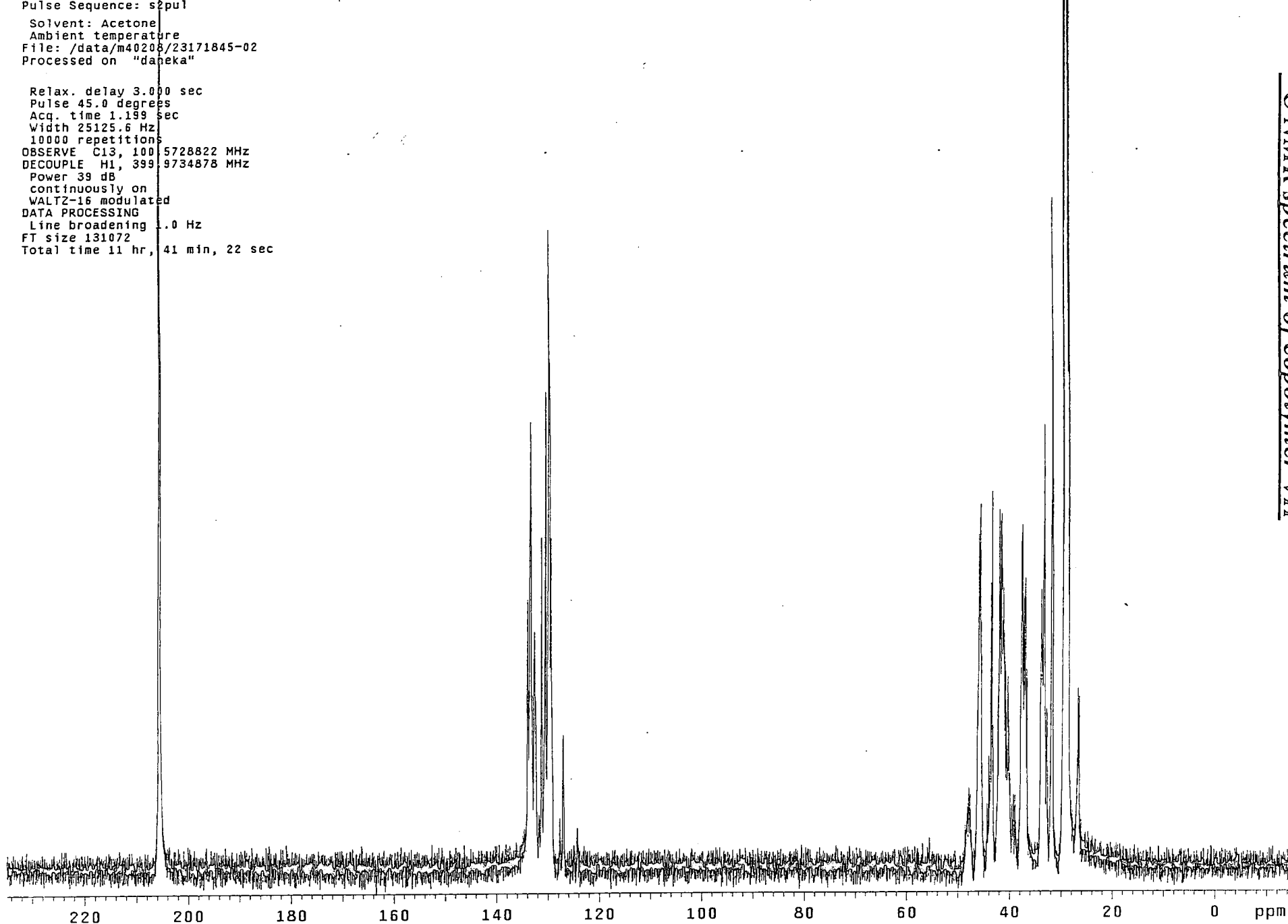
¹H NMR spectrum of copolymer VII



Pulse Sequence: s2pu1
Solvent: Acetone
Ambient temperature
File: /data/m40208/23171845-02
Processed on "dapaka"

Relax. delay 3.000 sec
Pulse 45.0 degrees
Acq. time 1.199 sec
Width 25125.6 Hz
10000 repetitions
OBSERVE C13, 100.5728822 MHz
DECOUPLE H1, 399.9734878 MHz
Power 39 dB
continuously on
WALTZ-16 modulated
DATA PROCESSING
Line broadening 1.0 Hz
FT size 131072
Total time 11 hr, 41 min, 22 sec

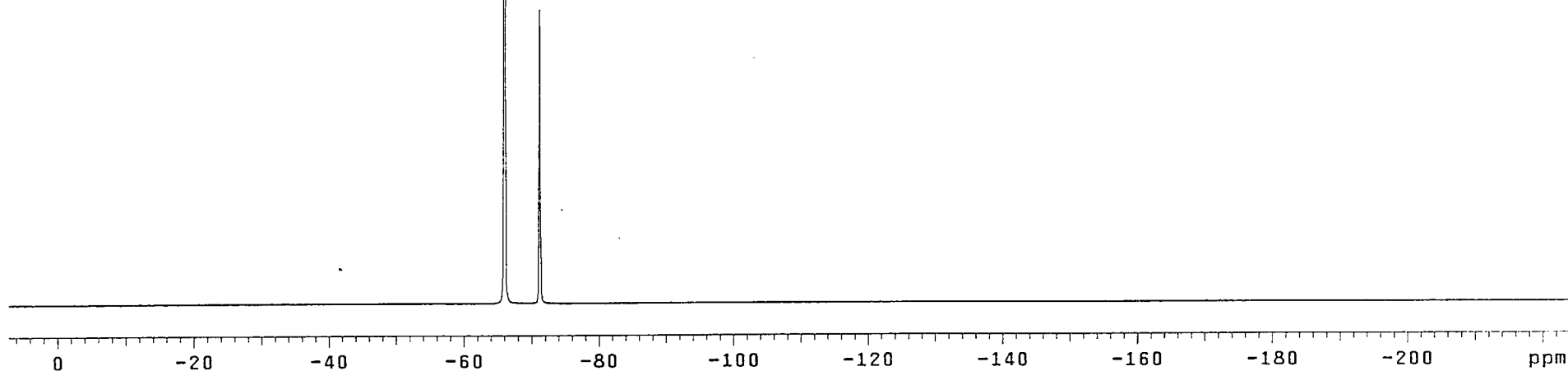
¹³C NMR spectrum of copolymer VII



Pulse Sequence: s2pu1
Solvent: Acetone
Ambient temperature
File: /data/m40208/23171900-03
Processed on "daneka"

Relax. delay 1.000 sec
Pulse 35.0 degrees
Acq. time 0.600 sec
Width 100.0 kHz
16 repetitions
OBSERVE F19, 376.3493461 MHz
DATA PROCESSING
Line broadening 1.7 Hz
FT size 262144
Total time 0 min, 25 sec

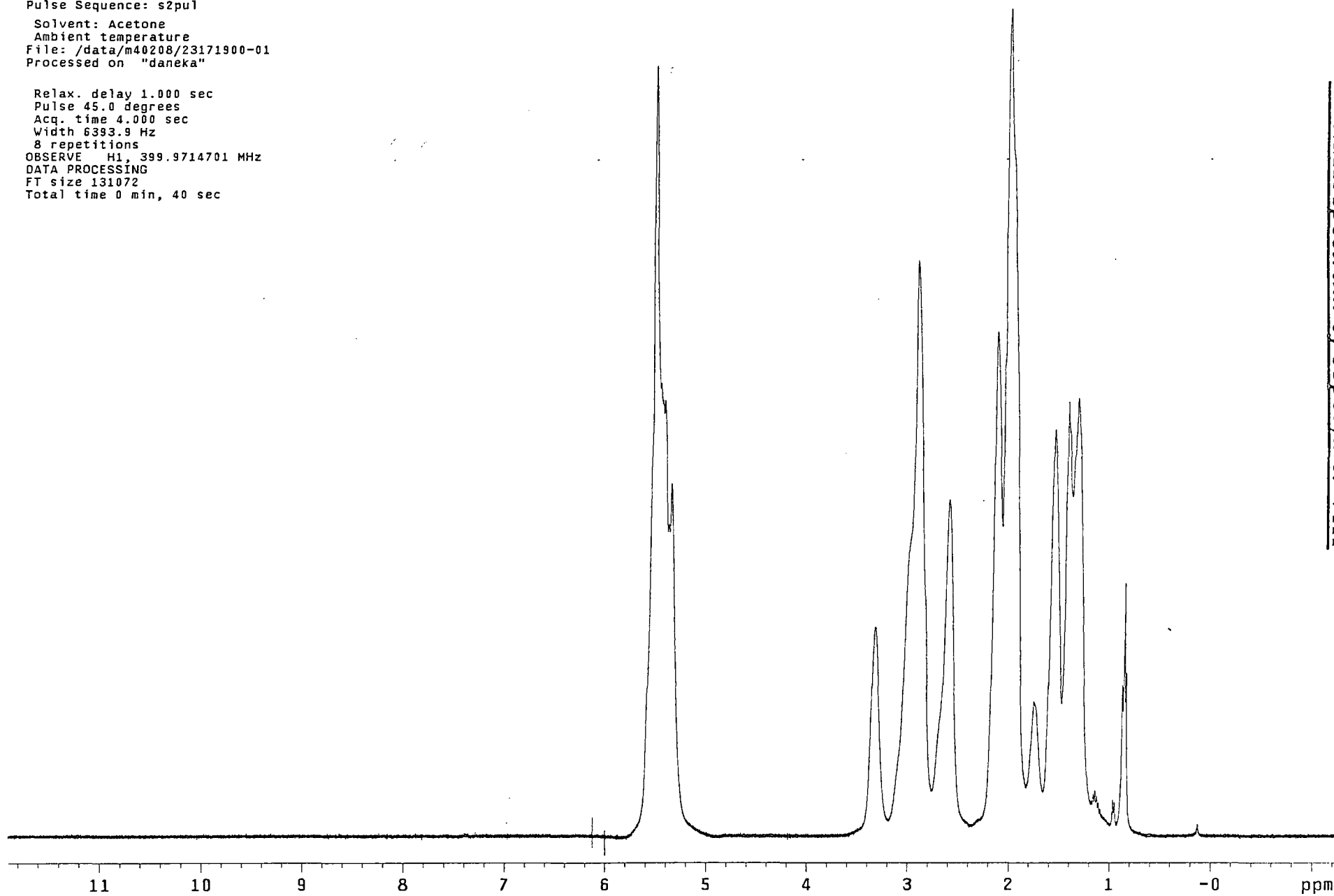
¹⁹F NMR spectrum of copolymer VIII



Pulse Sequence: s2pu1
Solvent: Acetone
Ambient temperature
File: /data/m40208/23171900-01
Processed on "daneka"

Relax. delay 1.000 sec
Pulse 45.0 degrees
Acq. time 4.000 sec
Width 6393.9 Hz
8 repetitions
OBSERVE H1, 399.9714701 MHz
DATA PROCESSING
FT size 131072
Total time 0 min, 40 sec

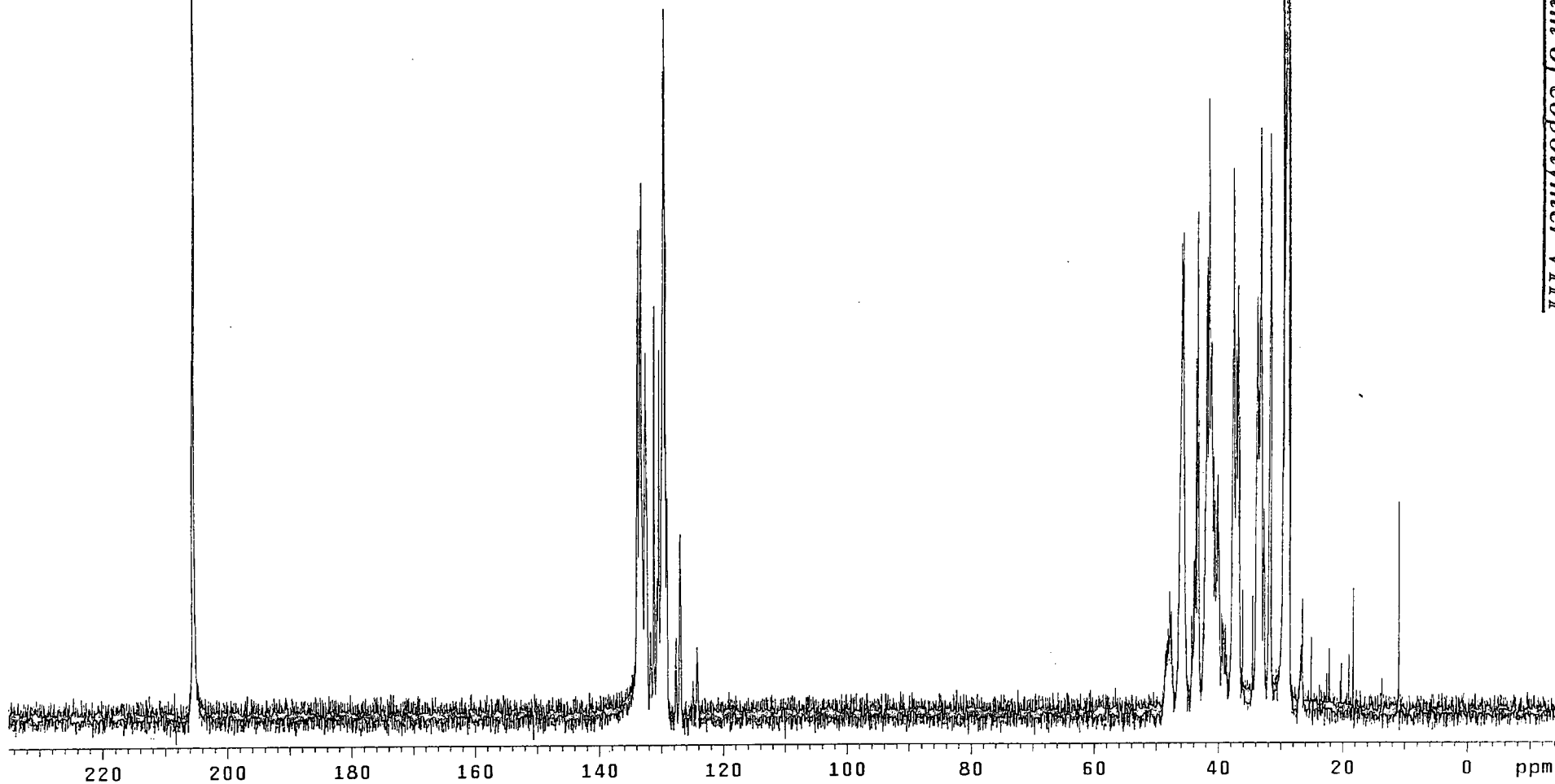
¹H NMR spectrum of copolymer VIII



Pulse Sequence: s2pu1
Solvent: Acetone
Ambient temperature
File: /data/m40208/23171900-02
Processed on "daheka"

Relax. delay 3.000 sec
Pulse 45.0 degrees
Acq. time 1.199 sec
Width 25125.6 Hz
10000 repetitions
OBSERVE C13, 100.5728822 MHz
DECOUPLE H1, 399.9734878 MHz
Power 39 dB
continuously on
WALTZ-16 modulated
DATA PROCESSING
Line broadening 1.0 Hz
FT size 131072
Total time 11 hr, 41 min, 22 sec

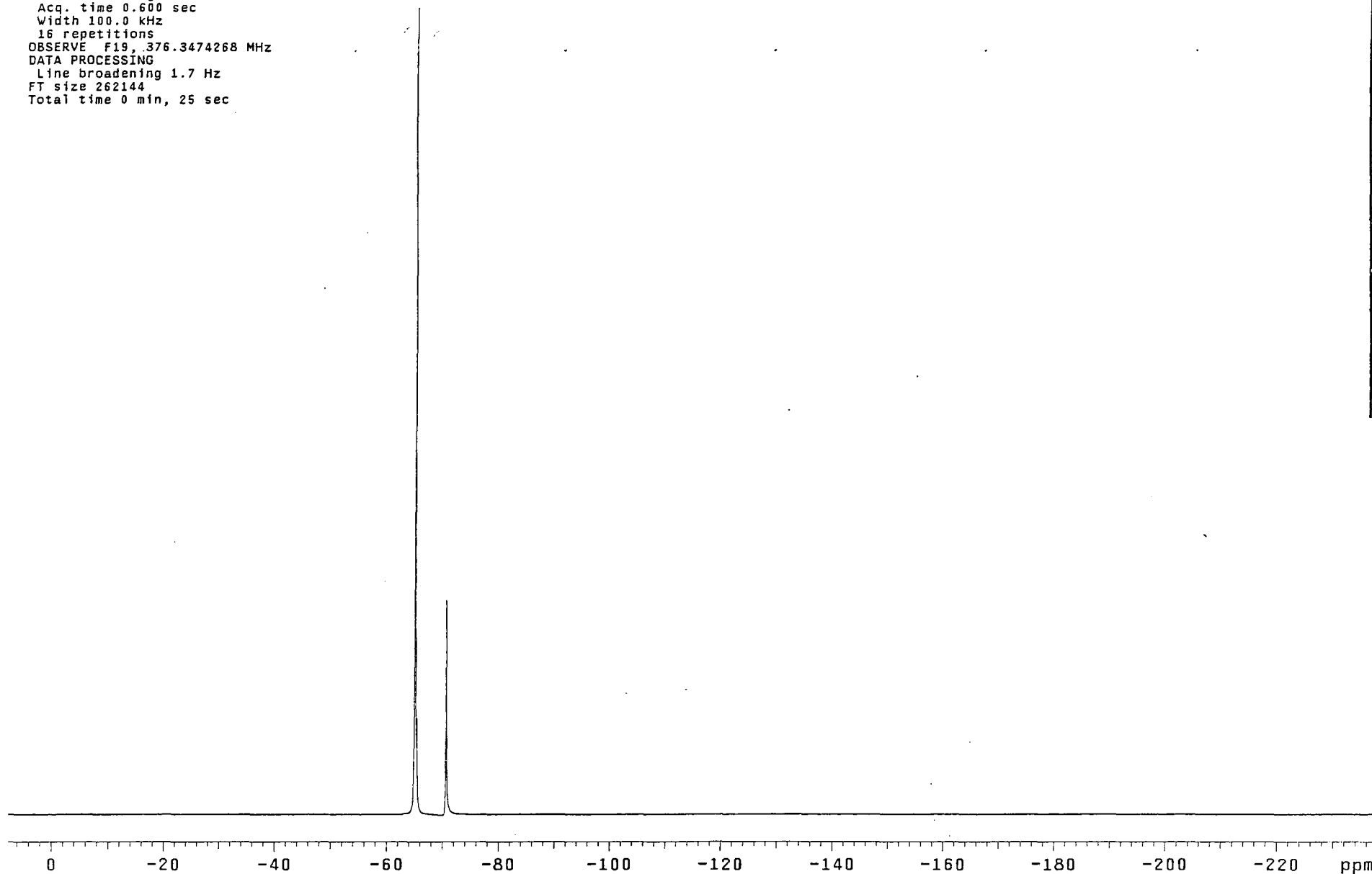
¹³C NMR spectrum of copolymer VIII



Pulse Sequence: s2pu1
Solvent: C6D6
Ambient temperature
File: /data/m40208/30171748-03
Processed on "daneka"

Relax. delay 1.000 sec
Pulse 35.0 degrees
Acq. time 0.600 sec
Width 100.0 kHz
16 repetitions
OBSERVE F19, 376.3474268 MHz
DATA PROCESSING
Line broadening 1.7 Hz
FT size 262144
Total time 0 min, 25 sec

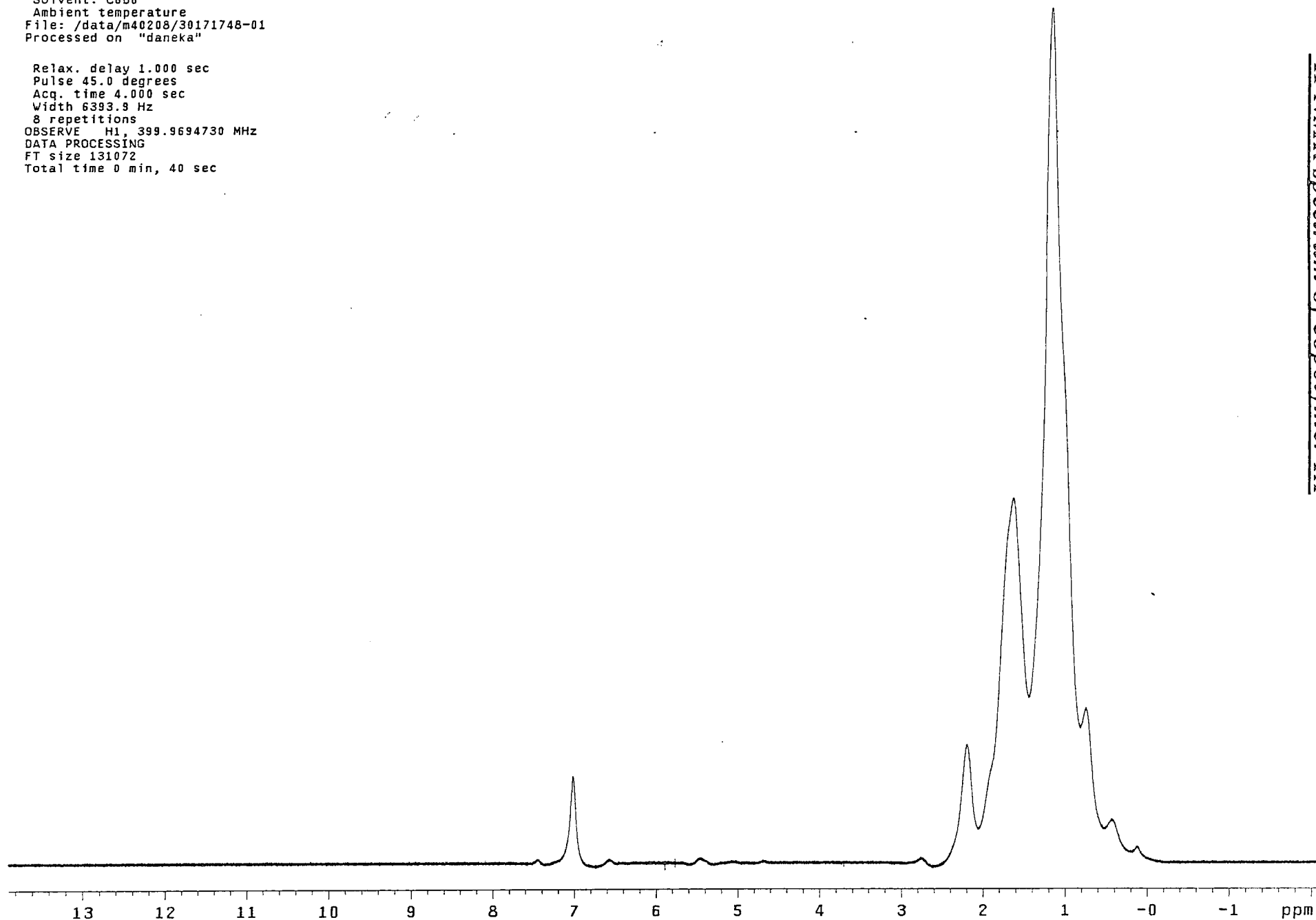
¹⁹F NMR spectrum of copolymer IX



Pulse Sequence: s2pu1
Solvent: C6D6
Ambient temperature
File: /data/m40208/30171748-01
Processed on "daneka"

Relax. delay 1.000 sec
Pulse 45.0 degrees
Acq. time 4.000 sec
Width 6393.9 Hz
8 repetitions
OBSERVE H1, 399.9694730 MHz
DATA PROCESSING
FT size 131072
Total time 0 min, 40 sec

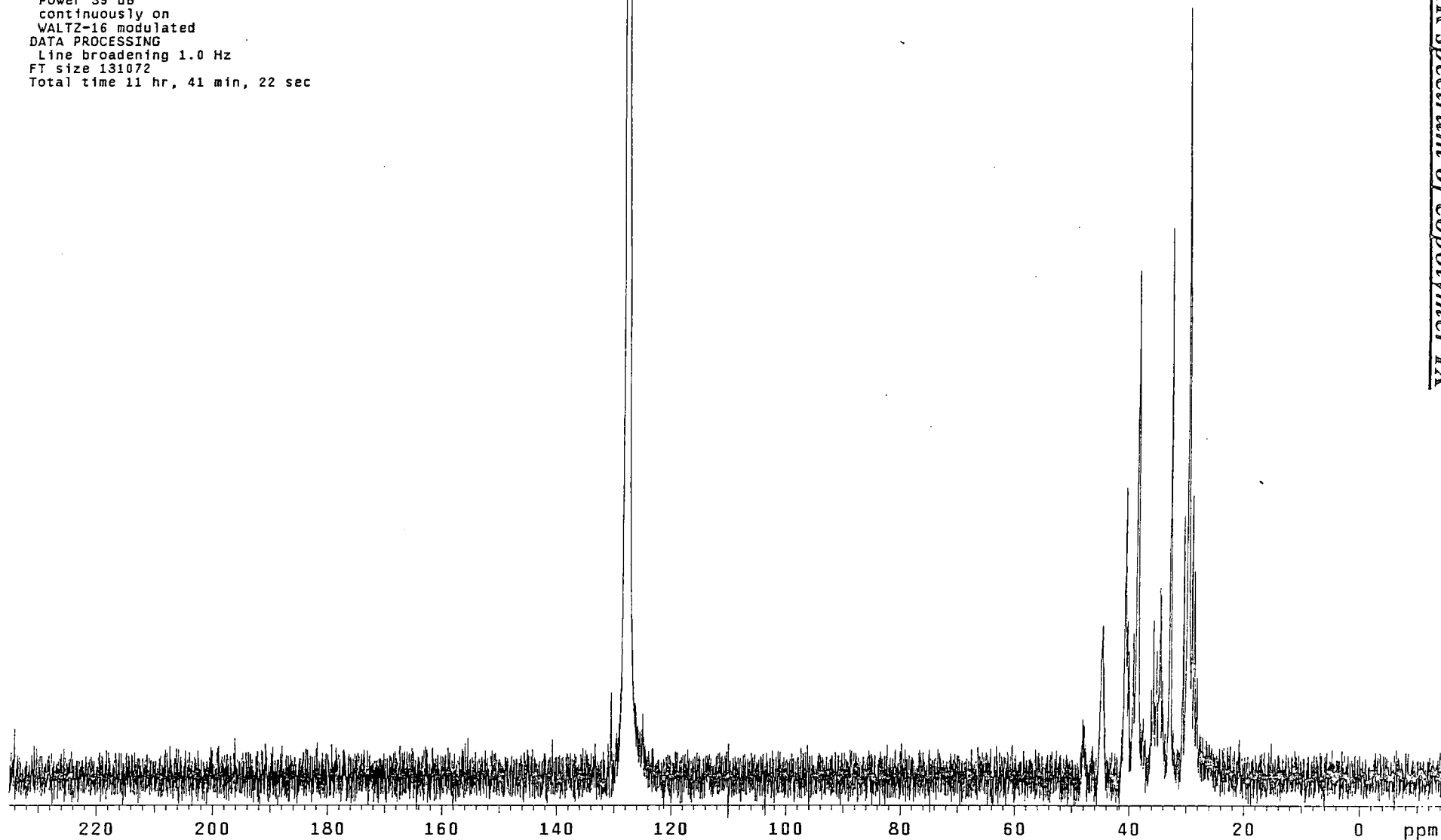
¹H NMR spectrum of copolymer IX



Pulse Sequence: szpu1
Solvent: C6D6
Ambient temperature
File: /data/m40208/30171748-02
Processed on "daneka"

Relax. delay 3.000 sec
Pulse 45.0 degrees
Acq. time 1.199 sec
Width 25125.6 Hz
10000 repetitions
OBSERVE C13, 100.5723692 MHz
DECOUPLE H1, 399.9714479 MHz
Power 39 dB
continuously on
WALTZ-16 modulated
DATA PROCESSING
Line broadening 1.0 Hz
FT size 131072
Total time 11 hr, 41 min, 22 sec

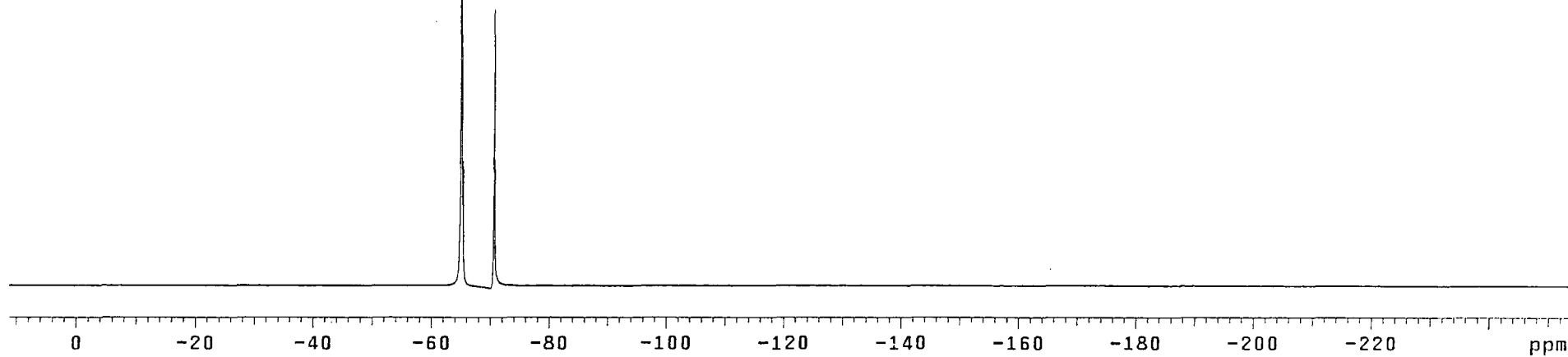
¹³C NMR spectrum of copolymer IX



Pulse sequence: zgpg30
Solvent: C6D6
Ambient temperature
File: /data/m40208/23171926-03
Processed on "daneka"

Relax. delay 1.000 sec
Pulse 35.0 degrees
Acq. time 0.600 sec
Width 100.0 kHz
16 repetitions
OBSERVE F19, 376.3474268 MHz
DATA PROCESSING
Line broadening 1.7 Hz
FT size 262144
Total time 0 min, 25 sec

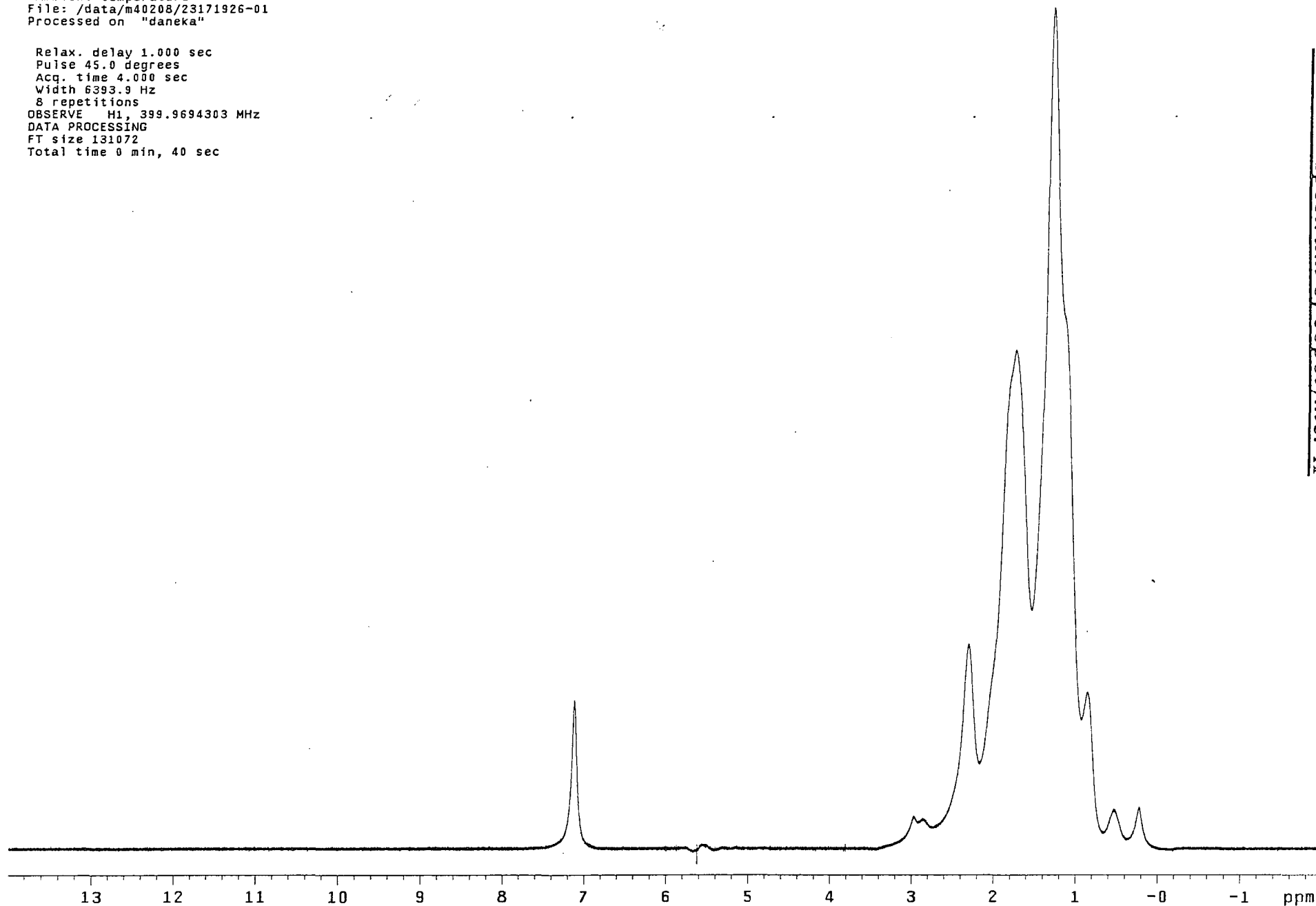
¹⁹F NMR spectrum of copolymer X



Pulse Sequence: s2pul
Solvent: C6D6
Ambient temperature
File: /data/m40208/23171926-01
Processed on "daneka"

Relax. delay 1.000 sec
Pulse 45.0 degrees
Acq. time 4.000 sec
Width 6393.9 Hz
8 repetitions
OBSERVE H1, 399.9694303 MHz
DATA PROCESSING
FT size 131072
Total time 0 min, 40 sec

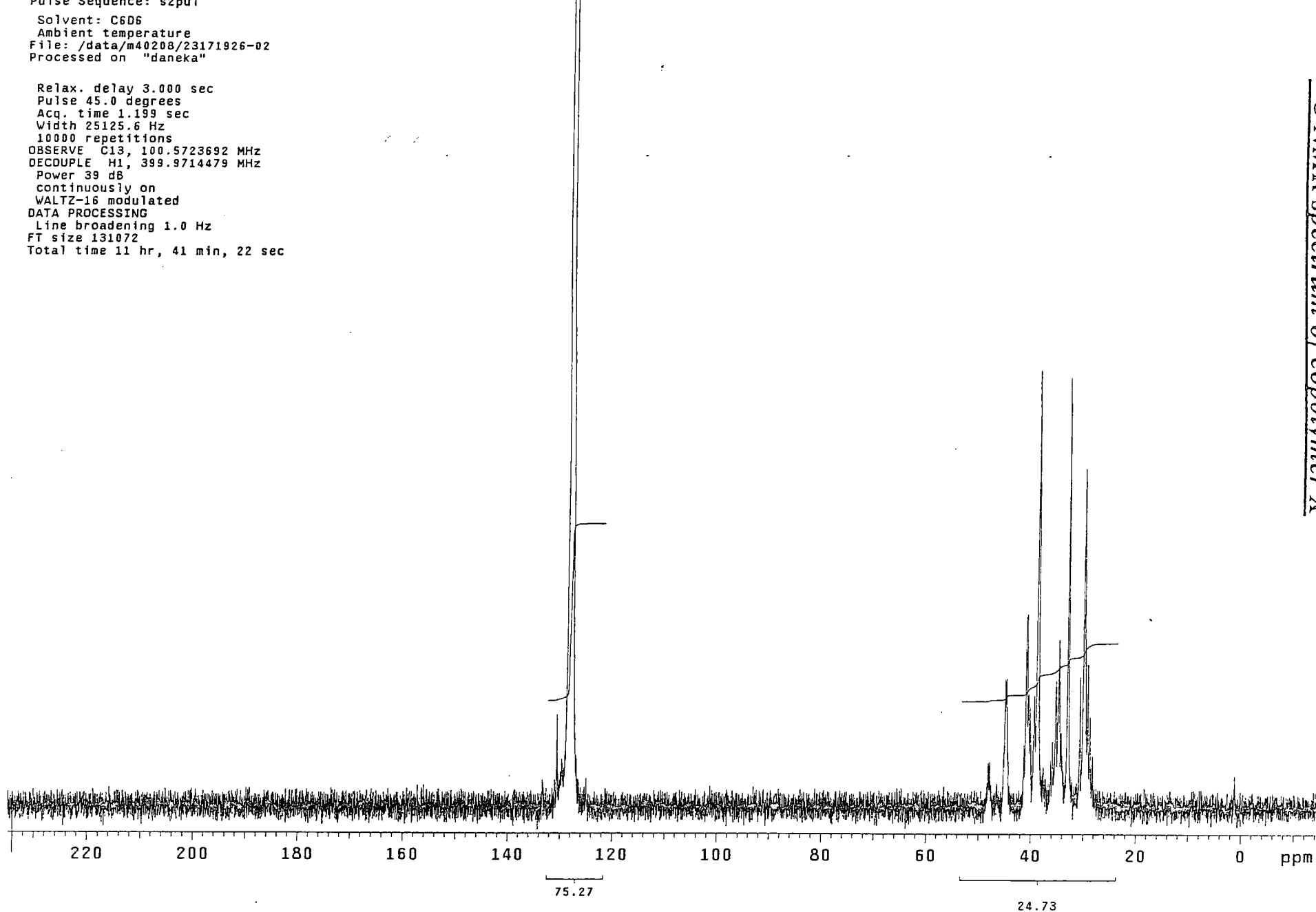
¹H NMR spectrum of copolymer X



Pulse sequence: szpul
Solvent: C6D6
Ambient temperature
File: /data/m40208/23171926-02
Processed on "daneka"

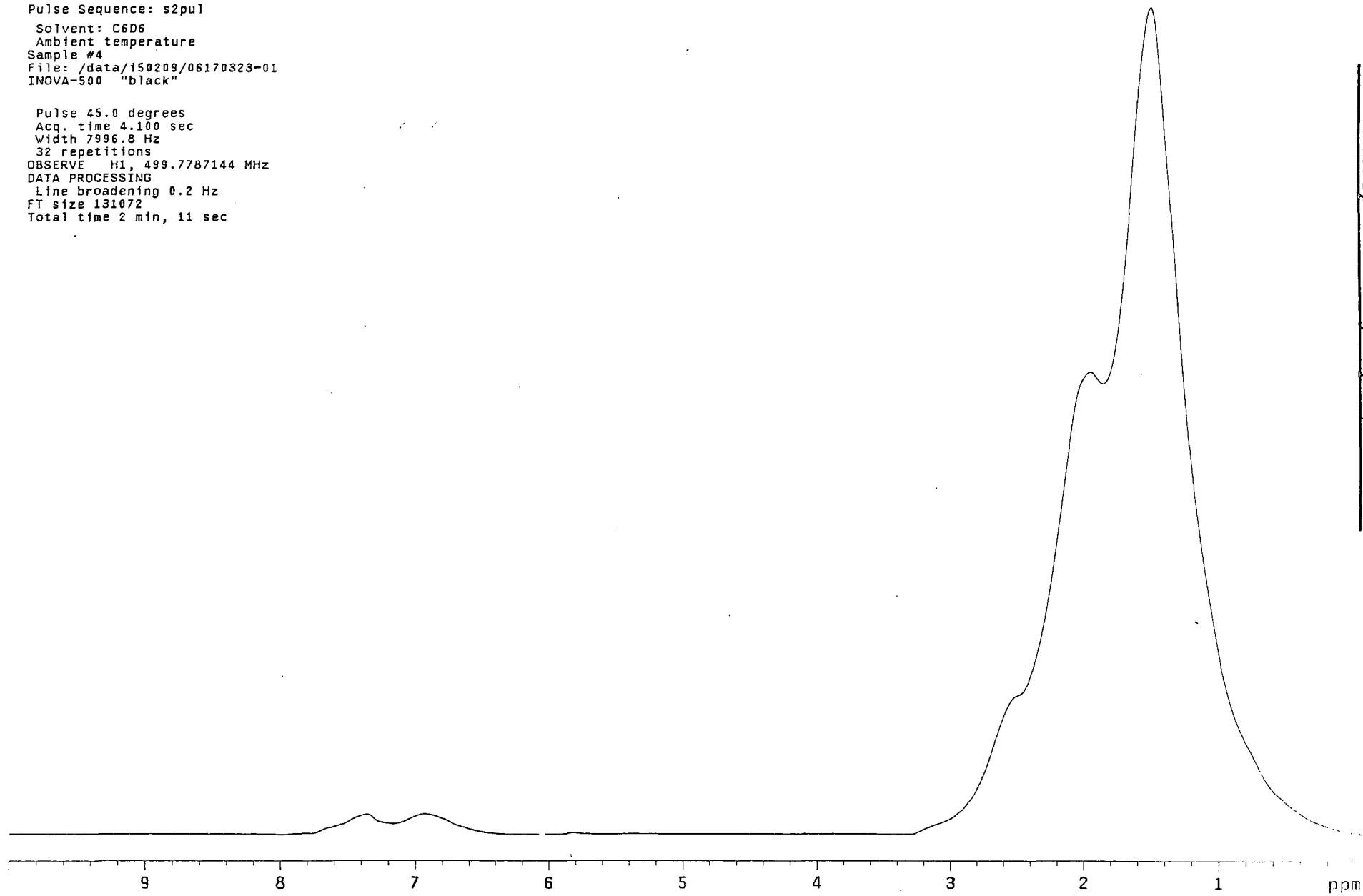
Relax. delay 3.000 sec
Pulse 45.0 degrees
Acq. time 1.199 sec
Width 25125.6 Hz
10000 repetitions
OBSERVE C13, 100.5723692 MHz
DECOUPLE H1, 399.9714479 MHz
Power 39 dB
continuously on
WALTZ-16 modulated
DATA PROCESSING
Line broadening 1.0 Hz
FT size 131072
Total time 11 hr, 41 min, 22 sec

¹³C NMR spectrum of copolymer X



File: /data/150209/06170323-01
Pulse Sequence: s2pu1
Solvent: C6D6
Ambient temperature
Sample #4
File: /data/150209/06170323-01
INOVA-500 "black"

Pulse 45.0 degrees
Acq. time 4.100 sec
Width 7996.8 Hz
32 repetitions
OBSERVE H1, 499.7787144 MHz
DATA PROCESSING
Line broadening 0.2 Hz
FT size 131072
Total time 2 min, 11 sec



¹H NMR spectrum of copolymer XII

Pulse Sequence: s2pu1
Solvent: C6D6
Ambient temperature
Sample #4, user 1-14-87
File: /data/i50209/06170323-02
INOVA-500 "black"

Relax. delay 3.000 sec
Pulse 45.0 degrees
Acq. time 1.311 sec
Width 31421.8 Hz
10000 repetitions
OBSERVE C13, 125.6694277 MHz
DECOUPLE H1, 499.7812133 MHz
Power 42 dB
continuously on
WALTZ-16 modulated
DATA PROCESSING
Line broadening 0.5 Hz
FT size 131072
Total time 11 hr, 59 min, 56 sec

¹³C NMR spectrum of copolymer XII

